

# **Catalytic Hydrogenolysis of Glycerol to 1-Propanol Using Bifunctional Catalysts in an Aqueous Media**

by

Chau Thi Quynh Mai

A thesis

presented to the University of Waterloo

in fulfillment of the

thesis requirement for the degree of

Doctor of Philosophy

in

Chemical Engineering

Waterloo, Ontario, Canada, 2016

© Chau Thi Quynh Mai

## **AUTHOR'S DECLARATION**

I hereby declare that I am the sole author of this thesis. This is a true copy of the thesis, including any required final revisions, as accepted by my examiners.

I understand that my thesis may be made electronically available to the public.

## Abstract

Biodiesel is an attractive alternative fuel obtained from renewable resources and glycerol is produced as a major byproduct in the biodiesel industry. Upgrading glycerol to other valuable chemicals will contribute to an economic sustainability of the biodiesel industry. Valuable commodity chemicals such as 1,2-propanediol (1,2-PD), 1,3-Propanediol (1,3-PD) and 1-Propanol (1-PO) could be produced by catalytic hydrogenolysis. Although much work has been done towards the conversion of glycerol to 1,2-PD and 1,3-PD, the direct conversion of glycerol to 1-PO has not received much attention. From an industry point of view, the production of 1-PO is very interesting. 1-PO has potential applications as a solvent, organic intermediate and can be dehydrated to produce “green“ propylene for the production of polypropylene. Therefore, the development of a new process for the efficient conversion of glycerol to 1-PO will contribute to new “green” chemicals which will benefit the environment and make biodiesel processes more profitable as 1 kg of glycerol is produced for every 10 kg of biodiesel.

In this research, heterogeneous hydrogenolysis of glycerol to 1-PO was carried out in a batch reactor using a bi-functional catalyst (prepared by a sequential impregnation method) in water, a green and inexpensive liquid medium. It was found that a bi-functional solid catalyst consists of a non-noble metal Ni for hydrogenation and an acidic function of silicotungstic acid (HSiW) supported on alumina ( $\text{Al}_2\text{O}_3$ ) to be an active catalyst for the one-pot synthesis of 1-PO from glycerol and  $\text{H}_2$  in a liquid phase reaction. A systematic study has been carried out to assess the effects of operating conditions on the glycerol conversion. The catalysts were characterized using BET, XRD,  $\text{NH}_3$ -TPD, TPR, TGA and FTIR techniques.

The effect of different metals (Cu, Ni, Pd, Pt and Cs) supported 30HSiW/ $\text{Al}_2\text{O}_3$  catalyst, heteroatom substitution (HSiW, HPW and HPMo) on NiHPA/ $\text{Al}_2\text{O}_3$  catalysts and 10Ni/30HSiW supported on different supports ( $\text{Al}_2\text{O}_3$ ,  $\text{TiO}_2$  and MCM-41) were studied to determine to what extent these components affect the catalytic activity of the NiHPAs/ $\text{Al}_2\text{O}_3$  catalysts for the hydrogenolysis of glycerol. The effect of the preparation process on the catalytic activity and the structure of the catalyst was also studied.

It was found that 1%Pt is the best promoter for the production of 1-PO in a stainless steel batch reactor (the selectivity to 1-PO was 59.2% at 45.3% conversion of glycerol). 1%Ni, a much

cheaper metal, has fairly comparable reactivity to 1%Pt (the selectivity to 1-PO was 54.7% at 39.2% conversion of glycerol). It was reported that the catalytic activity and thermal stability towards decomposition of the catalyst depends on heteroatom substitution. Using NH<sub>3</sub>-TPD, XRD and FTIR it was found that while the Keggin-structure of HSiW and HPW supported catalyst is stable up to a treatment temperature of 450°C, the Keggin-structure of a HPMo supported catalyst was decomposed even at a treatment temperature of 350°C; the decomposition of HPMo into MoO<sub>3</sub> is likely to be responsible for the inactivity of the NiHPMo catalyst for glycerol conversion. HPW and HPMo lost their acidity much more readily than HSiW, and a HSiW supported catalyst was the best candidate for 1-PO production. The catalytic activity and the acidity of 10Ni/30HSiW supported catalyst are influenced strongly by supporting 10Ni/30HSiW on different supports.

Using XRD and FTIR it was found that the thermal treatment during the preparation process indeed affected the structure and the activity of the catalyst to some extent. The loss in activity of the catalyst, the decomposition in Keggin-structure of HPAs occur if the treatment temperature is higher than 450°C.

It is important to note that this is the first report on a 10Ni/30HSiW supported catalyst developed for the one-pot hydrogenolysis of glycerol in a water media with high conversion of glycerol (90.1%) and high selectivity to 1-PO (92.9%) at 240°C and 580PSI hydrogen using a Hastelloy batch reactor. The activation energy  $E_a$  of this reaction is 124.1kJ/mol.

Reaction pathways for the hydrogenolysis of glycerol using a bifunctional catalyst 10Ni/30HSiW/Al<sub>2</sub>O<sub>3</sub> is proposed. It is believed that acidity plays an important role for the dehydration and Ni plays an important role for the hydrogenation. It is suggested that with acidic catalysts, the main route for the formation of 1-PO from glycerol is via either the hydrogenation of acrolein or further hydrogenolysis of 1,2-PD (and 1,3PD) where 1,2-PD (and 1,3-PD) and acrolein are the intermediate species in the formation of 1-PO from glycerol. The formation of 1,2-PD and 1,3-PD takes place through an initial dehydration of the primary or secondary hydroxyl groups on glycerol to give acetol or 3-hydroxypropanaldehyde (3-HPA). The hydrogen activated on the metal facilitates the hydrogenation of acetol or 3-HPA to release 1,2-PD or 1,3-PD respectively. However, dehydration of 3-HPA on the acid sites forms acrolein. Further hydrogenolysis of diols or hydrogenation of acrolein produces 1-PO.

1,3-PD that is a very high value-added chemical can also be obtained from hydrogenolysis of glycerol using a Ni-HSiW supported catalyst. To improve the selectivity of 1,3-PD it is suggested that the catalyst should have high hydrogenation activity for the intermediate 3-HPA. The equilibrium between acrolein and 3-HPA in the hydration-dehydration step is important, so it is essential to tune the bi-functional catalyst and the conditions of the reaction to form 1,3-PD from 3-HPA. A study of promoter effects for the activity of catalyst to form 1,3-PD is recommended.

## Acknowledgements

To achieve the Ph.D degree is my first important objective since I came to Canada. I was lucky to get the chance to accomplish my wish at the University of Waterloo. The Ph.D program is challenging both academically and personally. I appreciate the encouragement, support, instruction, tutorial, and cooperation provided by the Department of Chemical Engineering and the University of Waterloo during the past five years. Without this help, my study in pursuing this degree would have been much more difficult.

First of all, I would like to express my sincere gratitude to my supervisor, Professor Flora T.T. Ng for her academic instruction, research guidance, continuous encouragement, financial support and inspiration through the course of this research project. Her professional experience, active research attitude, and her keen judgement on the study direction are the guiding light in my study. Under her supervision my research skills have improved to a higher level. I would also show my gratitude to Professor Garry Rempel who gives me the chance to extend my knowledge in catalysis, the helpful discussions and suggestions, and his professional experience.

Secondly, I would extend my gratitude to the committee members in my Comprehensive Examination and the Oral Defence, Professor Bill Anderson, Professor Aiping Yu, Professor Zhongchao Tan, and Professor Ying Zheng for their constructive comments and contributions to this thesis. I would also show my gratitude to the lecturers of the four courses I took during my Ph.D program. They are Professor Garry Rempel, Professor Thomas A. Duever, Professor Zhongwei Chen and Professor Michael K.C. Tam. The study on these courses was very helpful in completing this thesis.

I would like to thank all the members of Professor Ng's research group during my study. Special thanks to Dr. Yuanqing Liu for helping me start the experiments with the autoclave, GC and catalyst preparation techniques. Thanks to Dr Guo - a visiting professor from China for helping me with the DRIFT and TPD techniques, and for sharing his valuable experience and knowledge. Thanks to Dr. Nagaraju Pasupulety for helping me with the TPD and XRD experiments. Thanks to Dr. Lei Jia for helping me with the RGA and TEM experiments. Thanks to all other members for their help with my experiments and their friendship: Ashish Gaurav, Lu Dong, Saurabh Patankar, Manish Tiwari. Thanks to the undergraduate students who helped to get the excellent

data: Aprajita Bansal, Beatriz Vieira, Hsin-Ya Lo, Gurjant Singh Sidhu, Eghosa Ogbeifun and Arnaud N. Gatera. Thanks to the members in Professor Rempel's group for their helping with the equipment: Dr. Allen Liu and Dr Karl Liu. I would acknowledge the kind assistance of Ralph Dickhout, Bert Habicher, Ravindra Singh and Rick Hecktus during my research.

As a daughter, I would like to bow my deep gratitude and my love to my parents, Cu Mai and Dong Phan. I appreciate them raising me up, providing me a comfortable growing up environment, supporting my education, and giving me their great selfless love. I would like to send my appreciation to my siblings, Phuong Mai and Khoa Mai, who supported and took care of my parents all the time during my study.

Finally, I want to express my deep gratitude to my husband, Hai Le, for his constant encouragement, understanding, and support throughout my study and my life. I also appreciate the birth of my sons, Son Le and Daniel Le, who gave me a lot of happiness during my study.

The financial support from the Natural Sciences and Engineering Research Council (NSERC) of Canada, Vietnam International Education Development (VIED) and PetroVietnam of Vietnam is gratefully appreciated.

## Table of Contents

Abstract.....	iii
Acknowledgements.....	vi
Table of Contents.....	viii
List of Figures.....	xi
List of Tables.....	xv
Nomenclature.....	xvii
Chapter One.....	1
General of Background.....	1
1.1 Introduction.....	1
1.2 Glycerol production and markets.....	2
1.3 Glycerol as a platform chemical.....	4
1.4 Converting glycerol into value-added products.....	5
1.5 Uses of 1,2-Propanediol, 1,3- Propanediol and 1-Propanol.....	8
1.5.1 1,2-Propanediol.....	8
1.5.2 1,3-Propanediol.....	8
1.5.3 1-Propanol.....	9
1.6 Research objective.....	10
Chapter Two.....	12
Literature Review.....	12
2.1 Introduction.....	12
2.2 Reaction mechanism for the heterogeneous hydrogenolysis of glycerol to lower alcohols.....	12
2.3 Heteropolyacids.....	18
2.4 Catalyst for production of 1,3-Propanediol from glycerol.....	20
2.4.1 Promoting effect of Tungsten-added catalysts in the generation of Brønsted acid.....	20
2.4.2 Noble metal based catalysts.....	22
2.5 Catalysts for production of 1-Propanol from glycerol.....	25
Chapter Three.....	27
Experimental Apparatus and Methods.....	27
3.1 Materials.....	27



3.2 Catalyst Preparation Methods .....	27
3.2.1 The preparation of metal heteropolyacids supported catalyst by impregnation .....	27
3.2.2 Loading Cs on 10Ni/30HSiW/Al <sub>2</sub> O <sub>3</sub> catalysts by ion-exchanged method.....	28
3.3 Autoclave Experimental Apparatus .....	28
3.3.1 Catalyst reduction apparatus.....	28
3.3.2 Autoclave apparatus .....	29
3.4 Products Analytical Apparatus and Method .....	30
3.4.1 Gas Chromatography (GC).....	30
3.5 Methods and Procedures for Catalyst Characterization Techniques.....	33
3.5.1 Ammonia Temperature Programmed Desorption (NH <sub>3</sub> -TPD).....	34
3.5.2 H <sub>2</sub> Temperature Programmed Reduction (TPR) .....	36
3.5.3 Brunauer Emmett Teller (BET) Surface Area.....	36
3.5.4 Thermal Gravimetric Analysis (TGA) .....	38
3.5.5 X-Ray Diffraction (XRD).....	38
3.5.6 Fourier transform infrared spectroscopy (FTIR) .....	39
Chapter Four .....	40
Conversion of glycerol to lower alcohols using 10Ni/30HSiW/Al <sub>2</sub> O <sub>3</sub> catalyst in a Stainless Steel batch reactor.....	40
4.1. Effect of metals on the hydrogenolysis of glycerol.....	40
4.2 Effect of Cs <sup>+</sup> on activity of 10Ni/30HSiW/Al <sub>2</sub> O <sub>3</sub> catalyst .....	48
4.3 Conclusions .....	61
Chapter Five.....	63
Conversion of glycerol to lower alcohols using 10Ni/30HSiW/Al <sub>2</sub> O <sub>3</sub> catalyst in a Hastelloy reactor .....	63
5.1 Repeatability of 10Ni/30HSiW/Al <sub>2</sub> O <sub>3</sub> Catalyst .....	63
5.2 Effect of experimental parameters .....	64
5.2.1 Effect of RPM.....	64
5.2.2 Effect of hydrogen pressure.....	69
5.2.3 Effect of water content .....	75
5.2.4 Effect of catalyst weight loading .....	79
5.2.5 Kinetic analysis.....	81

5.2.6 Effect of temperature and activation energy.....	83
5.3 Study of the effect of NiHSiW/Al <sub>2</sub> O <sub>3</sub> loading on Al <sub>2</sub> O <sub>3</sub> .....	88
5.3.1 Effect of HSiW loading on catalytic activity of the 10Ni/HSiW/Al <sub>2</sub> O <sub>3</sub> .....	88
5.3.2 Effect of different amounts Ni loading.....	95
5.3.3 Effect of catalyst preparation sequence on 10Ni/30HSiW/Al <sub>2</sub> O <sub>3</sub> catalysts .....	102
5.4 Proposed reaction mechanism using heterogeneous metal catalysts .....	108
5.5 Leaching and recyclability of catalyst.....	113
5.6 Conclusions .....	115
Chapter Six.....	117
Keggin type Heteropolyacid supported catalyst for hydrogenolysis of glycerol to 1-Propanol.	117
6.1 Efficient hydrogenolysis catalysts based on Keggin polyoxometalates.....	117
6.2 The effect of thermal treatment on activity and structure of 10Ni/30HSiW/Al <sub>2</sub> O <sub>3</sub> catalyst .....	126
6.3 Effect of different supports on activity of 10Ni/30HSiW supported catalyst.....	143
6.4 Conclusion.....	152
Chapter Seven .....	153
Conclusion and Recommendation .....	153
7.1 Conclusions on glycerol hydrogenolysis to 1-PO using 10Ni/30HSiW supported catalyst .....	153
7.2 Proposed reaction pathway.....	155
7.3 Recommendations .....	157
References.....	159
Appendix A Literature Data.....	177
Appendix B GC Calibration Curve.....	185
Appendix C Acid concentration calculation (mmol/g <sub>cat</sub> ).....	191
Appendix D Glycerol conversion, product selectivity and rate constant calculations .....	194
Appendix E Data of hydrogenolysis of Glycerol (some typical experiments) .....	198
Appendix F Permission to Re-print Copyrighted Material.....	202

## List of Figures

Figure 1-1 Global and United State crude glycerol production 2003–2023.....	4
Figure 1-2 Processes of catalytic conversion of glycerol into useful chemicals.....	6
Figure 1-3 Market Value of Different Value-added Products from Glycerol in 2016.....	7
Figure 2-1 Crystal structure of a typical Keggin-type heteropolyanion.....	19
Figure 2-2 Models proposed for the states of acidic protons and water in solid $H_3PW_{12}O_{40}$ .....	19
Figure 3-1 Diagram of the Catalyst Reduction Apparatus.....	29
Figure 3-2 An Autoclave Reactor System.....	29
Figure 3-3 A typical chromatogram of a GC calibration standard.....	32
Figure 3-4 Diagram of the Altamira AMI-200 Catalyst Characterization System.....	35
Figure 4-1 XRD patterns of 1 wt% metal loading on HSiW/Al <sub>2</sub> O <sub>3</sub> catalyst.....	42
Figure 4-2 XRD patterns of 1wt% and 10 wt% Ni loading on HSiW/Al <sub>2</sub> O <sub>3</sub> catalyst.....	42
Figure 4-3 NH <sub>3</sub> -TPD patterns of different metals loading on 30HSiW/Al <sub>2</sub> O <sub>3</sub> catalyst.....	43
Figure 4-4 NH <sub>3</sub> -TPD patterns of 1 wt % and 10 wt% Ni supported 30HSiW/Al <sub>2</sub> O <sub>3</sub> catalyst.....	43
Figure 4-5 Pseudo-first-order rate constants for the 10Ni/30HSiW/Al <sub>2</sub> O <sub>3</sub> catalysts using different starting material.....	47
Figure 4-6 NH <sub>3</sub> -TPD patterns for different Cs <sup>+</sup> exchanged.....	54
Figure 4-7 Effect of different Cs <sup>+</sup> content on acidity of catalyst.....	54
Figure 4-8 FT-IR spectra of 10Ni/30Cs <sub>x</sub> H <sub>4-x</sub> SiW/Al <sub>2</sub> O <sub>3</sub> .....	55
Figure 4-9 XRD patterns for the 10Ni/30Cs <sub>x</sub> H <sub>4-x</sub> SiW/Al <sub>2</sub> O <sub>3</sub> catalysts with different Cs <sup>+</sup> content.....	56
Figure 4-10 Effect of Cs <sup>+</sup> on Glycerol Hydrogenolysis and products selectivity as a function of time.....	59
Figure 5-1 Concentration profiles of different products using 10Ni/30HSiW/Al <sub>2</sub> O <sub>3</sub> catalyst reduced at 350°C.....	66
Figure 5-2 Concentration profiles of acetol, 12-PD and Acr using 10Ni/30HSiW/Al <sub>2</sub> O <sub>3</sub> catalyst reduced at 350°C.....	66
Figure 5-3 Pseudo-First-Order kinetics analyses in the presence 10Ni/30HSiW/Al <sub>2</sub> O <sub>3</sub> catalysts at different agigator speed.....	68

Figure 5-4 Effect of H <sub>2</sub> pressure on glycerol hydrogenolysis and products selectivity as a function of time.....	72
Figure 5-5 Pseudo-First-Order kinetics plots of H <sub>2</sub> pressure effect on hydrogenolysis of glycerol in the presence of 10Ni/30HSiW/Al <sub>2</sub> O <sub>3</sub> catalyst.....	74
Figure 5-6 Effect of water content on Glycerol Hydrogenolysis and product distribution.....	76
Figure 5-7 Pseudo-First-Order kinetics plots of effect of glycerol feed concentration on hydrogenolysis of glycerol in the presence of 10Ni/30HSiW/Al <sub>2</sub> O <sub>3</sub> catalyst.....	78
Figure 5-8 Effect of catalyst weight loading on Glycerol Hydrogenolysis and product distribution .....	80
Figure 5-9 Pseudo-First-Order kinetics plots of effect of catalyst weight loading on hydrogenolysis of glycerol in the presence of 10Ni/30HSiW/Al <sub>2</sub> O <sub>3</sub> catalyst.....	80
Figure 5-10 Effect of temperature on glycerol hydrogenolysis and products selectivity as a function of time.....	86
Figure 5-11 Pseudo-First-Order kinetics analyses for the 10Ni/30HSiW/Al <sub>2</sub> O <sub>3</sub> catalysts at different temperature .....	87
Figure 5-12 Calculation of the activation energy based on ln(k) and 1/T using the equation $\ln k = \ln A - E_a/R(1/T)$ .....	87
Figure 5-13 Effect of HSiW loading on Glycerol Hydrogenolysis and products selectivity as a function of time .....	91
Figure 5-14 Pseudo-First-Order kinetics plots of effect of HSiW loading on hydrogenolysis of glycerol in the presence of 10Ni/HSiW/Al <sub>2</sub> O <sub>3</sub> catalyst.....	91
Figure 5-15 NH <sub>3</sub> -TPD patterns of different HSiW loading.....	92
Figure 5-16 Effect of HSiW loading on acidity of the catalyst.....	93
Figure 5-17 XRD patterns for different HSiW loading.....	95
Figure 5-18 Effect of Ni loading on Glycerol Hydrogenolysis and products selectivity.....	97
Figure 5-19 Effect of Ni loading on glycerol hydrogenolysis and products selectivity as a function of time.....	98
Figure 5-20 Pseudo-First-Order kinetics plots of effect of Ni loading on hydrogenolysis of glycerol in the presence of Ni/30HSiW/Al <sub>2</sub> O <sub>3</sub> catalyst.....	99
Figure 5-21 NH <sub>3</sub> -TPD patterns for Ni loading.....	99

Figure 5-22 XRD patterns for different Ni loading catalyst.....	101
Figure 5-23 Effect of preparation sequence loading active components on glycerol hydrogenolysis and products selectivity as a function of time.....	104
Figure 5-24 Pseudo-First-Order kinetics plots of effect of sequence adding components on hydrogenolysis of glycerol in the presence of 10Ni/30HSiW/Al <sub>2</sub> O <sub>3</sub> catalyst.....	104
Figure 5-25 NH <sub>3</sub> -TPD patterns for method preparation.....	106
Figure 5-26 XRD patterns for method preparation.....	106
Figure 5-27 TPR patterns for sequence loading of component.....	107
Figure 5-28 Hydrogenolysis of glycerol and lower alcohols.....	108
Figure 6-1 Concentration profiles of different HPAs supported 10Ni/Al <sub>2</sub> O <sub>3</sub> catalyst at different reduction temperature at 350 and 450°C.....	120
Figure 6-2 Pseudo-First-Order kinetics plots of effect of HPAs on hydrogenolysis of glycerol in the presence of 10Ni/30HPA/Al <sub>2</sub> O <sub>3</sub> catalyst.....	121
Figure 6-3 NH <sub>3</sub> -TPD patterns for different HPAs reduced at 350 and 450°C.....	122
Figure 6-4 Total acidity amount for different HPAs reduced at 350 and 450°C.....	122
Figure 6-5 XRD patterns for different HPAs calcined at 350°C.....	125
Figure 6-6 FTIR patterns for different HPAs calcined at 350°C.....	125
Figure 6-7 Effect of calcination temperature on the conversion of glycerol and the distribution to products as a function of time .....	130
Figure 6-8 NH <sub>3</sub> -TPD patterns for catalyst calcined at different temperature.....	132
Figure 6-9 TPR patterns for catalyst calcined at different temperature.....	134
Figure 6-10 XRD signal for catalyst calcined at different temperature.....	134
Figure 6-11 FTIR signal for catalyst calcined at different temperature.....	135
Figure 6-12 Effect of reduction temperature on the conversion of glycerol and the distribution to products as a function of time.....	139
Figure 6-13 Pseudo-First-Order kinetics plots for 10Ni/30HSiW/Al <sub>2</sub> O <sub>3</sub> Catalyst reduced at different temperature.....	140
Figure 6-14 NH <sub>3</sub> -TPD patterns for catalyst reduced at different temperature.....	141

Figure 6-15 Effect of supports reduced at 350°C on the conversion of glycerol and the distribution to products as a function of time.....	146
Figure 6-16 Effect of supports reduced at 450°C on the conversion of glycerol and the distribution to products as a function of time.....	147
Figure 6-17 Effect of supports on Glycerol Hydrogenolysis and products selectivity.....	147
Figure 6-18 Pseudo-First-Order kinetic analysis of effect of support on hydrogenolysis of glycerol in the presence of 10Ni/30HSiW/Al <sub>2</sub> O <sub>3</sub> catalyst.....	148
Figure 6-19 NH <sub>3</sub> -TPD patterns for different support. ....	149
Figure 6-20 Effect of supports on total acidity and acid strength of catalyst reduced at 450°C..	150
Figure 6-21 Effect of acidity of catalyst on glycerol conversion and selectivity of products....	150
Figure 6-22 XRD patterns for different support.....	151

## List of Tables

Table 1-1 Physical properties of pure glycerol.....	3
Table 3-1 Detailed GC Method.....	31
Table 3-2 Retention Time and Response Factor for Each Compound.....	32
Table 4-1 Total acidity of catalysts.....	43
Table 4-2 Effect of metal loading on catalytic performance.....	46
Table 4-3 The hydrogenolysis of 1,2-PD, 1,3-PD and 1-PO.....	47
Table 4-4 Surface area and total acidity of 10Ni/30Cs <sub>x</sub> H <sub>4-x</sub> SiW/Al <sub>2</sub> O <sub>3</sub> catalyst.....	54
Table 4-5 Effect of Cs <sup>+</sup> on catalytic performance in the hydrogenolysis of Glycerol.....	57
Table 4-6 Effect of Cs <sup>+</sup> on catalytic performance of 30HSiW/Al <sub>2</sub> O <sub>3</sub> catalyst in the Hydrogenolysis of Glycerol.....	60
Table 5-1 Repeatability study on 10Ni/30HSiW/Al <sub>2</sub> O <sub>3</sub> catalyst.....	64
Table 5-2 Effect of agitator speed on the reaction rate and the distribution to products in the hydrogenolysis of Glycerol.....	65
Table 5-3 Effect of hydrogen pressure on the conversion of glycerol and the distribution to products in the hydrogenolysis of glycerol.....	70
Table 5-4 Effect of water content on the conversion of glycerol and the distribution to products in the hydrogenolysis of Glycerol.....	75
Table 5-5 Effect of catalyst weight loading on the conversion of glycerol and the distribution to products in the hydrogenolysis of Glycerol.....	79
Table 5-6 Effect of temperature on the conversion of glycerol and the distribution to products in the hydrogenolysis of glycerol.....	85
Table 5-7 Effect of temperature on the reaction rate of hydrogenolysis of glycerol.....	86
Table 5-8 Effect of HSiW loading on the conversion of glycerol and the distribution to products in the hydrogenolysis of Glycerol using 10Ni/Al <sub>2</sub> O <sub>3</sub> .....	89
Table 5-9 BET surface area and total acidity of different HSiW loading catalysts.....	94
Table 5-10 Effect of Ni loading on catalytic activity of the Ni/30HSiW/Al <sub>2</sub> O <sub>3</sub> .....	96
Table 5-11 BET surface are and acidities of different Ni loading catalysts.....	100

Table 5-12 Effect of different sequence loading active components on product distribution....	103
Table 5-13 Total acidity of different sequence HSiW loading catalysts.....	105
Table 5-14 Hydrogenolysis of different starting materials using 10Ni/30HSiW/Al <sub>2</sub> O <sub>3</sub> catalyst	109
Table 5-15 Continuing reaction without using 10Ni/30HSiW/Al <sub>2</sub> O <sub>3</sub> catalyst.....	113
Table 5-16 10Ni/30HSiW/Al <sub>2</sub> O <sub>3</sub> catalyst recycling study.....	114
Table 6-1 Effect of different HPAs supported 10Ni/Al <sub>2</sub> O <sub>3</sub> catalyst on the conversion of glycerol and the distribution to products in the hydrogenolysis of glycerol.....	119
Table 6-2 Effect of different HPAs supported 10Ni/Al <sub>2</sub> O <sub>3</sub> catalyst and reduction temperature on acidity and catalyst performance.....	123
Table 6-3 Effect of calcination temperature on the conversion of glycerol and the distribution to products in the hydrogenolysis of Glycerol.....	129
Table 6-4 Effect of calcination temperature on acidity of 10Ni/30HSiW/Al <sub>2</sub> O <sub>3</sub> catalyst.....	132
Table 6-5 Effect of reduction temperature on the conversion of glycerol and the distribution to products in the hydrogenolysis of Glycerol.....	138
Table 6-6 Effect of reduced temperature on acidity of 10Ni/30HSiW/Al <sub>2</sub> O <sub>3</sub> catalyst.....	142
Table 6-7 Effect of support on the conversion of glycerol and the distribution to products in the hydrogenolysis of Glycerol.....	145
Table 6-8 Surface area and acidities of 10Ni/30HSiW supported catalysts.....	149



## Nomenclature

1,2-PD = 1,2-propanediol

1,3-PD = 1,3-propanediol

1-PO = 1-propanol

3-HPA= 3-Hydroxypropionaldehyde

Acr = Acrolein

BET = Brunauer–Emmett–Teller

EG = Ethylene Glycol

FID = Flame Ionization Detector

FTIR = Fourier Transform Infrared Spectroscopy

GC = Gas Chromatography

GHG = Greenhouse Gas

HPAs = Heteropolyacids

HPMo = Phosphomolybdic acid

HPW= Phosphotungstic acid

HSiW = Silicotungstic acid

IMP = Impregnation

LD50 = Lethal Dose 50%

LDLO = Lethal Dose Low

PTFE = Polytetrafluoroethylene

RPM = Round per Minute

TCD = Thermal Conductive Detector

TGA = Thermal Gravimetric Analysis

TPD = Temperature Programmed Desorption

TPR = Temperature Programmed Reduction

wt% = weight percent

XRD = X-Ray Diffraction

# Chapter One

## General of Background

### 1.1 Introduction

Fossil oil is still the main source not only for energy but also for most of the chemical products used by modern society, including plastics, rubber, perfumes, and pharmaceuticals. Energy is essential not only in the industrial sector but also important over all aspects of society. The chemical industry is a cornerstone of human development that influences all aspects of modern society.

As a source of energy, fossil fuel is non-renewable, produces the pollutants that causes huge environmental issues and it is not easy to solve. It is important to use other alternative resources effectively, bring down the reliance on fossil feedstocks and the environmental influence of the production methods and products [1-3]. The foreseen depletion of petroleum together with an increased public concern on environmental issues and global climate change has increased the interest in the replacement of fossil-based chemicals by biomass-based chemicals [4]. It has motivated many researchers to focus on the conversion of fossil fuels to alternative sources of renewable energy and shift the petroleum-based society to green, environmentally friendly society.

In view of the fossil-based issues, the idea of green chemistry was developed [5]: “the chemical industry needs to be designed in the way that can minimize or eliminate the utilization and generation of polluted and toxic substances”. In addition, the use of catalysts, which are selective and recyclable, is one of the important principles of green chemistry.

Several substantial actions can be applied to utilize and modify renewable sources that could have an enormous influence on human activities. Such implementation can exist in different industries such as energy, polymer, textile, pharmaceutical, paints and coatings, food etc [4]. Essentially, they have given rise to a key research area for the replacement of fossil-based raw materials by biomass. Recently glycerol has emerged as a potential alternative to fossil-based raw materials and “glycerchemistry” [6, 7] has become an important developing sector that comprises replacing petroleum-based resources with glycerol as a bio feedstock in the chemical, solvent and fuel

industries [8]. Glycerol, also called 1, 2, 3-propanetriol, is a simple sugar alcohol with three hydroxyl groups. Generally, Glycerol can be obtained either as a by-product from fermentation or as a by-product in biodiesel production. Glycerol is considered by the US Department of Energy as one of the 12 building block chemicals obtained from biomass that can be utilized to produce other high value biomass-based chemicals [9]. Glycerol could be used to produce many valuable products via oxidation, esterification, hydrogenolysis and others [6]. Upgrading the value of glycerol will reduce the cost of biodiesel production and help the biodiesel industry.

For a successful bio-based economy, development of biomass-based chemicals and green catalyst will be important in order to convert to a limited number of building blocks to a range of secondary products for different applications [10, 1]. In the context of this thesis, glycerol was used as raw material for C3 platform chemicals such as 1,2-PD, 1,3-PD and 1-PO.

## **1.2 Glycerol production and markets**

Glycerol is a three carbon polyol which is hygroscopic, colorless, odorless viscous liquid under atmospheric condition. It is sweet tasting in its pure form and low toxicity. Glycerol finds a range of applications in industry and commerce such as: food industries, pharmaceuticals, personal cares, plasticizers, tobacco, emulsifiers, antifreeze and so on. It is also a very important raw material to produce many other chemicals [11]. Some physical characteristics of this compound are listed in Table 1-1.

Glycerol that is currently available on the market can be obtained by the chemical conversion of propylene (synthetic glycerol - 10% of the market) or from oleochemical industry especially as a main by-product in biodiesel production (bio-glycerol - 90 % of the market) [11, 12]. Biodiesel is produced from renewable sources, together with its biodegradability and non-toxic nature has become one of the most promising fuels for the future. The major co-product of this process is a glycerol. For every 9 kg of biodiesel produced approximately 1 kg of glycerol is produced as a byproduct [13]. A recent surge in the production of biodiesel has created a glut in the glycerol market. As a result, the value of both crude and refined glycerol has in general decreased over the years. Dow Chemical in Freeport Texas is the only supplier of synthetic glycerol in the US. However, the flood of biodiesel-derived glycerol causes this plant to close in January 2006 [14].

**Table 1-1** Physical properties of pure glycerol [11]

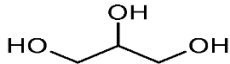
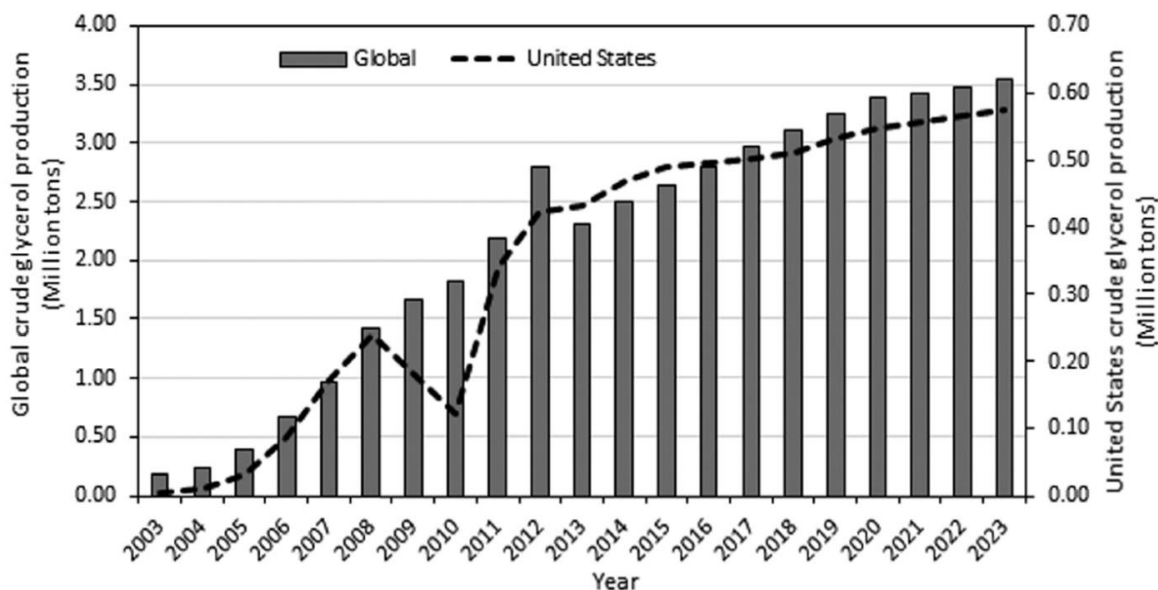
Chemical Structure	
Chemical Formula	$C_3H_8O_3$
Molecular Mass	$92.09 \text{ g}\cdot\text{mol}^{-1}$
Density (at 20 °C)	$1.261 \text{ g}\cdot\text{cm}^{-3}$
Caloric Value	$18 \text{ kJ}\cdot\text{g}^{-1}$
Melting Point	$18.0 \text{ }^\circ\text{C}$
Boiling Point (at 101.9 kPa)	$290.0 \text{ }^\circ\text{C}$
Electrical Conductivity (at 20 °C)	$0.1 \mu\text{S}\cdot\text{cm}^{-1}$

Fig. 1-1 shows a forecast of the crude glycerol production from the biodiesel industry in the United States and other countries in the last ten years and for the next ten years. A fast increase of glycerol production results in a saturation of the market causing prices of crude glycerol and refined glycerol to drop. The price of refined glycerol varied from \$0.2 to \$0.7/kg and crude glycerol from \$0.04/kg to \$0.33/kg over the past few years in the global market [15]. A flood in the glycerol market has established [16].

It has been proposed that once the glycerol price drops below US\$ 0.23 per kg it would open up the possibility of using glycerol as a biorefinery feedstock chemical [17]. Prior to the large scale production of biodiesel, the use of glycerol from biodiesel for this purpose was rarely investigated. However, as a large amount of crude glycerol is formed in biodiesel plants followed by a drop in the price of crude glycerol makes glycerol a valuable by-product which could be purified and sold to increase the profitability of the overall process [18].



**Figure 1-1** Global and United State crude glycerol production 2003–2023 [7]\*

\*Reprinted from Ye X. P. et al., ACS Symposium Series; American Chemical Society: Washington, DC, 2014, Chapter 3, pp. 43–80 with permission from ACS Publications

### 1.3 Glycerol as a platform chemical

Platform chemicals are substances with functional groups and are used as building blocks that can be converted to a wide range of chemicals or materials. Bio-based platform chemicals that are biodegradable provide a great opportunity for decarbonising everyday products and makes society more environmentally friendly [19]. Production and conversion of bio-derived platform chemicals is a very promising approach to provide a sustainable market and reduction of biofuel production cost [1, 20]. Glycerol is a polyol molecule rich in functionalities, unique structure, biocompatibility and biodegradability [21] which could become one of the most important platform chemicals for the biobased chemical industry [19]. Glycerol is considered by the US Department of Energy as one of the 12 building block chemicals obtained from biomass that can be utilized to produce other high value biomass-based chemicals [9].

These days, due to government policies to encourage the utilization of renewable resources and to fulfill the rising energy demand, biodiesel production has rapidly increased. The expansion of biodiesel production makes glycerol readily available and in large supply. The conversion of glycerol into other chemicals creates new opportunities for utilizing glycerol as the crude material [17]. Furthermore sustaining a good price for glycerol can boost other industries like biodiesel

which is struggling to gain a foothold. As a result upgrading the value of glycerol will reduce the cost of biodiesel production and help the biodiesel industry. Significant research has been focused recently on its conversion to value-added chemicals as a bio platform chemical to replace mainstream petroleum derived chemicals [17, 21, 22]. There are several chemicals which can be obtained from the hydrogenolysis of glycerol that have higher value than glycerol such as 1,2-propanediol (1,2-PD), 1,3-propanediol (1,3-PD) and 1-propanol (1-PO).

#### **1.4 Converting glycerol into value-added products**

Utilization of glycerol derived from the growing biodiesel industry is important to oleochemical industries [23]. In the past, the high value of glycerol made it economically unattractive as a feedstock chemical and the improvement of alternative processes for glycerol utilization is not properly considered [16]. Recently, an increase in glycerol supply and a drop in the price of crude glycerol make glycerol an important building block for the production of a variety of bio-based chemicals. Biodiesel, designated to be a future alternative fuel, produces crude glycerol as a waste byproduct. The conversion of this crude glycerol to value added products is a sustainable approach compared to petroleum-based products. Besides, upgrading of crude glycerol to value added products affects a substantial effect on the economy of the biodiesel sector. Over the past decades significant research efforts have been focused on the conversion of glycerol as a low-cost feedstock to other valuable chemicals and products. Because of the high functionality of glycerol (two primary and one secondary hydroxyl group), reactions can proceed along multiple reaction pathways to give mixtures of products. Several good review articles on glycerol conversion to value-added chemicals and products have been published. In 2008 Zhou C. H. et al. showed from a technical standpoint several different reaction pathways to produce other chemicals from glycerol (Fig. 1-2) [24].

In 2008 Pagliaro et al., recapped 22 different possible approaches that can be used to obtain different valuable products from glycerol and their industrial applications [25]. In 2015 Bagheri et. al. reviewed and highlighted many possible processes for the catalytic conversion of glycerol into useful chemicals [6]. Various reactions that are available to derive value added chemicals of commercial interest from glycerol such as hydrogenolysis of glycerol to propanediols, dehydration of glycerol into acrolein, steam reforming of glycerol to produce hydrogen were reported

[16,24,26,27]. Among the approaches hydrogenolysis of glycerol into lower alcohols have been reported as promising processes and can produce higher value products such as 1,2-propanediol

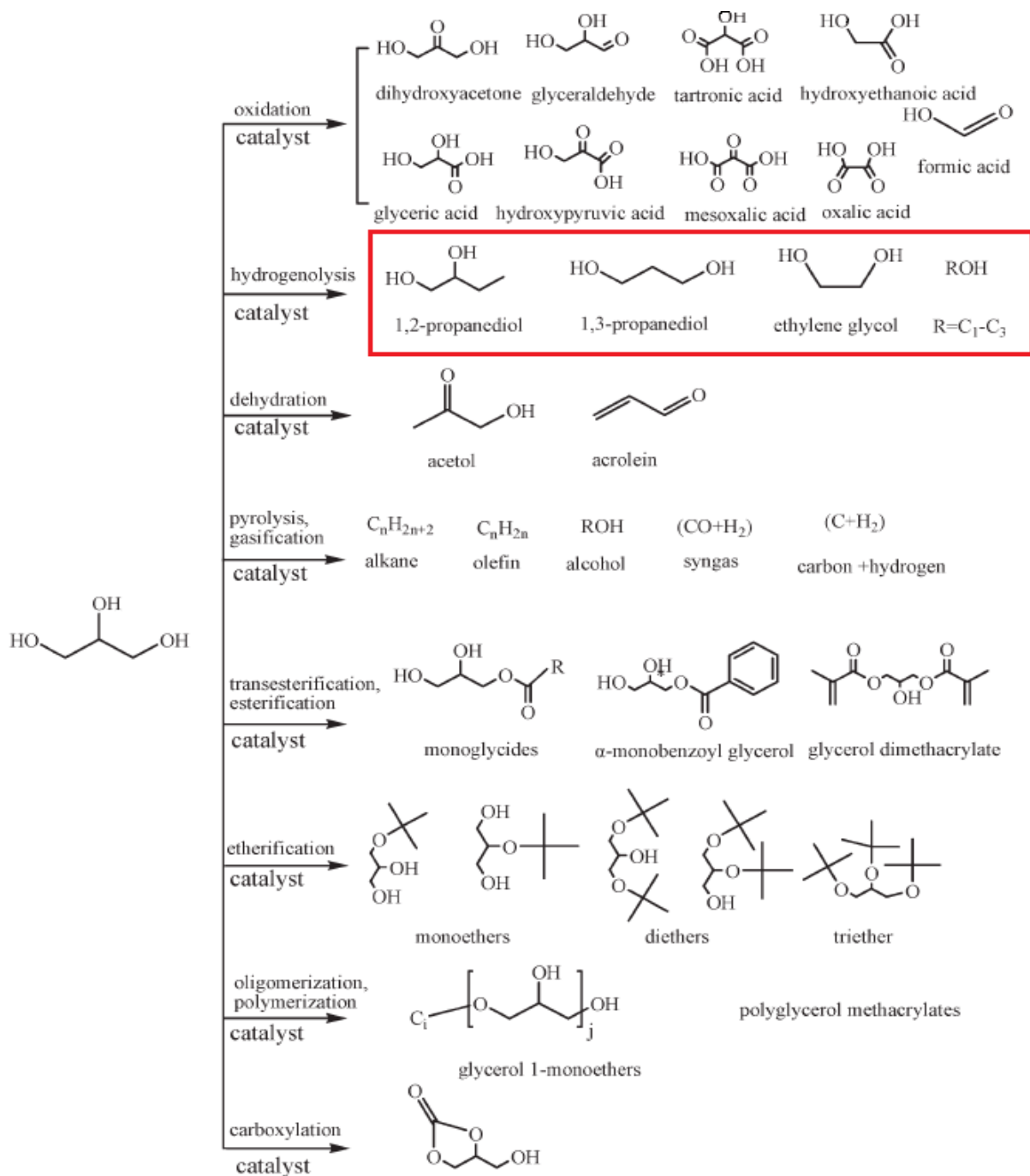


**Figure 1-2** Processes of catalytic conversion of glycerol into useful chemicals [24]\*

\*Reprinted from Zhou C.H. et al., Chemical Society Reviews, 2008, 37, pp. 527–549 with permission from the Royal Society of Chemistry

(1,2-PD), 1,3-propanediol (1,3-PD), and 1-propanol (1-PO). 1,2-PD is used primarily for commodity chemicals and is a green replacement for the toxic ethylene glycol for deicing aircraft. 1,3-PD is a valuable intermediate for the production of high value polymers such as polyester and polyurethane resins. 1-PO is useful as a solvent, organic intermediate and could be dehydrated to produce “green“ propylene for the production of polypropylene. The market value of these chemicals is shown in Fig. 1-3 [28a].

It is clear that 1,3-PD is the most valuable product among these alcohols, followed by 1-PO and 1,2-PD. Thus far, the most effective way to produce 1,3-PD is through fermentation [28b]; however, the low metabolic efficiency and poor compatibility with existing chemical plants make it less favorable. In recent year the glycerol hydrogenolysis of glycerol to 1,3-PD has been intensively developed; however, the selectivity of glycerol conversion to 1,3-PD is still limited. Selective hydrogenolysis of glycerol into 1,3-PD is much more challenging compared with the production of 1,2-PD or lower alcohols. The production of 1,2-PD has been studied extensively since a high yield of 1,2-PD can be obtained under mild reaction conditions [29]. From an industrial point of view, the production of 1-PO is also very interesting since it finds many applications as an important industrial intermediate; however, the production of 1-PO from glycerol has not received much attention. Therefore, the development of a new process for the efficient conversion of glycerol into propanediols and 1-PO will contribute to new “green” chemicals which will benefit the environment and make the biodiesel process more profitable. Until now among these alcohols only the product of 1,2-PD has been commercialized so there is a huge opportunity for the development of new process for 1-PO.

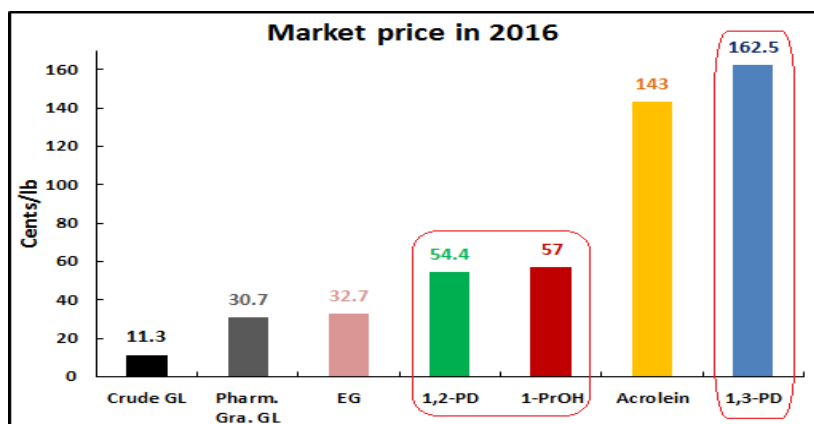


**Figure 1-3** The market value of different value-added products from glycerol in 2016 [28a]



## **1.5 Uses of 1,2-Propanediol, 1,3- Propanediol and 1-Propanol**

### **1.5.1 1,2-Propanediol**

1,2-propanediol (1,2-PD) which is a clear colorless viscous liquid is an important medium-value commodity chemical having a wide range of applications. It is used for making polyester resins, liquid detergents, pharmaceuticals, cosmetics, tobacco humectants, flavor and fragrance agents, personal care items, paints, animal feed, antifreeze compounds, etc. There has been a rapid expansion of the market for 1,2-PD as antifreeze as a de-icing agent due to the growing concern over the toxicity of ethylene glycol based products to humans and animals. 1,2-PD is conventionally produced by the hydration of propylene oxide [12]. The process based on a glycerol feedstock has been recognized as an economically, environmentally and sustainable method compared with the commercial petroleum-based route.

### **1.5.2 1,3-Propanediol**

1,3-propanediol (1,3-PD) which is a colorless liquid with a freezing point of  $-24^{\circ}\text{C}$  and a boiling point of  $214^{\circ}\text{C}$  has many uses. 1,3-PD is generally used as an industrial building block for producing polymers and composite materials; it is especially used as a monomer in the synthesis for new types of polyesters such as polytrimethylene and terephthalate. It has also found an application as a chemical intermediate in the manufacture of cosmetics, medicines and heterocyclic compounds [30]. Many products that may also contain 1,3-PD include adhesives, sealants, laminates, coatings, paints, perfumes, fragrances, personal care products and laboratory scale chemicals [31]. One of the most successful applications of 1,3-PD is the formulation of corterra polymers [32]. Industrial production of 1,3-PD is currently based on petroleum by hydroformylation of ethylene oxide or hydration of Acrolein [33]. As petroleum feedstocks become more limited and costs become higher, glycerol as a bio-feedstock has become a more attractive feedstock for 1,3-PD production. The production of 1,3-PD from bio-based glycerol has the potential to become an alternative for current industrial production based on petroleum feedstocks. Bio-derived 1,3-PD not only offers good market opportunities but also provides a cost effective method for its production. Many research groups have worked on the selective hydrogenolysis of glycerol to 1,3-PD; however, selective production of 1,3-PD from biomass-derived glycerol is still a challenge.

### 1.5.3 1-Propanol

1-Propanol (1-PO) which is a highly flammable, volatile, clear, colorless liquid with an alcohol-like, sweet and pleasant odor [33] is a major component of resins and is used as a solvent in the pharmaceutical, paint, cosmetics and cellulose ester industries [34,35]. Production and uses of 1-PO are associated with its transformation into related compounds such as propionic acid, propionaldehyde and trihydroxymethyl ethane, all of which are important chemical commodities. It also finds applications in the manufacture of flexographic printing ink and textiles [36,37], as a dispersing agent for cleaning preparations and floor wax, metal degreasing fluids, adhesives[38], a chemical intermediate in the manufacture of other chemicals[39]. More recently, it is being used as a hand disinfectant by health care workers. Besides its industrial uses, 1-PO is added to foods and beverages as a flavor (IPCS 1990). 1-PO can be esterified to yield diesel fuels and be dehydrated to yield propylene, which is currently derived from petroleum as a monomer for making polypropylene [40]. In addition, like the more familiar aliphatic alcohols of methanol, ethanol and butanol, 1-PO is considered as a potential high-energy biofuel. The use of 1-propanol recently has shown potential as the next-generation gasoline to petroleum substitute [35] which has promoted interest in its production. 1-PO is considered to be a better biofuel than ethanol since it has advantages over ethanol in terms of higher octane number, tends to have a higher energy content, lower hygroscopicity, water solubility, energy density, combustion efficiency, storage convenience. It is compatible with existing transportation infrastructures and pipelines [41] and is suitable for engine fuel usage [42]. However, the production of propanol is more difficult than that of other alcohols so up until now it has been too expensive to be a common fuel. In the petrochemical industry, 1-PO is currently produced via hydroformylation of ethylene to form propanal followed by hydrogenation to 1-PO [43]. It can also be recovered commercially as a by-product via the high pressure synthesis of methanol from carbon monoxide and hydrogen or by the vapor-phase oxidation of propane and from the reduction of propene-derived Acrolein. 1-PO recently has been obtained from glycerol by conversion of glycerol to 1,2-PD first, with 1,2-PD being subsequently converted to 1-PO [44-46]. In comparison with the process based on petroleum-derived ethylene, propylene, the production of 1-PO based on bio-based glycerol would be preferential in terms of sustainability and environmental efficiency.

## 1.6 Research objective

Selective conversion of glycerol to green valueable chemicals such as 1,3-PD, 1,2-PD and 1-PO is promising. In recent years, although significant work has been done towards glycerol hydrogenolysis to propanediols, the one-pot hydrogenolysis of glycerol to 1-PO has received limited attention. Therefore, the main focus of the research is to develop a selective catalyst for the hydrogenolysis of glycerol to green sustainable chemicals, especially the one pot synthesis of 1-PO. The hydrogenolysis of glycerol requires an acidic site for dehydration and a metal site for hydrogenation. HPAs are well known to be green, active catalysts for many of homogeneous and heterogeneous acid catalyzed reactions, in particular alcohol dehydration. Hence it is chosen as an acidic component for this research. The much lower price of Ni compared to noble metals is very attractive for a hydrogenation. This research work is devoted to the glycerol hydrogenolysis with the development of catalysts for the one-pot catalytic transformation of glycerol to high value-added chemicals over a Ni-based HSiW supported catalysts in a water media. Replacement of homogeneous hazardous catalyst by using as a solid, green catalyst, the use of water as green, cheap solvent will enable a greener chemical process. To my knowledge, this is the first time a bi-functional catalyst of Ni and HSiW supported on Al<sub>2</sub>O<sub>3</sub> was successfully prepared and used for the one-pot production of 1-PO from glycerol in water media using a batch reactor.

Although HPAs have high acidity and high catalytic activity, the high solubility in polar solvents such as water, the low surface area and the tendency to lose active sites and deactivation under thermal treatments leads to limitation their application. Therefore the effect of the thermal treatment on the stability and product selectivity in the glycerol hydrogenolysis is emphasized. The addition of Cs<sup>+</sup> to the catalyst was also explored since Cs<sup>+</sup> is known to modify the acidity of the HPAs. The effect of oxide supports for the HPAs was also explored as the supports could affect the surface area and the acidity of the catalysts. The catalyst development work for the research project are elaborated in the following 3 projects described below.

In the first project, a 10Ni/30HSiW/Al<sub>2</sub>O<sub>3</sub> catalyst (loaded with 10 wt% Ni and 30 wt% on Al<sub>2</sub>O<sub>3</sub>) was prepared and used for the hydrogenolysis of glycerol to lower alcohols such as 1,2-PD, 1,3-PD and 1-PO using a stainless steel batch reactor. The effect of different metals such as Pd, Pt and Cu on the catalyst activity was studied. Since a balance of metal and acidity can improve the performance of catalyst, Cs<sup>+</sup> was used to tune the acidity of the catalyst.

In the second project, the effect of different process parameters such as catalyst loading, H<sub>2</sub> pressure, glycerol and water concentration, temperature on the glycerol conversion and product selectivity were investigated. Some chemicals, notably acids, can affect the the surface of stainless steel reactor. Since a supported strong acid, HPA, was part of the catalyst used for the research, a Hastelloy reactor was used for the investigation of the effect of process parameters on the catalytic performance of the 10Ni/30HSiW/Al<sub>2</sub>O<sub>3</sub> catalyst.

In the third project, the affect of different factors on the properties of the heteropolyacids itself such as different Keggin type heteropolyaids, the thermal treatment and the support were investigated.

Various characterization techniques such as BET, XRD, TPR, TPD, TGA and FTIR were used to characterize the catalysts. The properties of the catalysts were used to explain the reactivity of the catalysts for the conversion and selectivities between the catalyst structure and the catalytic performance. A reaction pathway for the hydrogenolysis of glycerol to various products was proposed.

Finally, conclusions are drawn and recommendations are given for future work based on the results of these studies.

## Chapter Two

### Literature Review

#### 2.1 Introduction

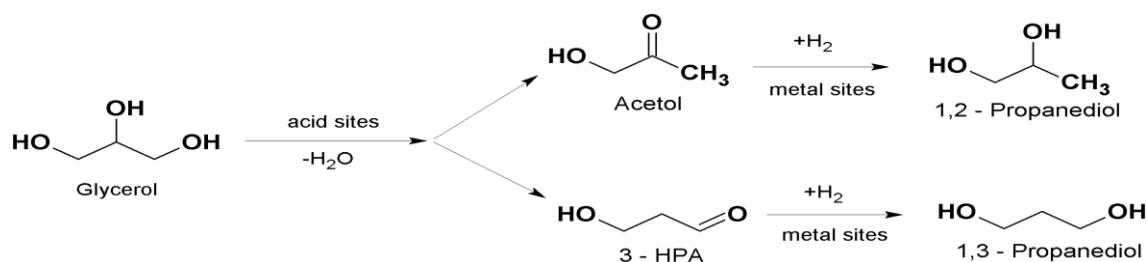
The excess of waste glycerol produced in the biodiesel industry may be used for the production of value-added chemicals to avoid waste disposal and increase process economy. Various reactions are available to derive value added chemicals of commercial interest from glycerol. Because of the high functionality of glycerol (two primary and one secondary hydroxyl groups), reactions can proceed along multiple reaction pathways to give mixtures of products. Therefore, careful development of catalysts and reaction conditions is of great importance to selectively obtain the desired products. The biodiesel industry currently regards glycerol as a waste by-product; however, with novel methods glycerol has the potential to be converted into other valuable products. Some of these value-added products are 1,2-PD, 1,3-PD and 1-PO. A literature review on reaction mechanism, hydrogenolysis of glycerol into these value-added chemicals using different catalysts is discussed in this section.

#### 2.2 Reaction mechanism for the heterogeneous hydrogenolysis of glycerol to lower alcohols

It is proposed that the hydrogenolysis of glycerol occurs via several parallel and consecutive reaction pathways, leading to a range of products such as 1,2-PD, 1,3-PD, 1-PO, 2-propanol, EG, lactic acid, ethanol, methanol. Therefore, it is a great challenge to design catalysts that can give a high yield of the desired products, especially 1,3-PD. In order to develop efficient catalysts, it is of great importance to understand the reaction mechanism since it can help to design further new catalysts and provide information for process optimization.

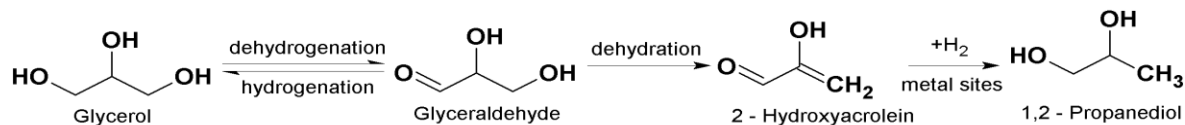
According to previous studies, there are some possible mechanisms for the production of lower alcohols such as 1,2-PD, 1,3-PD and 1-PO. The production of 1,2-PD or 1,3-PD was intensively studied and some possible pathways were proposed: the dehydration – hydrogenation mechanism and the dehydrogenation – dehydration – hydrogenation mechanism. In addition, the direct hydrogenolysis mechanism, the chelation – hydrogenolysis mechanism and the etherification –

hydrogenation mechanism have also been proposed. The dehydration – hydrogenation mechanism involves the dehydration of glycerol to acetol or 3-hydroxypropionaldehyde (3-HPA) and subsequent hydrogenation of these aldehydes to 1,2-PD or 1,3-PD (Scheme 2-1). The dehydration – hydrogenation pathway is usually feasible under acidic conditions where acid sites exist in the catalytic system [47-51]. The dehydration step occurs at the acid sites, and the hydrogenation step is catalyzed by the metal. According to this mechanism, most previous studies show that the reaction favors the formation of 1,2-PD. It was shown that generally the tungsten component is necessary to promote the selectivity to 1,3-PD since it is probably beneficial to induce Brønsted acid sites that can cleave the secondary – OH group in glycerol.



**Scheme 2-1** Dehydration – hydrogenation mechanism for the hydrogenolysis of glycerol [48]

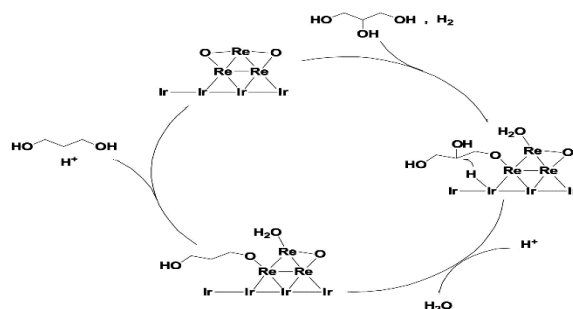
While the dehydration – hydrogenation mechanism is usually feasible in the presence of acid sites, the dehydrogenation – dehydration – hydrogenation mechanism (Scheme 2-2) is more dominant when the glycerol hydrogenolysis reaction is performed under basic conditions. The metal catalyst serves both dehydrogenating and hydrogenating functions in the total reaction process. It has been pointed out by Feng et. al. [52] that the production of 1,3-PD seems to be very difficult under basic conditions.



**Scheme 2-2** Dehydrogenation – dehydration – hydrogenation mechanism for the hydrogenolysis of glycerol to 1,2-PD [52]

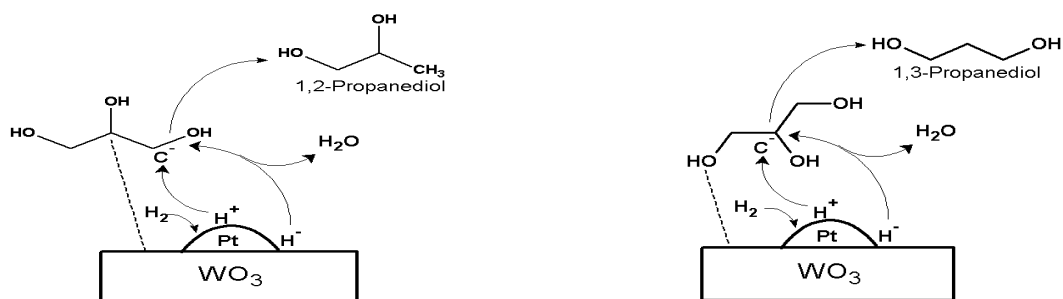
Tomishige et al. developed a metal – acid bifunctional catalyst system, which exhibited good performance for the hydrogenolysis of glycerol [47, 50]. He proposed that the mechanism of

glycerol hydrogenolysis using Rh–MO<sub>x</sub>/SiO<sub>2</sub> and Ir–MO<sub>x</sub>/SiO<sub>2</sub> (M = Re, Mo or W) catalysts [49, 51, 53]. A model of the transition state in the glycerol hydrogenolysis to 1,3-PD using Ir – ReO<sub>x</sub>/SiO<sub>2</sub> is shown in Scheme 2-3. First, glycerol is adsorbed on the surface of a ReO<sub>x</sub> cluster at the CH<sub>2</sub>OH group to form a terminal alkoxide. Meanwhile, hydrogen is activated on the Ir surface to form a hydride species. Next, the alkoxide located at the interface between ReO<sub>x</sub> and the Ir surface is attacked by the hydride species, and the OH<sup>-</sup> groups in the alkoxide are eliminated by releasing a water molecule. Finally, the hydrolysis of the reduced alkoxide gives the diol products.



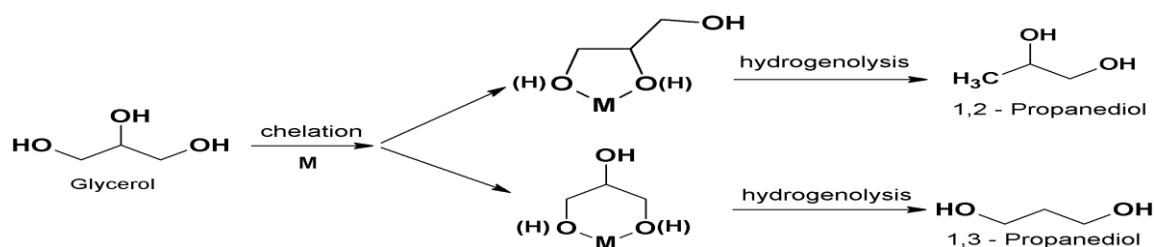
**Scheme 2-3** Direct hydrogenolysis mechanism for the hydrogenolysis of glycerol to 1,3-PD over Ir-ReO<sub>x</sub>/SiO<sub>2</sub> catalyst [51]

Besides the direct reaction mechanism, Qin et al. [54] and Liu et al. [55] proposed a different direct hydrogenolysis mechanism using WO<sub>x</sub>-supported Pt catalysts. This direct hydrogenolysis mechanism is distinguished by the heterolytic cleavage of hydrogen molecules to protons (H<sup>+</sup>) and hydrides (H<sup>-</sup>) at the interface of WO<sub>x</sub> and Pt. The strong interaction between Pt and WO<sub>x</sub> facilitates the heterolytic dissociation of hydrogen molecules. The proton formed will attack the primary or the secondary OH<sup>-</sup> group in the glycerol molecule by a protonation – dehydration, and form an intermediate oxocarbenium ion(I) or oxocarbenium ion(II), which is subsequently attacked by a proton (H<sup>+</sup>) to form 1,2-PD or 1,3-PD, respectively (Scheme 2-4).



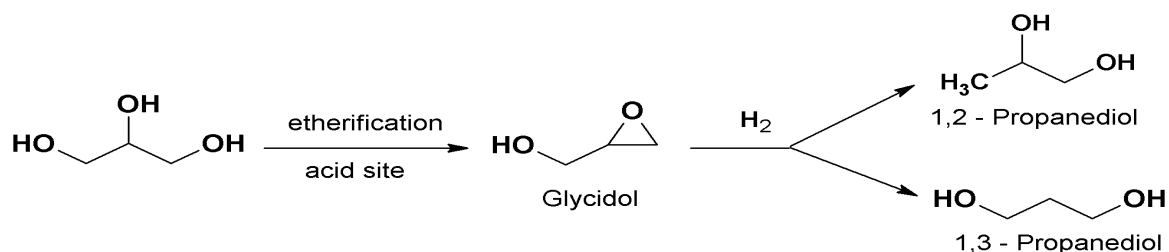
**Scheme 2-4** Direct hydrogenolysis mechanism for the hydrogenolysis of glycerol to Propanediols over Pt/WO<sub>x</sub> catalyst [54,55]

Chaminand et al. in 2004 [56] proposed a chelation – hydrogenolysis mechanism. It is suggested that the active metals (M) can be chelated by two hydroxyl groups from the glycerol molecule and thus modify the selectivity of the hydrogenolysis reaction. While 1,2-PD can be obtained via a 5-membered-ring chelation transition state, 1,3-PD can be obtained via a 6-membered-ring chelation transition state (Scheme 2-5).



**Scheme 2-5** Chelation – hydrogenolysis mechanism [56]

Wang et al. has proposed glycidol as an intermediate from the glycerol dehydration on acid sites. Using Cu-based catalysts Wang et al. [57] and Huang et al. [58] discovered evidence for the formation of glycidol (3-hydroxy-1,2-epoxypropane). Therefore, Feng et al. [52] proposed an etherification – hydrogenation mechanism for the hydrogenolysis of glycerol to propanediols. As shown in Scheme 2-6, glycidol is formed by the intramolecular etherification of two adjacent OH<sup>-</sup> groups in the glycerol molecule. Hydrogenation of glycidol via a ring-opening reaction can produce propanediols.

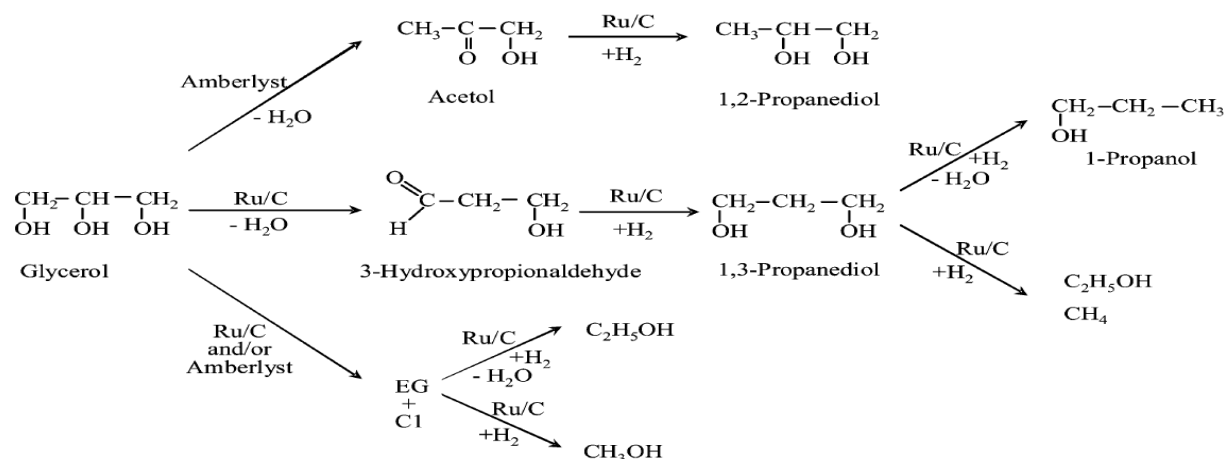


**Scheme 2-6** Etherification – hydrogenation mechanism [52]

1-Propanol (1-PO) is another valuable chemical produced from the hydrogenolysis of glycerol; however, the direct conversion of glycerol to 1-PO remains essentially unexplored. Some possible ways for the conversion of glycerol to 1-PO have been proposed through either propanediols or acrolein as an intermediate: further hydrogenolysis of propanediols or hydrogenation of acrolein.



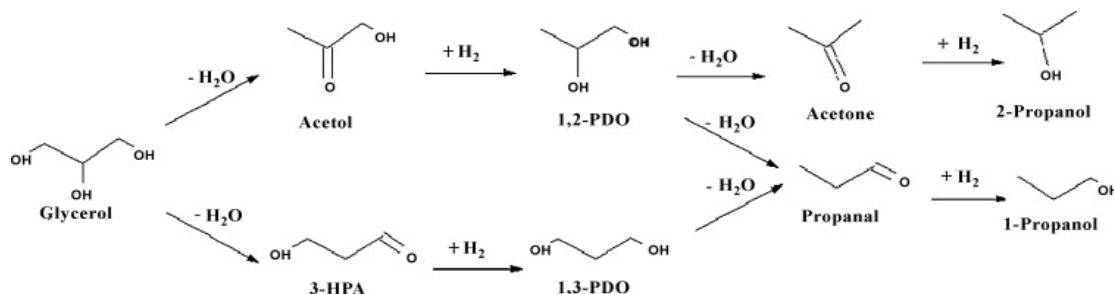
Miyazawa et al., [59] studied the reaction scheme of glycerol hydrogenolysis and degradation over Ru/C + Amberlyst and Ru/C catalyst in the aqueous solution. It is assumed that 1-PO is formed via 1,3-PD (Scheme 2-7).



**Scheme 2-7** Reaction scheme of glycerol hydrogenolysis and degradation reactions [59]\*

\*Reprinted from Miyazawa T. et al., J. Catal., 2006, 240, 213–221 with permission from Elsevier

Gandarias et. al., [50] proposed the hydrogenolysis of glycerol over Pt supported on an amorphous silica-alumina (Pt/ASA) (Scheme 2-8): glycerol is first dehydrated to either acetol or 3-HPA which is hydrogenated to 1,2-PD or 1,3-PD respectively with further hydrogenolysis of 1,2-PD or 1,3-PO to form 1-PO.

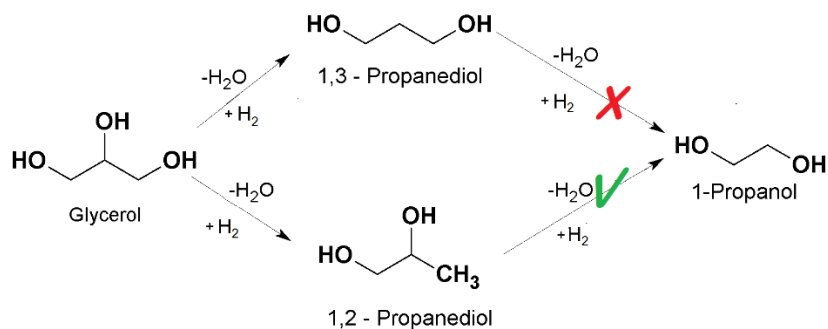


**Scheme 2-8** The hydrogenolysis of glycerol over Pt supported on an amorphous silica–alumina (Pt/ASA) [50]

Lin et. al. [60] used a sequential zeolitic packing and a Ni based catalysts as two-layer catalysts in a fixed-bed reactor to study the hydrogenolysis of glycerol and indicated most of 1-the PO in the products was generated from glycerol via a “sequential two-time dehydration-hydrogenation”

mechanism, with most of 1-PO coming from the hydrogenation of acrolein that was produced from the two-time dehydration of glycerol. Using sequential two-layer catalysts (zirconium phosphate layer was packed in the upper layer, the supported Ru catalysts were in the second layer) in a continuous-flow fixed-bed reactor for the conversion of glycerol to 1-PO, Wang et. al. [61] proposed the possible reaction route involved in glycerol hydrogenolysis. It was found that the two sequential-layers catalyst system can convert glycerol to 1-PO at complete glycerol conversion by a dehydration–hydrogenation route, where ZrP converted glycerol into acrolein while Ru/SiO<sub>2</sub> catalyst transformed acrolein into 1-PO.

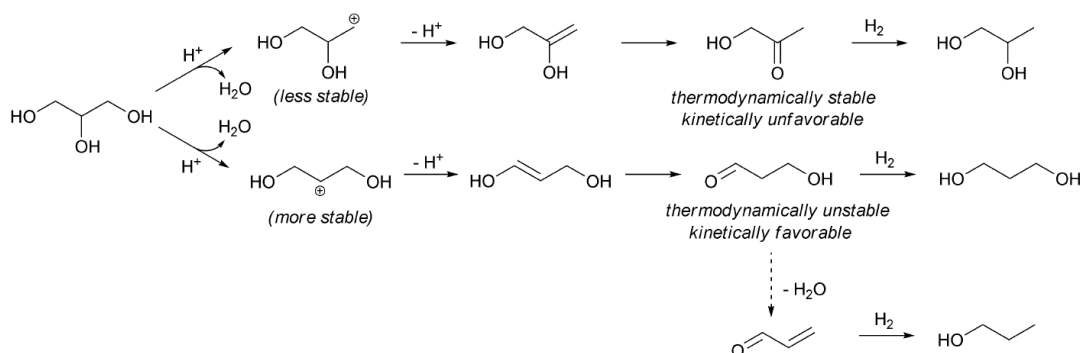
Yu et al., investigated the hydrogenolysis of glycerol to 1-PO in aqueous solutions using the catalyst of Ir/ZrO<sub>2</sub> [62] and confirmed in two separate experiments that the formation of 1-PO directly from 1,2-PD occurred at a considerably higher rate than that from 1,3-PD, and verified that 1-PO was mainly produced by the formation of 1,2-PD as an intermediate during the reaction. This pathway was also proposed by Sun et al. [81b] when they studied vapor-phase catalytic conversion of glycerol into propylene over WO<sub>3</sub>/Cu/Al<sub>2</sub>O<sub>3</sub> catalyst (Scheme 2-9).



**Scheme 2-9** Proposed reaction routes involved in glycerol hydrogenolysis over Ir/ZrO<sub>2</sub> catalyst [63]

Nakagawa Y. et al., [64] explained the formation of 1-PO using the metal–acid bifunctional catalyst system where the acid function plays a role in the dehydration reaction and the metal catalyzes the hydrogenation reaction (Scheme 2-10). It is assumed that the protonation of the secondary OH in glycerol and subsequent dehydration produces a more stable cationic intermediate than the protonation of terminal OH produces. The deprotonation of the cationic intermediates produces more 3-hydroxypropanal than acetol, although thermodynamically 3-

hydroxypropanal is less stable than acetol. The subsequent dehydration of 3-hydroxypropanal produces acrolein and finally 1-PO.



**Scheme 2-10** Elementary reactions in the dehydration of glycerol [64]\*

\*Reprinted from Nakagawa Y. et al., *Catal. Sci. Technol.*, 2011, 1, 179–190 with permission from the Royal Society of Chemistry

An enormous number of catalysts have been reported for the conversion of glycerol to lower alcohols. In this section, the literature reporting different types of catalyst are reviewed. The reported experimental results are listed in Table A in Appendix A.

## 2.3 Heteropolyacids

Heteropolyacids (HPAs) present several advantages as catalysts that make them economically and environmentally attractive [65, 66]. HPAs are very strong Brønsted acids, stronger than common inorganic acids (HCl, H<sub>2</sub>SO<sub>4</sub>...) and are even sometimes classified as super acids [50]. Moreover their acid–base and redox properties can be tuned by modifying their compositions. With a strong Brønsted character, approaching the superacidic region, HPAs represent a potential alternative to other acid systems and become the most interesting ones from a catalysis and industrial point of view.

Among the HPAs, the best known of these structures is the Keggin–type heteropolyacids. The Keggin–type heteropolyacids typically represented by the formula XM<sub>12</sub>O<sub>40</sub><sup>n-</sup> where X is the central atom or heteroatom, M (with M=W, Mo, V..) is the addenda atom and X (with X=P, Si, Ge or As) is the charge of the heteropoly anion itself (Fig. 1-4). The acidity of the HPAs strongly depends on the nature of the addenda atoms. The Brønsted acidity strongly decreases with the loss of constitutional water because all the residual protons are then localized (Fig. 1-5). The exchange

of the protons of the heteropoly acid by cations results in a decreased number of Brønsted acid sites. One important drawback of Keggin-type HPAs is their low specific surface area, a disadvantage which can be overcome by dispersing the HPAs on high surface area supports. The thermal stability is also influenced by the interaction between the heteropolyacids and the carrier substrate [67-69]. When using supported heteropoly acids, the acidity also depends on the support due to electro-static interactions.

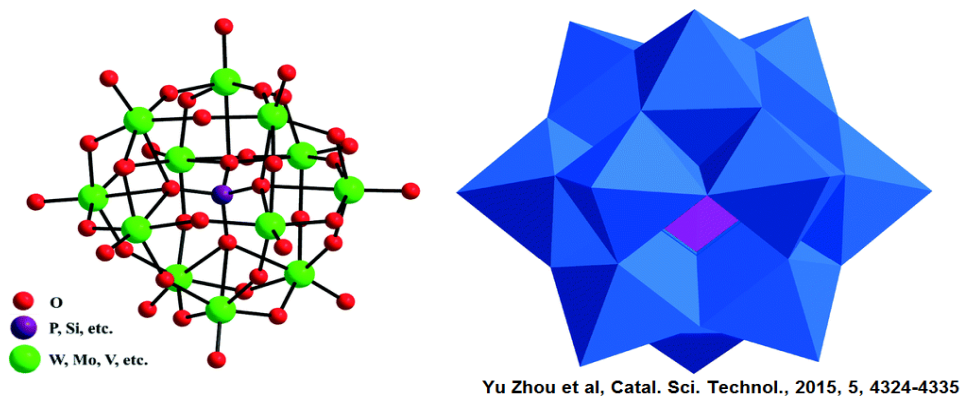


**Figure 2-1** Crystal structure of a typical Keggin-type heteropolyanion. (left) Ball-and-stick model; (right) polyhedral model [70] \*

\*Reprinted from Zhou Y. et al, Catal. Sci. Technol., 2015, 5, 4324-4335 with permission from the Royal Society of Chemistry

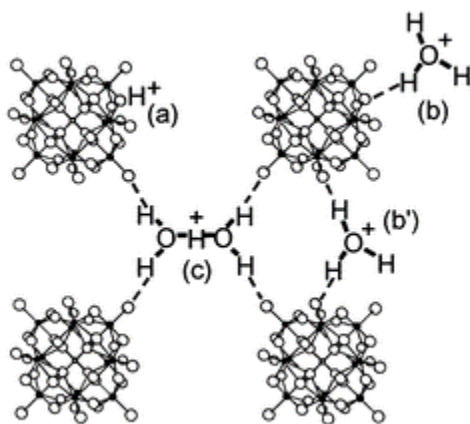


**Figure 2-2** Models proposed for the states of acidic protons and water in solid H<sub>3</sub>PW<sub>12</sub>O<sub>40</sub> [71]\*

\*Reprinted from Misono M., Chem. Commun., 2001, 1141–1152 with permission from the Royal Society of Chemistry

Although HPAs have good thermal stability in the solid state, better than other strong acids like ion exchange resins [65], the tendency to decompose the Keggin structure under thermal treatments always leads to the loss of active sites and deactivation [72-75]. Several ways of enhancement of the stability of the HPAs have been investigated. One way consists in the aforementioned exchange of addenda metal atoms. The second way consists of the preparation of HPA salts, which are known to be more stable than their parent acid due to the reduced number of protons needed in the final decomposition step of the HPA. Some studies were focused on the influence of the support on the thermal stability of the HPA. Apparently, Lewis acid supports (e.g. alumina, zirconia) increase the thermal stability of the HPA by electrostatic interactions [76]. Therefore, the properties of HPAs can be tuned via the proper selection of the central atom, the addenda atom, the counter-cations and the support to make the catalysts feasible.

## **2.4 Catalyst for production of 1,3-Propanediol from glycerol**

Several patents and papers have disclosed 1,3-PD production by the catalytic hydrogenolysis of glycerol in the presence of homogeneous or heterogeneous catalysts. In this section the available literature on the heterogeneous catalysts used for production of 1,3-PD from glycerol is presented.

### **2.4.1 Promoting effect of Tungsten-added catalysts in the generation of Brønsted acid**

Several research groups have pointed out the importance of Brønsted acid sites in 1,3-PD formation and it has been found that the 1,3-PD yield is approximately proportional to the concentration of the Brønsted acid sites since the Brønsted acid sites favor the removal of the secondary hydroxyl group of glycerol to 3-hydroxypropionaldehyde, which subsequently is hydrogenated by mainly Platinum to form 1,3-PD [77-87].

It is reported that Tungsten (W) compounds are widely used in various industrial processes such as oxidations, acid–base reactions, and photocatalytic reactions. The acidity of W oxide species has been proposed as playing a key role in the selective production of 1,3-PD [77,54,56,82,88]. It was found that H atom spillover onto the  $WO_x$  species forming  $W^{6-n}O_x-(nH^+)$  as Brønsted acid centers under the reaction conditions.  $H_2$  can restore the Brønsted acid sites by reduction of  $WO_x$  species or by formation of acidic  $H_xWO_3$  species. H atoms formed by  $H_2$  dissociation become involved not only in desorption of adsorbed intermediates, but also in the generation and maintenance of the Brønsted acid sites [83, 89, 90, 91]. In 2010 Gong et al. [82] prepared  $SiO_2$ -

supported Pt/WO<sub>3</sub>/TiO<sub>2</sub> catalysts. It was found that the main role of WO<sub>3</sub> is to regulate acidity of the catalyst by introducing Brønsted acid sites, which were shown to be essential for 1,3-PD formation. The optimal loadings of Ti and W as oxides were 10% and 5%, respectively, and the glycerol conversion and 1,3-PD selectivity reached 15.3% and 50.5%, respectively.

Heteropolyacids (HPAs) that possess unique properties such as Brønsted acidity, uniform acid sites and easily tunable acidity [92-94] compared to conventional solid acid catalysts such as oxides or zeolites make them economically, environmentally attractive [65,66]. Moreover their acid–base and redox properties can be tuned by modifying their compositions. HPAs have found many applications in the field of catalysis and the best known of these structures is the Keggin–type heteropolyacids. Among the HPAs, silicotungstic acid (HSiW) has been intensively investigated for the conversion of glycerol to propanediols since in the presence of water, HSiW having a lower oxidation potential and higher hydrolytic stability, is superior to other HPAs as a catalyst in a water medium [95]. HSiW is reported to be responsible for inducing the presence of Brønsted acid sites [77,96,97]. In 2012 Zhu et. al. [77] reported that supporting HSiW on Pt/SiO<sub>2</sub> has increased the acid sites, especially Brønsted acid sites and it is obvious that Brønsted acid sites are indispensable in order to produce 1,3-PD selectively. With the optimized catalyst of Pt-HSiW/SiO<sub>2</sub> and optimized conditions, glycerol conversion and 1,3-PD selectivity reached 81.2% and 38.7%, respectively for reactions carried out in an aqueous phase. In 2013, Zhang et. al. [83] developed a new method to synthesize mesoporous Ti–W oxides and investigated how tungsten oxide species affect catalyst texture. It was reported that the presence of strong Brønsted acid sites was suggested to be responsible for the superior performance for selective hydrogenolysis of glycerol to 1,3-PD. The excellent performance was attributed to the presence of a large amount of acid sites; in particular the Brønsted acid site. The catalyst 2Pt/Ti<sub>90</sub>W<sub>10</sub> exhibited high selectivity to 1,3-PD of 40.3% and promising catalytic activities (18.4% glycerol conversion) at 180°C, 5.5 MPA of hydrogen. In 2013 Zhu. Et. al. [79] carried out the hydrogenolysis of glycerol over zirconia supported bifunctional catalysts containing Pt and HPAs. Among the tested supported HPAs catalysts, HSiW exhibited superior performance. Addition of HSiW to Pt/ZrO<sub>2</sub> catalysts improved the catalytic activity (24.1% conversion) and 1,3-PD selectivity (48.1%) remarkably because of the enhanced Brønsted acid. In the same year Zhu et. al. [86] reported that addition of alkaline metals Li, K, Rb and Cs was a powerful approach to tune the acidic property of HSiW in terms of

Brønsted acid sites and Lewis acid sites and to control the catalytic performance in glycerol hydrogenolysis.

## **2.4.2 Noble metal based catalysts**

Since hydrogenolysis uses hydrogen as a reactant for the hydrogenation, the hydrogenolysis catalyst must have an ability to activate hydrogen molecules. Noble metals are well known to be able to activate hydrogen molecules and are widely used in hydrogenation catalysts.

### **2.4.2.1 Rh based catalyst**

Supported Rh catalysts show some activity in the reforming of aqueous glycerol to 1,3-PD. In 2004, Chaminad et al. [56] showed that when using a catalyst of Rh/C with a H<sub>2</sub>WO<sub>4</sub> additive the selectivity to 1,3-PD was 12% at 32% conversion after 168h and 1,3-PD/1,2-PD molar ratio of 2 from a sulfolane solution of glycerol at a temperature of 453K and pressure of 8 MPa hydrogen. In 2005, Kusunoki et al. [47] also reported that the addition of H<sub>2</sub>WO<sub>4</sub> to Rh/C enhanced the glycerol conversion and the selectivity to 1,3-PD, however, the activity was not so high. The selectivity to 1,3-PD was 20.9% at a conversion of 1.3% using 20w% glycerol aqueous, and initial H<sub>2</sub> pressure 8.0 MPa at 453K. In 2006, Miyazawa et. al. [59] tested the activity over M/C and M/C + Amberlyst catalysts (M = Pt, Rh, Pd, and Ru) for the reaction of glycerol. Among these catalyst, Rh-based + Amberlyst catalyst gave the highest selectivity to 1,3-PD of 9% at a conversion of 3% under the condition of 393K and 8MPa hydrogen. In 2007, Furikado et al. [48] compared the activity of various supported noble-metal catalysts (Rh, Ru, Pt and Pd over C, SiO<sub>2</sub> and Al<sub>2</sub>O<sub>3</sub>) for the hydrogenolysis of aqueous glycerol at a much lower temperature of 393K. Among the catalysts tested, Rh/SiO<sub>2</sub> gave the highest glycerol conversion and selectivity to 1,3-PD (7.2% and 7.9% respectively).

### **2.4.2.2 Pt based catalyst**

Supported Pt catalysts are some of the most active supported catalyst for the hydrogenolysis of glycerol to 1,3-PD and have been intensively studied by many researchers for the reforming of glycerol to 1,3-PD. In 2010 Gandarias et al. [50] reported the hydrogenolysis of aqueous glycerol over a platinum catalyst supported on acidic amorphous silica-alumina. At 493K and 4,5 MPa H<sub>2</sub> pressure, the selectivity to 1,3-PD was 4.5% at a conversion of 19.8%. In 2010, Qin et al. [54]

applied Pt/WO<sub>3</sub>/ZrO<sub>2</sub> catalysts for the hydrogenolysis of aqueous glycerol. Both the amounts of W and Pt greatly affected the performance. The highest activity was 46% for 1,3-PD selectivity and 72% of the glycerol conversion was obtained with the catalyst of 3w%Pt and 10w%W. In 2011, Oh et. al. [84] reported very selective 1,3-PD formation using a Pt sulfated zirconia. Using this catalyst under the condition of 443K for 24h with an initial H<sub>2</sub> pressure of 7.3 MPa, an 84% 1,3-PD selectivity was observed at 66.5% glycerol conversion in 1,3-dimethyl-2-imidazolidinone (DMI) solvent. In 2012, Mizugaki et. al. [98] investigated the addition effect of a secondary metal on a Pt/WO<sub>3</sub> catalyst. Among the additive metals tested (Al, V, Cr, Mn, Fe, Zn, Ga, Zr, Mo and Re), Al showed the best effect in performance for glycerol hydrogenolysis to 1,3-PD (44% selectivity at 90% conversion after 10h at 453K and 3MPa hydrogen in water without any additives). It was suggested that the positive effect of Al was related to the high performance of Pt–W catalysts on the Al-based supports. In 2013, Dam et al. [99] tested the effect of various tungsten-based additives for glycerol hydrogenolysis over commercial catalysts (Pd/SiO<sub>2</sub>, Pd/Al<sub>2</sub>O<sub>3</sub>, Pt/SiO<sub>2</sub> and Pt/Al<sub>2</sub>O<sub>3</sub>) in water at 473K. The highest conversion and selectivity (49% conversion, 28% selectivity) to 1,3-PD was achieved by using a Pt/Al<sub>2</sub>O<sub>3</sub> + HSiW catalyst at 473K and 4MPa hydrogen after 18 hours. In 2013, Arundhathi et. al. [100] reported a very good result using Pt/WO<sub>x</sub> on a boehmite (AlOOH) support. The 1,3-PD yield reached 66–69% after 12h at 453K and 5MPa hydrogen from aqueous glycerol and these values are the highest reported up until now. In 2013, Delgado [101] studied the influence of the nature of the support on the catalytic properties of Pt-based catalysts for the hydrogenolysis of glycerol. It was found that 1,3-PD is formed only under H<sub>2</sub> and should be produced from 3-HPA hydrogenation; the aldehyde being easily hydrogenated and never observed under their experimental conditions. It is important to mention that a noticeable formation of H<sub>2</sub> occurred under a N<sub>2</sub> atmosphere, providing aqueous phase reforming of glycerol on the Pt sites. Although titania is the best catalyst for the production of 1,2-PD under the reaction conditions studied, alumina is the most active catalyst for the production of 1,3-PD under a hydrogen atmosphere. It has been reported that under N<sub>2</sub>, the alumina supported catalyst yielded the highest amount of H<sub>2</sub>, and this catalyst can also give the most 1,3-PD under H<sub>2</sub> (at a conversion of 10%, the selectivity was 12.1%). Longjie et. al. [55] prepared a Pt catalyst supported on mesoporous WO<sub>3</sub> which gave 39.3% of 1,3-PD selectivity at 18% conversion. The activity and selectivity were much higher than those of Pt/commercial WO<sub>3</sub> catalysts (29.9% selectivity and 4.5% conversion). In 2013 Zhu et. al. [78] reported that catalysis



of 2Pt–15HSiW/ZrO<sub>2</sub> for glycerol hydrogenolysis. Although this study focused on the production of propanols, good 1,3-PD selectivity was obtained (~40% selectivity at ~60% conversion at 433K, 5MPa, 10wt% of aqueous glycerol). In 2014 the same group [102] prepared a series of SiO<sub>2</sub> modified Pt/WO<sub>x</sub>/ZrO<sub>2</sub> catalysts with various SiO<sub>2</sub> content for glycerol hydrogenolysis to improve 1,3-PD selectivity. Among them, the 5PtW/ZrSi catalyst showed superior activity and provided maximum 1,3-PD selectivity, of up to 52.0% at a conversion of 54.3% at 180°C, 5.0 MPa. Pt–HSiW/ZrO<sub>2</sub> was further improved by modification with alkali metals (Li, K, Rb and Cs) [79]. Among them, Pt–LiHSiW/ZrO<sub>2</sub> showed a higher activity and 1,3-PD selectivity than the unmodified catalyst, attaining 43.5% conversion and 53.6% 1,3-PD selectivity at 453K. In 2014, Deng et al. [103] investigated the particle size effect of a series of carbon nanotubes (CNTs) supported Pt-Re bimetallic catalysts for glycerol hydrogenolysis. It was found that the scission of the secondary C–O bond of glycerol was favored over larger sized Pt-Re/CNTs catalysts, leading to the formation of 1,3-PD. Under a temperature of 170°C and 4 MPA hydrogen, after 8 hours, the conversion was 20% and the selectivity to 1,3-PD was 13%.

#### **2.4.2.3 Ru based catalyst**

In comparison to Pt and Rh, Ru added catalysts are less active for the conversion of glycerol to 1,3-PD. In 2014, Vanama P.K., et al. [104] reported on the catalytic behavior of Ru/MCM-41 catalysts for the hydrogenolysis of glycerol in the vapor phase at 230°C. It was found that the conversion of glycerol was 62% and the selectivity to 1,3-PD was 20% with a ruthenium loading of 3 wt%.

#### **2.4.2.4 Non-noble metal based catalysts**

For the hydrogenolysis of glycerol to 1,3-PD; since 3-HPA is an unstable intermediate that easily further dehydrates to acrolein it is often preferred to use noble metals for the hydrogenation of 3-HPA to 1,3-PD. Non-noble metals are rarely used for the hydrogenolysis of glycerol to 1,3-PD and there are only a few papers that have been published on this topic. In 2009 Huang L. et al. [105] prepared a Cu–HSiW/SiO<sub>2</sub> catalyst and applied it for the vapor-phase hydrogenolysis of glycerol. At optimum conditions (483K, 0.54 MPa H<sub>2</sub>, without water), conversion and 1,3-PD selectivity reached 83.4% and 32.1%, respectively. It was found that the presence of water decreased both the activity and 1,3-PD selectivity of the Cu–HSiW/SiO<sub>2</sub> catalyst. In 2011, Feng

et. al. [106] studied the gas phase hydrogenolysis of glycerol using a series of Cu/ZnO/MO<sub>x</sub> catalysts (MO<sub>x</sub>=Al<sub>2</sub>O<sub>3</sub>, TiO<sub>2</sub>, and ZrO<sub>2</sub>) at 240–300°C under 0.1MPa of H<sub>2</sub>. The Cu/ZnO/TiO<sub>2</sub> catalyst favored the formation of 1,3-PD with a maximum selectivity of 10% at a high reaction temperature of 280°C. The results showed that the selectivity to 1,3-PD increased with increasing reaction temperature. It was suggested that the weak acid sites favor the dehydration of glycerol to 3-hydroxypropanal (3-HPA), resulting in the formation of 1,3-PD and the strong acid sites favor the dehydration of glycerol to hydroxyacetone, which can be hydrogenated to 1,2-PD. More reported numerical results regarding this process are listed in Table A-2 in Appendix A.

## 2.5 Catalysts for production of 1-Propanol from glycerol

The initial goal of the present work was the investigation and development of heterogeneous catalysts for the hydrogenolysis reaction of glycerol to 1,3-PD. During the development, a catalyst was discovered surprisingly to catalyze the reaction with high yield of 1-PO from glycerol. 1-PO was identified as a side product during the overhydrogenolysis reaction of glycerol to diols and so far not much work has been carried out on this topic. In 2007 Furikado et al. [48] achieved high selectivity of 41.3% to 1-PO over Rh/SiO<sub>2</sub> at 120°C and 8.0 MPa in the presence of Amberlyst during glycerol hydrogenolysis. In 2008 Kurosaka et al. [88] reported a significant amount of 1-PO (28% yield) was formed using Pt/WO<sub>3</sub>/ZrO<sub>2</sub> in 1,3-dimethyl-2-imidazolidinone at 130°C and 4.0 MPa hydrogen; probably because of the severe reaction conditions employed. In 2010 Quin L.Z. et al. [54] reported that a 56.2% yield of 1-PO was obtained in a fixed bed reactor using the catalyst 4.0Pt/WZ10 (containing 10 wt% tungsten and calcined at 700°C) at 130°C and 4 MPa H<sub>2</sub>. It was assumed that the production of 1-PO could increase if the reaction pressure and calcination temperature were increased. The deoxygenation of glycerol is proposed to occur by an ionic mechanism, involving proton transfer and hydride transfer steps. The excess amount of protons and hydride ions may enhance the consecutive deoxygenation of propanediols to propanols. In 2010, 2011 Tomishige et al. [53, 107] reported that 1-PO can be obtained with a yield of 20.72% and 23.9% respectively by using Ir/SiO<sub>2</sub> modified with a Re species and sulfuric acid additive at 120°C and 8MPa hydrogen. In 2011 Thibault et al. [108] obtained a 18% yield to 1-PO from glycerol hydrogenolysis at 200°C and 3.45 MPa hydrogen using a homogenous Ru complex and methane sulfonic acid in a water–sulfolane mixed solvent. In 2011, Ryneveld et. al. [75] reported that a 42.8% yield of 1-PO could be obtained for the conversion of glycerol using commercial

Ni/SiO<sub>2</sub> catalysts at 320°C and 6MPa hydrogen. In 2012, Zhu et. al. [77] obtained a 32.7% yield of 1-PO in the hydrogenolysis of glycerol to 1,3-PD over Pt-HSiW/SiO<sub>2</sub> at 200°C and 5MPa hydrogen. It was found that the selectivity of 1-PO increased linearly with increasing temperature as the higher temperature facilitated the overhydrogenolysis of propanediols. Following this paper, in the same year Zhu S. published a paper on the one-step hydrogenolysis of glycerol to biopropanols using Pt-HSiW/ZrO<sub>2</sub> catalysts providing a high yield of 1-PO and 2-PO at 200°C and 5MPa (80% yield). It was found that with respect to the selectivity, the increase of hydrogen pressure favored the sequential hydrogenolysis of propanediols to produce propanols. Using Ni instead of Pt, Zhu et. al. reported that the yield of 1-PO was rather low, only 4% [78]. Generally, the catalysts that are effective for the selective hydrogenolysis of glycerol to 1,3-PD have a potential for the production of 1-PO from glycerol. However, these systems need a high pressure of hydrogen and Rh-based or Pt based catalysts are expensive. Although Ni, a nonprecious metal can also be used for hydrogenation reactions [75, 109-112], the use of supported Ni catalysts for the chemical transformation of glycerol to 1,3-PD and 1-PO has appeared less frequently in the literature and the yield of 1-PO is still low even under severe reaction conditions.

The 1-PO is usually a by-product of glycerol hydrogenolysis to 1,2-PD and 1,3-PD and the yield of 1-PO is rather low. Recently there are a few reports on the conversion of glycerol-derived propanediols to 1-PO; however; not much research has been done on the conversion of glycerol to 1-PO directly. In 2010 Amada Y et al reported that using RhReO<sub>x</sub>/SiO<sub>2</sub> (Re/Rh ¼ 0.5) catalyst can obtain high yields of 1-PO (66%) by the hydrogenolysis of 1,2-PD at 393 K and 8.0 MPa initial H<sub>2</sub> pressure [45]. In 2014 Peng et. al reported a process for the conversion of 1,2-PD to 1-PO over a ZrNbO catalyst with the selectivity to propanol reaching approximately 39% at 85.0% 1,2-PD conversion at 290°C under 1 atm N<sub>2</sub>; the weak Brønsted acid sites may play a crucial role in the conversion of 1,2-PD to 1-PO [113]. In an attempt to elucidate the role of propanediols as the intermediates to 1-PO in the hydrogenolysis of glycerol Ryneveld et. al. found that using Ni/Al<sub>2</sub>O<sub>3</sub> and Ni/SiO<sub>2</sub> catalysts in the hydrogenolysis of 1,3-PD, 1-PO was produced as the main product [30]. Recently, the sequential two-layer catalysts for the hydrogenolysis of glycerol in continuous-flow fixed-bed reactor was studied for the production of 1-PO but the selectivity to 1-PO is still low with maximum selectivity at 69% [60, 61, 63]. More reported numerical results regarding this process are listed in Table A-3 in Appendix A.

## Chapter Three

### Experimental Apparatus and Methods

In this chapter, the procedure of catalyst preparation and loading of different composition are introduced. The analytical methods employed in this work are outlined including the quantitative analysis of liquid products by gas chromatography. The specifications of the batch autoclave reaction for glycerol hydrogenolysis to produce lower alcohol and the procedures of liquid sampling are explained. The detailed catalyst characterization techniques are described including temperature programmed desorption (TPD), X-Ray diffraction (XRD), Thermogravimetric analysis (TGA), BET surface area and Fourier Transform InfraRed spectroscopy (FTIR).

#### 3.1 Materials

Glycerol ( $\geq 99.5\%$ ), 1,2-Propanediol ( $\geq 98\%$ ), 1,3-Propanediol (99%), and 1-Propanol (anhydrous 99.7%) were obtained from Sigma-Aldrich. Ni(II) nitrate hexahydrate ( $\text{Ni}(\text{NO}_3)_2 \cdot 6\text{H}_2\text{O}$ , crystalline,  $\geq 99.0\%$ ), Copper(II) nitrate hemi (pentahydrate) ( $\text{Cu}(\text{NO}_3)_2 \cdot 2.5\text{H}_2\text{O}$ ,  $\geq 98.0\%$ ), Platinum chloride ( $\text{H}_2\text{PtCl}_6 \cdot 6\text{H}_2\text{O}$ ), Palladium acetate ( $\text{Pd}(\text{OAc})_2$ ,  $\geq 98\%$ ), aluminum oxide (corundum,  $\alpha\text{-Al}_2\text{O}_3$ , 99%, 100 mesh) and Tungstosilicic acid hydrate ( $\text{H}_4\text{SiW}_{12}\text{O}_{40} \cdot n\text{H}_2\text{O}$ , anhydrous basis) were purchased from Sigma-Aldrich, Canada. High purity grade hydrogen and nitrogen were purchased from Praxair Canada and were used directly from the cylinders.

#### 3.2 Catalyst Preparation Methods

In this section, the procedures of preparing catalysts via different preparation methods including the methods of loading different promoters are introduced.

##### 3.2.1 The preparation of metal heteropolyacids supported catalyst by impregnation

Different metals and supports of the HPAs catalysts were prepared by the incipient wetness impregnation method similar to that previously described [104]. The catalyst support was impregnated with a desired amount of HPAs aqueous solution by slowly adding small quantities of the HPAs solution to a well stirred weighed amount of support at room temperature. The mixture was blended well to ensure the support remained dry throughout the solution addition process

(until all the desired amount of HPAs is impregnated). Then the powder was dried at 393 K overnight and calcined at 623K for 5 h in air. The HPAs/support samples obtained were further impregnated with an aqueous solution of the metal precursor following: the same procedure as the previous step to obtain an appropriate amount of metal loading. After drying at 393 K, the samples were calcined in air at 623K for 5 h. The catalysts are labelled as xM/yHPAs /support, where x, y represents the nominal weight loading of metal and HPAs respectively. Before carrying out an experiment the catalyst was reduced in hydrogen for 5 hours.

### **3.2.2 Loading Cs on 10Ni/30HSiW/Al<sub>2</sub>O<sub>3</sub> catalysts by ion-exchanged method**

The 10Ni/30Cs<sub>x</sub>H<sub>4-x</sub>SiW/Al<sub>2</sub>O<sub>3</sub> catalysts were prepared via ion exchange. A set of cesium-exchanged HSiWs were prepared by an ion-exchange method with a variation of cesium content. A known amount of cesium chloride (CsCl, Sigma-Aldrich) was dissolved in distilled water then the desired amount of 10Ni/30HSiW/Al<sub>2</sub>O<sub>3</sub> was added to this solution and aged for 4 hours without mixing. After that, the round bottle with the aged solution was evaporated on an oil bath at 70°C until the solvent evaporated completely. Then the catalyst was dried in an oven at 110°C overnight. Finally, it was calcined at 350°C for 5 h to yield the 10Ni/30Cs<sub>x</sub>H<sub>4-x</sub>SiW/Al<sub>2</sub>O<sub>3</sub>.

## **3.3 Autoclave Experimental Apparatus**

In this section, the experimental apparatus for the experiments carried out in an autoclave are introduced including the catalyst reduction and reaction systems.

### **3.3.1 Catalyst reduction apparatus**

Before each experiment was carried out, the catalyst was reduced in a quartz tubular reactor. The reactor is enclosed by a furnace controlled by a temperature controller as shown in Fig. 3-1. The pre-weighed catalyst particles were placed on a catalyst bed made from quartz in the tubular reactor and the reactor was placed into the furnace; a thermocouple was placed into the tube below the catalyst bed. The reactor was heated to the designated temperature under a continuous high purity helium flow. After the temperature was reached, the three-way valve was adjusted to let a continuous high purity hydrogen gas flow upward through the catalyst bed for 5 hours. Then the furnace was turn off and the catalyst particles were cooled to room temperature under a helium flow.

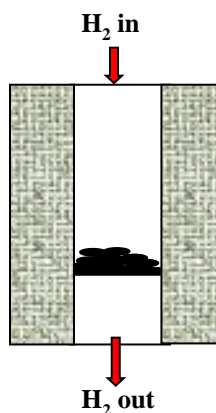


**Figure 3-1** Diagram of the catalyst reduction apparatus

### 3.3.2 Autoclave apparatus

Two mini bench top reactors made of two different materials which as illustrated in Fig. 3-2 were used for the catalyst activity tests in this thesis. One is a 300ml Parr Instrument 4182 Series constructed of Stainless Steel T316 and another is a 300mL Parr Instrument 4560 Series constructed of hastelloy. The reactors are sealed with a PTFE O-ring seal. The maximum operating conditions were rated to be 360°C and 3000PSI. An impeller was connected to a magnetic drive for mixing. The reactor temperature was monitored with a thermocouple and the temperature was controlled by a Parr Instrument 4848 Series (for hastelloy reactor) and Parr Instrument 4842 Series (for Stainless Steel T316) reactor controller. Over-pressure protection was provided by a rupture disk made from Au and rated to fail at 2500 psi purchased from Fike Corp. A sampler was equipped for taking liquid samples at different time intervals during the reaction.

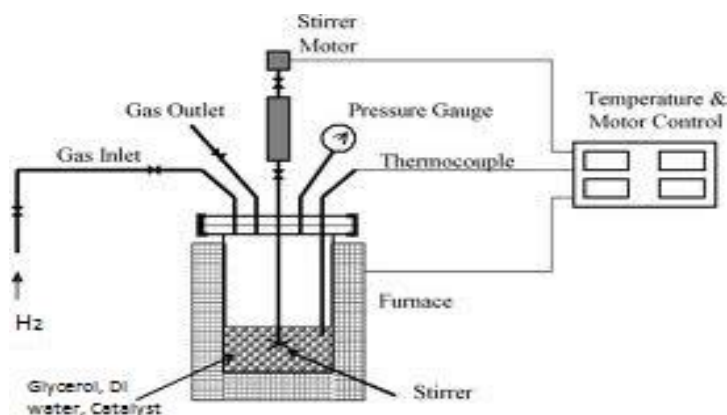


**Figure 3-2** An autoclave reactor system

### 3.4 Products Analytical Apparatus and Method

In this section, the apparatus for products analysis and the mathematic analytical method are introduced.

#### 3.4.1 Gas Chromatography (GC)

Reaction product samples were taken at different time intervals during the reaction, cooled to room temperature, and were firstly centrifuged using an IEC CL31 multispeed centrifuge purchased from Thermo Electron Corp. at 8000RPM for 10 minutes to separate the large catalyst particles from the liquid product samples. Then the centrifuged liquid samples were filtered through a polyethersulfone syringe membrane with 0.2 $\mu$ m pore size to further separate the fine particles remaining in the liquid samples. These samples were analyzed by an Agilent Technologies 6890N Gas Chromatograph equipped with a flame ionization detector (FID). All the samples were injected automatically by an Agilent Technologies 7863 Series auto-injector with a 5 $\mu$ L syringe. A J&W Scientific DB-WAX megabore capillary column (30m x 0.53mm I.D. x 10 $\mu$ m film thickness) was used for separation of different species. The GC method parameters were list in Table 3-1.

A solution of 1-butanol with a known amount of internal standard was prepared a priori and used for analysis. 1,4-butanediol was chosen as the internal standard since it is not one of the product species and it exhibits similar properties to the components because it contains two hydroxyl groups. An internal standard solution was prepared by adding 5g of 1,4-butanediol into 1L of 1-butanol. The standards were purchased from Sigma Aldridge Co. Canada. Before the experimental samples were injected into the GC, a calibration for each sample standard was carried out. The samples were prepared for analysis by adding around 120 mg of product sample to 1 mL of prepared solution in a 2 mL glass vial. A 1  $\mu$ L portion of the sample was injected into the column. Fig. 3-3 depicts of chromatogram of one calibration standard with all possible products, the species in an unknown sample can be determined based on the retention time of standards as listed in Table 3-2.

Using the standard calibration curves that were prepared for all the components, the integrated areas were converted to weight percentages for each component present in the sample. For each data point, the theoretical selectivity of products was calculated.

**Table 3-1** Detailed GC method

Inlet	Volume Injected	1 $\mu$ L
	Inlet Temperature	300 °C
	Carrier Gas	He
	Inlet Pressure	5 psi
	Total Flow	100 mL/min
Oven Temperature Profile	Initial Temperature	100 °C
	Hold	2 min
	Ramp1	10°C /min to 133 °C
	Ramp2	1°C /min to 143 °C
	Ramp3	10°C /min to 200 °C
	Hold	15 min
FID Detector	Detector Temperature	300 °C
	H <sub>2</sub> Flow	40 mL/min
	Air Flow	450 mL/min
	Makeup Gas	He
	Makeup Flow	45 mL/min

A multiple-point internal standard method was used for the GC calibration. 6 calibration standards which contained different amounts of each product species (50mg, 100mg, 150mg, 200mg, 250mg, 600mg) in 5mL of internal standard solutions were prepared for analysis. Then the response factor of each component can be calculated using Equation 3-1. The calibrated response factor of each species is listed in Table 3-2 and the calibration curves are shown in Appendix B.



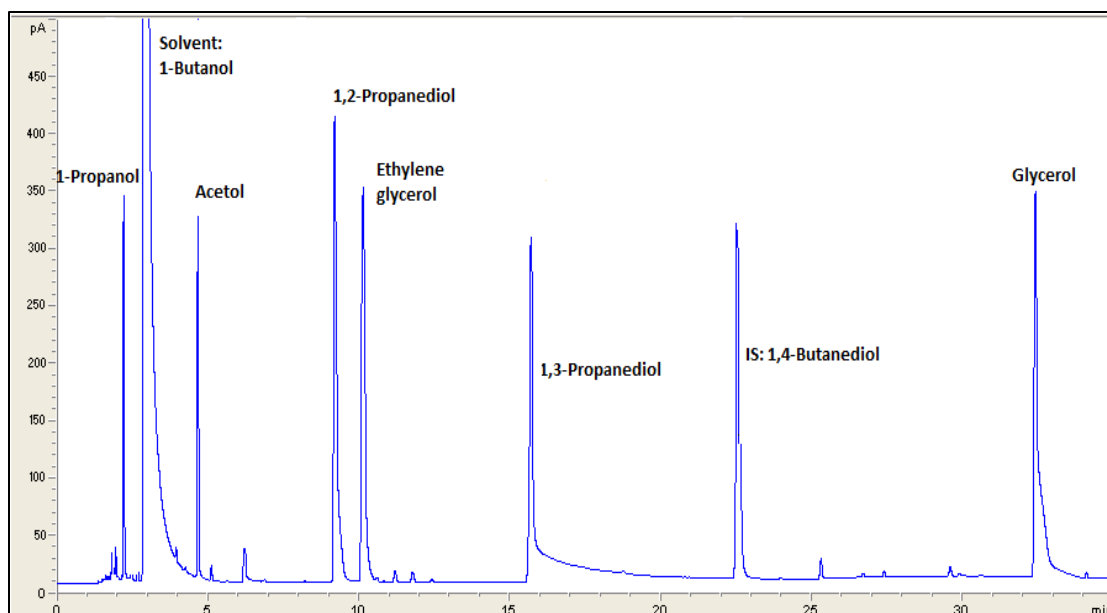


**Figure 3-3** A typical chromatogram of a GC calibration standard

$$\frac{m_i}{m_{I.S.}} = k_i \frac{A_i}{A_{I.S.}} \quad \text{Equation 3-1}$$

where,

$m_i$ ,  $A_i$  -- mass and area of each species respectively

$m_{I.S.}$ ,  $A_{I.S.}$  -- mass and area of internal standard respectively

$k_i$  -- response factor of each species

**Table 3-2** Retention Time and Response Factor for Each Compound

Compound	1-PO	1-Butanol	Acetol	1,2-PD	EG	1,3-PD	1,4-Butanediol	GL
<b>Retention Time (min)</b>	<b>2.129</b>	<b>2.788</b>	<b>4.57</b>	<b>9.165</b>	<b>10.09</b>	<b>15.61</b>	<b>22.35</b>	<b>32.23</b>
<b>Response Factor</b>	<b>0.791</b>	<b>-</b>	<b>1.518</b>	<b>1.242</b>	<b>1.668</b>	<b>1.215</b>	<b>1.0</b>	<b>1.645</b>

Equation 3-2 was used to calculate the mass of each species in the sample. The glycerol conversion, 1-PO selectivity and yield of each product were calculated on a carbon basis from Equation 3-3 to Equation 3-6.

### Equation 3-2

$$m_i = m_{I.S.} k_i \frac{A_i}{A_{I.S.}}$$

### Equation 3-3

$$Glycerol\_conversion = \frac{\sum mole\_of\_all\_carbon\_based\_product}{\sum mole\_of\_all\_carbon\_based\_product + mole\_of\_glycerol\_remain}$$

### Equation 3-4

$$1\_PO\_selectivity = \frac{mole\_of\_1\_PO}{\sum mole\_of\_all\_carbon\_based\_product}$$

### Equation 3-5

$$13\_PD\_selectivity = \frac{mole\_of\_13\_PD}{\sum mole\_of\_all\_carbon\_based\_product}$$

### Equation 3-6

$$Yield_i\% = \frac{mole\_of\_product\_i}{\sum mole\_of\_all\_carbon\_based\_product + mole\_of\_glycerol\_remain} * 100\%$$

## 3.5 Methods and Procedures for Catalyst Characterization Techniques

In order to study the physicochemical properties such as surface area, structure and acidity of the catalysts and the relationship between the catalyst structures and catalytic activity to understand the performance of the catalyst, some catalyst characterization experiments were carried out. The different techniques used included: temperature programmed desorption (TPD), H<sub>2</sub> Temperature Programmed Reduction (TPR), powder X-ray diffraction (XRD), BET surface area analysis, Thermal Gravimetric Analysis (TGA) and Fourier Transformed Infrared (FTIR) spectroscopy. In this section, the methods and procedures for the catalyst characterization techniques are briefly introduced.

### 3.5.1 Ammonia Temperature Programmed Desorption (NH<sub>3</sub>-TPD)

NH<sub>3</sub> Temperature programmed desorption is one of the most widely used and flexible techniques for determining the amount and strength of acid sites of the catalysts due to the simplicity of the technique. Determining the quantity and strength of the acid sites on the catalyst surface is crucial to understanding and predicting the performance of a catalyst.

Preparation: Samples are usually degassed at 100°C for one hour in flowing helium/argon to remove water vapor and to avoid pore damage from steaming which may alter the structure of the support. The samples are then temperature programmed to a certain temperature and held at that temperature for sometime to remove strongly bound species and activate the sample. Finally the sample is cooled to 120°C in a stream of flowing helium/argon

Adsorption: The sample is saturated with the basic probe at 120°C; this temperature is used to minimize physisorption of the ammonia. For ammonia, two techniques are available to saturate the sample: pulsing the ammonia using the loop or continuously flowing ammonia. Pulsing the ammonia allows the user to compare the quantity of ammonia adsorbed (via pulse adsorption) to the quantity desorbed for the subsequent TPD. After saturation with ammonia, the sample is purged for a minimum of one hour under a flow of helium to remove any of the physisorbed probe.

Desorption: The TPD is easily performed by ramping the sample temperature at 10°C/minute to a given temperature. It is a good rule of thumb that the end temperature during the TPD should not exceed the maximum temperature used in the preparation of the sample. Exceeding the maximum preparation temperature may liberate additional species from the solid unrelated to the probe molecule and cause spurious results. During the TPD of ammonia, the built-in thermal conductivity detector (TCD) will monitor the concentration of the desorbed species. For the reactive probes (propyl amines), a mass spectrometer is required to quantify the density of acid sites. For these probes, several species may be desorbing simultaneously: ammonia.

NH<sub>3</sub> Temperature programmed desorption was used to determine the amount and strength of acid sites of the catalysts. Lower temperature desorption corresponds to weak acid sites and higher temperature to medium, strong acid sites. The catalyst was saturated under a flow of ammonia after which the temperature of the sample was gradually increased and the amount of ammonia desorbed was recorded as a function of time. The temperature at which ammonia desorbs is

associated with a particular type of acid site. Altamira AMI-200 Catalyst Characterization System was used for the TPD experiments. The catalyst powder was screened through a sieve to make sure that the particles with a size between 250 $\mu\text{m}$  and 500 $\mu\text{m}$  were collected for the TPD analysis. In a typical experiment, approximately 120mg of catalyst was weighed and placed in a quartz U-tube reactor. The catalyst sample was packed in one side of the U-tube reactor on a quartz wool bed that was made of a small amount of quartz wool placed on both ends of the catalyst sample. The U-tube was then secured to the sample station and enclosed by a furnace integrated with a thermocouple. Prior to the TPD studies, the catalyst sample was reduced under a flow of 5% H<sub>2</sub> (balanced Argon) at a volumetric flow rate of 30ml/hr at 300°C for 1h. After reduction, the catalyst was cooled down to 50°C and was saturated by passing 5% NH<sub>3</sub> (balance Argon) at a flow rate of 30ml/min for 1h and subsequently flushed with an Argon flow (30ml/min) at 50°C for 1h to remove the physisorbed ammonia. Then TPD analysis was carried out by heating the catalyst from ambient temperature to 750°C at a heating rate of 10°C/min for NH<sub>3</sub> desorption. After the catalyst TPD experiment, 5 pulses of a known volume (i.e. the sample loop volume of 524.0  $\mu\text{L}$ ) of 5% NH<sub>3</sub> (balance Argon) were injected directly into the TCD without passing through the U tube for calibration; the number of moles of ammonia injected can be calculated from the ideal gas law. The ammonia concentration in the effluent stream was monitored with a thermal conductivity detector and the area under the peak was integrated using software to determine the amount of desorbed ammonia. The flow diagram for this system is shown in Fig. 3-4.

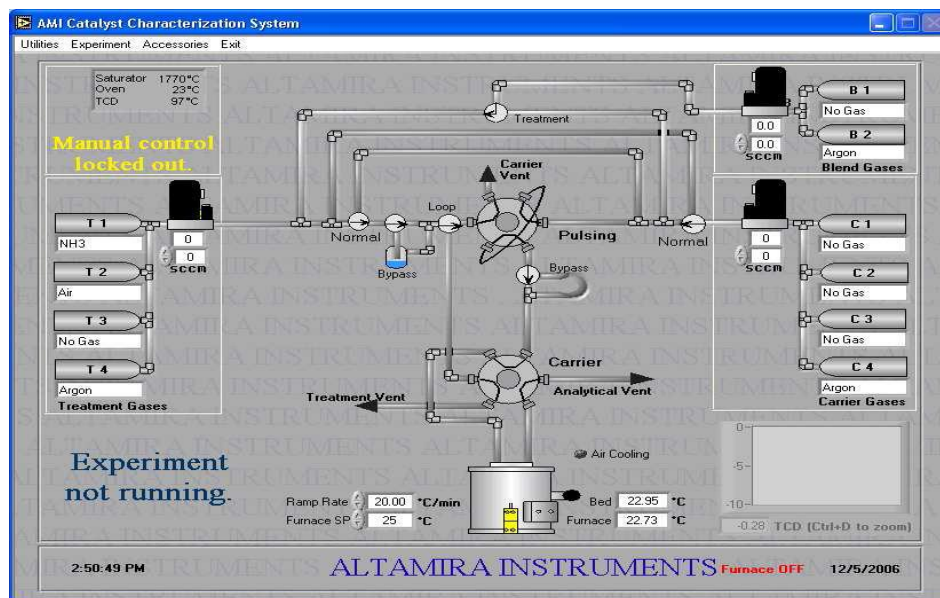


**Figure 3-4** Diagram of the Altamira AMI-200 Catalyst Characterization System

The number of moles of NH<sub>3</sub> desorbed during desorption step can be calculated using Equation 3-7 and Equation 3-8.

$$\text{Calibration\_Value} = \frac{0.524\text{ml} \times 5.16\% \text{NH}_3}{\text{mean\_calibration\_area}} \quad \text{Equation 3-7}$$

$$\text{Uptake}(\mu\text{mole} / \text{gcat}) = \frac{\text{analytical\_area} \times \text{calibration\_value}}{\text{sample\_weight} \times 24.5} \quad \text{Equation 3-8}$$

### 3.5.2 H<sub>2</sub> Temperature Programmed Reduction (TPR)

Temperature-Programmed Reduction (TPR) was used to reveal the number of reducible species present on the catalyst surface and the temperature at which the reduction of each species occurs. The TPR analysis begins by flowing an analysis gas (typically hydrogen in an inert carrier gas such as argon) through the sample, usually at ambient temperature. While the gas is flowing, the temperature of the sample is increased linearly with time and the consumption of hydrogen by the adsorption/reaction is monitored. Changes in the concentration of the gas mixture downstream from the reaction cell are determined. This information yields the volume of hydrogen uptake. In this research, TPR experiments have been carried out to determine the appropriate reduction temperature for each catalyst. The catalyst was loaded and reduced as described in section 3.4.1 for NH<sub>3</sub>-TPD. In a typical experiment, approximately 60mg of catalyst was weighed and placed in a quartz U-tube reactor. The catalyst is reduced while the temperature is increased to find the optimum reduction temperature. The catalyst was firstly heated to 200°C and kept at 200°C for 60 minutes under 30ml/min Argon flow to remove all the moisture and other species absorbed on the catalyst surface. Then the catalyst was heated under 30ml/min 5% H<sub>2</sub> balanced with Argon at a heating rate of 5°C/min until 900°C and then the temperature was held at 900°C for 15 minutes.

### 3.5.3 Brunauer Emmett Teller (BET) Surface Area

The BET technique is a common technique used to measure the specific surface area of a material by adsorbing gas molecules on a solid surface. The concept of the BET theory is an extension of the Langmuir adsorption theory from monolayer to multilayer adsorption. Adsorption is the phenomenon of gas molecules sticking to the surface of a solid. The concentrations of gas

(adsorbate) will be different on the solid (adsorbent) under different conditions, and this effect can be used to determine the area of solid materials.

In a gas sorption experiment, the material is first heated and degassed by vacuum or inert gas purging in order to remove any contaminants, volatile organics. A controlled amount of inert gas such as nitrogen (N<sub>2</sub>), argon (Ar), or krypton (Kr) is then introduced, which adsorbs on the surface of the material. The sample is placed under vacuum at a low temperature, usually at the boiling point of liquid nitrogen (-195.6°C). The sample is then subjected to a wide range of pressures. The amount of gas molecules adsorbed will vary as the pressure of the gas is varied. When the quantity of adsorbate on a surface is measured over a wide range of relative pressures at constant temperature, the result is an adsorption isotherm. The resulting adsorption isotherm is analyzed according to the BET method. The BET surface area can be calculated via equation 3-9:

$$\frac{P}{n(P_0-P)} = \frac{1}{cn_m} + \frac{c-1}{cn_m} * \frac{P}{P_0} \quad \text{Equation 3-9}$$

where P, P<sub>0</sub>, c, n, n<sub>m</sub> are the adsorption pressure, the saturation pressure, a constant, the amount adsorbed (weight of adsorbate) at the relative pressure P/P<sub>0</sub>, and the monolayer capacity (weight of adsorbate constituting a monolayer of surface coverage), respectively [114]. Through the slope and intercept of a plot of P/[n(P<sub>0</sub>-P)] against (P/P<sub>0</sub>), n<sub>m</sub> can be determined. The cross-sectional area (ACS) occupied by one N<sub>2</sub> adsorbate molecule is 16.2Å<sup>2</sup>. The BET surface area can be calculated using equation 3-10:

$$A = \frac{A_{CS} * n_m * N_A}{M_{N_2}} \quad \text{Equation 3-10}$$

Where, N<sub>A</sub> is the Avogadro's number, and M<sub>N<sub>2</sub></sub> is the molar mass of N<sub>2</sub>, 28g mol<sup>-1</sup>. The specific surface area is then calculated by dividing the area A by the sample weight.

In this thesis research, the BET surface area was determined using a Micromeritics Gemini VII instrument with nitrogen physisorption at 77 K, taking 0.162 nm<sup>2</sup> as the cross sectional area for di-nitrogen. The analysis was carried out on calcined catalyst. Catalyst samples were degassed under nitrogen at 300°C in 3 hours to desorb the moisture on the catalyst surface then cooled down to room temperature and weighed before proceeding BET analysis.

### 3.5.4 Thermal Gravimetric Analysis (TGA)

Thermo Gravimetric Analysis (TGA), an analytic technique that measures the weight loss (or weight gain) of a material against temperature or time technique, can provide information on the thermal stability of the compound in the solid state and the amount of crystal waters present. TGA is an analytic technique that measures the weight loss (or weight gain) of a material against temperature or time. As materials are heated, they can lose weight from drying, evaporation and decomposition. Some materials can gain weight by reacting with the air.

A TGA Q500 was used for TGA thermal analysis. The pan was filled with around 10mg of catalyst sample. Then the sample was heated under 100ml/min air flow from room temperature to 900 °C.

### 3.5.5 X-Ray Diffraction (XRD)

XRD was used to study the composition of the catalysts. It is also useful to determine if the material under investigation was crystalline or amorphous. The calcined catalyst was attacked by X-rays at various angles. Intensity of the reflected X-rays depends on the relative arrangement of atoms in the crystal. The angle of X-rays reflected from crystal depends on the dimensional characteristics of the lattice. Each material has a unique X-ray diffraction pattern.

The XRD patterns were obtained on a Bruker D8 Focus model. The configuration included power of 40 kV, current intensity, 1.0 mm divergence slit, 1.0 mm anti-scattering slit, 0.1 mm detector slit and 0.6 mm receiving slit. Cu  $\alpha$  radiation wave length was set to 1.54 Å; the  $2\theta$  angle was set at 20°-80° with a ramp 0.02° per minute. The catalyst was crushed well to produce fine particles before doing experiment.

The average crystallite size was calculated using the Scherrer equation. If there is no inhomogeneous strain, the crystallite size D can be estimated from the peak width by the Scherrer's formula:

$$D = k\lambda/B(2\theta)\cos\theta$$

where  $\lambda$  is the X-ray wavelength, B is the full width of height maximum of a diffraction peak,  $\theta$  is the diffraction angle, and k is the Scherrer constant which is of the order unity for usual crystal.

### 3.5.6 Fourier transform infrared spectroscopy (FTIR)

The use of FTIR as a characterization technique is based on the vibrational frequencies of the chemical bonds. The vibrational motions of the chemical bonds in a material have frequencies in the infrared regime. In the infrared technique, the intensity of a beam of infrared radiation is measured before ( $I_0$ ) and after ( $I$ ) its interaction with the sample as a function of light frequency. The plot of  $I/I_0$  versus frequency is the “infrared spectrum”. By using FTIR, information about the identities, surrounding environments and concentrations of the chemical bonds in the material can be obtained [115]. FTIR spectra are capable in revealing information about the functional group present within a molecule. Infrared spectroscopy FTIR can then supply a “fingerprint” of the compound made showing the typical M-O bond vibration peaks, where M can be the addenda or the heteroatom. FTIR spectroscopy was performed in order to observe any significant changes in the chemical structures of the Keggin anion of the catalyst.

FTIR analyses of the catalysts were recorded using a Nicolet 6700 FTIR spectrum from Thermo Electron Corporation using a KBr disc technique and working with resolution of  $4\text{ cm}^{-1}$  in the middle range. The spectra were recorded with 32 scans between  $400$  and  $4400\text{ cm}^{-1}$  with a resolution of  $4\text{ cm}^{-1}$ . For the FTIR analysis, the samples were analyzed after dilution in KBr as follows. Approximately  $5\text{ mg}$  (2.5wt.%) sample is well mixed into  $200\text{ mg}$  fine alkali halide (here KBr is used) powder and then finely ground and put into a pellet-forming die. A force of approximately  $10$  tons is applied under a vacuum of several mm Hg for several minutes to form transparent pellets. Before forming the KBr powder into pellets, it was pulverized to 200 mesh max. and then dried at approximately  $110\text{ }^\circ\text{C}$  for three hours. When performing measurements, the background was measured with an empty pellet holder inserted into the sample chamber. The chemical bonds present in the structure of the materials were identified by this analysis technique.



## Chapter Four

### **Conversion of glycerol to lower alcohols using 10Ni/30HSiW/Al<sub>2</sub>O<sub>3</sub> catalyst in a Stainless Steel batch reactor**

Much work has been done towards the hydrogenolysis of glycerol to 1,3-PD and 1,2-PD, however, routes to lower alcohols, such as 1-PO have been less frequently reported. A literature review showed that various heterogeneous systems including Rh, Ru, Pt, PtRu, Cu systems and Raney Ni are studied for the hydrogenolysis of glycerol to lower alcohols. Surprisingly, the use of supported Ni systems as catalysts towards the chemical transformation of glycerol, especially towards the formation of lower alcohols, has appeared less frequently in the literature. Therefore the main purpose of this chapter was the production of lower alcohols, primarily 1,3-PD and 1-PO from glycerol using 10Ni/30HSiW/Al<sub>2</sub>O<sub>3</sub> catalysts in a stainless steel batch reactor.

In this chapter, the effect of metals of Pt, Pd, Ni and Cu and the effect of Cs<sup>+</sup> substitution of H<sup>+</sup> on the activity and selectivity of the catalyst for the hydrogenolysis of glycerol in a batch reactor was investigated. The catalysts were synthesized in our lab via an impregnation method, and then crushed and sieved to less than 250µm before testing to minimize internal mass transfer effects. Prior to each experiment, the catalyst was reduced in a quartz tubular reactor at 350°C for 5h. Reactions were performed in a 300ml Parr Instrument 4182 Series constructed of stainless steel T316. After sealing the reactor the reaction mixture was purged with N<sub>2</sub> gas several times and then with H<sub>2</sub> gas while stirring gently at 50 RPM to remove all the oxygen from the headspace and any dissolved oxygen in the solvent. The reactor was then pressurized to the target pressure and heated to the required temperature. When the reactor had just reached the required temperature, the stirring speed was increased to 700 RPM at which point the first sample at 0 hour was taken. The progress of the reaction was followed by sampling at regular intervals during the reaction. The reactor was maintained at 240°C during the reaction.

#### **4.1. Effect of metals on the hydrogenolysis of glycerol**

Since hydrogenolysis requires hydrogen for hydrogenation, the hydrogenolysis catalyst must have an ability to activate hydrogen molecules. In this section different metals supported on 30HSiW/Al<sub>2</sub>O<sub>3</sub> catalysts were studied for the hydrogenolysis of glycerol. Noble metals are well

known to be able to activate hydrogen molecules and are widely used as hydrogenation catalysts. Pt supported HPAs catalyst is one of the most active supported catalysts for the hydrogenolysis of glycerol and has been intensively studied by many researchers for the upgrading of glycerol to other value-added chemicals [77-79, 86]. Although research has been carried out towards the hydrogenolysis of glycerol to 1,2-PD and 1,3-PD, hardly any work has been reported on the one-pot direct conversion of glycerol to 1-PO. For the conversion of glycerol to 1-PO, noble metals such as Rh, Ru, Pt are often used but the selectivity to 1-PO can reach only as high as of 80%. [45, 78, 116]. A non-noble metal such as Cu has also been intensively investigated for the upgrading of glycerol [63, 105, 117] but the catalysts does not show their effectiveness toward selectivity of 1-PO. Ni-based catalysts show acceptable activities and selectivities at moderate costs of manufacturing, especially as compared to the costs associated with catalysts based on noble metals. Ni-based catalysts can also have high catalytic activity and selectivity for the hydrogenation of aldehydes especially in converting 3-HPA (3-hydroxypropionaldehyde) to 1,3-PD [112, 118-121]. However, to date Ni supported catalysts have not been reported for the one-pot hydrogenolysis of glycerol to produce 1-PO. The production of 1-PO either was carried out under high temperature (320°C), high pressure of H<sub>2</sub> (6MPAa) in fix-bed reactor or the catalyst was packed in a sequential two-layer catalysts [122] and the selectivity of 1-PO is still low.

In the present section, bi-functional catalysts were synthesized with different metals (i.e. Ni, Pd, Pt, Cu) and HSiW supported on Al<sub>2</sub>O<sub>3</sub> as bifunctional catalysts by a sequential impregnation method for the one-pot hydrogenolysis of glycerol to lower alcohols, in particular, to 1-PO. The catalysts were characterized using XRD and NH<sub>3</sub>-TPD techniques. A comparison of the reactivity and the product selectivity of the Ni catalyst with the Pd, Pt and Cu catalysts were carried out. Rate constants for the conversion of glycerol, 1,2-PD and 1,3-PD, 1-PO was determined for a 10Ni/30HSiW/Al<sub>2</sub>O<sub>3</sub> catalyst and a reaction pathway was proposed.

### **Experiment condition**

The effect of metals on the overall reaction is studied by carrying out the hydrogenolysis of glycerol using different metals loading under the same reaction condition. Prior to each experiment, the catalyst was reduced in a quartz tubular reactor at 350°C. The experiment was performed at 240°C, 700RPM under 880 H<sub>2</sub> pressure using 4g of metal supported 30HSiW/Al<sub>2</sub>O<sub>3</sub>

catalyst, 30g of glycerol, 70g deionized water in 8 hours. The properties of the prepared catalysts were characterized using  $\text{NH}_3$ -TPD, XRD techniques.

## Results and discussion

### Characterization of catalysts

The catalysts were characterized by XRD and  $\text{NH}_3$ -TPD techniques to study the relationship between catalytic activity and catalyst properties in particular the acid concentration of the catalysts.

XRD patterns of all catalysts are shown in Fig. 4-1 and 4-2. It can be seen that the XRD patterns are similar for all the catalyst with 1 wt% Pt, 1 wt% Pd, 1 wt% Ni supported on 30HSiW/ $\text{Al}_2\text{O}_3$ . In all the samples, no diffraction lines due to Ni, Pd and Pt were observed. Hence the XRD patterns suggest that at a low level of metal loading of 1 wt% that the metal oxide species is present in a highly dispersed amorphous state. In Fig. 4-2, the XRD patterns show that when Ni loading increases from 1 wt% to 10 wt%, the diffraction peak of NiO was observed. Thus the nickel oxide is present in a highly dispersed amorphous state at 1 wt % Ni in the sample and as a crystalline NiO phase at a 10 wt% Ni loading.

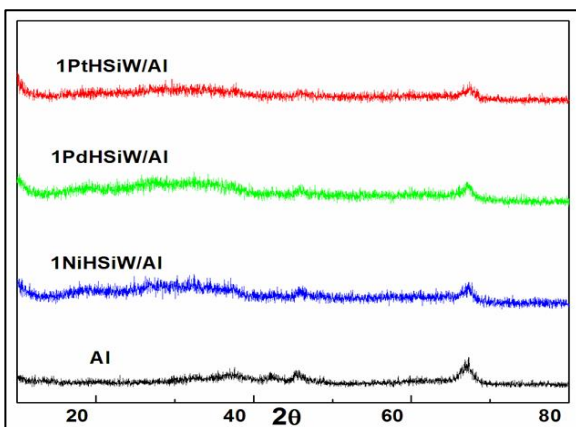


**Figure 4-1** XRD patterns of 1 wt% metal loading on HSiW/ $\text{Al}_2\text{O}_3$  catalyst

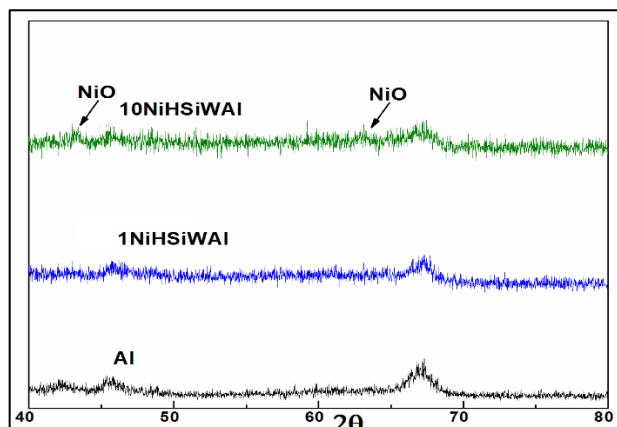


**Figure 4-2** XRD patterns of 1wt% and 10 wt% Ni loading on HSiW/ $\text{Al}_2\text{O}_3$  catalyst

The  $\text{NH}_3$ -TPD measurements were carried out to compare the acidity of different metal supported 30HSiW/ $\text{Al}_2\text{O}_3$ . The  $\text{NH}_3$ -TPD profiles are shown in Fig. 4-3 and 4-4. The TPD data was

deconvoluted into 3 peaks (namely weak, medium and strong acid sites) using a Gaussian fitting method. The results are shown in Table 4-1.

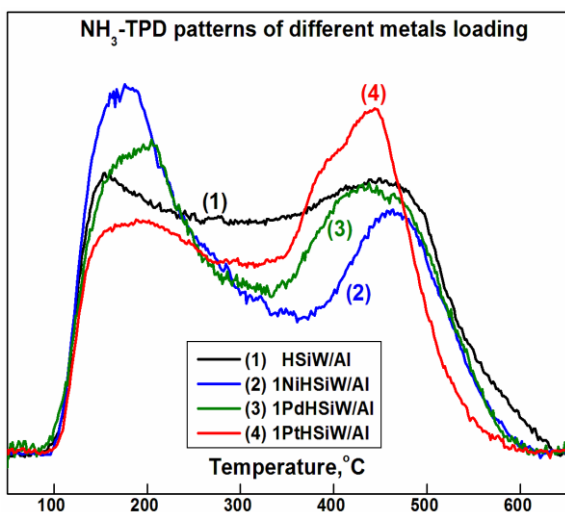


**Figure 4-3** NH<sub>3</sub>-TPD patterns of different metals (Ni, Pd, Pt) loading on 30HSiW/Al<sub>2</sub>O<sub>3</sub> catalyst

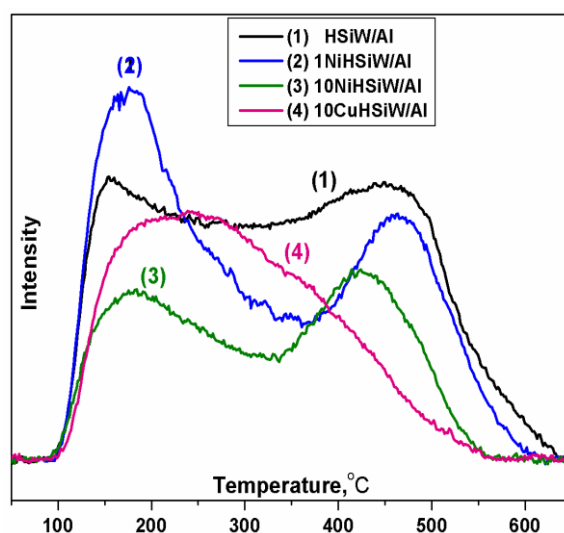


**Figure 4-4** NH<sub>3</sub>-TPD patterns of 1 wt % and 10 wt% Ni supported 30HSiW/Al<sub>2</sub>O<sub>3</sub> catalyst

**Table 4-1** Total acidity of catalysts

Catalyst	Weak acid site mmol/g /(Temp.)	Medium acid site mmol/g /(Temp.)	Strong acid site mmol/g /(Temp.)	Total acid amount, mmol/g
30HSiW/Al <sub>2</sub> O <sub>3</sub>	0.149/ (155°C)	0.379/ (243°C)	0.461/ (439°C)	0.989
1Ni/30HSiW/Al <sub>2</sub> O <sub>3</sub>	0.228/ (167°C)	0.308/ (259°C)	0.330/ (460°C)	0.866
1Pd/30HSiW/Al <sub>2</sub> O <sub>3</sub>	0.205/ (172°C)	0.242/ (254°C)	0.425/ (442°C)	0.873
1Pt/30HSiW/Al <sub>2</sub> O <sub>3</sub>	0.235/ (178°C)	0.194/ (281°C)	0.441/ (428°C)	0.869
10Ni/30HSiW/Al <sub>2</sub> O <sub>3</sub>	0.124/ (162°C)	0.233/ (246°C)	0.215/ (427°C)	0.572
10Cu/30HSiW/Al <sub>2</sub> O <sub>3</sub>	0.108/ (162°C)	0.201/ (230°C)	0.347/ (345°C)	0.657

As it can be seen from Table 4-1, 1wt% metal loading decreases the total acidity of the 30HSiW/Al<sub>2</sub>O<sub>3</sub> catalyst by approximately 10%. A decrease in acidity may possibly be due to the covering of acid sites by metal, or from the direct anchoring of metals on proton sites, and or from blockage of the access to the acid sides by metal particles. However, the total acidity of the 1wt % of Ni, Pd or Pt supported 30HSiW/Al<sub>2</sub>O<sub>3</sub> catalysts is quite similar. Although the total acidity of

the catalyst does not depend on the type of metal loading, the distribution of the strength and amount of the acid sites appear to be dependent on the type of metal, however the variation is not very significant.

Fig. 4-4 shows that an increase in Ni loading from 1wt% to 10 wt% leads to a significant decrease in the acidity of the catalyst. This suggests the possibility in covering the acid sites by adding metal or direct anchoring on proton sites, and from blockage of acid channels by metal particles. The addition of 10 wt% Cu causes a significant reduction in the strength of the acid sites of the catalyst. As can be seen from Table 4-1, the amount of weak and medium acid sites diminishes, and interestingly the amount of strong acid sites increases but the peak shifts to a lower temperature (345°C compared with 427°C for the catalyst with 10% Ni) indicating a lower acid strength.

### **Activity test results**

To establish the role played by the metallic sites of the catalyst in the hydrogenolysis of glycerol, a series of metal (Pt, Pd, Ni and Cu) supported 30HSiW/Al<sub>2</sub>O<sub>3</sub> catalysts were prepared and used for the conversion of an aqueous solution of a 30wt. % glycerol initial concentration under an initial H<sub>2</sub> pressure of 880PSI at room temperature . The main products observed in the liquid phase were: acetol, 1,2-PD, 1,3-PD, acrolein (Acr), 1-PO and ethylene glycol (EG). Some other products (OP) such as methanol, ethanol were also obtained. In addition, some other products were detected but not identified (UIP).

The conversion and product selectivity data for the catalysts are shown in Table 4-2. The first set of experiments were performed with 1% metal loading of Ni, Pd and Pt onto 30HSiW/Al<sub>2</sub>O<sub>3</sub> and compared with the parent catalyst 30HSiW/Al<sub>2</sub>O<sub>3</sub>. The data shows that these metals affect both the glycerol conversion and product distribution. It is interesting to observe that the addition of Pt, Pd and Ni increased the glycerol conversion which could be attributed to the higher hydrogenation activity of these metals. The dehydration of glycerol to form acetol or 3-HPA shown in Scheme 4-1 is reversible. Hydrogenation of the intermediates formed from the dehydration of glycerol will shift the equilibrium to 1,2-PD or 1,3-PD and increases the conversion of glycerol. Besides differences in glycerol conversion, the product distribution of the parent catalyst is also quite different than those with added Ni, Pt, Pd. The parent catalyst yields a higher selectivity to acrolein but no 1,3-PD is detected. Dehydration of the secondary alcohol group in glycerol will produce 3-

HPA which could either be further dehydrated to form acrolein or hydrogenated to produce 1,3-PD. Since the parent catalyst is the most acidic catalyst in this study but deficient in effective hydrogenation sites, hence acrolein was obtained in high selectivity and interestingly no 1,3-PD was detected. Addition of 1 wt% of Ni, Pd, Pt significantly increases the conversion of glycerol due to the hydrogenation of the dehydration intermediates acetol or 3-HPA to produce 1,2-PD or 1,3-PD respectively. Further hydrogenolysis of 1,2-PD or 1,3-PD produces 1-PO. While addition of 1 wt% Pt to the parent catalyst increases glycerol conversion with a higher selectivity to 1,3-PD and 1-PO, it is interesting to observe addition of 1 wt% Ni also promotes the hydrogenolysis of glycerol to 1-PO with activity and selectivity similar to that of Pt and Pd.

The nominal weight loading of Ni in Ni/30HSiW/Al<sub>2</sub>O<sub>3</sub> was increased to 10wt% in an attempt to promote the hydrogenolysis and conversion of glycerol. The reactivity was also compared with a catalyst with 10wt% Cu loading on 30HSiW/Al<sub>2</sub>O<sub>3</sub> under the same reaction conditions. As can be observed from Table 4-2, by increasing the Ni loading from 1 wt % to 10 wt% Ni there was a decrease in the conversion of glycerol; however, it increases the selectivity to 1,2 PD and 1-PO and reduces the selectivity of the unidentified products (UIP). A higher Ni loading apparently increases the selectivity to lower alcohols possibly due to the increased hydrogenation activity. As discuss above, a higher loading of Ni decreases the strong acidic sites of the catalyst (Fig. 4-4 and Table 4-1) which caused the decrease in the conversion of glycerol as the first step for glycerol conversion is the acid catalyzed dehydration. Since Ni, an inexpensive transition metal has activity comparable to Pt, the activity of another inexpensive transition metal was also investigated. Surprisingly, the catalytic activity of the 10 wt% Cu loaded catalyst decreased remarkably. The selectivity to lower alcohols such as 1,2-PD and 1-PO is low; also no 1,3-PD or EG were detected using a Cu supported 30HSiW/Al<sub>2</sub>O<sub>3</sub> catalyst. Interestingly acrolein was obtained. The product selectivity suggests that Cu is not effective for hydrogenation under this reaction condition. It is worth noting that the strength of the acid sites of the Cu loaded catalyst is much less than the other metals (Fig. 4-4, Table 4-1). Whilst the strength of acid sites affects dehydration which is reflected in lower glycerol conversion; the lower selectivity to the desired products is attributed to the lower hydrogenation activity of Cu compared to Ni, Pd and Pt.

**Table 4-2** Effect of metal loading on catalytic performance

Entry	Catalyst	Conv mol%	Selectivity, mol%								
			1,3PD	1,2PD	Ac	EG	1-PO	Acr	MeOH	EtOH	UIP
1	30HSiW/Al <sub>2</sub> O <sub>3</sub>	14.5	0.0	0.0	6.0	0.0	30.5	19.7	5.3	9.1	29.4**
2	1Ni/30HSiW/Al <sub>2</sub> O <sub>3</sub>	39.2	3.0	4.1	3.3	0.0	54.7	3.4	3.4	2.9	25.2*
3	1Pd/30HSiW/Al <sub>2</sub> O <sub>3</sub>	34.1	5.4	4.7	4.1	0.0	51.4	1.9	4.1	8.7	21.7*
4	1Pt/30HSiW/Al <sub>2</sub> O <sub>3</sub>	45.3	10.5	5.7	2.5	1.8	59.2	1.9	0.0	5.1	13.3*
5	10Ni/30HSiW/Al <sub>2</sub> O <sub>3</sub>	33.2	7.9	10.5	3.8	4.4	60.7	1.5	1.8	4.8	4.6*
6	10Cu/30HSiW/Al <sub>2</sub> O <sub>3</sub>	18.0	0.0	4.2	5.3	0.0	31	12.6	0.0	8.2	42.9**

**Reaction condition:** M/30HSiW/Al<sub>2</sub>O<sub>3</sub> catalyst (M: Pt, Pd, Ni, Cu), 240°C, 880PSI initial H<sub>2</sub>, 30g of glycerol (30wt%), 70g of DI water, 4g catalyst, 8 hours. U.I.P.: unidentified products (\*: one heavy product, \*\*: some light and heavy products)

In order to elucidate the reaction pathway for glycerol conversion, the hydrogenolysis of 1,2-PD, 1,3-PD, 1-PO over 10Ni/30HSiW/Al<sub>2</sub>O<sub>3</sub> was also evaluated under conditions similar to that of glycerol and the results are presented in Table 4-3. The pseudo first order rate constants for the conversion of glycerol, 1,2-PD, 1,3-PD and 1-PO under the same reaction conditions were calculated and are presented in Fig. 4-5. As can be seen the conversion of 1,3-PD was lower than that of glycerol and 1,2-PD, the pseudo first order rate constants for the conversion of 1,2-PD and 1,3-PD shows the rate constants for the conversion of 1,2-PD is 15 times faster than for 1,3-PD. Therefore, 1-PO is mainly produced from 1,2-PD with a high conversion of 1,2-PD and high selectivity to 1-PO. Since the conversion of 1-PO was much lower than that of 1,2-PD and 1,3-PD, it can be assumed that 1-PO is stable under the reaction condition and becomes the final product in the hydrogenolysis of glycerol using 10Ni/30HSiW/Al<sub>2</sub>O<sub>3</sub>. It is interesting to note that ethylene glycol was obtained in the glycerol hydrogenolysis, however, it was not detected in the hydrogenolysis of 1,2-PD and 1,3-PD suggesting that ethylene glycol was produced directly from glycerol by a C–C bond cleavage reaction. In the reaction of glycerol and 1,2-PD, ethanol was observed which can be formed via sequential hydrogenolysis of ethylene glycol or decomposition of 1,2-PD.

**Table 4-3** The hydrogenolysis of 1,2-PD, 1,3-PD and 1-PO

Reactant	Glycerol	1,2PD	1,3PD	1-PO
Conversion, mol%	33.2	98.1	26.4	8.5
Selectivity, mol%				
Acetol	3.8	0.6	0.0	0.0
1,2PD	7.9	-	0.0	0.0
1,3PD	10.5	0.0	-	0.0
1-PO	60.7	90.8	77.4	-
EG	4.4	0.0	0.0	0.0
MeOH	1.8	0.0	0.0	0.0
EtOH	4.8	2.1	15.0	20.7
Acr	1.5	0.0	0.8	0.0
Propanal	0.0	4.5	0.0	79.3
UIP	4.6	2.6	6.8	0.0

**Reaction condition:** 10Ni/30HSiW/Al<sub>2</sub>O<sub>3</sub> catalyst, 240°C, 880PSI initial H<sub>2</sub>, 30g of glycerol (30wt%), 70g of DI water, 4g catalyst, 8 hours

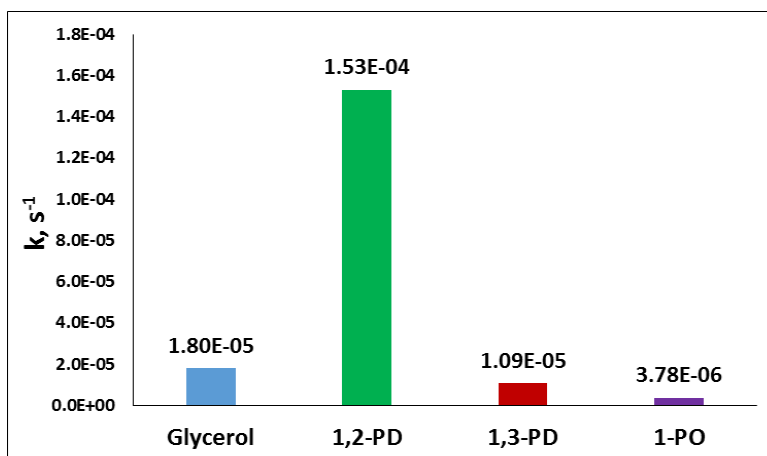


**Figure 4-5** Pseudo-first-order rate constants for the 10Ni/30HSiW/Al<sub>2</sub>O<sub>3</sub> catalysts using different starting material. **Reaction condition:** 240°C, 880PSI H<sub>2</sub>, 700RPM, 4g catalyst, 30g of glycerol (30wt%), 70g of DI water.

It is interesting to note that the rate constant for the conversion of 1,2-PD is the highest, followed by glycerol. The conversion of 1,3-PD is slower than the glycerol conversion while the conversion



of 1-PO is the slowest. These rate constants provide important formation on the proposed reaction pathway for glycerol hydrogenolysis and also the product selectivity.

## Summary

Ni, Pd, and Pt promote the activity of the 30HSiW/Al<sub>2</sub>O<sub>3</sub> supported catalyst for the conversion of glycerol to higher value chemicals such as 1,3-PD, 1,2-PD and in particular 1-PO. Among these metals, Pt is the best promoter for the production of 1,3-PD, a very high value intermediate for valuable polymers. Although it is reported that Cu possesses good hydrogenation activity that is comparable with Ni, Cu does not show activity for the production of 1,3-PD under this reaction conditions. Interestingly Ni, a much cheaper metal, has fairly comparable reactivity to Pt.

The much lower price of Ni compared to Pt is very attractive for a new green process development for the conversion of glycerol to sustainable higher value products. To obtain a desired product selectively, the control of reaction conditions and catalyst properties such as acid strength, the amount of appropriate acid sites and metal hydrogenation activity will be needed. Optimization of the catalyst preparation techniques and a balance of Ni and HiSiW loading on various supports could lead to high yields of value-added chemicals from glycerol. Due to the inexpensive Ni-based catalyst and the high selectivity, an economical production of green and sustainable 1-PO from glycerol hydrogenolysis may be feasible for future commercial development. 1-PO is mainly produced from 1,2-PD with a high conversion of 1,2-PD and high selectivity to 1-PO and 1-PO is stable under the reaction condition and is assumed as the final product in the hydrogenolysis of glycerol using 10Ni/30HSiW/Al<sub>2</sub>O<sub>3</sub>.

## 4.2 Effect of Cs<sup>+</sup> on activity of 10Ni/30HSiW/Al<sub>2</sub>O<sub>3</sub> catalyst

In this section, effect of Cs<sup>+</sup> exchanged H<sup>+</sup> in the 10Ni30HSiW/Al<sub>2</sub>O<sub>3</sub> catalyst was investigated for hydrogenolysis of glycerol.

Although HPAs are useful solid catalysts, the specific surface area of these solid materials is very low making low dispersion, agglomeration or leaching of HPAs still a crucial limitation. In order to increase the efficiency of HPA-catalyzed processes these disadvantages have to be overcome. One of the possible solutions is synthesizing salts of them since the protons in Keggin HPAs can be readily exchanged, totally or partially, by different cations without affecting the primary Keggin

structure of the heteropoly anion. It is reported that the presence of counter cations such as  $\text{Cs}^+$ ,  $\text{Rb}^+$ ,  $\text{K}^+$  in replacement of protons can modify the physicochemical properties (reduces water solubility and simultaneously increases specific surface area [123] of heteropolyacids ) therefore the method to control these properties can be established by exchange of protons by various alkaline metals in different concentrations [85]. In this way, a partial neutralization of HPA's with these cations is achieved and insoluble salts of HPA's are obtained that also contribute to improve their catalytic activity by increasing the HPA dispersion [124]. It is evident that the protons in the heteropolyacids are the source of catalyst activity because most of the completely cation exchanged salts were inactive in acid-base catalysis. It has been reported that acidic HSiW promotes the condensation of formaldehyde and methyl formate to methyl glycolate and methyl methoxy acetate whereas completely cation exchanged compounds are inactive [125]. Haber et al. [126] studied the synthesis of metal salts of HPA's in pure form and also supported them on silica and tested them in dehydration of ethanol and hydration of ethylene. It was reported that the structure of salts of heteropolyacids were affected by the type of counter cation present. Salts with small cations like Fe, Co, Ni or Na resembled the parent HPA, as they were water soluble, nonporous and had low surface areas. On the other hand, salts of HPA with large monovalent cations such as  $\text{NH}_4^+$ ,  $\text{K}^+$ , and  $\text{Cs}^+$  were water insoluble, had rigid micro/mesoporous tertiary structure and had high surface areas [126, 127]. Kozhevnikov stated that when in the form of salts, thermal stability of heteropolyacids is higher than their acid forms [128].

The most-studied insoluble salt of HPAs is Cs salt that is a well-known acidic catalyst in which the residual protons are more acidic than the homogeneous acid catalysts (e.g.  $\text{H}_2\text{SO}_4$ ). Partial substitution of protons of HPAs by  $\text{Cs}^+$  results in a higher thermal stability. When in the form of salts, thermal stability of heteropolyacids is higher than their acid forms. It is reported that properties of HPAs such as solubility, crystalline structure, porosity, surface area, amount of water of crystallization and thermal stability are sensitive to the amount of  $\text{Cs}^+$  substituted [124, 129,130]. Alkaline substituted of  $\text{Cs}^+$  HPAs catalysts have also attracted much attention due to their high surface area and tunable porosity which enable them for the use in dehydration reaction. [131-133]. Okuhara et al. [134] concluded that the pore size of the acidic Cs salts ( $\text{Cs}_x\text{H}_{3-x}\text{PW}_{12}\text{O}_{40}$ ) was controlled by the  $\text{Cs}^+$  content, the shape selective catalysis was observed and the acidic Cs salts were strongly acidic and when compared to the zeolites  $\text{SO}_4^{2-}/\text{ZrO}_2$ , they were more catalytically active for decomposition of esters and alkylation in liquid-solid reaction system. In

1995, Essayem et. al. confirmed that the Cs salts of  $H_3PW_{12}O_{40}$  exhibit a much higher surface area than their acid analog and the enhancement of the surface area results obviously in a strong increase in specific catalytic activity in the conversion of methanol to dimethyl ether. The amount of acidity and the acid strength depends differently on the Cs content [135]. In 1998 Bardin et al.[136] tested the heteropolyacid  $H_3PW_{12}O_{40}$  and its Cs salts  $Cs_xH_{3-x}PW_{12}O_{40}$  ( $x = 1, 2, 2.5, 3$ ) for isomerization and it was found that incorporation of Cs into the heteropolyacid decreased the acidic protons available for catalysis, increased the specific surface area, and increased the thermal stability. In 2013 E. Rafiee et. al. investigated the activity of  $Cs_xH_{3-x}PW_{12}O_{40}$  ( $X = 0, 1, 2, 2.5$  and 3) catalysts in the synthesis of  $\beta$ -ketoenol ethers [137]. It was reported that activity; acidity, solubility and consequently, recoverability of these catalysts are related to Cs content. Shaimaa M. Ibrahim also mentioned in his work that the catalytic activity and selectivity towards dehydration and dimerization processes of the catalysts are much affected by the number of substituted acid protons by alkali metal. The surface area of the supported Cs or K salts of HPW increased progressively by increasing the number of protons substituted by  $Cs^+$  or  $K^+$  which resulted to an increase in the catalytic activity [138]. Narasimharao et. al. investigated the relations in structure–activity and Cs-doped heteropolyacids catalysts for biodiesel production [139]. It was found that the total acid site density decreases with  $Cs^+$  exchange. All samples with  $x > 1$  are resistant to leaching and can be recycled without major loss of activity in particular  $Cs_{2.3}H_{0.7}PW_{12}O_{40}$  can be used without loss of activity or selectivity. Pesaresi et. al. [140] used Cs-doped  $H_4SiW_{12}O_{40}$  catalysts for biodiesel applications and it is found that low loadings  $\leq 0.8$  Cs per Keggin, (trans) esterification activity arises from homogeneous contributions. However, higher degrees of substitution result in entirely heterogeneous catalysis, with rates proportional to the density of accessible acid sites present within mesopores. In 2015 Sujiao et. al. [141] studied  $Cs_xH^{3+}_{n-x}PMo_{12-n}VnO_{40}$  catalysts ( $n=0, 1, 2, x=0.5-3.0$ ) in the direct hydroxylation of benzene reaction. It is found that the leaching of catalyst decreases significantly with increasing the Cs content.

Although considerable research has studied the effect of Cs substituted HPAs catalyst to improve the catalytic activity in reactions, there are only a few reports on the effect of  $Cs^+$  exchanged HPAs catalyst for the glycerol conversion. Alhanash et. al. [85] demonstrated that the water-insoluble Cs heteropoly salt,  $Cs_{2.5}H_{0.5}PW_{12}O_{40}$ , possessing strong Brønsted acid sites and high water tolerance is an active catalyst for the dehydration of glycerol to acrolein. The catalyst exhibits high initial activity, with a glycerol conversion of 100% at 98% acrolein selectivity. Recently, Atia et

al. [72] investigated a series of Li, K and Cs modified HSiW catalysts for glycerol dehydration and found that addition of alkaline metals Li, K and Cs has greatly improved the desired acrolein selectivity and activity. The incorporation of alkaline metals into HPAs helps to regulate to some extent the dispersion of active species on the support surface, strengthen the water-tolerance and simultaneously adjust the acidity, resulting in increased activity and stability, particularly in polar water medium. In 2012 Haider et. al. [142] found that Cs-doped HSiW supported on a mixture of theta and delta phases of alumina was stable for up to 90-h reaction time and gave a maximum selectivity of 90% acrolein at 100% glycerol conversion. It's suggested that the origin of the long-term stability is related to the strength of the partially doped silicotungstic acid on the alumina support. Doping with Cs maintains the Keggin structure of HSiW, resulting in long-term stability and the high acrolein yield observed. The binding strength of the partially doped silicotungstic acid on the alumina was found to be crucial to sustain the supported Keggin structure and hence the acidity of the active sites resulting in a high acrolein yield. Zhu, et. al. reported that the addition of Cs by ion exchange tunes the acidic properties of HSiW and hence could affect the catalytic performance for glycerol hydrogenolysis [86].

From our previous work, it is reported that the 10Ni/30HSiW/Al<sub>2</sub>O<sub>3</sub> catalyst is a potential candidate for 1-PO production. It is therefore valuable to investigate the effect of Cs<sup>+</sup> substitution to improve the selectivity and stability of the HSiW supported catalysts and to control the acidic properties for glycerol conversion. In the present work, we exchanged protons with the Cs ion for the hydrogenolysis of glycerol to lower alcohols, in particular, to 1-PO. A series of different Cs<sup>+</sup> content of Keggin-type HPAs 10Ni/30H<sub>4-x</sub>Cs<sub>x</sub>SiW/Al<sub>2</sub>O<sub>3</sub> (x=0-4) were prepared and the activity test of catalysts for the hydrogenolysis of glycerol was carried out in a stainless steel batch reactor. The catalysts were characterized using BET, FTIR, XRD and NH<sub>3</sub>-TPD techniques. The effect of Cs<sup>+</sup> exchanged H<sup>+</sup> on the activity of Ni-free 30HSiW/Al<sub>2</sub>O<sub>3</sub> (30Cs<sub>x</sub>H<sub>4-x</sub>SiW/Al<sub>2</sub>O<sub>3</sub>) (x=0-4) catalysts were also studied for comparison.

#### **4.2.1 Experimental conditions**

##### **Catalyst preparation**

The 10Ni30Cs<sub>x</sub>H<sub>4-x</sub>SiW/Al<sub>2</sub>O<sub>3</sub> (or 30Cs<sub>x</sub>H<sub>4-x</sub>SiW/Al<sub>2</sub>O<sub>3</sub>) catalysts were prepared via ion exchange. A set of cesium-exchanged HSiWs were prepared by an ion-exchange method with a

variation of cesium content. A known amount of cesium chloride (CsCl, Sigma-Aldrich) was dissolved in distilled water then added to a desired amount of 10Ni30HSiW/Al<sub>2</sub>O<sub>3</sub> (or 30HSiW/Al<sub>2</sub>O<sub>3</sub> was added to this solution) and aged for 4 hours without mixing. After that, the round bottle with the aged solution was evaporated on an oil bath at 70°C until the solvent evaporated completely. Then the catalyst was dried in an oven at 110°C overnight. Finally, it was calcined at 350°C for 5 h to yield the 10Ni30Cs<sub>x</sub>H<sub>4-x</sub>SiW/Al<sub>2</sub>O<sub>3</sub> (or 30Cs<sub>x</sub>H<sub>4-x</sub>SiW/Al<sub>2</sub>O<sub>3</sub>). Before carrying out an experiment the catalyst was reduced with hydrogen at 350°C for 5 hours.

### **Experimental condition**

The effects of the different cesium (Cs<sup>+</sup>) content on catalytic performance was performed in a 300ml Stainless Steel Parr batch autoclave using 30g glycerol, 70g DI water, 580PSI Hydrogen at 240°C. 700 RPM and 4g of catalysts 10Ni/30Cs<sub>x</sub>H<sub>4-x</sub>SiW/Al<sub>2</sub>O<sub>3</sub> (x=0-4). The main products observed in the liquid phase were: Acetol, 1,2-Propanediol (1,2-PD), 1,3-Propanediol (1,3-PD), 1-Propanol (1-PO) and ethylene glycol (EG). Some other products such as methanol (MeOH), ethanol (EtOH), acrolein (Acr) were also obtained and named as other products (O.P.). The properties of the prepared catalysts were characterized using BET, TPD, XRD and FTIR techniques.

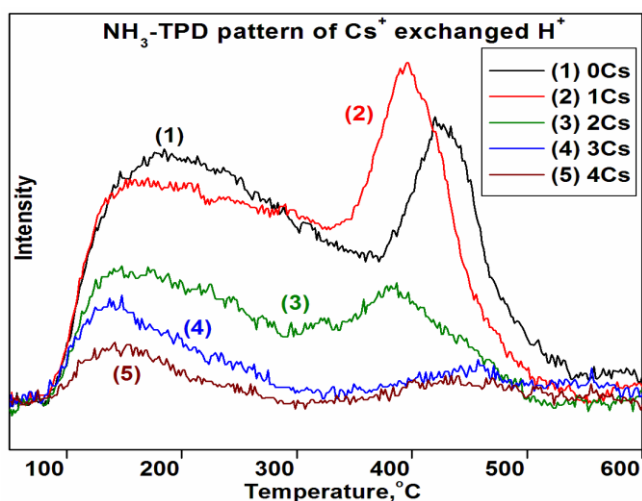
### **Results and discussion**

#### **Characterization of catalysts**

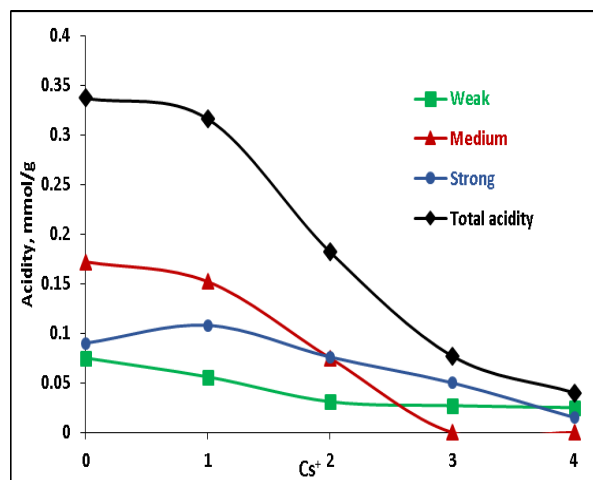
Acid properties of the catalyst with different Cs<sup>+</sup> content were explored by NH<sub>3</sub>-TPD from 50 to 750°C to determine the quantity of acid sites on the catalyst surface and the distribution of acid strength of the catalyst in order, to find a comprehensive correlation between Cs<sup>+</sup> content with catalytic activity and acid property of the 10Ni/30HSiW/Al<sub>2</sub>O<sub>3</sub> catalysts. Fig. 4-6 shows the profiles of NH<sub>3</sub>-TPD desorption from the catalysts. As can be seen, all samples presented a broad profile between 100 and 550°C, revealing that the acid property and surface acid sites were widely distributed and indicating the presence of different acid sites with different strengths. The TPD data was then de-convoluted into 3 peaks (namely weak, medium and strong acid sites) using a Gaussian fitting method and the results are shown in Table 4-4.

Table 4-4 showed that generally  $\text{Cs}^+$  exchanged  $\text{H}^+$  decreases the total acidity of the  $10\text{Ni}/30\text{HSiW}/\text{Al}_2\text{O}_3$  catalyst. When the  $\text{Cs}^+$  loading is less than 1, the acidity is very similar to the parent catalyst with four protons, on further increase in  $\text{Cs}^+$  loading from 1 to 3, the acidity decreases almost linearly and gradually tails off at  $\text{Cs}^+$  loading of 4 when all the protons are replaced nominally (Fig. 4-7). The exchange of  $\text{Cs}^+$  also causes a modification in the distribution of the acid strength of the catalysts. It was found that the strength of medium acid sites was significantly affected by adding  $\text{Cs}^+$ . With a  $\text{Cs}^+$  content from 0 to 2, 3 peaks of weak, medium and strong acid sites were observed, and with further increasing of  $\text{Cs}^+$  to 3 and 4, the medium acid sites significantly diminished and only 2 peaks of weak and strong acid sites remained. It is noticed that the exchange of 3 and 4  $\text{Cs}^+$  resulted in a complete removal of medium acid sites but an increase of the strength of strong acid site as the peak shifts to a higher temperature of  $442^\circ\text{C}$ . The above results clearly showed that these catalysts possess different acid sites, while catalysts with  $0\text{Cs}^+$ ,  $1\text{Cs}^+$  and  $2\text{Cs}^+$  have medium acid sites, catalysts with  $3\text{Cs}^+$  and  $4\text{Cs}^+$  do not. With an increase of  $\text{Cs}^+$  content from 0 to 2, the acid strength of all acid sites (weak, medium and strong) of the catalysts decreased gradually, and the desorbed ammonia peaks of catalysts with  $0\text{Cs}^+$ ,  $1\text{Cs}^+$  and  $2\text{Cs}^+$  shift to lower temperature. It is noticed that there is a significant drop in medium acid sites when 3 protons were substituted by  $3\text{Cs}^+$  or all the 4 protons was totally substituted with  $4\text{Cs}^+$  (the amount of medium acid site almost drop to nearly  $0\text{mmg/g}$  respectively). These results illustrated that  $\text{Cs}^+$  substitution decreases both the amount of acidity and the acid strength of the catalysts. It is believed that  $\text{Cs}^+$  eliminates the acid sites of catalyst by replacing the proton source and an inverse relationship (Table 4-7) is observed between  $\text{Cs}^+$  content and acid concentration on the catalysts.

Surface area of  $10\text{Ni}/30\text{Cs}_x\text{H}_{4-x}\text{SiW}/\text{Al}_2\text{O}_3$  ( $x=0-4$ ) catalyst was determined by BET and presented in Table 4-4. As can be seen the surface area of the  $10\text{Ni}/30\text{HSiW}/\text{Al}_2\text{O}_3$  catalyst increased with the increasing of  $\text{Cs}^+$  content, which was similar to the reports in the literature [143] with an exception of the catalyst with the full substitution of protons where the surface area significantly decreases. This impact of  $\text{Cs}^+$  ions on surface area has also been reported for  $\text{Cs}^+$  exchanged  $\text{HSiW}$  on silica and aluminosilicate supports [144]. It is noticed that, although the substitution of proton by  $\text{Cs}^+$  increases the surface area slightly, it does not increase the acidity of the catalyst to any extent.



**Figure 4-6** NH<sub>3</sub>-TPD patterns for different Cs<sup>+</sup> exchanged H<sup>+</sup>



**Figure 4-7** Effect of different Cs<sup>+</sup> content on acidity of catalyst

**Table 4-4** Surface area and total acidity of 10Ni/30Cs<sub>x</sub>H<sub>4-x</sub>Si W/Al<sub>2</sub>O<sub>3</sub> catalyst

Catalyst	BET, m <sup>2</sup> /g	Weak acid site mmol/g / (Temp.)	Medium acid site mmol/g / (Temp.)	Strong acid site mmol/g / (Temp.)	Total acid amount, mmol/g
10Ni/30H <sub>4</sub> SiW/Al <sub>2</sub> O <sub>3</sub>	18.3	0.075/ (160°C)	0.172/ (264°C)	0.090/ (429°C)	0.337
10Ni/30Cs <sub>1</sub> H <sub>3</sub> SiW/Al <sub>2</sub> O <sub>3</sub>	22.5	0.056/ (151°C)	0.152/ (258°C)	0.108/ (400°C)	0.316
10Ni/30Cs <sub>2</sub> H <sub>2</sub> SiW/Al <sub>2</sub> O <sub>3</sub>	27.5	0.031/ (151°C)	0.075/ (213°C)	0.076/ (382°C)	0.182
10Ni/30Cs <sub>3</sub> H <sub>1</sub> SiW/Al <sub>2</sub> O <sub>3</sub>	29.1	0.027/ (152°C)	-	0.050/ (442°C)	0.077
10Ni/30Cs <sub>4</sub> SiW/Al <sub>2</sub> O <sub>3</sub>	17.6	0.025/ (155°C)	-	0.015/ (442°C)	0.040

Heteropoly anions (primary structure of oxoanions) can be determined by FT-IR that is an informative fingerprint of the Keggin heteropoly cage structure to confirm the structural integrity of the Keggin unit of these catalysts. The FTIR spectra of Keggin anions present in the catalyst should appear between 700 and 1100cm<sup>-1</sup> [145].

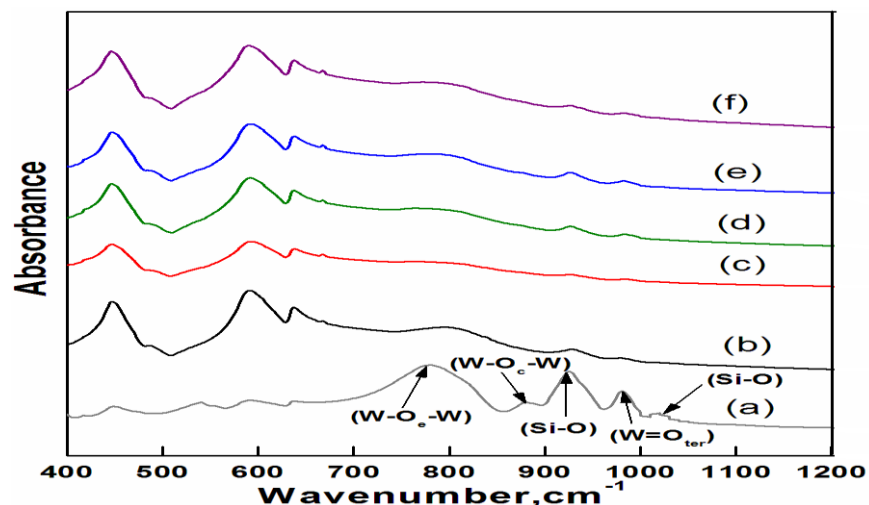


**Figure 4-8** FT-IR spectra of (a) 30HSiW/Al<sub>2</sub>O<sub>3</sub>, (b) 10Ni/30HSiW/Al<sub>2</sub>O<sub>3</sub>, (c) 10Ni/30Cs<sub>1</sub>H<sub>3</sub>SiW/Al<sub>2</sub>O<sub>3</sub>, (d) 10Ni/30Cs<sub>2</sub>H<sub>2</sub>SiW/Al<sub>2</sub>O<sub>3</sub>, (e) 10Ni/30Cs<sub>3</sub>H<sub>1</sub>SiW/Al<sub>2</sub>O<sub>3</sub> and (f) 10Ni/30Cs<sub>4</sub>SiW/Al<sub>2</sub>O<sub>3</sub>.

Fig. 4-8 shows the infrared spectra of the catalyst with different Cs<sup>+</sup> content after calcination at 350°C. The fingerprint bands of the HSiW Keggin anion appeared at 978, 915, and 798 cm<sup>-1</sup>, which could be assigned to the typical antisymmetric stretching vibrations of W=O, Si-O, and W-O<sub>e</sub>-W (W-O<sub>e</sub> - stretch vibration of W-O<sub>6</sub> octahedrons that share a vertex or an edge) [145] was observed which provided the evidence for the retention of the Keggin ion structure on the surface of HSiW supported catalysts. These results indicate that the Keggin structure of catalyst remains unaltered after substitution of H<sup>+</sup> by Cs<sup>+</sup> on 10Ni/30HSiW/Al<sub>2</sub>O<sub>3</sub> catalyst.

To help elucidate if the structural transformations accompany Cs<sup>+</sup> doping, the 10Ni/30Cs<sub>x</sub>H<sub>4-x</sub>SiW/Al<sub>2</sub>O<sub>3</sub> samples were also examined by powder XRD. The XRD pattern of Cs<sup>+</sup> content was depicted in the Fig. 4-9.

Fig. 4-9 provides clear evidence that recrystallization of the 10Ni/30Cs<sub>x</sub>H<sub>4-x</sub>SiW/Al<sub>2</sub>O<sub>3</sub> catalyst accompanies Cs<sup>+</sup> doping, consistent with proton exchange. As seen from the XRD pattern without adding Cs<sup>+</sup> the diffraction peaks that have been assigned to the protons of the secondary structure were observed at 2θ=7.5°, 8.9°, 9.3°, 28.5°, 29.0°. With increasing Cs<sup>+</sup> substitution, a variation in the diffraction peaks was observed. It can be seen that when the amount of hydrogen protons decreased, the intensity of the diffraction peaks assigned to the hydrogen protons decreased also. This result is consistent with that published by Guo et. al where an increase of Cs<sup>+</sup> content increased the surface area of the HPAs while the acidity decreased due to substitution of protons



by  $\text{Cs}^+$  [146]. Meanwhile the diffraction peaks that are assigned to  $\text{Cs}^+$  substituted HSiW were observed with  $2\theta$  diffraction bands at  $10.7^\circ$ ,  $18.5^\circ$ ,  $23.9^\circ$ ,  $26.2^\circ$ ,  $30.4^\circ$ ,  $35.8^\circ$  and  $39^\circ$ . The intensity of these increased with increasing  $\text{Cs}^+$  content. As a result,  $\text{Cs}^+$  containing catalysts had better crystal stability than those without  $\text{Cs}^+$ . Moreover, the greater content of  $\text{Cs}^+$  corresponded to a more stable crystal structure [143, 147] due possibly to the modification of the crystal structure of HSiW by the larger  $\text{Cs}^+$  radius. There is no evidence of new peaks that suggest changes in the Keggin structure.

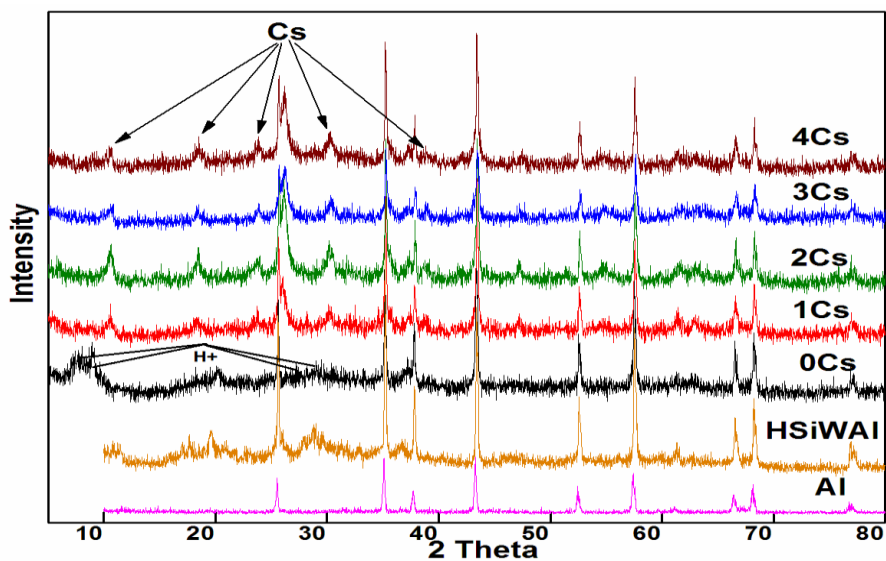


**Figure 4-9** XRD patterns for the  $10\text{Ni}/30\text{Cs}_x\text{H}_{4-x}\text{SiW}/\text{Al}_2\text{O}_3$  catalysts with different  $\text{Cs}^+$  content

### Activity test results

To investigate the effect of  $\text{Cs}^+$  on the catalyst performance in the hydrogenolysis of glycerol, a series of different  $\text{Cs}^+$  exchanged  $10\text{Ni}/30\text{Cs}_x\text{H}_{4-x}\text{SiW}/\text{Al}_2\text{O}_3$  ( $x=0-4$ ) catalysts were carried out in a batch reactor for the conversion of an aqueous solution of a 30 wt% glycerol initial concentration under an initial  $\text{H}_2$  pressure of 880 PSI. The main products observed in the liquid phase were: acetol (Ac), 1,2-PD, 1,3-PD, 1-PO and ethylene glycol (EG). Some other products such as methanol (MeOH), ethanol (EtOH) and minor Acrolein (Acr) were also obtained in these experiments. Catalytic performance of the  $10\text{Ni}/30\text{Cs}_x\text{H}_{4-x}\text{SiW}/\text{Al}_2\text{O}_3$  catalysts is shown in Table 4-5 and Fig. 4-10.

**Table 4-5** Effect of Cs<sup>+</sup> on catalytic performance in the hydrogenolysis of Glycerol

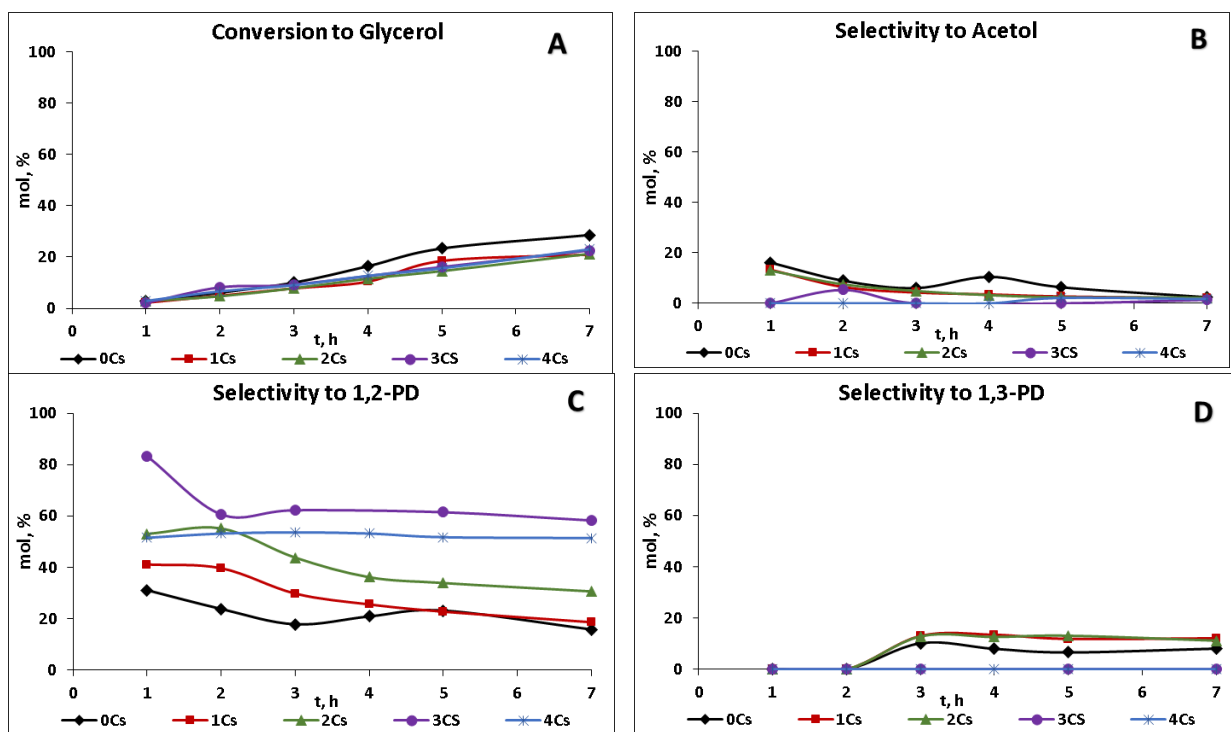
Catalyst	Conv mol%	Selectivity, mol%						
		1,3-PD	1,2-PD	Ac	EG	1-PO	EtO	MeOH
10Ni/30HSiW/Al <sub>2</sub> O <sub>3</sub>	28.6	8.0	15.8	2.4	5.4	65.1	3.3	0.0
10Ni/30Cs <sub>1</sub> H <sub>3</sub> SiW/Al <sub>2</sub> O <sub>3</sub>	21.0	12.1	18.5	2.0	6.5	58.1	2.8	0.0
10Ni/30Cs <sub>2</sub> H <sub>2</sub> SiW/Al <sub>2</sub> O <sub>3</sub>	21.3	11.2	30.6	2.3	10.9	42.4	2.6	0.0
10Ni/30Cs <sub>3</sub> H <sub>1</sub> SiW/Al <sub>2</sub> O <sub>3</sub>	22.6	0.0	58.2	1.4	21.7	12.5	5.1	1.1
10Ni/30Cs <sub>4</sub> SiW/Al <sub>2</sub> O <sub>3</sub>	23.1	0.0	51.4	1.7	29.5	4.7	9.8	2.9

**Reaction Condition:** 10Ni/30Cs<sub>x</sub>H<sub>4-x</sub>SiW<sub>10</sub>/Al<sub>2</sub>O<sub>3</sub> (x=0-4) catalyst, 240°C, 700RPM, 4g catalyst, 30g of glycerol (30wt%), 70g of DI water and 880PSI of H<sub>2</sub>, 7hours.

As seen in Table 4-5, significant difference in product distribution with respect to different Cs<sup>+</sup> substituted catalysts was observed, although Cs<sup>+</sup> has little effect on glycerol conversion. When 1H<sup>+</sup> was substituted by 1Cs<sup>+</sup>, the glycerol conversion decreases from 28.6% to around 21%; however no significant decrease in the conversion of glycerol was observed for higher concentration of Cs<sup>+</sup> exchanged catalysts (x=2,3,4). The pseudo first order rate constant for the conversion of glycerol also indicates the same reactivity trend [Fig. 4-10H]. This reactivity trend was similar to the trend in the strength of weak acid sites. However there is a clear correlation between product distribution and the number of H<sup>+</sup> exchanged by Cs<sup>+</sup>. The increase in the selectivity of 1,2-PD and EG was observed for all the catalysts containing Cs<sup>+</sup>. This result suggests that the formation of 1,2-PD and EG may be due to a competitive cleavage between the C–O bonds and C–C bonds in the rate determining steps. Increasing the number of H<sup>+</sup> substituted by Cs<sup>+</sup> increased the selectivity to EG and 1,2-PD while the selectivity to 1,3-PD and 1-PO decreased. The selectivity to 1-PO was observed to decrease (from 65% to 4.7%) by increasing Cs<sup>+</sup> substitution from 0 to 4, while that of the 1,2-PD and EG increased from about 20% to 52.1% and from 6.3% to 29.9% respectively. This result indicates that selectivity to 1-PO favorably occurred at low loading of Cs<sup>+</sup>. At high content of Cs<sup>+</sup> the elimination of proton of the heteropolyacids apparently suppress the further hydrogenolysis of 1,2-PD to 1-PO. Such changes in selectivity could be attributed to the changes in the acidity of catalysts. It is clear from Table 4-4 that an inverse correlation is observed between Cs<sup>+</sup> content and the acidity distribution and amount over a HSiW supported 10Ni/Al<sub>2</sub>O<sub>3</sub> catalyst. It was also noticed that the fully substituted

(10Ni/30Cs<sub>4</sub>SiW/Al<sub>2</sub>O<sub>3</sub>) catalyst (i.e. 4H<sup>+</sup> substituted by 4 Cs<sup>+</sup>) with low amount of acid sites is essentially inactive for the production of 1-PO (selectivity to 1-PO was 4.7%). It is important to point out that at a high level of Cs<sup>+</sup> substitution (at 3 and 4 Cs<sup>+</sup> substitution), no 1,3-PD was detected. Therefore the hydrogenolysis of glycerol from 1,3-PO requires Brønsted acid sites.

Fig. 4-10 shows the catalytic performance of the 10Ni/30Cs<sub>x</sub>H<sub>4-x</sub>SiW/Al<sub>2</sub>O<sub>3</sub> catalyst for the hydrogenolysis of glycerol as a function of reaction time. It can be seen that as the reaction proceeds, the conversion of glycerol and the selectivity of 1-PO gradually increase. The selectivity of 1,2-PD (the intermediate for 1-PO) increases at the beginning of the reaction and then slightly decreases with the reaction time. Interestingly, 1,3-PD was not detected at the first hour of sampling but observed during the 2<sup>nd</sup> hour of sampling indicating that it is produced from an intermediate such as 3-HPA. 1,3-PD does not convert to 1-PO readily and hence remains fairly constant after it is produced [219]. Increasing the Cs<sup>+</sup> content in the catalyst increases not only the selectivity to EG but also the formation rate of this product; the more Cs<sup>+</sup> substituted H<sup>+</sup>, the sooner EG was formed [Fig. 4-10G]. Clearly, the selectivity to 1,2-PD and EG essentially increased with an increase in Cs<sup>+</sup>. Hence it can be inferred that acidity plays an important role in the hydrogenolysis of propanediols to 1-PO.



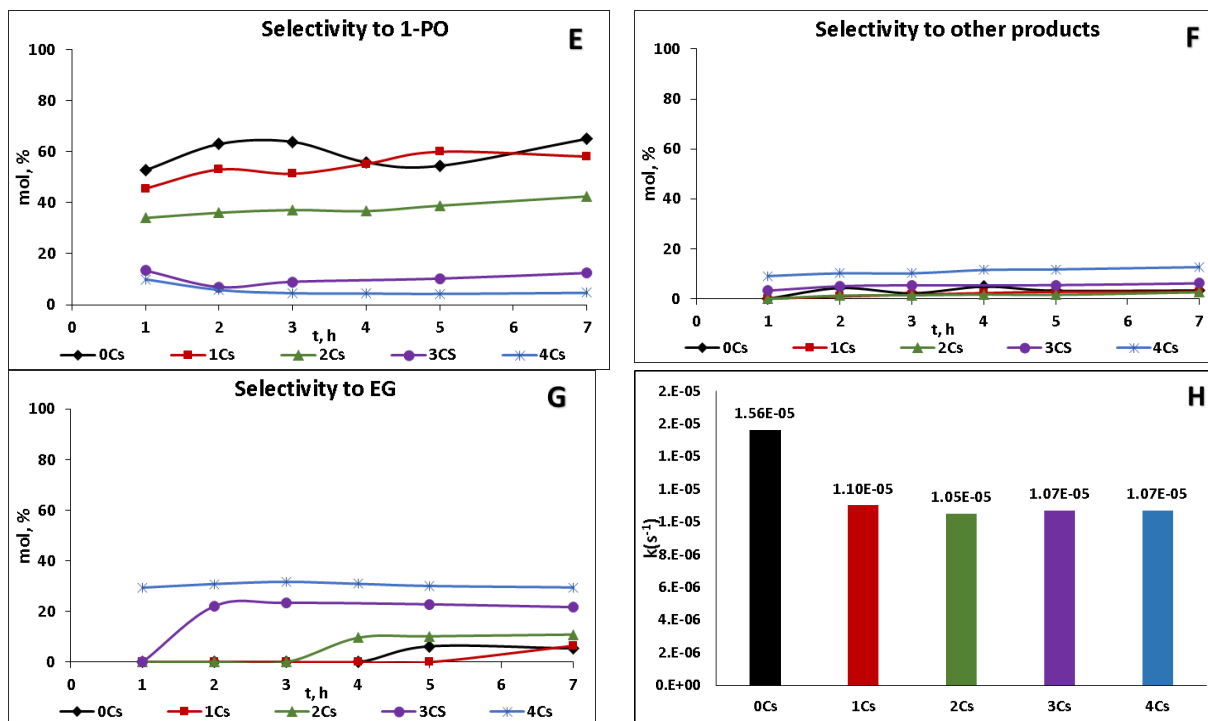


**Figure 4-10** Effect of Cs<sup>+</sup> on Glycerol Hydrogenolysis and products selectivity as a function of time; A) Glycerol Conversion; B,C,D,E,F,G) Selectivity of acetol, 1,2-PD, 1,3-PD, 1-PO, other products and EG, Cs, respectively; H) The Pseudo-First-Order rate constant k. **Reaction conditions:** 10Ni/30Cs<sub>x</sub>H<sub>4-x</sub>SiW/Al<sub>2</sub>O<sub>3</sub> (x=0-4) catalyst, 240°C, 700RPM, 4g catalyst, 30g of glycerol (30wt%), 70g of DI water and 880PSI of H<sub>2</sub>, 7hours

One possible explanation of the Cs<sup>+</sup> effect on EG selectivity may be due to the promotion of the retro-aldol reaction. The formation of 1,2-PD and EG from glycerol under alkaline conditions was reported by many authors [148-151], This reaction route involves a reversible dehydrogenation of glycerol to glyceraldehyde (GA) on the metal surface. The product of the dehydrogenation reaction can then undergo a C–O scission by dehydration or a C–C scission via the retro-aldol mechanism in the aqueous phase to form 1,2-PD or EG respectively.

As shown from the experimental data, apparently the Cs-free (10Ni/30HSiW/Al<sub>2</sub>O<sub>3</sub>) catalyst favored the C–O bond breakage leading to the formation of 1,2-PD, 1,3-PD and 1-PO instead of EG. However, the catalysts with higher Cs<sup>+</sup> substitution favored the cleavage of the C–C bond to produce EG attributed to the decrease in the acidity of the catalyst. Moreover, the high EG selectivity was obtained over high Cs<sup>+</sup>, which might originate from the decrease in acidity of the catalyst.

To reveal the effect of Cs<sup>+</sup> alone on the catalyst without the Ni hydrogenation function, a series of different Cs<sup>+</sup> exchanged Ni-free 30HSiW/Al<sub>2</sub>O<sub>3</sub> (30Cs<sub>x</sub>H<sub>4-x</sub>SiW/Al<sub>2</sub>O<sub>3</sub>) catalysts were prepared and the activity of the catalysts were studied in a batch reactor for the conversion of an aqueous solution of a 30 wt% glycerol initial concentration under an initial H<sub>2</sub> pressure of 880 PSI.

The catalytic performance of 30Cs<sub>x</sub>H<sub>4-x</sub>SiW/Al<sub>2</sub>O<sub>3</sub> catalysts modified by different Cs<sup>+</sup> substitution are presented in the Table 4-6. As can be seen from Table 4-6, the support Al<sub>2</sub>O<sub>3</sub> alone is not active for glycerol conversion. The Ni-free (30HSiW/Al<sub>2</sub>O<sub>3</sub>) catalyst is not active for the production of diols such as 1,2-PD, 1,3-PD or EG. Furthermore the catalyst was deactivated significantly after 2 or more H<sup>+</sup> were substituted by Cs<sup>+</sup>. The conversion of glycerol decreased from 15.3% to only 1.1 % when all the H<sup>+</sup> was substituted by Cs<sup>+</sup>. This was also observed by Haider et. al. for the catalytic dehydration of glycerol to acrolein [142]. It was found that over a 0.05 M Cs<sup>+</sup>-doped HSiW catalysts, a selectivity of acrolein of 96% at 100% glycerol conversion was obtained. However, the catalyst was deactivated when the concentration of Cs<sup>+</sup> increased to 0.35M and that of selectivity to acrolein of 0% at 2% glycerol conversion was obtained. This loss of catalytic activity may be due to hydrocarbons deposited on the active sites and/or blockage of the catalyst pores. Without Ni for hydrogenation of the dehydrated or dehydrogenated intermediates shown in Scheme 1 and 2, only further cracking or oligomerization to light and heavy products will occur and cause catalyst deactivation.

**Table 4-6** Effect of Cs<sup>+</sup> on catalytic performance of 30HSiW/Al<sub>2</sub>O<sub>3</sub> catalyst in the Hydrogenolysis of Glycerol

Catalyst	Conv. mol%	Selectivity, mol%						
		1,3-PD	1,2-PD	Acetol	EG	1-PO	Acr	OP
Al <sub>2</sub> O <sub>3</sub>	0.0	0.0	0.0	0.0	0.0	0.0	0.0	0.0
30HSiW/Al <sub>2</sub> O <sub>3</sub>	15.3	0.0	0.0	6.0	0.0	30.5	24.8	36.7**
30Cs <sub>1</sub> H <sub>3</sub> SiW/Al <sub>2</sub> O <sub>3</sub>	13.2	0.0	0.0	6.0	0.0	35.4	26.8	31.8*
30Cs <sub>2</sub> H <sub>2</sub> SiW/Al <sub>2</sub> O <sub>3</sub>	4.8	0.0	0.0	13.8	0.0	21.9	47.9	16.1*
30Cs <sub>3</sub> H <sub>1</sub> SiW/Al <sub>2</sub> O <sub>3</sub>	2.6	0.0	0.0	19.1	0.0	31.5	48.0	1.5*
30Cs <sub>4</sub> SiW/Al <sub>2</sub> O <sub>3</sub>	1.1	0.0	0.0	27.5	0.0	40.4	31.0	1.2*

**Reaction Condition:**  $30\text{Cs}_x\text{H}_{4-x}\text{SiW}_{10}/\text{Al}_2\text{O}_3$  ( $x=0-4$ ) catalyst,  $240^\circ\text{C}$ , 700RPM, 4g catalyst, 30g of glycerol (30wt%), 70g of DI water and 880PSI of  $\text{H}_2$ , 7hours. \*OP: MeOH, EtOH, Unidentified light products, \*\*OP: MeOH, EtOH, Unidentified light and heavy products

## Summary

Results of the runs with different  $\text{Cs}^+$  loading suggested that  $\text{Cs}^+$  has little effect on the glycerol conversion; however it shows a significant effect on the product distribution – due to reduction of acidity. The  $10\text{Ni}/30\text{HSiW}/\text{Al}_2\text{O}_3$  catalyst was found to be an effective catalyst for the production of 1-PO, whereas,  $\text{Cs}^+$  exchanged catalyst becomes effective for the production of 1,2-PD and EG. With an increase in  $\text{Cs}^+$  content, the selectivity for 1-PO decreases but the selectivity to 1,2-PD and EG increases. A greater quantity of acid sites of a certain strength corresponded to a higher selectivity of 1-PO. Although the substitution of proton by  $\text{Cs}^+$  can improve the surface area of the catalyst to some extent, it does not enhance the catalyst activity; besides there was an inverse correlation between  $\text{Cs}^+$  and the quantity and nature of acid sites. XRD data shows that hydrogen protons in the secondary structure may be replaced by  $\text{Cs}^+$  that corresponds to the decrease in the acidity of the catalyst. Although the acidity of catalyst decreases significantly, the Keggin structure of catalyst remains unaltered after substitution of protons by  $\text{Cs}^+$  on  $10\text{Ni}/30\text{HSiW}/\text{Al}_2\text{O}_3$ . Among the catalysts tested,  $1\text{Cs}^+$  catalyst showed the best catalytic performance for 1,3-PD and 1-PO; however, fully substituted  $10\text{Ni}/30\text{Cs}_4\text{SiW}/\text{Al}_2\text{O}_3$  is catalytically inert for production of 1-PO as it possesses very low acid sites. Ni plays an important role for the production of lower alcohols due to its hydrogenation activity. Without Ni, the substitution of  $\text{H}^+$  by  $\text{Cs}^+$  decreases the activity of  $30\text{HSiW}/\text{Al}_2\text{O}_3$  significantly.

## 4.3 Conclusions

Among the metals (Cu, Ni, Pd, and Pt) supported on  $30\text{HSiW}/\text{Al}_2\text{O}_3$ , Pt is the best promoter for the production of 1,3-PD from glycerol using. Ni a much cheaper metal has fairly comparable reactivity to Pt. Although it is reported that Cu possesses good hydrogenation activity that is comparable with Ni, Cu does not show activity for the production of 1,3-PD under this reaction conditions.

Cs<sup>+</sup> has little effect on the glycerol conversion; however it shows a significant effect on the product distribution – due to reduction of acidity. The 10Ni/30HSiW/Al<sub>2</sub>O<sub>3</sub> catalyst was found to be an effective catalyst for the production of 1-PO, whereas, the Cs<sup>+</sup> exchanged catalyst becomes effective for the production of 1,2-PD and EG. A greater quantity of acid sites of a certain strength corresponded to a higher selectivity of 1-PO. XRD data shows that hydrogen protons in the secondary structure may be replaced by Cs<sup>+</sup> that corresponds to a decrease in the acidity of the catalyst. Among the catalysts tested, 1Cs<sup>+</sup> catalyst showed the best catalytic performance for 1,3-PD and 1-PO; however, fully substituted NiCs<sub>4</sub>SiW<sub>12</sub>O<sub>40</sub> is catalytically inert for the production of 1-PO as it possesses very low acid sites.

Ni plays an important role for the production of lower alcohols due to its hydrogenation activity. Without Ni, the substitution of H<sup>+</sup> by Cs<sup>+</sup> decreases the activity of 30HSiW/Al<sub>2</sub>O<sub>3</sub> significantly. To obtain a desired product selectively, the control of reaction conditions and catalyst properties such as acid strength, the amount of appropriate acid sites and metal hydrogenation activity will be needed. Optimization of the catalyst preparation techniques and a balance of Ni and HSiW loading on various supports could lead to high yields of value-added chemicals from glycerol. 1-PO is mainly produced from 1,2-PD with a high conversion of 1,2-PD and high selectivity to 1-PO and 1-PO is stable under the reaction condition and is assumed as the final product in the hydrogenolysis of glycerol using 10Ni/30HSiW/Al<sub>2</sub>O<sub>3</sub>. Due to the inexpensive Ni-based catalyst and the high selectivity, an economical production of green and sustainable 1-PO from glycerol hydrogenolysis may be feasible for future commercial development.

## Chapter Five

### Conversion of glycerol to lower alcohols using 10Ni/30HSiW/Al<sub>2</sub>O<sub>3</sub> catalyst in a Hastelloy reactor

With some chemicals, notably acids, metal loss over the entire surface from the steel reactor may occur and affect the entire experiment. The 10Ni/30HSiW/Al<sub>2</sub>O<sub>3</sub> catalyst is a potential catalyst for the production of higher sustainable chemicals from glycerol. However the leaching of heteropoly species in a polar media is an issue. Due to the high acidity of the heteropoly acid, a corrosion-resistant Hastelloy reactor was used for this study on the effect of process parameters on the conversion and selectivity. Ni and HSiW supported alumina can serve as bifunctional catalysts to effectively convert glycerol in a water medium under a hydrogen atmosphere. The strong acidity of the supported HSiW facilitates the dehydration of glycerol while the moderate hydrogenation activity of Ni allows selective hydrogenation of the aldehyde groups in the intermediate products. In this study, we study the effect of different factors on the catalytic performance.

#### 5.1 Repeatability of 10Ni/30HSiW/Al<sub>2</sub>O<sub>3</sub> Catalyst

A repeatability study of the catalyst with 10Ni/30HSiW/Al<sub>2</sub>O<sub>3</sub> has been carried out using 95% confidence interval to ensure the experimental error is acceptable. Three experiments with this catalyst were conducted under the same reaction conditions. The 95% confidence interval (C.I.) and the standard deviation ( $\sigma$ ) is calculated using Equation 5-1 and Equation 5-2 and the results are shown in Table 5-1.

$$95\% C.I. = \left[ \bar{x} - 1.96 \times \frac{\sigma}{\sqrt{n}}, \bar{x} + 1.96 \times \frac{\sigma}{\sqrt{n}} \right] \quad \text{Equation 5-1}$$

$$\sigma = \left( \sqrt{\frac{\sum (x_i - \bar{x})^2}{n}} \right) \quad \text{Equation 5-2}$$



**Table 5-1** Repeatability study on 10Ni/30HSiW/Al<sub>2</sub>O<sub>3</sub> catalyst

Run	Glycerol Conversion	1-PO Sel	1-PO Yield	Acetol Sel	1,2-PD Sel.	OP Sel
$x_1$	67.43	93.22	62.85	0.72	1.35	4.71
$x_2$	65.43	91.21	59.68	0.78	1.53	6.48
$x_3$	67.42	91.20	61.49	0.55	1.71	6.54
$\bar{x}$	66.76	91.88	61.34	0.68	1.53	5.91
$\sigma$	0.94	0.95	1.30	0.10	0.14	0.85
$\frac{\sigma}{\sqrt{n}}$	0.54	0.55	0.75	0.06	0.08	0.49
95% C.I.	66.76±1.06	91.88±1.07	61.34±1.47	0.68±0.11	1.53±0.16	5.91±0.96

**Reaction condition:** 10Ni/30HSiW/Al<sub>2</sub>O<sub>3</sub> catalyst, 240°C, 880PSI initial H<sub>2</sub>, 30wt% (30g) Glycerol, 2g catalyst, 7 hours.

As shown in Table 5-1, the selected catalyst exhibit perfect reproducibility in the hydrogenolysis reaction and the 95% confidence interval for 1-PO selectivity using the 10Ni/30HSiW/Al<sub>2</sub>O<sub>3</sub> catalyst is [90.80%; 92.95%]

## 5.2 Effect of experimental parameters

### 5.2.1 Effect of RPM

Due to the existence of a three-phase reaction, gas-liquid, liquid-solid, and intra particle diffusional resistances may influence the rate and selectivity of the chemical reaction [152]. It is thought that the increase in stirring rate can increase the mass transfer of gases into liquid and also from liquid to solid surface that leads to increase in the dissolution rate of H<sub>2</sub>. Here the effect of the stirring speed on the reaction rate of hydrogenolysis of glycerol was investigated.

### Experiment condition

The effect of agitator speed on the overall reaction was examined by varying the agitation speed over the range of 300 RPM to 700RPM under otherwise same reaction conditions. The experiment was performed at 240°C under 580PSI of H<sub>2</sub> pressure using 2g of 10Ni/30HSiW/Al<sub>2</sub>O<sub>3</sub> catalyst, 30g of glycerol (30wt %), 70g of DI water over 7hours. Two catalysts reduced at different temperature were studied. One was reduced at 350°C and another was reduced at 450°C for 5 hours.

## Results and discussion

First the catalysts reduced at 350°C were studied. The results obtained from the hydrogenolysis of glycerol at different agitation speed are presented in the Table 5-2 (Entry 1 to 3) and plotted in Fig. 5-1 and Fig. 5-2. The main products observed in the liquid phase were: acetol, 1,2-PD, 1,3-PD, acrolein (Acr), 1-PO and ethylene glycol (EG). Some other products (OP) such as methanol, ethanol were also obtained. The data shows that using the catalyst reduced at 350°C the agitation speed did affect the conversion of glycerol and the distribution of products. When the speed of agitator was increased from 300RPM to 500RPM, the conversion of glycerol increased from 65% to 84% and the selectivity to 1-PO increased from 87.2 to 91.8% respectively; where as, the selectivity to acetol, 1,2-PD and Acr as intermediate species decreased. A further increase in stirrer speed to 700 RPM did not affect the conversion and selectivity. This indicated that at 500RPM external mass transfer effects were eliminated.

**Table 5-2** Effect of agitator speed on the reaction rate and the distribution to products in the hydrogenolysis of Glycerol

Red. Temp	RPM	Conv mol%	Selectivity, mol%						
			13PD	12PD	Acetol	EG	1-PO	Acr	OP
350	300	64.9	0.0	1.3	0.9	0.0	87.2	5.1	5.6
	500	84.3	0.0	0.0	0.5	0.0	91.8	3.8	3.9
	700	81.1	0.0	0.0	0.6	0.0	90.6	3.7	5.1
450	300	41.2	0.0	3.0	1.9	0.0	80.4	9.6	5.0
	700	43.8	0.0	2.9	1.2	0.0	80.9	5.4	9.5

**Reaction Condition:** 10Ni/30HSiW/Al<sub>2</sub>O<sub>3</sub> catalyst, 240°C, 700RPM, 2g catalyst, 30g of glycerol (30wt%), 70g of DI water and 580PSI of H<sub>2</sub>. OP: By-products included methanol and ethanol.

Fig. 5-1 depicts the concentration profile as a function of time of the catalyst reduced at 350°C. From Fig. 5-1, it can be observed that as the reaction proceeds, the concentration of glycerol decreases and the concentration of 1-PO increases. Since the concentration of acetol, 1,2-PD and Acr was too low to be observed from Fig. 5-1, the concentration profile of acetol, 1,2-PD and Acr are depicted separately in Fig. 5-2 to find the correlation between the intermediate species and the speed of agitation.

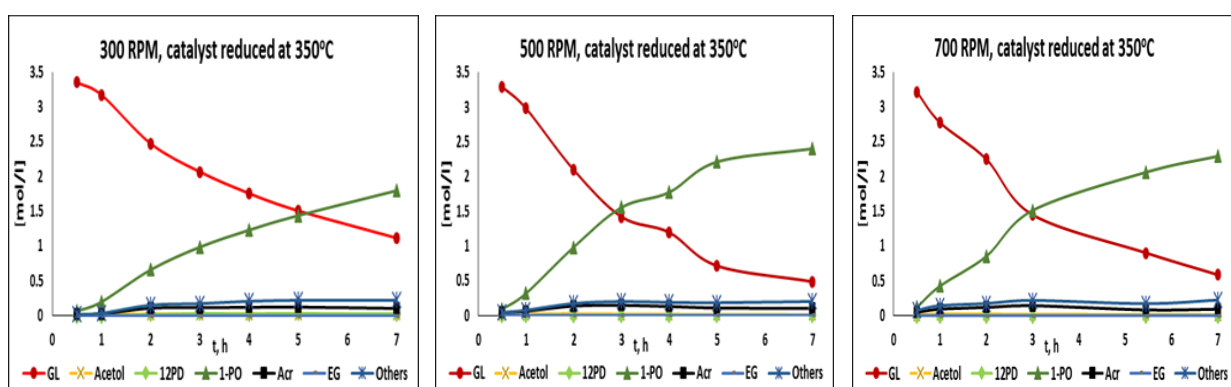


**Figure 5-1** Concentration profiles of different products using 10Ni/30HSiW/Al<sub>2</sub>O<sub>3</sub> catalyst reduced at 350°C. **Reaction conditions:** 240°C, 580 H<sub>2</sub>, 30g of glycerol (30wt %), 70g of DI water, 2g catalyst

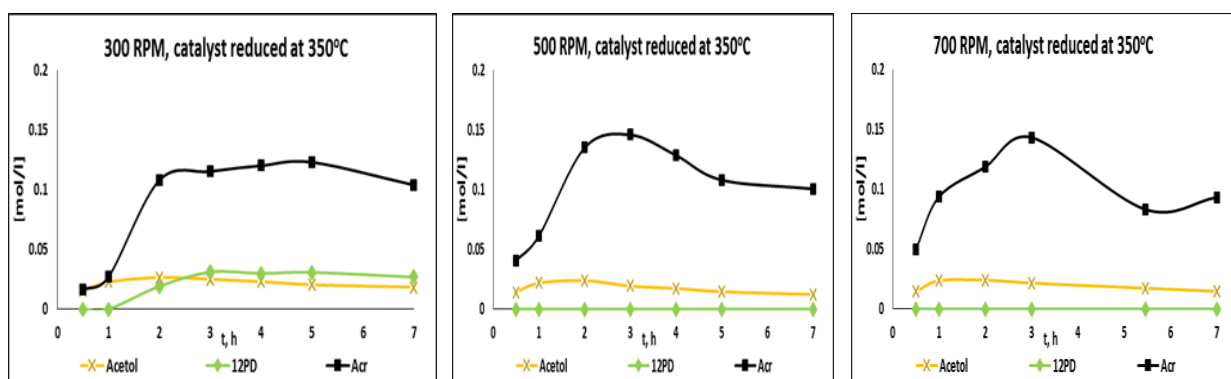


**Figure 5-2** Concentration profiles of acetol, 12-PD and Acr using 10Ni/30HSiW/Al<sub>2</sub>O<sub>3</sub> catalyst reduced at 350°C. **Reaction conditions:** 240°C, 580 H<sub>2</sub>, 30g of glycerol (30wt%), 70g of DI water, 2g catalyst

As can be seen in Fig. 5-2, the concentration of acetol and Acr, intermediates to 1,2-PD and 1-PO respectively, increases at the beginning of the reaction and then decreases with the reaction time and did not depend on the agitation speed. However, the pattern of 1,2-PD concentration is not similar to acetol concentration. When the agitation speed is low at 300RPM, 1,2PD is still detectable and the concentration of 1,2-PD as the intermediate of 1-PO increases at the beginning of the reaction and then decreases with the reaction time. However, when the speed was increased to 500RPM, 1,2-PD became undetectable. Furthermore an increase in the agitation speed to 700 RPM did not result in an increase in the conversion of glycerol; however it still affected the product distribution slightly and 1,2-PD was also undetectable. The selectivity to 1-PO slightly decreases while the selectivity to by products increases. This decrease in the 1-PO selectivity could be due to the formation of by-products such as methanol and ethanol through side reactions.

Results showed that a speed of 500RPM is sufficient to allow further hydrogenolysis of 1,2-PD or hydrogenation of Acr to 1-PO but not increase the side reactions to produce by products. There are always other by-products formed during the reaction time. The pseudo-first-order rate constant also provides evidence of the effect of stirring speed on the reaction rate (Fig. 5-3).

Catalysts reduced at 450°C were also studied to see if the stirring speed still affects the hydrogenolysis of glycerol. The data is presented in the Table 5-2 (entry 4 and 5). It is evident that increasing the reduction temperature decreases the catalyst activity significantly; however the performance of the catalyst was independent of agitation speed over the range of 300 RPM to 700 RPM, and the reaction rate is almost identical (Fig. 5-3). It is noted that the agitation speed did not result in a change in both the conversion of glycerol and the distribution of products; the conversion of both catalysts is around 42%.

Normally, if a process is controlled by diffusion, the reaction rate would also linearly increase with increasing stirring speed; whereas if the process was controlled by chemical reaction, reaction rate will no longer change when the stirring speed reaches a certain value [153]. In the case of when the catalyst is reduced at 350°C, as can be observed from the data when the stirring speed was lower than 500 RPM, the reaction rate constant  $k$  increases with stirring speed increasing, the glycerol concentration decreased faster at 500-700 RPM compared with 300 RPM (Fig. 5-3). When the stirring speed was over 500 rpm, the reaction rate constant  $k$  seems to be constant and does not change much with stirring speed.

By increasing stirring rate, the mass transfer of reactants (glycerol, H<sub>2</sub>) from the bulk to catalyst surface is increased. The H<sub>2</sub> was supplied continuously throughout the entire experiment so the quantity of H<sub>2</sub> was sufficient for the entire experiment. Therefore most probably the rate of reaction at stirring rates higher than 500 RPM is controlled by a surface reaction and mass transfer should not be an issue. However, a similar phenomenon was not observed on the catalyst reduced at 450°C and it is suggested that the rate of reaction of this catalyst is controlled by the surface reaction even at 300 RPM since the conversion is slower for this catalyst.

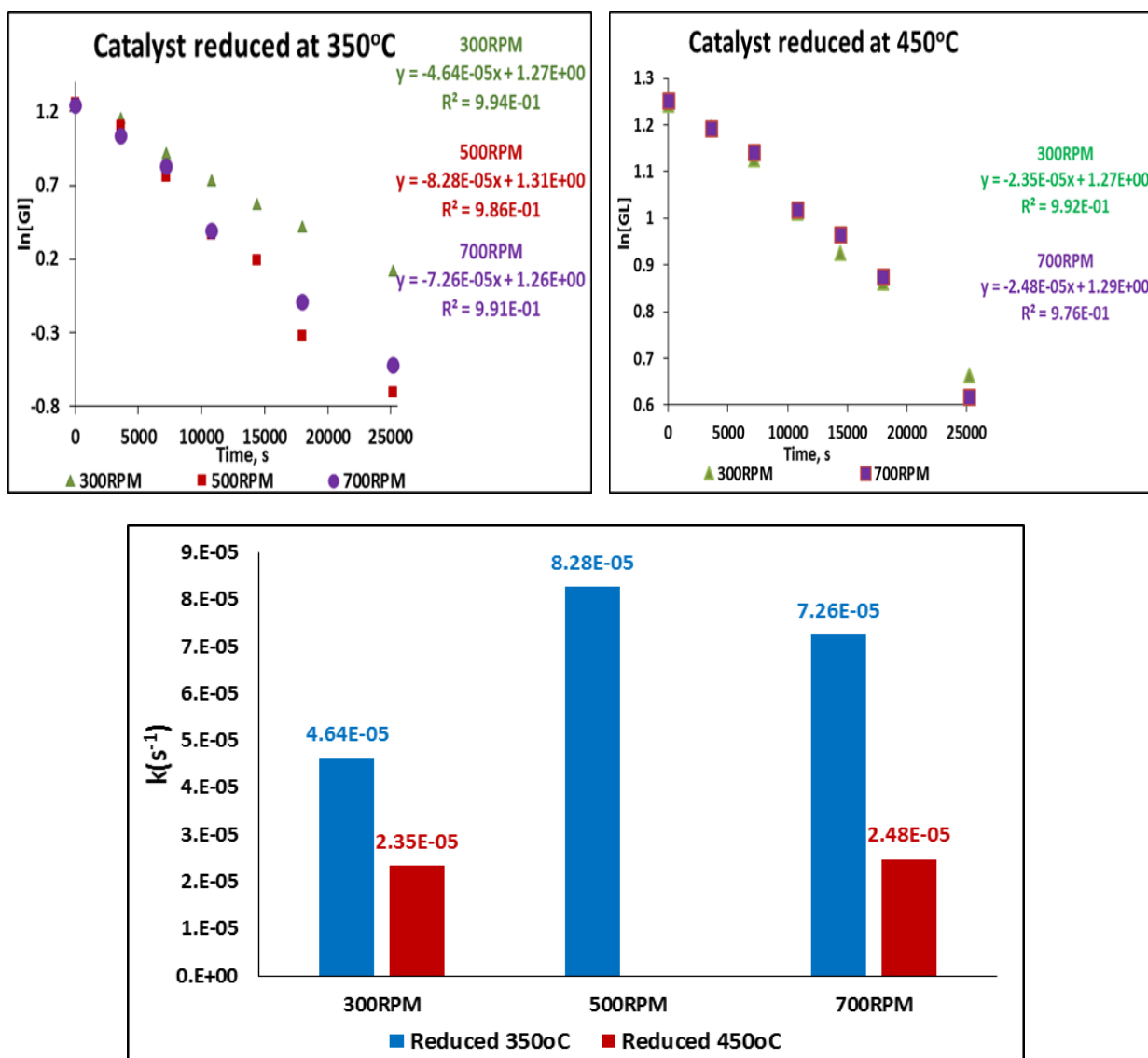


**Figure 5-3** Pseudo-First-Order kinetic analyses in the presence 10Ni/30HSiW/Al<sub>2</sub>O<sub>3</sub> catalysts at different agitator speed. **Reaction condition:** 240°C, 580 H<sub>2</sub>, 30g of glycerol (30wt%), 70g of DI water, 2g catalyst

## **Summary**

This study showed that at stirring speeds higher than 500RPM the diffusion process was much faster than the chemical reaction, and diffusion was not the limiting factor for the reaction. Hence a stirring speed of 500RPM is sufficient to overcome diffusional limitations for the hydrogenolysis of glycerol to the products for the catalyst reduced at 350°C. However, for the catalyst reduced at 450°C even at 300 RPM the hydrogenolysis catalyzed by this catalyst is already chemically controlled.

### **5.2.2 Effect of hydrogen pressure**

Molecular hydrogen is a reactant in hydrogenolysis reactions. High hydrogen pressure will increase the cost of purchase, transportation and storage of gaseous hydrogen. Optimizing hydrogen can bring about a number of different benefits and add value to the process. Therefore, a minimum hydrogen pressure in the reactor is required for complete catalytic conversion of glycerol to desired products. Above this hydrogen pressure, catalytic reaction rates are expected to be independent of hydrogen pressure due to the limited adsorption capacity of the catalyst. Therefore optimal operating pressures for hydrogenolysis of glycerol to other products will balance the higher costs of high pressure equipment with decreased yields at lower pressures. Here the effect of H<sub>2</sub> pressure on reaction rate of hydrogenolysis of glycerol was investigated for different pressures of hydrogen over the range 290 - 800 PSI.

### **Experimental condition**

The effect of hydrogen pressure pressure on the overall reaction is studied by carrying out the hydrogenolysis of glycerol at 290, 580 and 800PSI of hydrogen pressure under otherwise the same reaction conditions. The experiment was performed at 240°C under the selected H<sub>2</sub> pressure using 2g of 10Ni/30HSiW/Al<sub>2</sub>O<sub>3</sub> catalyst, 30g of glycerol (30wt%), 70g of DI water, over 7hours. Prior to the experiment the catalyst was reduced at 350°C for 5 hours.

### **Results and discussion**

The effect of hydrogen pressure on the catalytic performance of 10Ni/30HSiW/Al<sub>2</sub>O<sub>3</sub> catalyst is listed in the Table 5-3 and Fig. 5-4. The main products observed in the liquid phase were: acetol, 1,2-PD, 1,3-PD, acrolein (Acr), 1-PO and ethylene glycol (EG). Some other products (OP) such as methanol (MeOH), ethanol (EtOH) were also obtained. However at low H<sub>2</sub> pressures of 290PSI, some other light unidentified products (UIP) were also detected.

**Table 5-3** Effect of hydrogen pressure on the conversion of glycerol and the distribution to products in the hydrogenolysis of glycerol

<b>P<sub>H<sub>2</sub></sub></b> <b>PSI</b>	<b>k<sub>obs</sub></b> <b>s<sup>-1</sup></b>	<b>Conv.</b> <b>mol%</b>	<b>Selectivity, mol%</b>						
			<b>1,3-PD</b>	<b>1,2-PD</b>	<b>Acetol</b>	<b>EG</b>	<b>1-PO</b>	<b>Acr</b>	<b>OP</b>
<b>0</b>		<b>22.9</b>	<b>0.0</b>	<b>0.0</b>	<b>17.3</b>	<b>0.0</b>	<b>13.9</b>	<b>13.4</b>	<b>55.4*</b>
<b>290</b>	<b>8.94E-5</b>	<b>87.5</b>	<b>0.0</b>	<b>1.5</b>	<b>1.8</b>	<b>0.0</b>	<b>76.9</b>	<b>8.1</b>	<b>11.7*</b>
<b>580</b>	<b>7.00E-5</b>	<b>81.1</b>	<b>0.0</b>	<b>0.0</b>	<b>0.6</b>	<b>0.0</b>	<b>90.6</b>	<b>3.7</b>	<b>5.1**</b>
<b>800</b>	<b>3.41E-5</b>	<b>53.7</b>	<b>0.9</b>	<b>1.2</b>	<b>0.6</b>	<b>0.0</b>	<b>92.9</b>	<b>1.6</b>	<b>2.8**</b>

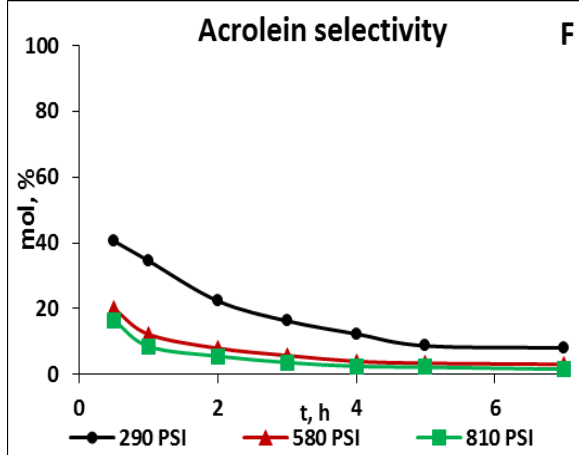
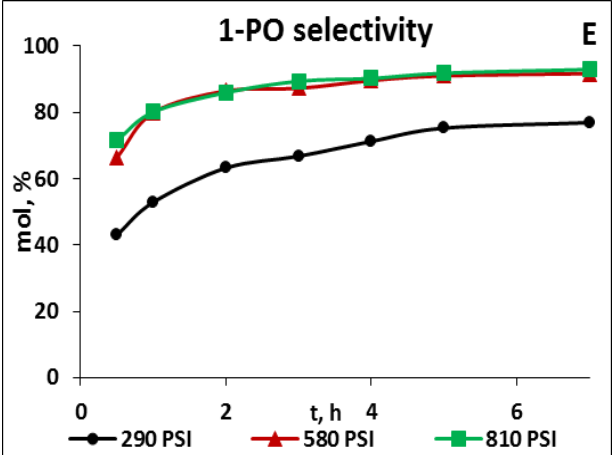
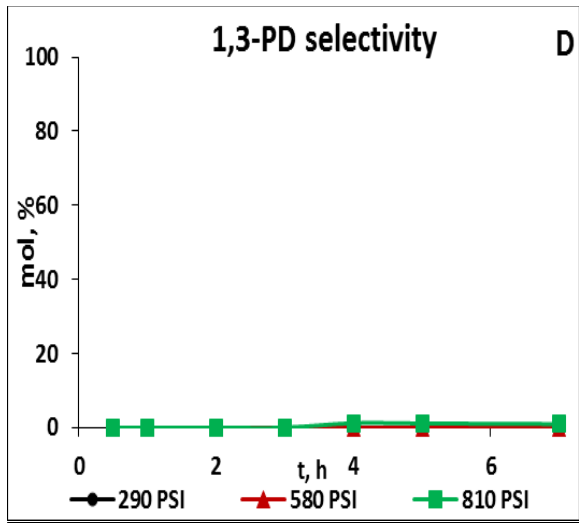
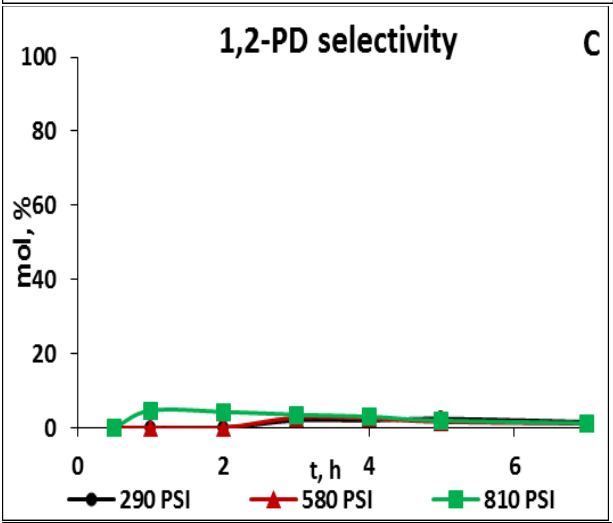
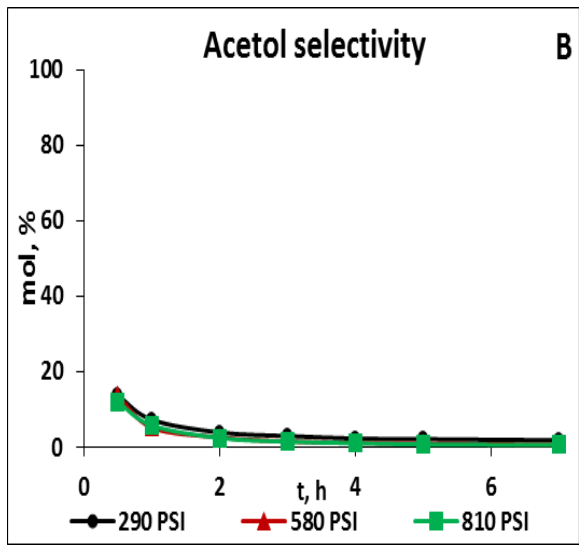
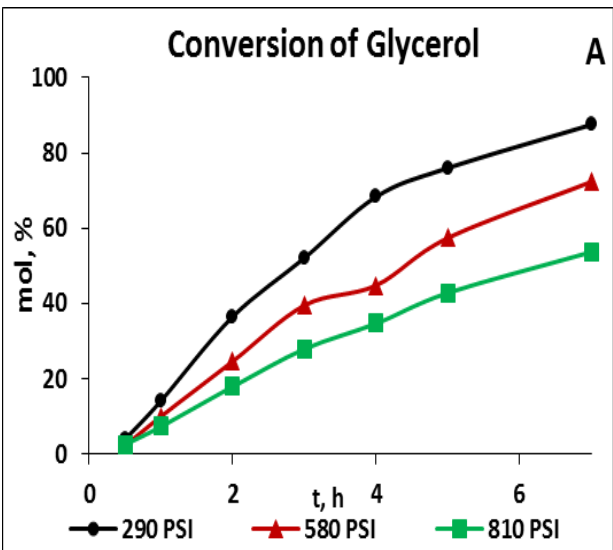
**Reaction condition:** 10Ni/30HSiW/Al<sub>2</sub>O<sub>3</sub> catalyst, 240°C, 700RPM, 2g catalyst, 30g of glycerol (30wt%), 70g of DI water, and H<sub>2</sub>, \*OP: MeOH, EtOH and light unidentified, \*\*: EtOH, MeOH

As can be seen from the Table 5-3, the hydrogen pressure dramatically influenced both the glycerol conversion and the distribution of products; the conversion of glycerol and selectivity to intermediate species such as acetol, 1,2-PD and Acr decreased monotonously with increasing hydrogen pressure; whereas, the selectivity to 1-PO increased. Without H<sub>2</sub> (under N<sub>2</sub>), the conversion of glycerol and selectivity to 1-PO is low (22.9% and 13.9% respectively), selectivity to acetol and acrolein is high (17.3% and 13.4% respectively) and significant by-products were produced. Once H<sub>2</sub> (290PSI) was introduced, the conversion of glycerol and selectivity to 1-PO significantly increased to 87.5% and 76.9% respectively. It's thought that H<sub>2</sub> promotes the hydrogenation of intermediate species so drives the hydrogenolysis reaction forward led to an increase in the conversion of glycerol. However, a further increase of H<sub>2</sub> pressure caused a decrease in the conversion of glycerol. At low H<sub>2</sub> pressure of 290PSI, although the conversion of glycerol is high of 87.5% but the selectivity to 1-PO is much lower (76.9%); the selectivity of

acetol and Acr is also high compared to other H<sub>2</sub> pressures. When the H<sub>2</sub> pressure was increased from 290PSI to 580PSI the selectivity to 1-PO significantly increased from 76.9% to 91.7%, but the conversion of glycerol decreased from 87.5% to 72.3% respectively. A further increase of H<sub>2</sub> pressure to 800PSI caused a decrease in the conversion of glycerol to only 53.7%; however, it only affects slightly the selectivity to 1-PO, the selectivity to 1-PO increases about 1% from 91.7% to 92.6%; 1,3-PD starts to be produced; meanwhile the selectivity of Acr decreased significantly to 1.6%. The abundance of Acr (8.1%) at a low H<sub>2</sub> pressure of 290PSI and this Acr significantly decreased to 1.6% at a high H<sub>2</sub> pressure of 800PSI suggesting that at low H<sub>2</sub> pressure, hydrogenation has a low rate compared to the one was at high pressure (Since hydrogen was supplied continuously throughout the reaction, the quantity of H<sub>2</sub> was sufficient for the entire experiment). It's again believed that 1-PO was produced by hydrogenation of Acr. The glycerol conversion and product selectivity as a function of time are shown in Fig. 5-4.

It can be observed from Fig. 5-4 that when the H<sub>2</sub> pressure is increased from 290PSI to 800PSI, the selectivity to 1-PO (E) is increased but the selectivity to acrolein (F) is decreased. This maybe due to the fact that H<sub>2</sub> promotes the hydrogenation of acrolein to 1-PO. This result was consistent with that of Mengpan et al [154] reported in their paper which reported on a study of the catalytic transformation of glycerol to 1-PO over the two layer catalysts (ZrP, coupling with 2%Ru/SiO<sub>2</sub>). The selectivity of 1-PO was enhanced from 32.0% to 76.5% while the selectivity of Acr decreased sharply from 47.2% to 2.3% as the hydrogen pressure was increased from 0.5 MPa to 2 MPa, the hydrogenation rate of the second layer of the 2%Ru/SiO<sub>2</sub> catalyst increased greatly. They found that the Acr conversion was more than 99% and the selectivity to 1-PO reached 96% using Ru/SiO<sub>2</sub> catalyst with the feed of 10% acrolein in a fixed-bed reactor, at temperature 315°C; H<sub>2</sub> pressure of 2 MPa and suggested that the hydrogenation of Acr to 1-PO is a fast reaction.





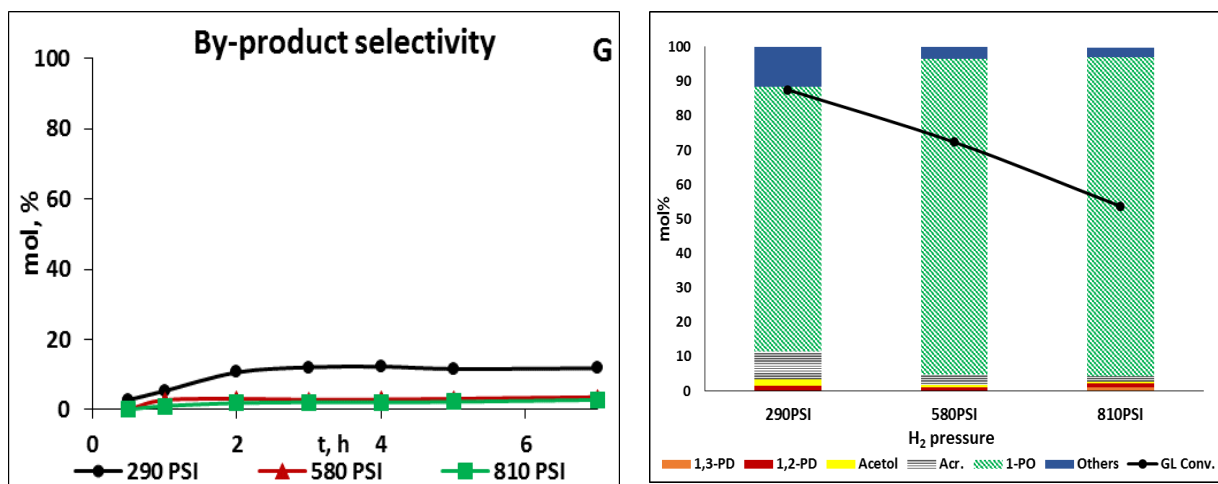


**Figure 5-4** Effect of H<sub>2</sub> pressure on glycerol hydrogenolysis and products selectivity as a function of time: a) Glycerol conversion; B,C,D,E,F,G) Acetol, 1,2PD, 1,3-PD, 1-PO, Acr and OP selectivity respectively; **Reaction condition:** 10Ni/30HSiW/Al<sub>2</sub>O<sub>3</sub> catalyst, 240°C, 700RPM, 2g catalyst, 30g of glycerol (30wt%), 70g of DI water and H<sub>2</sub>.

It is reported that the solubility of hydrogen in water is proportional to the hydrogen pressure [155]; so it is expected that a high conversion of glycerol should be observed at high H<sub>2</sub> pressure. However in this work the reaction rate (Fig. 5-5) decreased with an increase in H<sub>2</sub> pressure. It is suggested that an increase in H<sub>2</sub> pressure may promote the reduction of W resulting in lower acidic activity towards the dehydration step that decreases the conversion of glycerol [209]. Silicotungstic acid single crystals can be reversibly reduced to heteropolyblues as reported by Karwowska et al. [156]. Indeed, it was observed that at high pressure of H<sub>2</sub>, the solution of the product and the catalyst itself became a darker blue colour than it was at low pressure indicating a higher concentration of heteropolyblues. Although there is a decrease in glycerol conversion at high pressure, it is believed that the high H<sub>2</sub> pressure is necessary for hydrogenation step, to suppress side reactions and decrease the formation of undesired products. Therefore an optimal operating H<sub>2</sub> pressures is required to obtained high yield of 1-PO. It was found that reductive conditions (under hydrogen) are rather unfavorable [157] for the thermal stability of the HPA at higher temperatures.

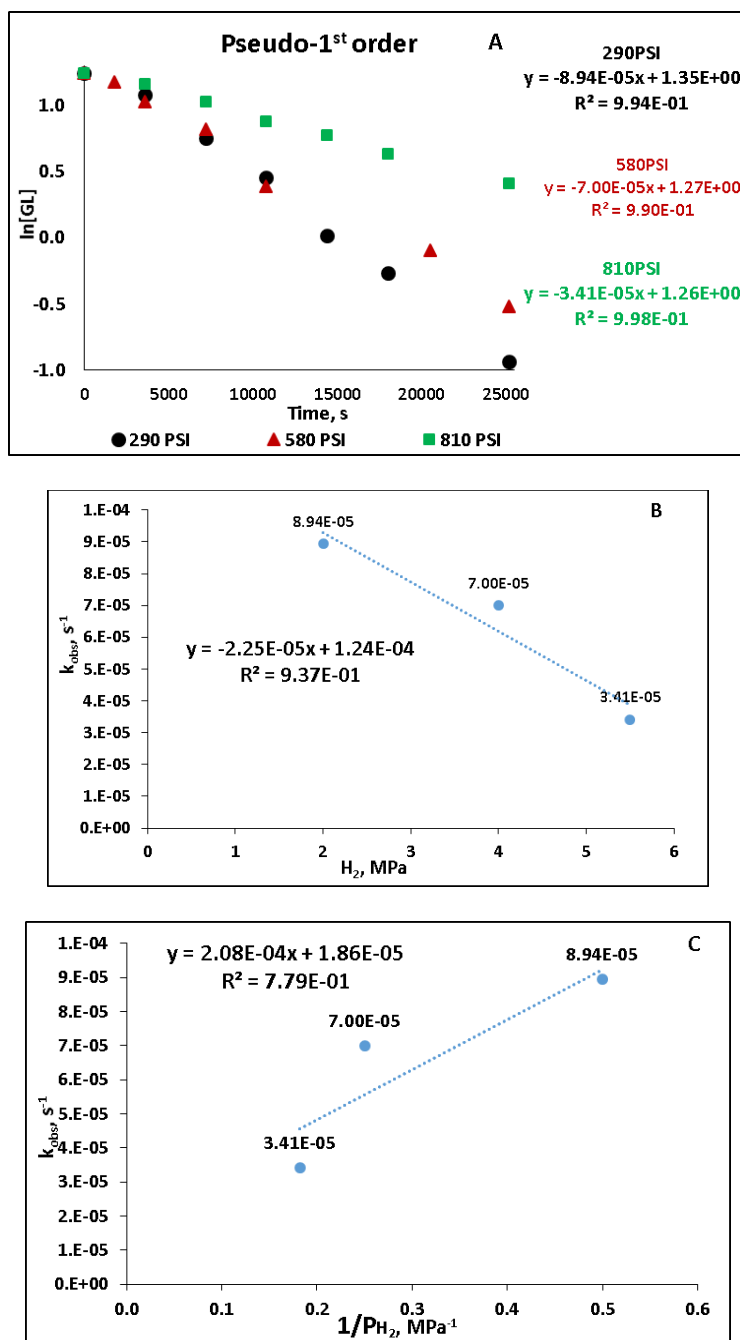


**Figure 5-5** Pseudo-First-Order kinetic plots of  $H_2$  pressure effect on hydrogenolysis of glycerol in the presence of 10Ni/30HSiW/Al<sub>2</sub>O<sub>3</sub> catalyst; **Reaction condition:** 240°C, 700RPM, 2g catalyst, 30g of glycerol (30wt%), 70g of DI water and  $H_2$

### Summary

It can be seen that the conversion of glycerol is inversely proportional to the hydrogen pressure at pressure higher than 290PSI. This can possibly be attributed to increased hydrogen pressures

actually inhibited the reactions due to competitive adsorption of hydrogen to the catalyst surface and the displacement of intermediate products, or the reduction of W under high pressure of H<sub>2</sub> results in the reduction of activity of the catalyst for the dehydration step. However a high H<sub>2</sub> pressure is necessary to suppress the undesired dehydration or side reactions and decrease the undesired products. Optimal operating H<sub>2</sub> pressures are required to obtain high yield of 1-PO.

### **5.2.3 Effect of water content**

Water is not only a solvent for the reaction but also a product of the hydrogenolysis of glycerol. Removal of water from the product drives the hydrogenolysis reaction forward. Besides it is preferable to use a concentrated feed in order to reduce the energy cost of heating water and to increase reactor efficiency (reactor space time). Therefore in this part the effect of water content (aqueous glycerol feed concentration) on the overall reaction was selected for study on the impact of diluents.

#### **Experimental condition**

The effect of water content on the overall reaction is studied by carrying out the hydrogenolysis of glycerol at 20, 40, 70, 90wt % water under the otherwise the same reaction conditions. The experiment was performed at 240°C under 580PSI H<sub>2</sub> pressure using 2g (6.5wt%) of 10Ni/30HSiW/Al<sub>2</sub>O<sub>3</sub> catalyst, 30g of glycerol, for 7hours. The catalysts were reduced at 450°C for 5h.

#### **Results and discussion**

Table 5-4 provides a summary of the effect of initial water content on overall glycerol conversion and product distribution. The main products observed in the liquid phase were: acetol, 1,2-PD, 1,3-PD, acrolein (Acr) and 1-PO. Some other products (OP) such as methanol (MeOH), ethanol (EtOH) and ethylene glycol (EG) were also obtained.

As can be seen from the Table 5-4, Fig 5-6 and Fig 5-7, as the water content increased, the conversion of glycerol and selectivity to both 1,2-PD and acrolein decreased. This may be due to the fact that as water content is increased, the equilibrium is driven in the backward direction. However, the selectivity to 1-PO slightly increased.

**Table 5-4** Effect of water content on the conversion of glycerol and the distribution to products in the hydrogenolysis of Glycerol

Water wt%	$k_{obs}$ s <sup>-1</sup>	Conv mol%	Selectivity, mol%					
			13PD	12PD	Acetol	1-PO	Acr.	OP*
20	3.25E-5	54.0	0.0	3.9	1.2	72.1	5.9	16.9
40	2.78E-5	48.3	0.0	3.4	1.2	76.5	5.4	13.5
70	2.46E-5	43.8	0.0	2.9	1.2	80.9	5.4	9.6
90	1.92E-5	36.4	0.0	5.9	0.0	81.2	2.2	10.7

**Reaction condition:** 10Ni/30HSiW/Al<sub>2</sub>O<sub>3</sub> catalyst, 240°C, 700RPM, 30g of glycerol, 6.5wt% catalyst (2g), 7 hours, and 580PSI of H<sub>2</sub>. \*OP: By-products included methanol, ethanol and EG

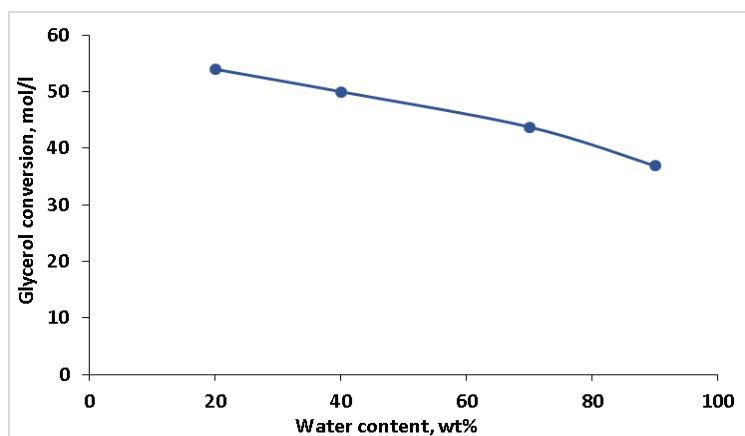
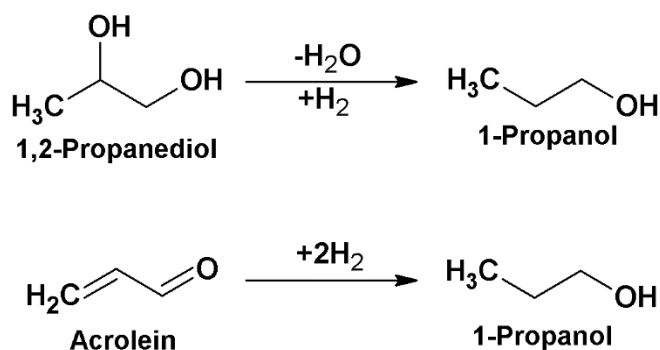


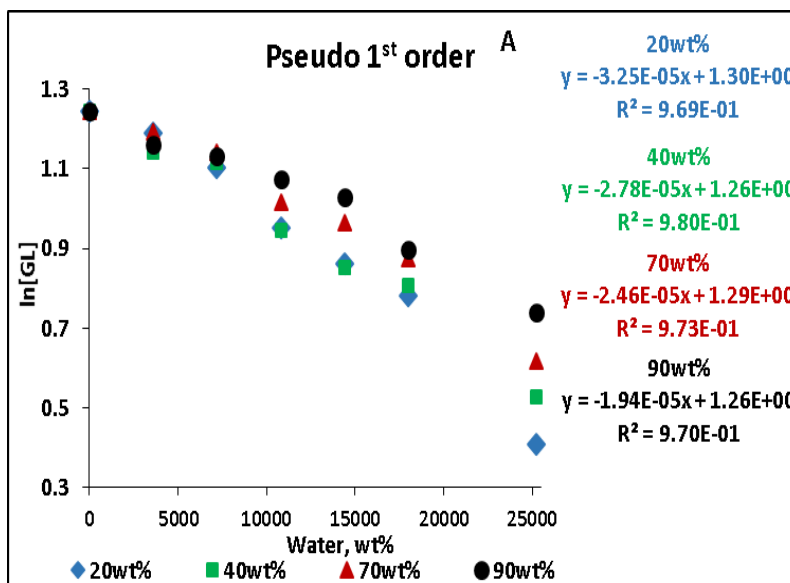
**Figure 5-6** Effect of water content on Glycerol Hydrogenolysis and product distribution; **Reaction condition:** 10Ni/30HSiW/Al<sub>2</sub>O<sub>3</sub> catalyst, 240°C, 700RPM, 30g of glycerol, 6.5wt% (2g) of catalyst and 580PSI H<sub>2</sub>.

Dilute feed solutions increase the selectivity to 1-PO but decrease the conversions of glycerol and intermediate species of acrolein and 1,2-PD or vice versa. This changing tendency can be explained: the decrease of water content leads to an increase in the glycerol conversion so the yield of 1,2-PD and/or acrolein as a primary product will increase. However 1,2-PD and/or acrolein is suggested as an intermediate species to 1-PO, so the amount of 1,2-PD and/or acrolein increases with increasing glycerol concentration, while the available number of catalytic sites (i.e., the

amount of catalyst) is constant. As a result, less active sites becomes available for the conversion of 1,2-PD and/or acrolein to 1-PO, so more 1,2-PD and/or acrolein can be retained and less 1-PO is produced. Based on stoichiometric calculation (Scheme 5-1), it is showed that 1 mol of H<sub>2</sub> is required to convert 1 mol of 1,2-PD to 1mol of 1-PO but it is required 2 mol of H<sub>2</sub> to convert 1 mol of Acr to 1mol of 1-PO. Although it is required more H<sub>2</sub> to convert an intermediate specie of acrolein to 1-PO than to convert of 1,2-PD to 1-PO, for the entire reaction it will need the same amount of H<sub>2</sub> whether 1-PO is obtained from 1,2-PO or acrolein, i.e. 2 mol of H<sub>2</sub> is required to produce 1 mol of 1-PO from 1 mol of glycerol.



**Scheme 5-1** The production of 1-PO from 1,2-PD and Acr



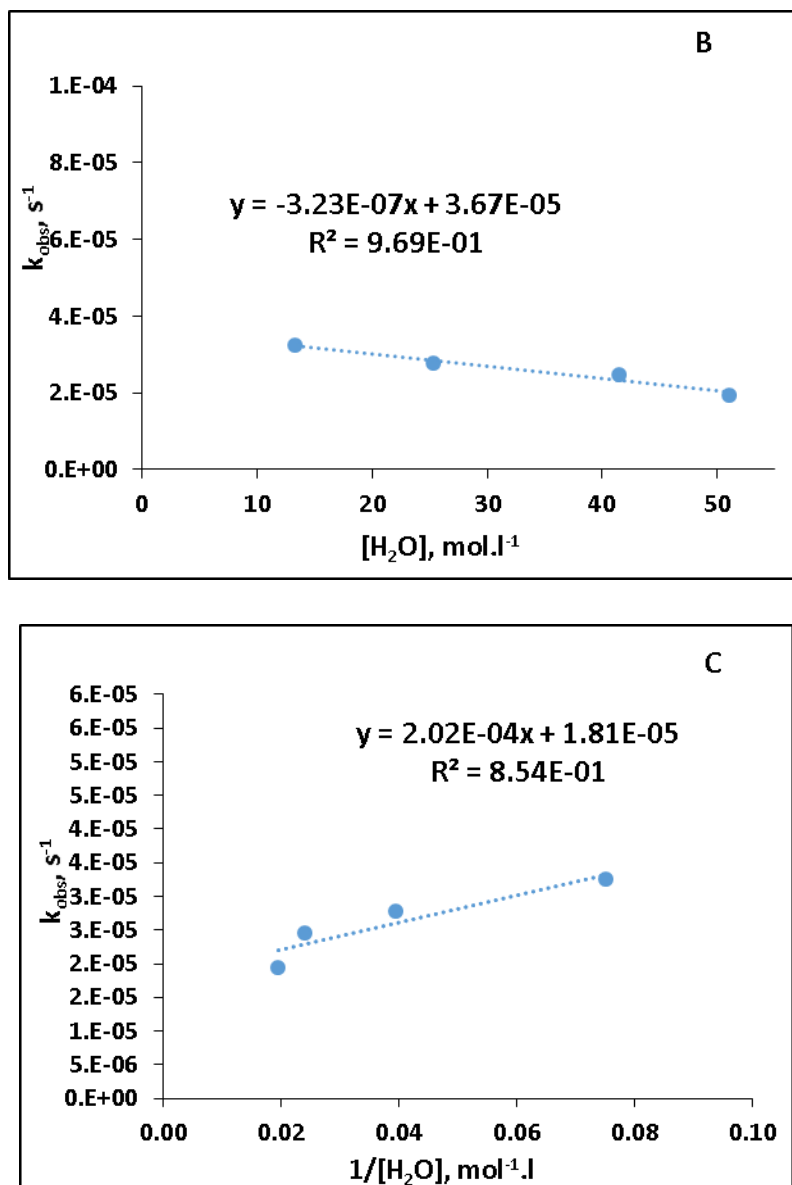


**Figure 5-7** Pseudo-First-Order kinetic plots of the effect of water content feed concentration on hydrogenolysis of glycerol in the presence of 10Ni/30HSiW/Al<sub>2</sub>O<sub>3</sub> catalyst; **Reaction condition:** 240°C, 700RPM, 30g of glycerol, 2g (6.5wt%) of catalyst, and 580PSI H<sub>2</sub>

### Summary

Dilute feed solutions increase the selectivity to 1-PO but lower the conversions of glycerol. Increasing the glycerol concentration (decreasing the initial water content) decreased the selectivity to 1-PO but the selectivity to 1,2-PD and acrolein increased. The increase in the concentration of glycerol results in less active sites becoming available for the conversion of 1,2-

PD and/or acrolein to 1-PO. Optimal glycerol feed concentration is required to obtain a high yield of 1-PO.

#### 5.2.4 Effect of catalyst weight loading

The amount of catalyst present in the reaction mixture is an important parameter that influences the rate of reaction. The amount of solid catalyst determines the total amount of surface area of the catalyst and the number of sites available for the reaction. When the amount of catalyst increases the amount of sites available for the reactants to get adsorbed onto and react also increases. In this part of the research, reactions were performed to determine the impact of catalyst loading on conversion of glycerol to other products.

#### Experiment condition

The effect of catalyst loading on the overall reaction is studied by carrying out the hydrogenolysis of glycerol using a different weight of catalyst over the range of 2.5, 4.5 and 6.5 wt% under otherwise the same reaction conditions. The experiment was performed at 240°C, 700 RPM under 580 H<sub>2</sub> pressure using 10Ni/30HSiW/Al<sub>2</sub>O<sub>3</sub> catalyst, 30g of glycerol (30wt. %), 70g of DI water, for 7 hours.

#### Results and discussion

Table 5-5 and Fig. 5-8 provide a summary of the effect of catalyst loading on the overall glycerol conversion and product distribution. The main products observed in the liquid phase were: acetol, 1,2-PD, 1,3-PD, Acr, 1-PO and EG. Some other products (OP) such as methanol (MeOH), ethanol (EtOH) were also obtained.

**Table 5-5** Effect of catalyst loading on the conversion of glycerol and the distribution to products in the hydrogenolysis of glycerol

Cat wt%	Conv mol%	k <sub>obs</sub> , s <sup>-1</sup> E-5	Selectivity, mol%						
			1,3-PD	1,2-PD	Acetol	EG	1-PO	Acr	OP*
2.5	55.4	3.62	0.0	0.0	1.0	0.0	90.6	5.1	3.2
4.5	68.7	5.13	0.0	0.8	0.7	0.0	92.0	3.5	3.1



6.5    81.1    7.00    0.0    0.0    0.6    0.0    90.6    3.7    5.1

**Reaction condition:** 10Ni/30HSiW/Al<sub>2</sub>O<sub>3</sub> catalyst, 240°C, 700RPM, 30g of glycerol, 70g of DI water and 580PSI of H<sub>2</sub>. \*OP: By-products included methanol and ethanol

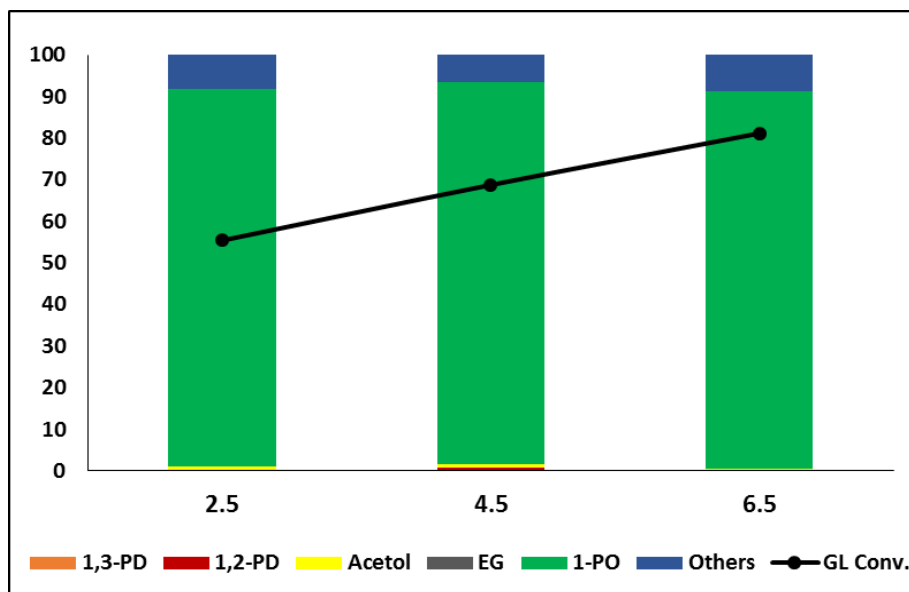


**Figure 5-8** Effect of catalyst weight loading on Glycerol Hydrogenolysis and product distribution; **Reaction condition:** 10Ni/30HSiW/Al<sub>2</sub>O<sub>3</sub> catalyst, 240°C, 700RPM, 30g of glycerol (30wt%), 70g of DI water and 580PSI H<sub>2</sub>.

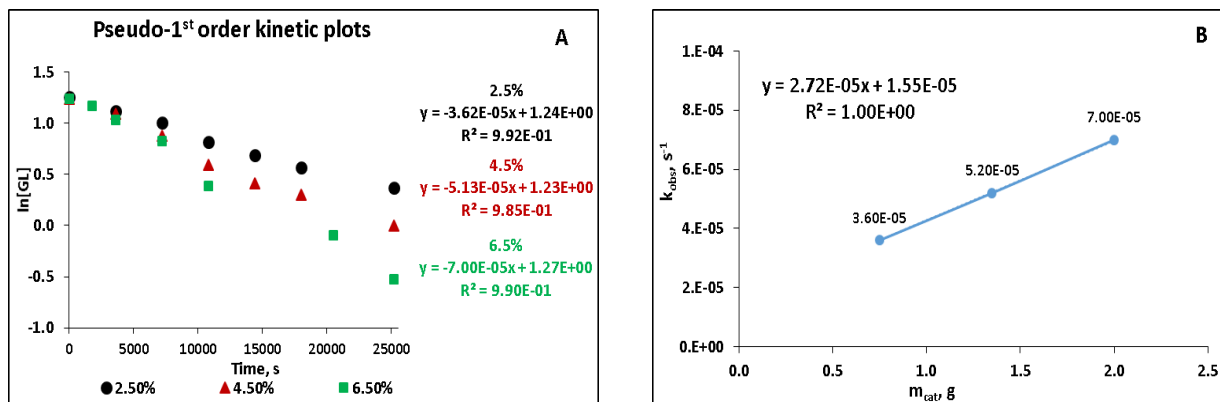


**Figure 5-9** Pseudo-first-order kinetic plots of effect of catalyst weight loading on hydrogenolysis of glycerol in the presence of 10Ni/30HSiW/Al<sub>2</sub>O<sub>3</sub> catalyst; **Reaction condition:** 240°C, 700RPM, 30g of glycerol (30wt%), 70g of DI water, and 580PSI H<sub>2</sub>

As can be seen, while the glycerol conversion increased monotonously with increasing catalyst loading, the product distribution is only affected slightly. The selectivity to acetol decreased with an increase in catalyst loading, and the selectivity to by products is the lowest at 4.5% catalyst loading. It is suggested that higher catalyst loading provides more active sites for the hydrogenolysis reaction of both glycerol to 1,2-PD and 1,2-PD can undergo further hydrogenolysis to propanol. However, further increases in catalyst loading could provide excess active sites resulting in increased exposure of 1-PO to produce undesired products causing a slight increase in selectivity of by-products. According to Fig. 5-9, it is also evident that the reaction rate of the hydrogenolysis reaction increased with an increase in catalyst loading.

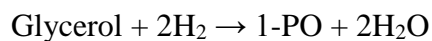
## Summary

Conversion increased with catalyst loading, but selectivity had a maximum of 92.7% at 4.5% loading. It is assumed that high catalyst loadings may result in an increase in the decomposition of the desired product or promote side reactions. Optimal catalyst loading is required to obtain a high yield of 1-PO.

### 5.2.5 Kinetic analysis

Based on the sampling data, the rate constant and the kinetics could be determined.

For the reaction of glycerol and H<sub>2</sub> the reaction to produce 1-Propanol can be written as:



The empirical rate law will be of the form:

$$-\frac{d[\text{GL}]}{dt} = k[\text{GL}]^a[\text{H}_2]^b[\text{H}_2\text{O}]^c[\text{cat}]^d$$

where a, b, c, d are the reaction orders with respect to Glycerol, H<sub>2</sub>, H<sub>2</sub>O and catalyst respectively

Since [cat], [H<sub>2</sub>] and [H<sub>2</sub>O] are constant,

$$-\frac{d[\text{GL}]}{dt} = k_{\text{obs}}[\text{GL}]^a$$

where  $k_{\text{obs}} = k[\text{H}_2]^b[\text{H}_2\text{O}]^c[\text{cat}]^d$

we will have a new constant that is called  $k_{\text{obs}}$  since this will be the rate constant that we “observe” in our experiment.

The effect of catalyst weight loading was studied. As can be seen from Fig. 5.9A the experimental data showed  $\ln[\text{GL}]$  vs. time is a straight line, thus it is suggested that the reaction is first-order in GL. The plot of  $\ln[\text{GL}]$  vs. time is represented by the equation 5-1.

$$-\frac{d[\text{GL}]}{dt} = k_{\text{obs}}[\text{GL}] \quad (5-1)$$

To study the reaction order with respect to catalyst,  $1/[\text{H}_2]$ , and  $1/[\text{H}_2\text{O}]$ , a set of observed rate constants of catalyst,  $1/[\text{H}_2]$ , and  $1/[\text{H}_2\text{O}]$  are presented in Table 5-5, 5-3 and 5-4. The values of the observed rate constants were plotted as a function of each parameter respectively (Figure 5-9B, 5-5C and 5-7C). If the order of the reaction with respect to catalyst,  $1/[\text{H}_2]$ , and  $1/[\text{H}_2\text{O}]$  is 1 then it is expected that  $k_{\text{obs}}$  vs each parameter will be a linear, otherwise the order of reaction is not 1. The data that are shown in each figure (Fig. 5-9B, 5-5C and 5-7C) indicate that the reaction is first order with respect to catalyst,  $1/[\text{H}_2]$ , and  $1/[\text{H}_2\text{O}]$ ; and we can obtain the actual rate constant from the slope of the line.

Therefore, the rate of glycerol disappearance is:

$$-\frac{d[\text{GL}]}{dt} = k \frac{[\text{GL}][\text{cat}]}{[\text{H}_2][\text{H}_2\text{O}]}$$

$P_{\text{H}_2}$  and  $[\text{H}_2\text{O}]$  are constant, and then

$$-\frac{d[\text{GL}]}{dt} = k_{\text{obs}}[\text{GL}] \quad \text{where } k_{\text{obs}} = k \frac{[\text{cat}]}{[\text{H}_2][\text{H}_2\text{O}]} = k_{\text{cat}}[\text{cat}], \quad \text{where } k_{\text{cat}} = k \frac{1}{[\text{H}_2][\text{H}_2\text{O}]} \quad (5-2)$$

From Fig. 5-9B on plotting the value of the observed rate constants as a function of catalyst loading, we found that the actual rate constant from the slope of the line is  $k_{\text{cat}} = 2.7\text{E-}5 \text{ s}^{-1}\text{g}^{-1}$ . Then

$$-\frac{d[\text{GL}]}{dt} = 2.7\text{E-}5[\text{cat}][\text{GL}]$$

From (5-2) we have

$$\mathbf{k = k_{\text{cat}}[\text{H}_2][\text{H}_2\text{O}] = 2.7\text{E-}5 \text{ s}^{-1}\text{g}^{-1} \cdot 4\text{MPa} \cdot 41.5 \text{ mol.l}^{-1} = 4.5\text{E-}3 \text{ s}^{-1}\text{g}^{-1}\text{MPa} \cdot \text{mol.l}^{-1}}$$

Catalyst loading and  $[\text{H}_2\text{O}]$  are constant, and then

$$-\frac{d[GL]}{dt} = k_{\text{obs}}[GL] \text{ where } k_{\text{obs}} = k \frac{[cat]}{[H_2][H_2O]} = k_{H_2} \frac{1}{[H_2]}, \text{ where } k_{H_2} = k \frac{[cat]}{[H_2O]} \quad (5-3)$$

From Fig. 5-5C on plotting the value of the observed rate constants as a function of  $H_2$ , we found the actual rate constant from the slope of the line is  $k_{H_2} = 2.1E-4 \text{ MPa}\cdot\text{s}^{-1}$ .

From (5-3) we have

$$k = k_{H_2} \frac{[H_2O]}{[cat]} = 2.1E-4 \text{ MPa}\cdot\text{s}^{-1} \cdot 41.5 \text{ mol}\cdot\text{l}^{-1} \cdot (1/2) \text{ g}^{-1} = 4.3E-3 \text{ g}^{-1} \text{ s}^{-1} \text{ MPa}\cdot\text{mol}\cdot\text{l}^{-1}$$

Catalyst and  $[H_2]$  are assumed constant, and then

$$-\frac{d[GL]}{dt} = k_{\text{obs}}[GL] \text{ where } k_{\text{obs}} = k \frac{[cat]}{[H_2][H_2O]} = k_{H_2O} \frac{1}{[H_2O]}, \text{ where } k_{H_2O} = k \frac{[cat]}{[H_2]} \quad (5-4)$$

From Fig. 5-7C, on plotting the value of the observed rate constants as a function of  $H_2O$ , we found that the actual rate constant from the slope of the line is  $k_{H_2O} = 2.0E-4 \text{ mol}\cdot\text{l}^{-1}\cdot\text{s}^{-1}$ .

$$\text{From (5-4) we have } k = k_{H_2O} \frac{[H_2]}{[cat]} = 2.0E-4 \text{ mol}\cdot\text{l}^{-1}\cdot\text{s}^{-1} \cdot 4 \text{ MPa} \cdot (1/2) \text{ g}^{-1} = 4.0E-4 \text{ g}^{-1} \text{ s}^{-1} \text{ MPa}\cdot\text{mol}\cdot\text{l}^{-1}$$

The results showed that the actual rate constant are similar when ( $H_2O$ ,  $H_2$ ) or (catalyst,  $H_2O$ ) are kept constant and  $k \sim 4.5E-3 \text{ s}^{-1} \text{ g}^{-1} \text{ MPa}\cdot\text{mol}\cdot\text{l}^{-1}$ . However, when the catalyst and  $H_2$  were constant, the actual rate constant becomes lower and  $k \sim 4.0E-4 \text{ s}^{-1} \text{ g}^{-1} \text{ MPa}\cdot\text{mol}\cdot\text{l}^{-1}$ . The reason may be because for this set of experiments the catalysts were reduced at high temperature of  $450^\circ\text{C}$ , while for other two sets of experiments (when catalyst and  $[H_2O]$  or  $[H_2O]$  and  $[H_2]$  were kept constant) the catalysts were reduced at lower temperature of  $350^\circ\text{C}$ . It is observed from the section 6.2.2 that the catalyst loses its acidity that results in the loss of its activity when it is reduced at temperature above  $400^\circ\text{C}$ . Therefore the actual rate constant of the reaction using the catalyst reduced at  $450^\circ\text{C}$  is lower than that of the reaction using the catalyst reduced at  $350^\circ\text{C}$ .

## 5.2.6 Effect of temperature and activation energy

Temperature plays an important role in the hydrogenolysis of glycerol. Since temperature can affect the rate of the hydrogenation. Increasing temperature leads to change in rates of adsorption, desorption that can cause a change in hydrogenation step and the overall reaction. In this section, the reactions were performed to determine the impact of temperature on the rate of the

hydrogenolysis of glycerol to other products. The value of the activation energy was also calculated.

### **Experimental condition**

The effect of temperature on the overall reaction is studied by carrying out the hydrogenolysis of glycerol at 230 to 260°C under the otherwise the same reaction conditions. The experiment was performed at 580PSI H<sub>2</sub> pressure using 2g of 10Ni/30HSiW/Al<sub>2</sub>O<sub>3</sub> catalyst, 30g of glycerol (30wt%), 70g of DI water, for 7hours. The catalysts were reduced at 400°C for 5 hours.

### **Results and discussion**

The effect of temperature on the catalytic performance of the 10Ni/30HSiW/Al<sub>2</sub>O<sub>3</sub> catalyst is presented in the Table 5-6 and Fig. 5-10. The main products observed in the liquid phase were: acetol, 1,2-PD, 1,3-PD, Acr, 1-PO and EG. Some other products (OP) such as methanol (MeOH), ethanol (EtOH) were also obtained.

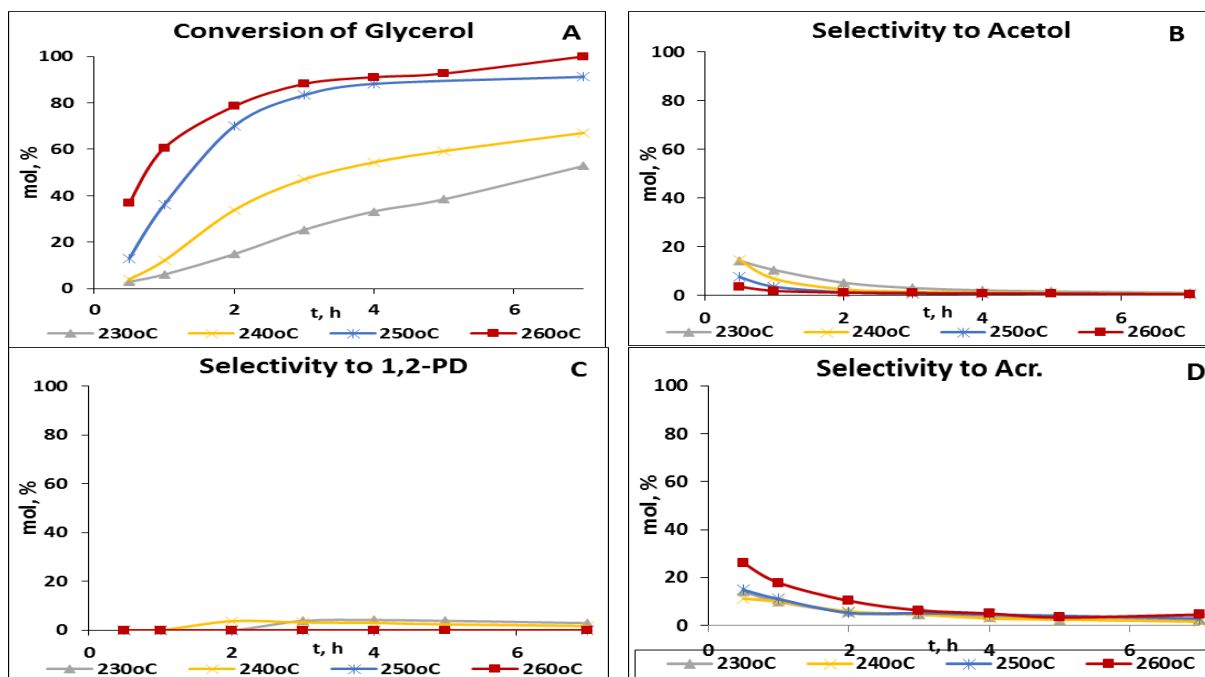
As can be seen, the temperature affects significantly the conversion of glycerol and the degradation of 1,2-PD. The glycerol conversion and by-products increased monotonously with increasing catalyst loading, while the selectivity to 1,2-PD and acetol decreased. At 260°C, the conversion of glycerol reached 100%. On increasing temperature from 230°C to 260°C the selectivity of 1,2-PD decreased from 2.9% to an undetectable level, meanwhile the selectivity to 1-PO slightly increased initially and then went through a maximum of 91.2% at 240°C. Further increases in temperature from 250°C to 260°C decreased the selectivity of 1-PO significantly to 84.2% at 100% conversion of glycerol.

Although high temperature favors 1-PO production, it also promotes the degradation of 1-PO. Over the range of 230 to 250°C, the effect of temperature on the selectivity to 1-PO distribution was not significant (selectivity to 1-PO reaches around 90%). However at higher temperature of 260°C the degradation of 1-PO occurs significantly, more than other light products which were produced leading to a decrease in selectivity of 1-PO to 84.2% and an increase in selectivity to other products (9.1%). This indicated that at a high temperature of 260°C, excessive hydrogenolysis resulted in the degradation of 1-PO or in increase side reactions.

**Table 5-6** Effect of temperature on the conversion of glycerol and the distribution to products in the hydrogenolysis of glycerol

T, °C	Conv. mol%	Selectivity, mol%						
		13-PD	12-PD	Acetol	EG	1-PO	Acr	OP*
230	53.0	0.0	2.9	0.9	0.0	90.3	2.2	3.7
240	67.4	0.0	1.7	0.6	0.0	92.4	1.6	3.7
250	91.2	0.0	0.0	0.4	0.0	90.8	2.8	6.0
260	100.0	0.0	0.0	0.4	1.2	84.8	4.5	9.1

**Reaction condition:** 10Ni/30HSiW/Al<sub>2</sub>O<sub>3</sub> catalyst, 240°C, 700RPM, 2g catalyst, 30g of glycerol (30wt%), 70g of DI water, 580PSI of H<sub>2</sub>, 7hours. \*OP: By-products included methanol and ethanol.



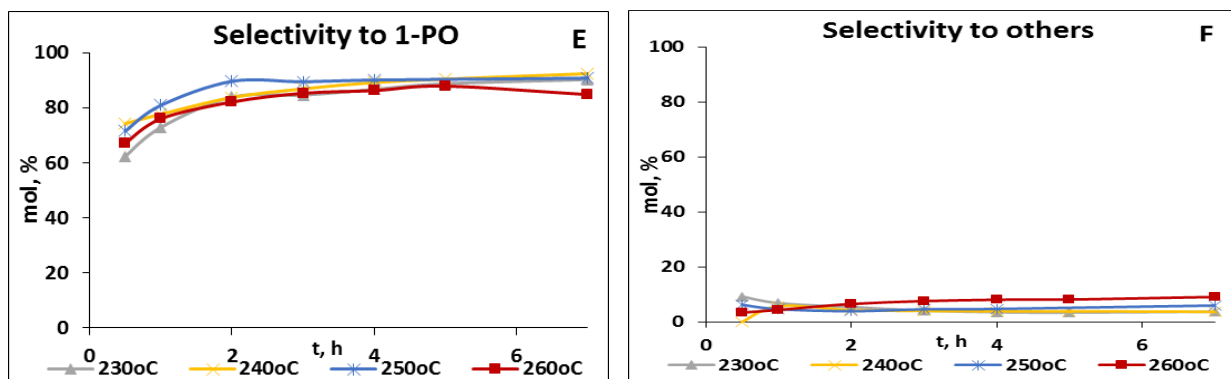


**Figure 5-10** Effect of temperature on glycerol hydrogenolysis and products selectivity as a function of time; A) Glycerol Conversion; B,C,D,E,F) Selectivity of acetol, 1,2-PD, Acr., 1-PO, other products, respectively; **Reaction condition:** 10Ni/30HSiW/Al<sub>2</sub>O<sub>3</sub> catalyst, 240°C, 700RPM, 2g catalyst, 30g of glycerol (30wt%), 70g of DI water and 580 PSI of H<sub>2</sub>.

### Activation energy

Based on the analyses of Pseudo-First-Order kinetic, the observed rate constants at different reaction temperature, and the activation energy for the 10Ni/30HSiW/Al<sub>2</sub>O<sub>3</sub> catalyst was calculated and is presented in Table 5-7.

**Table 5-7** Effect of temperature on the reaction rate of hydrogenolysis of glycerol

T, °C	k <sub>obs</sub> , s <sup>-1</sup>	T (K)	1/T*K <sup>-1</sup>	Ln(k <sub>obs</sub> )
230	3.30 E-05	503	0.00199	-10.32
240	4.77 E-05	513	0.00195	-9.95
250	1.14 E-04	523	0.00191	-9.08
260	1.58 E-04	533	0.00188	-8.75

Ea/R is the slope of the line given in the Fig 5-12. The activation energy is **E<sub>a</sub> = 124.1 kJ/mol**. Up to date there is no work has done on the activation energy for the hydrogenolysis of glycerol to 1-PO.

### Summary

It was shown in this study that with an increase in temperature from 230 to 260°C, there was a remarkable increase in the glycerol conversion from 53 to 100%. The selectivity of 1,2-PD

decreased gradually with an increase in temperature and was undetectable at 250°C. This indicated that 1,2-PD mostly undergoes hydrogenolysis to form 1-PO at 250°C. The selectivity of 1-PO was stable at around 90% until 250°C but significantly drop from 90% to 84% at 260°C. This suggests that 1-PO may be degraded at high temperature of 260°C.

Increasing temperature may promote further hydrogenolysis of 1,2-PD to 1-PO. However excessive heat may cause the degradation of 1-PO to other products or other side reaction. Therefore it is suggested that operation at higher pressures may prevent degradation of products. It is found that the activation energy of the hydrogenolysis of glycerol to 1-PO using a catalyst of 10Ni/30HSiW/Al<sub>2</sub>O<sub>3</sub> is of 124.1 kJ/mol and it is chemically kinetically controlled.

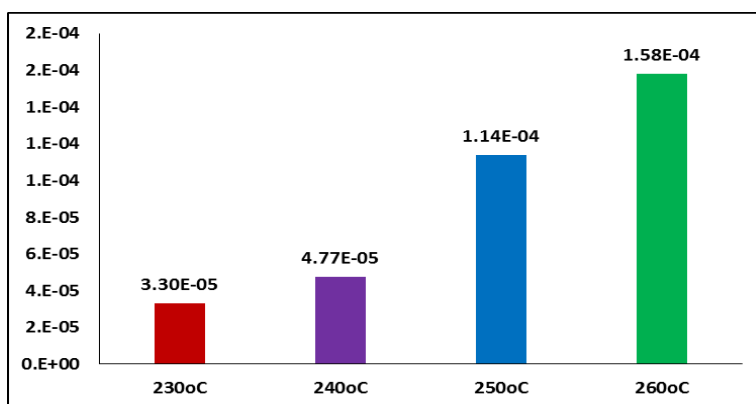


**Figure 5-11** Pseudo-first-order kinetic analysis for the 10Ni/30HSiW/Al<sub>2</sub>O<sub>3</sub> catalysts at different temperature (230, 240, 250 and 260°C). **Reaction condition:** 240°C, 580PSI of H<sub>2</sub>, 700RPM, 2g of catalyst, 30g of glycerol (30wt%), 70g of DI water.

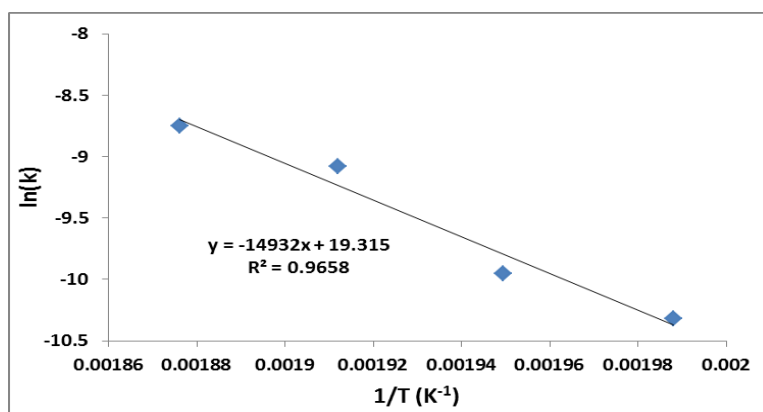


**Figure 5-12** Calculation of the activation energy based on  $\ln(k_{\text{obs}})$  and  $1/T$  using the equation  $\ln k = \ln A - E_a/R(1/T)$



### **5.3 Study of the effect of NiHSiW/Al<sub>2</sub>O<sub>3</sub> loading on Al<sub>2</sub>O<sub>3</sub>**

Bifunctional catalysis involving successive chemical steps on two independent types of sites plays an important role for hydrogenolysis of glycerol. The investigation of the effect of metal–acid balance on bifunctional catalysts is important.

Therefore, the effect of active component content was studied by varying the weight loading of HSiW and Ni to find out the effect of component content and the optimum composition. First the weight loading of HSiW was studied and then the optimum HSiW weight loading was chosen to study the effect of Ni loading. The active components were added in sequence so the effect of the sequence of adding the active component was also studied.

#### **5.3.1 Effect of HSiW loading on catalytic activity of the 10Ni/HSiW/Al<sub>2</sub>O<sub>3</sub>**

In this part the effect of HSiW loading on the catalyst activity of 10Ni/HSiW/Al<sub>2</sub>O<sub>3</sub> for the hydrogenolysis of glycerol was studied. The weight loading of HSiW on the catalysts was varied from 0 to 30wt% while the loading of Ni is set at 10wt% in order to investigate the influence of HSiW loading on the catalytic activities of the 10Ni/HSiW/Al<sub>2</sub>O<sub>3</sub> catalysts.

#### **Experimental condition**

The effect of HSiW loading on the catalyst activity was studied by varying the weight loading of HSiW on the catalysts from 0 to 30wt%, the hydrogenolysis of glycerol was carried out at 290, 580 and 800PSI of hydrogen pressure under otherwise the same reaction conditions. The experiment was performed at 240°C under 580PSI H<sub>2</sub> pressure using 2g of 10Ni/30HSiW/Al<sub>2</sub>O<sub>3</sub> catalyst, 30g of glycerol (30wt%), 70g of DI water, for 7hours. The catalysts were reduced at 450°C for 5 hours.

#### **Results and discussion**

The conversion of the glycerol and product distribution observed as a function of time at different HSiW loadings are shown in Fig. 5-13 and the data are summarized in Table 5-8. The main products observed in the liquid phase were: acetol, 1,2-PD, 1,3-PD, Acr, 1-PO and EG. Some other products (OP) such as methanol (MeOH), ethanol (EtOH) were also obtained.

The Fig 5-13 shows that for all catalysts, as the reaction proceeds, the conversion of glycerol and the selectivity of 1-PO gradually increase (Fig 5-13 A and D), while the selectivity of acetol, 1,2-PD and acrolein (the intermediate species) increases at the beginning of the reaction and then slightly decreases with increasing reaction time (Fig 5-13 B, C and E).

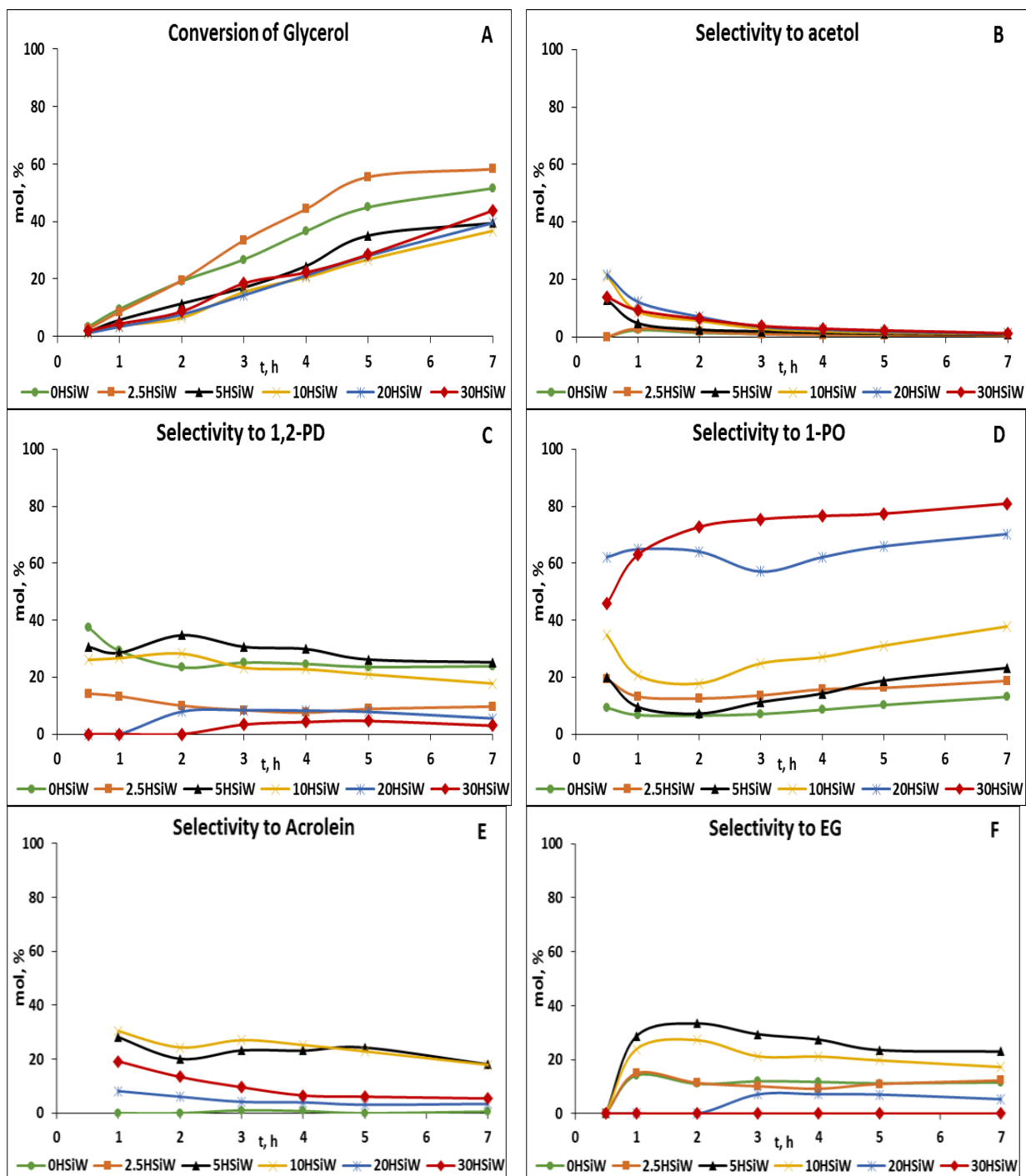
**Table 5-8** Effect of HSiW loading on the conversion of glycerol and the distribution to products in the hydrogenolysis of glycerol using 10Ni/Al<sub>2</sub>O<sub>3</sub>

HSiW, wt%	Conv. mol%	Selectivity, mol%						
		1,3-PD	1,2-PD	Acetol	EG	1-PO	Acr	OP*
0	51.6	0.0	23.8	0.6	11.5	13.0	0.0	51.1
2.5	58.2	0.0	9.7	0.5	12.3	18.7	0.3	58.5
5	39.5	0.0	25.2	0.8	23.0	23.2	0.6	27.2
10	37.2	0.0	17.5	1.0	17.0	37.1	1.0	26.4
20	39.8	0.0	5.4	1.1	5.3	69.2	3.4	15.6
30	43.8	0.0	2.9	1.2	0.0	79.7	5.4	10.8

**Reaction condition:** 10Ni/xHSiW/Al<sub>2</sub>O<sub>3</sub> catalyst (x=0, 2.5, 5, 10, 20 and 30wt%), 240°C, 700RPM, 2g catalyst, 30g of glycerol (30wt%), 70g of DI water and 580PSI of H<sub>2</sub>.\* OP: By-products included only MeOH and EtOH

As can be seen from the Table 5-8, the variation of HSiW loading over the range from 0 to 30wt% influences both the glycerol conversion and the product distribution. The selectivity to acetol, Acr and 1-PO gradually increased with an increase in HSiW loading. However the conversion of glycerol and selectivity of by-products first increased and then decreased, both of them went through a maximum of 58.2% and 58.5% respectively at 2.5wt% of HSiW loading. The selectivity to 1,2-PD and EG also went through a maximum of 25.2% and 23% respectively at 5wt% HSiW loading. Using the HSiW-free catalyst (i.e. Ni/Al<sub>2</sub>O<sub>3</sub>) and low loading of HSiW of 2.5wt%, the primary product was by products (mainly ethanol) with a selectivity of 51.1%, whereas only minor amount of 1-PO (13%) was obtained. This result suggested that at low HSiW loading (below 10wt%) the sequential hydrogenolysis capability of HSiW supported Ni/Al<sub>2</sub>O<sub>3</sub> catalyst was not effective to catalyze the sequential hydrogenolysis of 1,2-PD to 1-PO. Besides, the catalyst was also not active for the production of acrolein through the consequence dehydration of glycerol and

the selectivity to acrolein is low, being less than 1%. This maybe due to the low acidity of the catalyst at low HSiW loading.



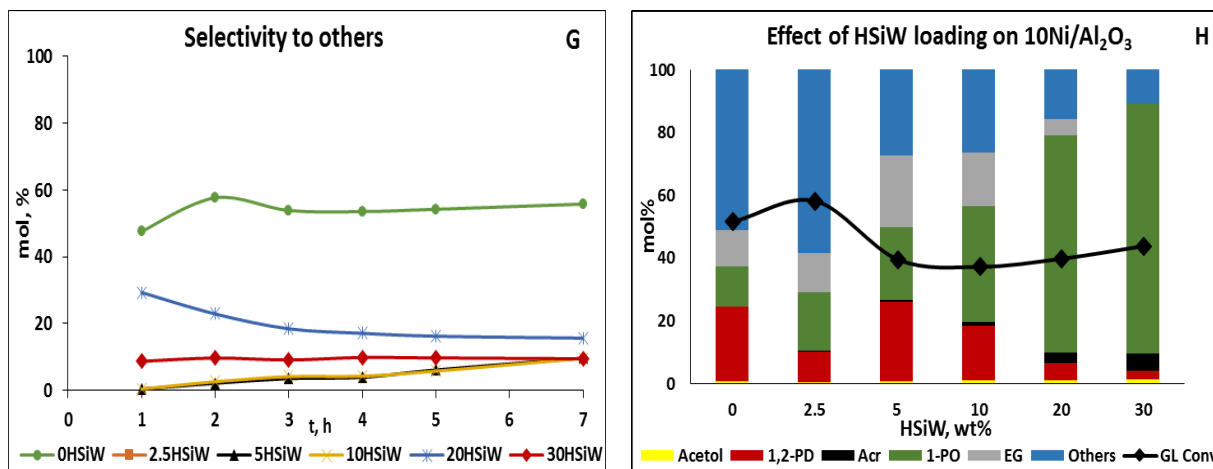


**Figure 5-13** Effect of HSiW loading on Glycerol Hydrogenolysis and products selectivity as a function of time; A) Glycerol Conversion; B,C,D,E,F,G) Selectivity of acetol, 1,2-PD, 1-PO, Acr., other products, respectively. H) A comparison in catalytic performance. **Reaction condition:** 10Ni/HSiW/Al<sub>2</sub>O<sub>3</sub> catalyst, 240°C, 700RPM, 2g catalyst, 30g of glycerol (30wt%), 70g of DI water and H<sub>2</sub>.

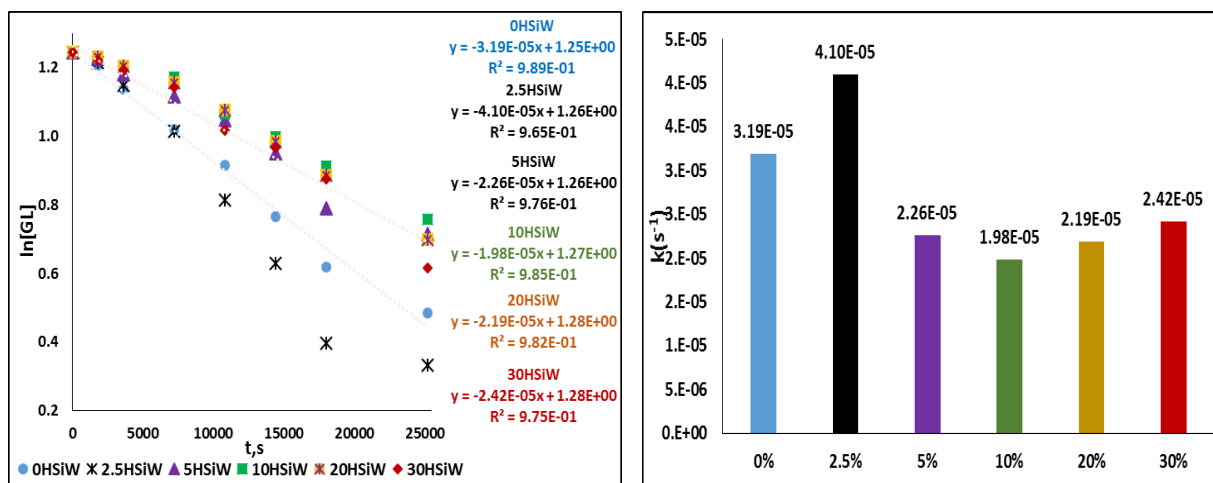


**Figure 5-14** Pseudo-First-Order kinetic plots of effect of HSiW loading on hydrogenolysis of glycerol in the presence of 10Ni/HSiW/Al<sub>2</sub>O<sub>3</sub> catalyst; **Reaction condition:** 240°C, 700RPM, 30g of glycerol (30wt%), 70g of DI water, 2g catalyst, and 580PSI H<sub>2</sub>

With a loading of HSiW higher than 10wt% the sequential hydrogenolysis capability of the catalyst was elevated considerably and the sequence of dehydration of glycerol was also promoted. As can be seen, when the loading of HSiW was below 10wt% the selectivity to 1-PO and Acr is as low as 37.1% and 1% respectively at 37.2% conversion of glycerol. When the HSiW loading was

increased to 20wt% the glycerol conversion increased slightly to 39.5% but 1-PO and Acr selectivity jumped up to 70.2% and 3.4% respectively. The selectivity to 1-PO and Acr reached the highest value of 80.9% and 5.4% at 43.8% conversion of glycerol with 30wt% HSiW loading. It is suggested that the loading of HSiW should be higher than 20wt% to promote the further hydrogenolysis of 1,2-PD to 1-PO or the production of Acr for the sequence of dehydration of Acr to 1-PO. It is believed that such changes in selectivity are likely related to the acidity of catalysts. Hence it is believed that HSiW played an important role in the production of 1-PO.

### Characterization of catalysts

Acid properties of the catalyst with different HSiW content were explored by  $\text{NH}_3$ -TPD from 50 to 750°C to determine the quantity of acid sites on the catalyst surface and the distribution of acid strengths of the catalyst and thus, to find a comprehensive correlation between HSiW content with catalytic activity and acid property of the 10Ni/xHSiW/ $\text{Al}_2\text{O}_3$  catalysts. Fig. 5-15 shows the profiles of  $\text{NH}_3$  desorbed from the studied catalysts. The correlation between the loading of HSiW and acidity of the catalyst are depicted in the Fig. 5-16A. The TPD data was deconvoluted into 3 peaks (namely weak, medium and strong acid sites) using a Gaussian fitting method, the quantity of acid sites of the catalysts is recorded in Table 5-9 and was then correlated with the catalytic activity of the catalysts.

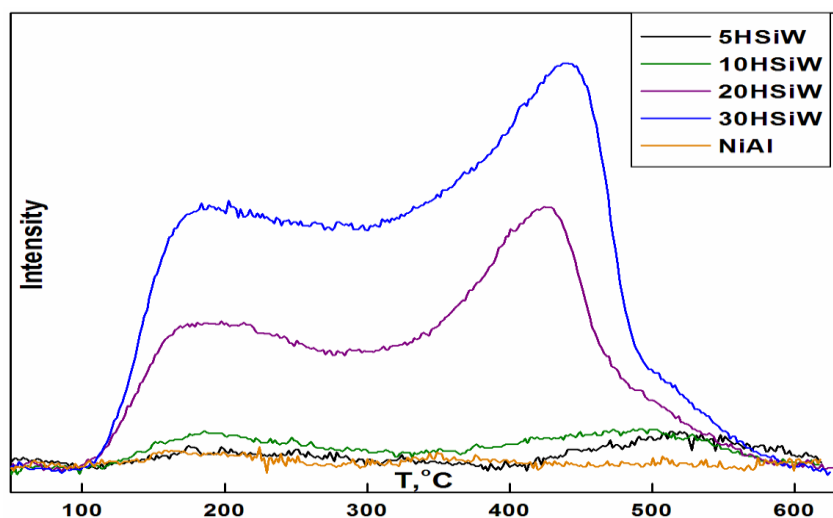
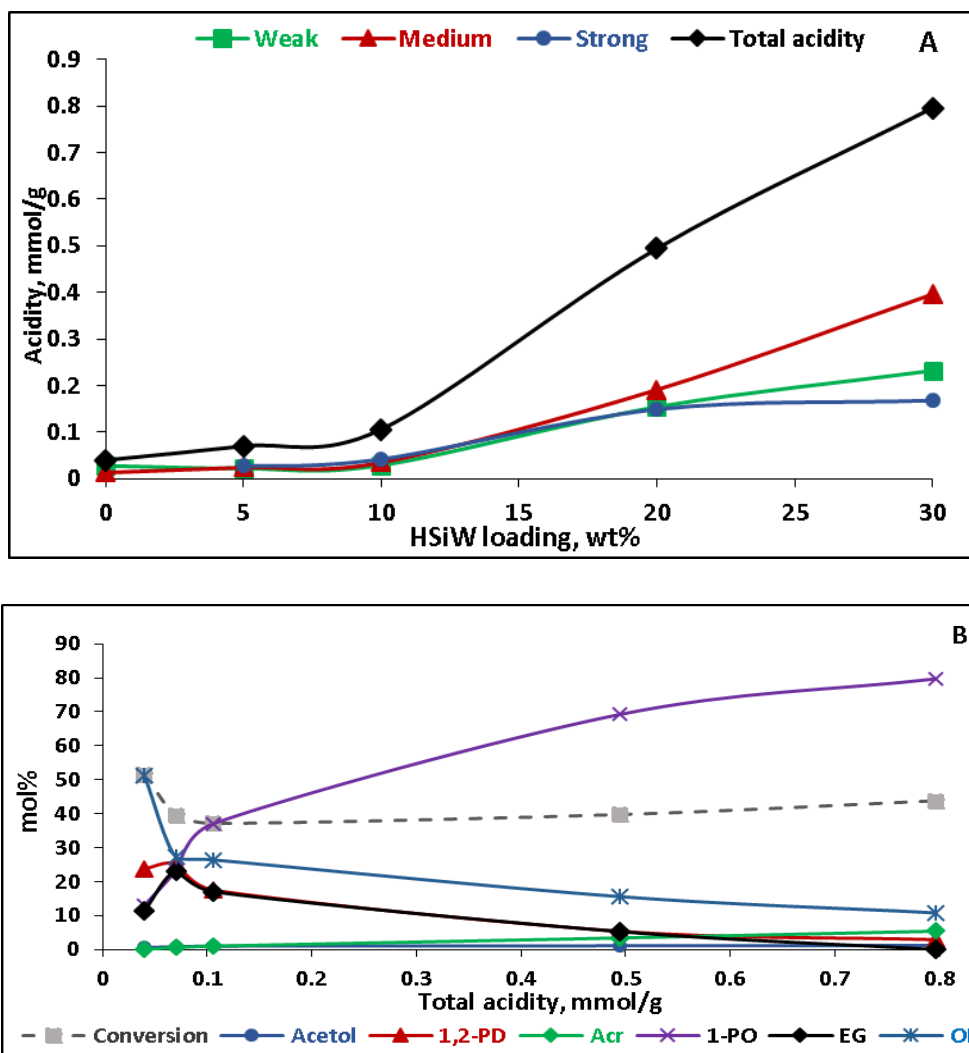


Figure 5-15  $\text{NH}_3$ -TPD patterns of different HSiW loading



**Figure 5-16** A. Effect of HSiW loading on acidity of the catalyst; B. Effect of total acidity of the catalyst on the conversion of glycerol and selectivity to products

The data shows that the total acidity of the catalyst and the strength of medium acid sites monotonously increased with increasing of HSiW loading. At low loading of HSiW below 10wt%, there is essentially no effect on acidity. However, with a further increase in HSiW loading to 20wt%, the total acidity increased significantly. It is noted that the selectivity to 1-PO behaves in parallel with the acidity and the strength of medium acid sites, while the selectivity to 1,2-PD and EG decreases with the loading level and is inversely proportional to the strength of medium acid sites. It is suggested that total acid amount and medium acid site of the catalyst favor the formation of 1-PO but disfavor 1,2-PD and EG.

At a low loading level of HSiW, although the dispersion is high, the direct interaction between the surface and heteropolyacids are rather strong, causing sometimes decomposition of heteropolyacids. NH<sub>3</sub> adsorption shows that at low HSiW loading the strength of strong acid sites is high (a shift toward higher temperature from 420°C to 480°C). The total acidity linearly increases with the amount of HSiW loading. It shows the dependencies of the reactions with the loading amount of HSiW on the catalysts.

The effect of different HSiW loading on catalyst surface area was investigated by N<sub>2</sub> adsorption–desorption isotherms. BET surface area was calculated by desorption isotherms and the result is listed in Table 5-9. It is interesting to note that there is a slight increase in the surface area of the catalyst from 17.9 to 20.9m<sup>2</sup>/g after HSiW was loaded onto 10Ni/Al<sub>2</sub>O<sub>3</sub> suggesting that the pores of alumina are not blocked by the HSiW. However, a further increase of HSiW loading does not improve the surface area of the catalyst.

**Table 5-9** BET surface area and total acidity of different HSiW loading catalysts

<b>HSiW, wt %</b>	<b>SAA m<sup>2</sup>/g</b>	<b>Weak acid site mmol/g /(Temp.)</b>	<b>Medium acid site mmol/g /(Temp.)</b>	<b>Strong acid site mmol/g /(Temp.)</b>	<b>Total acid amount, mmol/g</b>
<b>0</b>	<b>17.9</b>	<b>0.028/(175°C)</b>	<b>0.013/(350°C)</b>	<b>-</b>	<b>0.041</b>
<b>5</b>	<b>20.9</b>	<b>0.022/(187°C)</b>	<b>0.024/(270°C)</b>	<b>0.027/(480°C)</b>	<b>0.073</b>
<b>10</b>	<b>20.9</b>	<b>0.029/(190°C)</b>	<b>0.035/(282°C)</b>	<b>0.042/(476°C)</b>	<b>0.106</b>
<b>20</b>	<b>21.1</b>	<b>0.154/(186°C)</b>	<b>0.191/(324°C)</b>	<b>0.149/(420°C)</b>	<b>0.494</b>
<b>30</b>	<b>21.2</b>	<b>0.232/(189°C)</b>	<b>0.396/(335°C)</b>	<b>0.168/(436°C)</b>	<b>0.796</b>

X-ray diffraction was carried out to identify the crystalline structure of the catalysts. The X-ray patterns for different HSiW loading are shown in Fig. 5-17. Generally, bulk HSiW exhibits characteristic crystalline peaks at 8°~10°, 20°~24°, 26°~28°, 32°~35° [158]. It can be seen that no diffraction peaks corresponding to HSiW can be observed in the XRD pattern for 5 and 10wt % HSiW supported 10Ni/Al<sub>2</sub>O<sub>3</sub> catalyst, suggesting that HSiW was well dispersed on Al. As the loading amount exceeds 10wt%, some characteristic crystalline peaks of HSiW gradually evolve. This is a clear indication that large crystals of HSiW form which subsequently lower the HSiW dispersion. It is believed that, heteropoly ions strongly interact with supports at the loading below 10%, while the bulk properties of these materials prevail at high loading. This can explain why the

acidity of the catalyst was low, being extremely low when the loading of HSiW is below 10wt% and the acidity increases significantly at high loading.

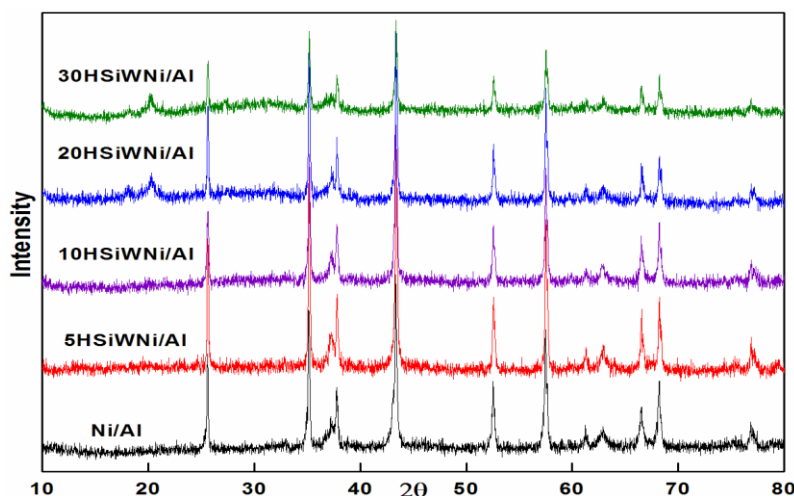


**Figure 5-17** XRD patterns for different HSiW loading

## Summary

The variation of HSiW loading over the range of 0 to 30wt% influences both the glycerol conversion and product distribution. The total acidity linearly increases with an increase in HSiW loading. Acidity can promote the production of 1-PO but decreases the production of 1,2-PD and EG. The loading of HSiW should be sufficiently high, i.e. 20wt % or higher) to promote the further hydrogenolysis of 1,2-PD to 1-PO. 30wt% HSiW loading shows the highest activity in the production of 1-PO.

### 5.3.2 Effect of different amounts Ni loading

It was found that 30wt% HSiW on a 10Ni/Al<sub>2</sub>O<sub>3</sub> catalyst shows the highest activity in the production of 1-PO. In this part of the research work the effect of Ni loading on the catalyst activity of Ni/30HSiW/Al<sub>2</sub>O<sub>3</sub> for the hydrogenolysis of glycerol was studied.

### Experimental condition

The loading of Ni on the catalysts was varied from 0 to 15wt% to investigate the influence of Ni loading on the catalytic activities of the  $\gamma$ -Ni/30HSiW/Al<sub>2</sub>O<sub>3</sub> catalysts. The experiment was performed at 240°C, under 580PSI of H<sub>2</sub> pressure using 2g of Ni supported 30HSiW/Al<sub>2</sub>O<sub>3</sub>



catalyst, 30g of glycerol (30wt%), 70g of DI water, 700RPM for 7hours. The catalysts were reduced at 450°C for 5 hours.

## Results and discussion

The conversions of the glycerol observed for different Ni loadings are shown in Fig. 5-18, 5-19 and the data are summarized in Table 5-9. The main products observed in the liquid phase were: acetol, 1,2-PD, 1,3-PD, Acr, 1-PO and EG. Some other products (OP) such as methanol (MeOH), ethanol (EtOH) were also obtained. However at low Ni loading of 0 and 1wt%, there are some other light and heavy unidentified products also produced.

The data shows that, the variation of Ni loading over the range of 0 to 15wt% influences both the glycerol conversion and product distribution. Among the catalysts, 5wt%Ni loading is most effective for the conversion of glycerol to 1-PO. On increasing the Ni loading from 0 to 15wt%, the conversion of glycerol and selectivity to Acr decreases gradually from 59% to 37.2% and 41.5% to 4.3% respectively; however the selectivity to different products is affected in a different manner. While the selectivity to 1-PO went through a maximum of 86.8%, the selectivity to by-products went through a minimum of 2.7% at 5wt % Ni loading.

**Table 5-10** Effect of Ni loading on catalytic activity of the Ni/30HSiW/Al<sub>2</sub>O<sub>3</sub>

Ni wt%	Acidity mmol/g	Conv %	Selectivity, %						
			1,3PD	1,2PD	Ac	EG	1-PO	Acr	OP
0	0.273	59.0	0.0	0.0	0.6	0.0	10.1	41.5	47.8*
1	1.297	53.4	0.0	0.0	1.3	0.0	41.7	42.0	15.0*
5	0.823	44.9	0.0	1.6	1.5	0.0	86.8	7.4	2.7
10	0.796	43.8	0.0	2.9	1.2	0.0	80.9	5.4	9.6
15	0.530	37.2	0.0	6.7	1.5	6.1	68.2	4.3	13.2

**Reaction condition:** yNi/30HSiW/Al<sub>2</sub>O<sub>3</sub> (y= 0,1,5,10 and 15wt%) catalyst, 240°C, 700RPM, 2g catalyst, 30g of glycerol (30wt%), 70g of DI water and 580PSI of H<sub>2</sub>. \*: By-products included methanol, ethanol and unidentified light ad heavy

For the Ni-free catalyst (i.e. HSiW/Al<sub>2</sub>O<sub>3</sub> catalyst) and a catalyst with 1wt % Ni loading, Acr is dominant (around 42%), 1-PO was produced at low selectivity (10.1% and 41.7% respectively) and no 1,2-PD was obtained. With increasing of Ni loading to 5wt%, the selectivity to 1-PO significantly increases to 86.8%, whereas Acr decreased to a lower level of around 7% and 1,2-PD appeared at 1.6% selectivity. However, further increase of the Ni loading led to a decrease in selectivity to 1-PO, whereas the selectivity to 1,2-PD increases gradually to 6.7% with 15% Ni loading, the selectivity to Acr continuously decreased to 4.3%. It should be noted that further increase of Ni loading from 5wt% to 15wt% leads to an increase in the selectivity to other by-products including methanol and ethanol. As can be seen from the Fig. 5-18, the selectivity of 1-PO went through a maximum while the selectivity to by-products went through a minimum of at 5wt% Ni loading. The selectivity to Acr decreased but the selectivity to 1,2-PD increased. It is believed that part of 1-PO came from the hydrogenation of acrolein that was produced from the consecutive dehydration of glycerol which was also reported by Xufeng L. in 2014 [122]. Therefore, an increase in Ni loading can promote the hydrogenation of acrolein to 1-PO leading to a decrease in the selectivity of acrolein but can also cause a decrease in acidity of the catalyst. This decrease in acidity can slow down the dehydration step that results in a decrease in conversion of glycerol and suppresses further hydrogenolysis of 1,2-PD to 1-PO.

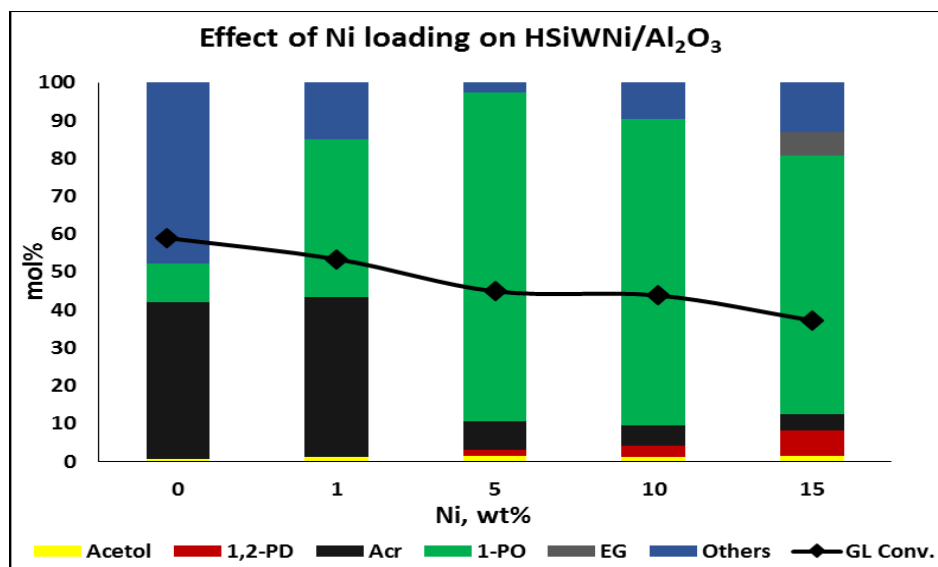


**Figure 5-18** Effect of Ni loading on glycerol hydrogenolysis and products selectivity; **Reaction condition:**  $\gamma$ Ni/30HSiW/Al<sub>2</sub>O<sub>3</sub> ( $\gamma$  = 0,1,5,10 and 15wt%) catalyst, 240°C, 700RPM, 2g catalyst, 30g of glycerol (30wt%), 70g of DI water and 580 PSI of H<sub>2</sub>

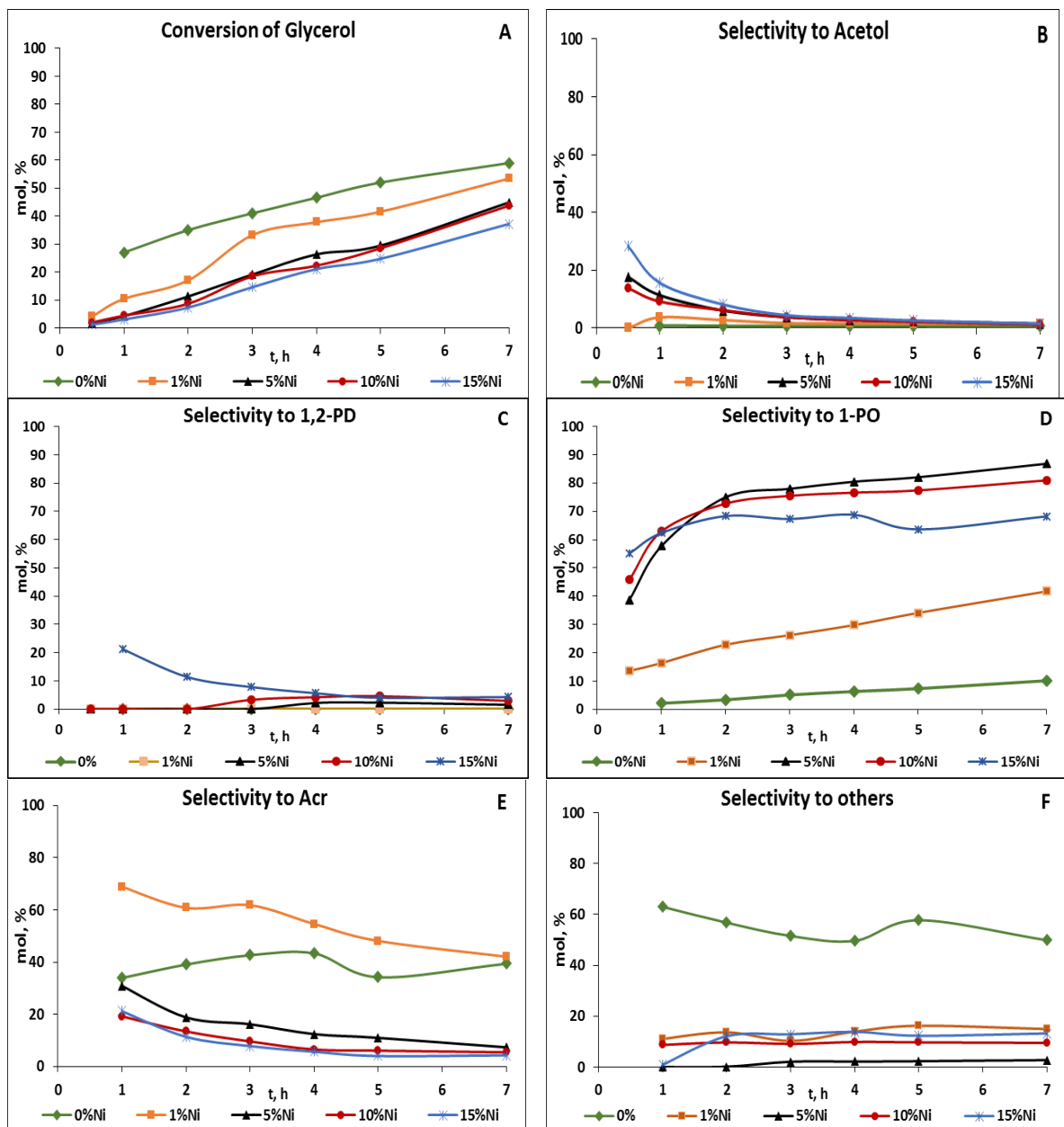


**Figure 5-19** Effect of Ni loading on glycerol hydrogenolysis and products selectivity as a function of time. A) Glycerol Conversion; B,C,D,E,F) Selectivity of acetol, 1,2-PD, 1-PO, Acr., other products, respectively. **Reaction condition:**  $y\text{Ni}/30\text{HSiW}/\text{Al}_2\text{O}_3$  ( $y=0, 1, 5, 10$  and  $15\text{wt}\%$ ) catalyst,  $240^\circ\text{C}$ ,  $700\text{RPM}$ ,  $2\text{g}$  catalyst,  $30\text{g}$  of glycerol ( $30\text{wt}\%$ ),  $70\text{g}$  of DI water and  $580\text{ PSI}$  of  $\text{H}_2$ .

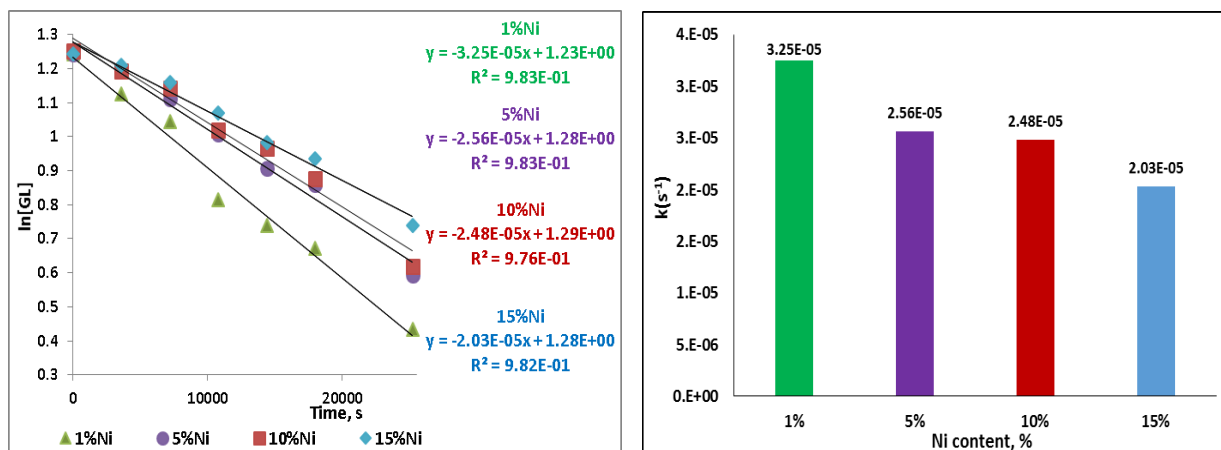


**Figure 5-20** Pseudo-First-Order kinetic plots of effect of Ni loading on hydrogenolysis of glycerol in the presence of Ni/30HSiW/Al<sub>2</sub>O<sub>3</sub> catalyst; **Reaction condition:** 240°C, 700RPM, 2g catalyst, 30wt% (30g) aqueous glycerol and 580PSI H<sub>2</sub>

### Characterization of catalysts

To examine surface acidity, NH<sub>3</sub>-TPD was performed. The TPD data was deconvoluted into 3 peaks (namely weak, medium and strong acid sites) using a Gaussian fitting method, the quantity of acid sites of the catalysts is shown in Table 5-11 and Fig. 5-21 and was then correlated with the catalytic activity of the catalysts.

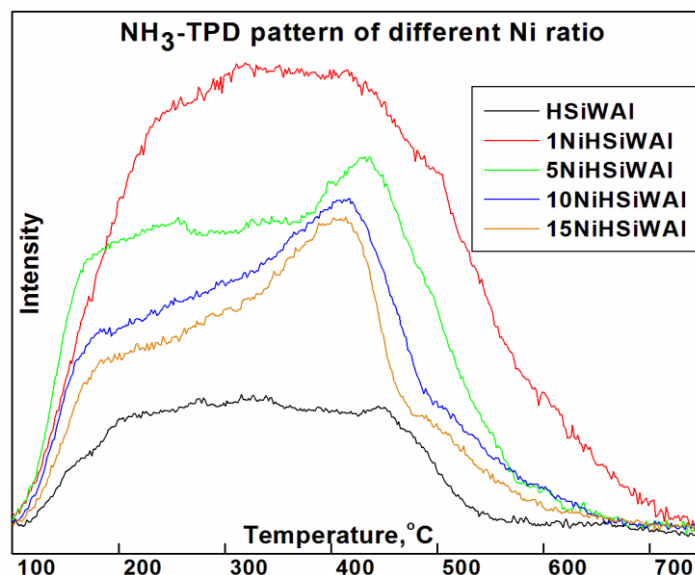


**Figure 5-21** NH<sub>3</sub>-TPD patterns for Ni loading

**Table 5-11** BET surface area and acidities of different Ni loading catalysts

Ni wt%	SAA m <sup>2</sup> /g	Weak acid site mmol/g / (Temp.)	Medium acid site mmol/g / (Temp.)	Strong acid site mmol/g / (Temp.)	Total acid amount, mmol/g
0	17.7	0.031/(200°C)	0.205/(325°C)	0.038/(457°C)	0.273
1	15.2	0.214/(214°C)	0.273/(304°C)	0.811/(437°C)	1.297
5	17.9	0.084/(95°C)	0.538/(236°C)	0.201/(440°C)	0.823
10	21.2	0.232/(189°C)	0.396/(335°C)	0.168/(436°C)	0.796
15	22.2	0.106/(189°C)	0.277/(309°C)	0.148/(408°C)	0.530

As can be seen, the total number of acidic sites decreases with increasing Ni content. A decrease in acidity may possibly be due to the covering of acid sites by Ni or it can be suggested that this behavior may result from direct anchoring on proton sites which forms blockage of acid channels by Ni particles. It is important to note that Ni-free catalyst possesses low acidity (0.273mmol/g) compared to that of the Ni supported catalyst. It maybe due to the fact that the Ni-promoted catalysts in the presence of hydrogen increases the acidity that might be attributed to the formation of water molecules during the reduction which could facilitate the formation of active Brønsted acid sites which are considered to be the active reaction sites [83, 89-91]. However the strength of acid sites does not follow this pattern. Among the catalysts, 5wt % Ni loading catalyst has its weak and medium acid sites at its lowest strength; and there was a significant shift toward lower temperature (shift of weak and medium acid sites from around 200°C to 95° C and 300°C to 236°C respectively). This decrease in the strength of the acid site of the 5wt % Ni loading catalyst may result in a proper balance between acid sites and metal sites so that an improvement in the activity of the catalyst toward the production of 1-PO from glycerol.

BET surface area was calculated from desorption isotherms and the results are listed in Table 5-10. As can be seen, the surface area increases with an increase in Ni loading. However, the increase in surface area does not seem to affect either the catalyst activity or acidity.

To examine structural changes induced into its active phase, XRD was performed and the results are shown in Fig. 5-22.

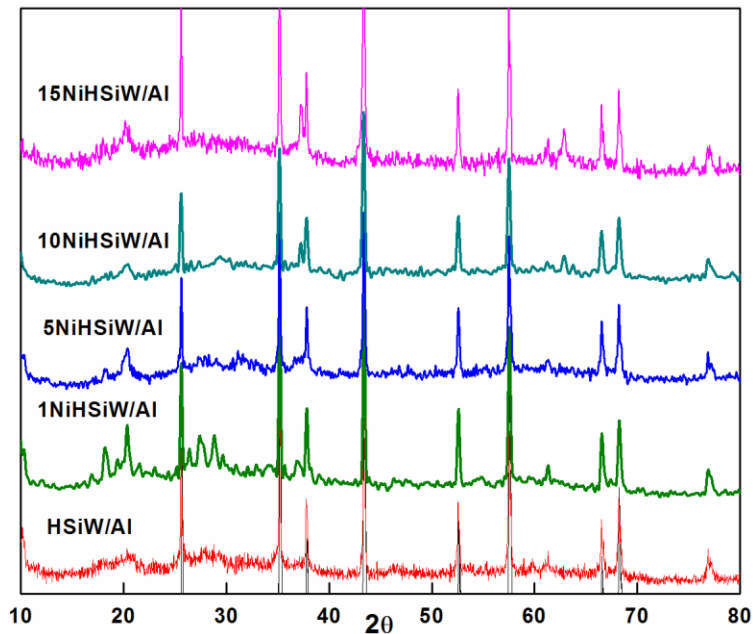


**Figure 5-22** XRD patterns for different Ni loading catalyst.

As can be seen from the XRD pattern, no diffraction peaks of NiO ( $2\theta = 37.3^\circ, 44.3^\circ$  and  $62.9^\circ$ ) are observed for the Ni loadings of up to 5wt % suggesting that Ni was dispersed well; either in an amorphous nature of Ni in the catalyst or that the size of Ni is smaller than the XRD detection limit. Further increase in the Ni loadings to 15wt %, results in diffraction peaks attributed to the NiO phase that can be observed and the intensities became stronger with a further increase of metal loading. As the loading of Ni is increased the reason for the formation of diffraction peaks attributed to the NiO might be due to the inhomogeneous distribution of the Ni species or the particle becoming larger due to agglomeration when Ni was loaded at high levels. Furthermore the intensities of the diffraction peaks attributed to the HSiW phase have been observed and the intensities became weaker with an increase in metal loading. It is believed that in the case of impregnated catalysts, the metal and the support are two separate phases and their interaction does not lead to any major change in the support structure. As a result the diffraction peaks attributed to the HSiW would decrease with increasing metal loading, since the added metal covers the pore walls and eventually fills up the pores.

### Summary

The variation of Ni loading over the range of 0 to 15wt% influences both the glycerol conversion and product distribution. It is found that the catalyst having 5wt loading of Ni is the best catalyst

compared to the others; it can give the highest selectivity to 1-PO, reducing the by-products as a result of better dispersion of NiO on the surface of the catalyst. It is believed that part of 1-PO came from the hydrogenation of acrolein that was produced from the consecutive dehydration of glycerol. The total number of acidic sites and the acid strength was found to decrease with increasing Ni content. A decrease in acidity may possibly be due to the covering of acid sites by Ni or it can be suggested that this behavior may result from direct anchoring on proton sites and from blockage of acid channels by Ni particles. To achieve good performance, catalysts must have a proper balance between acid sites and metal sites.

### **5.3.3 Effect of catalyst preparation sequence on 10Ni/30HSiW/Al<sub>2</sub>O<sub>3</sub> catalysts**

The catalyst was prepared by impregnation of the components in sequence. So the active components can be added in different sequences and this change in sequence may influence the activity and selectivity of the catalyst. Here the effect of the preparation sequence was examined by varying the order of component adding.

#### **Experimental condition**

The experiment was performed at 240°C under 580PSI of H<sub>2</sub> pressure using 2g of 10Ni/30HSiW/Al<sub>2</sub>O<sub>3</sub> catalyst, 30g of glycerol, 70g DI water, for 7 hours. The catalyst was reduced at 450°C for 5 hours.

#### **Results and discussion**

The effect of preparation sequences on the hydrogenolysis of glycerol are summarized in Table 5-12 and depicted in the Fig. 5-23. The main products observed in the liquid phase were: acetol, 1,2-PD, 1,3-PD, Acr, 1-PO and EG. Some other products (OP) such as methanol (MeOH), ethanol (EtOH) were also obtained.

As can be seen from the data, the method of preparation shows little effect on the catalyst activity in both the conversion of glycerol and product distribution. Among the catalysts, the one prepared by the co-impregnation method is the most effective with high conversion of glycerol and the selectivity of acrolein is low. When the component of HSiW was added first, the selectivity to 1-PO and the conversion of glycerol was low but the selectivity to 1,2-PD was high compared to other catalysts. It is suggested that there may be a decrease in acidity of the catalyst that can affect

the dehydration of glycerol and suppress further hydrogenolysis of 1,2-PD to 1-PO. In contrast, when Ni was loaded first, the selectivity to Acr was the highest. This may be due to the hydrogenation of Acr to 1-PO slowdown (that may be caused by a decrease in Ni sites after loading of HSiW on 10Ni/Al<sub>2</sub>O<sub>3</sub> so lower acrolein exposure to Ni for hydrogenation). The catalysts prepared by the co-impregnation method show the highest pseudo-first-order pseudo-first-order rate constant compared to the other methods of preparation (Fig. 5-24).

**Table 5-12** Effect of different sequence loading active components on product distribution

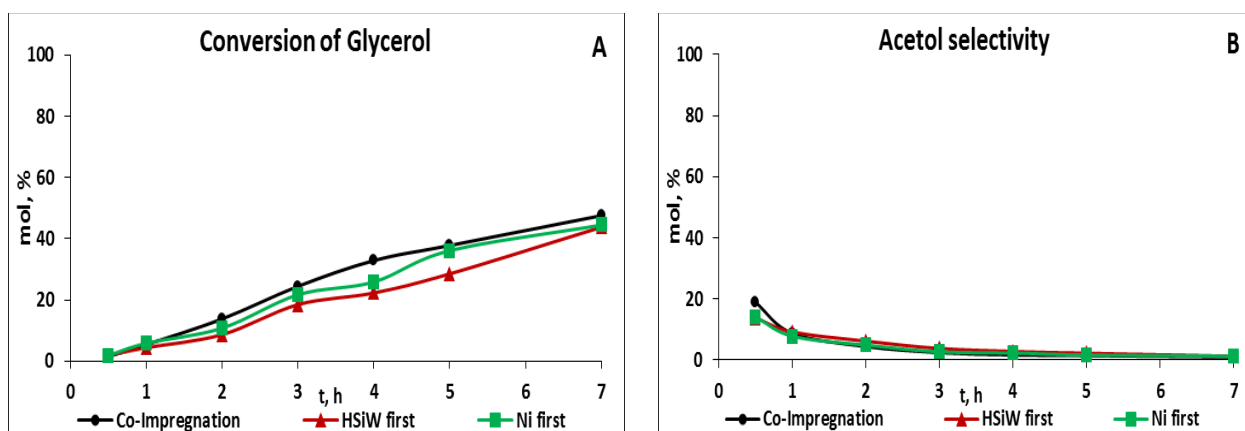
Sequence of loading *	Acidity mmol/g	Conv. mol%	Selectivity, mol%						
			1,3-PD	1,2-PD	Acetol	EG	1-PO	Acr	OP**
*HSiW first	0.796	43.8	0.0	2.9	1.2	0.0	80.9	5.4	9.5
*Ni first	0.858	44.5	0.0	1.6	1.2	0.0	86.6	7.2	3.4
*Co-imp	1.264	47.6	0.0	2.2	1.0	0.0	86.9	4.8	5.1

**Reaction condition:** 10Ni/30HSiW/Al<sub>2</sub>O<sub>3</sub> catalyst, 240°C, 700RPM, 2g catalyst, 30g of glycerol (30wt%), 70g of DI water and 580PSI of H<sub>2</sub>. \*\* OP: By-products included methanol and ethanol

\***HSiW first:** The HSiW was added first then Ni was loaded onto 30HSiW/Al

\***Ni first:** The Ni was added first then HSiW was loaded onto 10Ni/Al

\***Co-Imp:** catalyst prepared by Co-Impregnation method





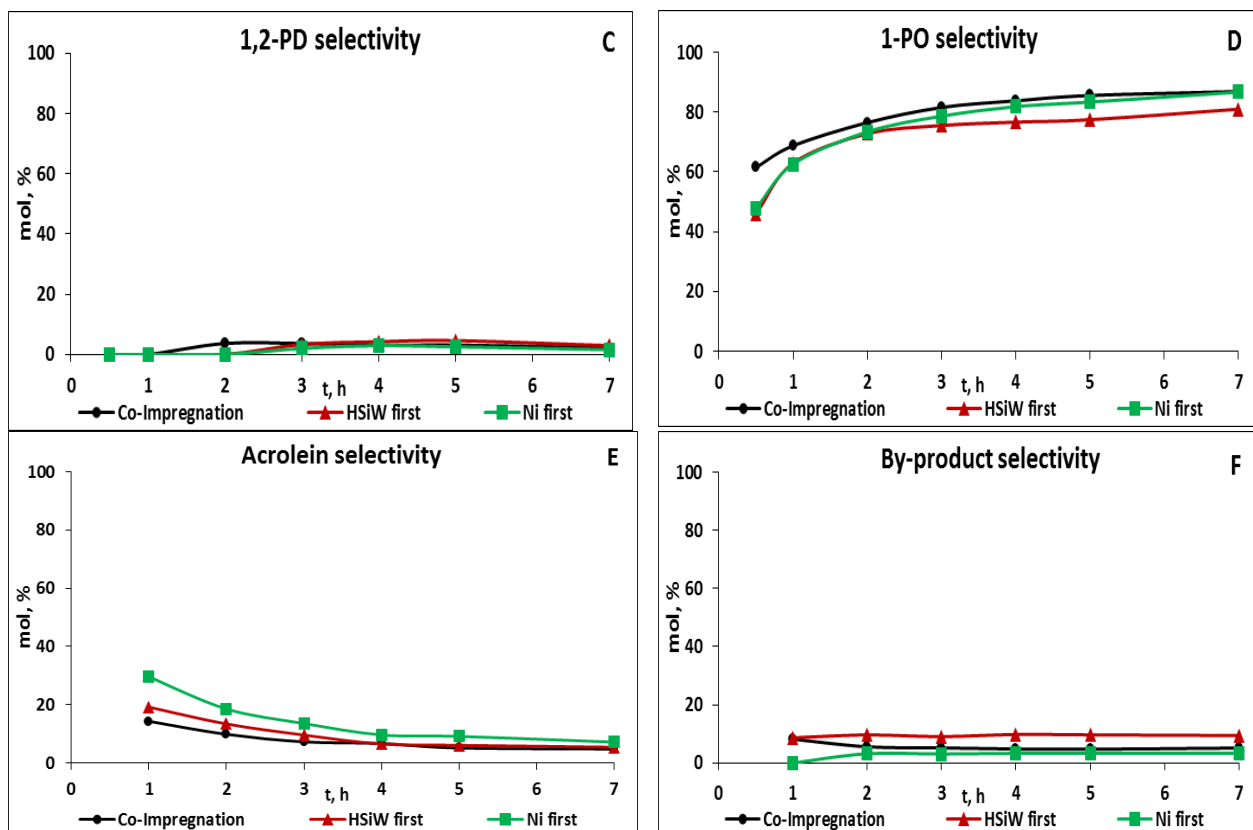


**Figure 5-23** Effect of preparation sequence loading active components on glycerol hydrogenolysis and products selectivity as a function of time. A) Glycerol Conversion; B,C,D,E,F) Selectivity of acetol, 1,2-PD, 1-PO, Acr., other products, respectively. **Reaction condition:** 10Ni/30HSiW/Al<sub>2</sub>O<sub>3</sub> catalyst, 240°C, 700RPM, 2g catalyst, 30g of glycerol (30wt%), 70g of DI water and 580 PSI of H<sub>2</sub>.

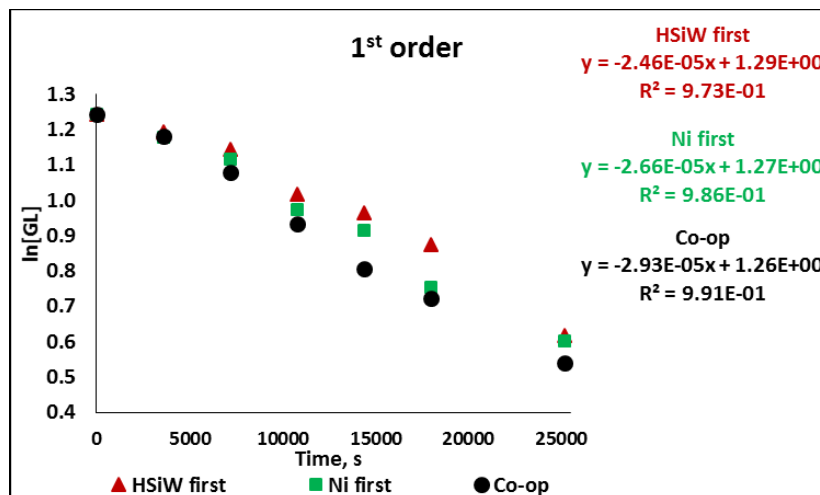


**Figure 5-24** Pseudo-First-Order kinetic plots of effect of sequence adding components on hydrogenolysis of glycerol in the presence of 10Ni/30HSiW/Al<sub>2</sub>O<sub>3</sub> catalyst; **Reaction condition:** 240°C, 700RPM, 2g catalyst, 30g of glycerol (30wt%), 70g of DI water and 580PSI H<sub>2</sub>

### Characterization of catalysts

To examine surface acidity, NH<sub>3</sub>-TPD was performed. The TPD data was deconvoluted into 3 peaks (namely weak, medium and strong acid sites) using a Gaussian fitting method, the quantity of acid sites of the catalysts was recorded and is shown in Table 5-13 and was then correlated with the catalytic activity of the catalysts. Among the catalysts, the catalyst that is prepared by co-impregnation has the highest acidity; however the strength of strong acid sites is the lowest (427°C). The acidity of the catalyst significantly decreases when active sites were doped in sequence. It is suggested that when the component was added in sequence the interaction between component species and support may be stronger causing the catalyst to become harder to reduce and affect the balance between the acid site and the metal site that leads to the reduction in total acidity of the catalyst. When HSiW was added first, the decrease in acidity may be caused by the covering of acid sites by Ni loading or it can be suggested that this behavior may result from direct anchoring on proton sites and from blockage of acid channels by Ni particles.

**Table 5-13** Total acidity of different sequence HSiW loading catalysts

Sequence	Weak acid site mmol/g / (Temp.)	Medium acid site mmol/g / (Temp.)	Strong acid site mmol/g / (Temp.)	Total acid amount, mmol/g
<b>HSiW first</b>	<b>0.232/(189°C)</b>	<b>0.396/(335°C)</b>	<b>0.168/(436°C)</b>	<b>0.796</b>
<b>Ni first</b>	<b>0.228/(203°C)</b>	<b>0.428/(347°C)</b>	<b>0.202/(450°C)</b>	<b>0.858</b>
<b>Co-imp</b>	<b>0.367/(189°C)</b>	<b>0.421/(363°C)</b>	<b>0.475/(427°C)</b>	<b>1.264</b>

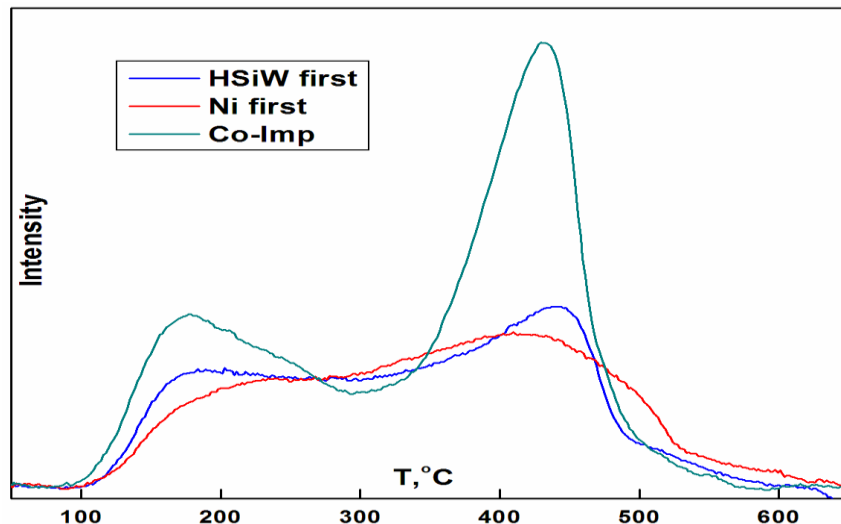


**Figure 5-25** NH<sub>3</sub>-TPD patterns for method preparation

X-ray diffraction was carried out to identify the crystalline structure of the catalysts. The X-ray patterns for different sequence loading are shown in Fig. 5-26.

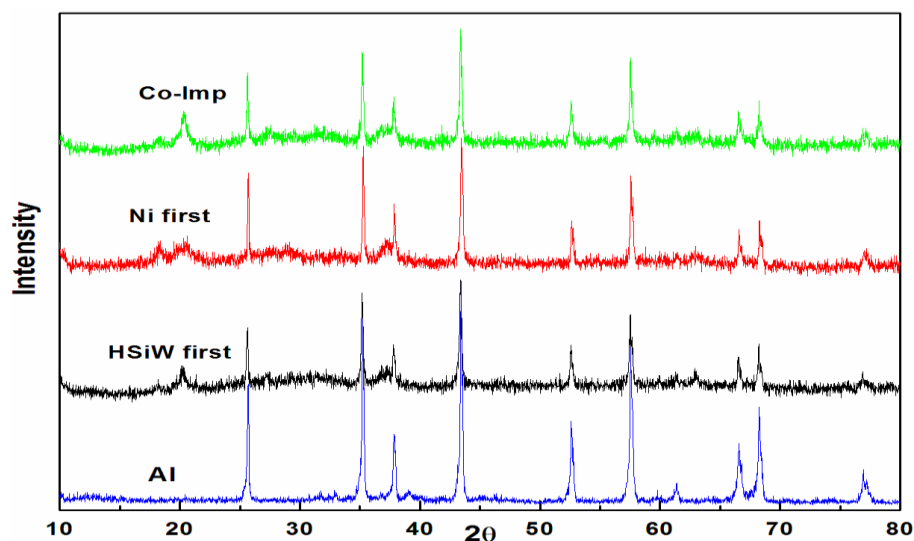


**Figure 5-26** XRD patterns for method preparation

The XRD pattern of the pure support shows the peaks of alpha alumina. Compared with the XRD pattern of Al, the peak intensity of the XRD pattern for all the catalysts diminishes. For all catalysts the reflection of SiW is observed but the intensity is slightly different. The diffraction lines corresponding to the reflections of HSiW ( $2\theta = 22^\circ \sim 24^\circ$ ,  $26^\circ \sim 28^\circ$ ,  $32^\circ \sim 35^\circ$ ) can be observed in all the XRD patterns of the catalyst, indicating that the layer formation of the HSiW phase at high loading of 30% HSiW on the surface of the Al. It should be noted that the peak intensity of HSiW

for (HSiW first) catalyst is weaker than for the others, which implies that either (HSiW first) the catalyst favors the dispersion of HSiW species on the surface of Al or the covering of HSiW by addition of Ni. However, the peak intensity of the NiO species ( $2\theta = 37.3^\circ, 44.3^\circ$  and  $62.9^\circ$ ) is similar for all catalysts

Aiming to understand the differences in reduction behavior coming from the preparation methodologies, TPR studies were performed on all the catalyst samples and the result are shown in Fig 5-27.

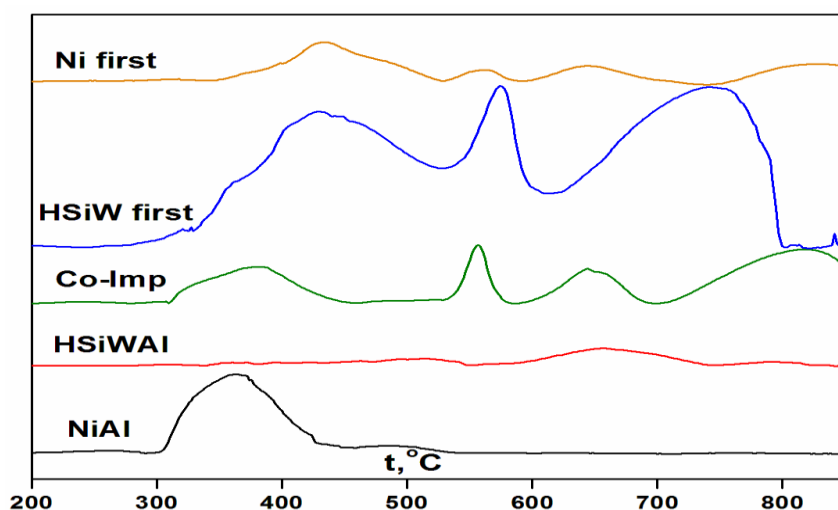


**Figure 5-27** TPR patterns for sequence loading of component

As seen in Fig. 5-27, the TPR pattern of the all 3 catalysts shows  $H_2$  consumption peaks with a maxima around  $800^\circ C$ . The 2 lower temperature peaks between  $300$  and  $500^\circ C$  are attributed to the reduction of highly dispersed NiO species that interact strongly with Al, and the higher temperature peak to the reduction of larger NiO clusters, but also in contact with Al.

As for the catalyst that Ni was added first, a displacement of the maximum of the first peak to a higher reduction temperature and is seen to overlap with the second peak and its height decreases, indicating the formation of particles with less interaction with Al, and therefore is harder to reduce.

For the catalyst that is prepared by the co-impregnation method, the reduction peaks of Ni shift toward lower temperature and overlap with the first peak, the reducibility of Ni is improved if the catalyst is prepared by the co-impregnation method.

## Summary

Briefly, the sequence of adding the catalyst component during the preparation of catalyst can affect the catalyst activity and the catalyst properties. Among these catalysts, the catalyst prepared by co-impregnation is the most effective for the hydrogenolysis of glycerol to 1-PO with high selectivity to 1-PO and low by-products production. Furthermore the catalyst prepared by the co-impregnation method possesses the highest acidity among others.

## 5.4 Proposed reaction mechanism using heterogeneous metal catalysts

In order to elucidate the reaction sequence of glycerol hydrogenolysis and understand the hydrogenolysis pathway of glycerol to lower alcohols the role of the intermediates 1,2-PD, 1,3-PD, 1-PO over Ni/HSiW/Al was investigated under conditions similar to that of the hydrogenolysis of glycerol and the results are presented in Table 5-14 and Fig 5-28.

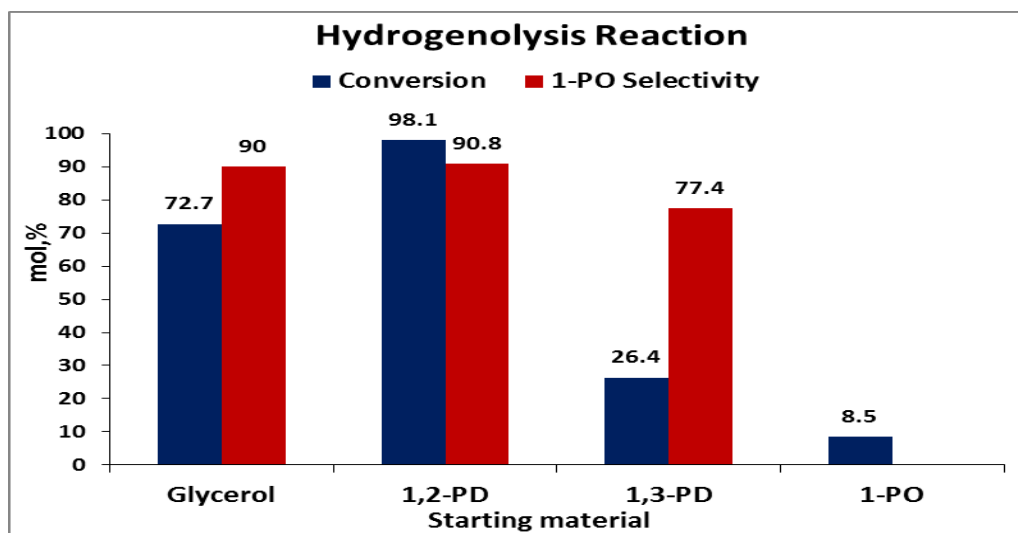


**Figure 5-28** Hydrogenolysis of glycerol and lower alcohols. **Reaction condition:** 10Ni/30HSiW/Al<sub>2</sub>O<sub>3</sub> catalyst, 240°C, 700RPM, 2g catalyst, 30g of glycerol (30wt%), 70g of DI water and 580PSI of H<sub>2</sub>, catalysts were reduced at 350°C for 5h.

The results show that with the same catalytic system the hydrogenolysis of 1,3-PD and 1-PO is not as effective as the hydrogenolysis of glycerol and 1,2-PD. While the conversion of 1,3-PD and 1-PO was low (26.4% and 8.5% respectively), the conversion of glycerol and 1,2-PD was much higher (71% and 98.1% respectively). Using different starting materials, 1-PO is always a major

product; however, the selectivity of 1-PO derived from 1,3-PD is low (only 77.4%) compared to 1-PO derived either from glycerol (90%) or from 1,2-PD (90.8%). With respect to the formation of ethylene glycol, it was obtained from glycerol hydrogenolysis; however, it was not detected in the 1,2-PD and 1,3-PD hydrogenolysis, suggesting that ethylene glycol was produced directly from glycerol by a C–C bond cleavage reaction. In the reaction of glycerol and 1,2-PD, ethanol was observed which can be formed via sequential hydrogenolysis of ethylene glycol or decomposition of 1,2-PD. Since the conversion of 1-PO was much lower than that of 1,2-PD and 1,3-PD it can be assumed that 1-PO is stable under the reaction conditions and can be considered as the final product in the hydrogenolysis of glycerol using the catalyst 10Ni/30HSiW/Al<sub>2</sub>O<sub>3</sub> under the reaction conditions. In the hydrogenolysis of 1-PO using 10Ni/30HSiW/Al<sub>2</sub>O<sub>3</sub> catalyst, 1-propanaldehyde is produced as the major product. Using 10Ni/30HSiW/Al<sub>2</sub>O<sub>3</sub> catalyst, it was clear that 1-PO was formed mainly from the further hydrogenolysis of 1,2-PD and it is evident that ethylene glycol was not obtained from 1,2-PD. It is thought that the pathway for the conversion of glycerol using 10Ni/30HSiW/Al<sub>2</sub>O<sub>3</sub> catalyst would involve glycerol dehydration to acetol or 3-HPA on acid sites, followed by hydrogenation of acetol or 3-HPA on metal sites to produce 1,2-PD or 1,3-PD respectively. Then further hydrogenolysis of 1,2-PD or 1,3-PD will produce 1-PO. Therefore the role of Ni and HSiW for hydrogenation and dehydration respectively in the hydrogenolysis of glycerol was studied in this respect.

**Table 5-14** Hydrogenolysis of different starting materials using 10Ni/30HSiW/Al<sub>2</sub>O<sub>3</sub> catalyst

\*a: Unreduced catalyst

\*b: HSiW/Al catalyst

\*c: Ni/Al catalyst

	1	2	3	4	5	6	7	8
Reactant	Glycerol	Glycerol	Glycerol <sup>a*</sup>	Glycerol <sup>b</sup>	Glycerol <sup>c*</sup>	12PD	13PD	1PO
Gas	Nitrogen	Hydrogen						
Conversion	22.9	72.3	71.6	69.0	56.3	98.1	26.4	8.5
Selectivity								
Acetol	17.3	0.6	1.1	0.6	0.5	-	-	-
1,2PD	-	1.1	-	-	20.4	-	-	-
1-PO	13.9	91.2	67.6	10.1	13.4	90.8	77.4	-
EG	-	-	-	-	11.8	-	-	-

<b>MeOH</b>	-	<b>1.3</b>	<b>1.4</b>	-	<b>2.4</b>	-	-	-
<b>EtOH</b>	<b>4.9</b>	<b>2.7</b>	<b>1.6</b>	-	<b>51.5</b>	<b>2.1</b>	<b>15</b>	<b>20.7</b>
<b>Acr</b>	<b>13.4</b>	<b>2.9</b>	<b>25.9</b>	<b>39.4</b>	-	-	<b>0.8</b>	-
<b>Propanal</b>	-	-	-	-	-	<b>4.5</b>	-	<b>79.3</b>
<b>UIP</b>	<b>50.5**</b>	<b>0.2*</b>	<b>2.4**</b>	<b>49.9**</b>	-	<b>2.6*</b>	<b>6.8*</b>	-

**Reaction condition:** 10Ni/30HSiW/Al<sub>2</sub>O<sub>3</sub> catalyst, 240°C, 700RPM, 2g catalyst, 30g of glycerol (30wt%), 70g of DI water and 580PSI of H<sub>2</sub>, catalysts were reduced at 350°C for 5h.

\*UIP: unidentified light products; \*\*UIP: unidentified light and heavy products

To explore a bifunctional metal-acid catalysed pathway for the hydrogenolysis of glycerol in a batch autoclave, first the dehydration of glycerol on 10Ni/30HSiW/Al<sub>2</sub>O<sub>3</sub> catalyst was tested under the same conditions applied to glycerol hydrogenolysis without addition of H<sub>2</sub> as a reactant for the hydrogenation step (N<sub>2</sub> was used instead of H<sub>2</sub>) (Table 5-14, column 1). Without H<sub>2</sub>, the reaction was slow, yielding acetol and acrolein in moderate selectivity (12.5% and 12% respectively) and selectivity to 1-PO is low (15.6%) at only 24.9% conversion of glycerol compared to the reaction with H<sub>2</sub> in which the conversion of glycerol and selectivity to 1-PO increase significantly to 72.7% and 90% respectively (column 2). Since metal is required for hydrogenation, the non-reduced catalyst was tested to elucidate the role of the metal (Table 5-14, column 3). The data show that without reducing, the activity of the catalyst is similar to the reduced catalyst with respect to glycerol conversion; however, the product distribution is influenced significantly. Compared to the reduced catalyst (column 2) the selectivity to 1-PO decreased from 90% to 67.6%; however, the selectivity of acrolein increased from 2.9% to 25.9%. The result show that the unreduced catalyst lost its activity or has hydrogenation activity severely reduced for the hydrogenation of acrolein to 1-PO.

Then the dehydration of glycerol using the catalyst without Ni addition was tested (Table 5-14, column 4). As can be seen from the Table 5-14, the catalyst affects slightly the catalyst activity in terms of the conversion of glycerol which reaches 69%; however, it affects the product distribution significantly. The selectivity to 1-PO significantly decreases from 90% to around 10% whereas the selectivity to acrolein increases from 2.9% to 39.4%. This again suggests that Ni is required to hydrogenate acrolein to 1-PO. Then the role of Ni was studied using only a metal of Ni supported alumina (Table 5-14, column 5). The data shows that 1,2-PD is produced as a major desired product with a selectivity of 20.4% and ethanol as a main by-product whereas 1-PO was produced in low

selectivity of 13.4%. The low 1-PO selectivity is expected to be due to lack of acidity for further hydrogenolysis of 1,2-PD to 1-PO, and Ni alone promotes the rupture of C-C bonds to produce ethanol. These results support the bifunctional mechanism for glycerol hydrogenolysis over the 10Ni/30HSiW/Al<sub>2</sub>O<sub>3</sub> catalyst.

It is well-known from the literature that acid catalysts can be used to carry out dehydration of alcohols in which the alcohol can be protonated by a Brønsted acid. Acidic sites can donate a proton to the reactant molecule and form a carbocation transition state that is the primary driver of the activity and selectivity of the reaction. In the dehydration of the alcohol, the acid catalyst tends to favor removal of hydroxyl groups from carbons that form a more stable carbocation. Primary alcohols are generally less reactive than the corresponding secondary alcohols due to the smaller electron-releasing inductive effect of one alkyl group as compared to two alkyl groups while the secondary carbocation is more stable than the primary carbocation [159,160].

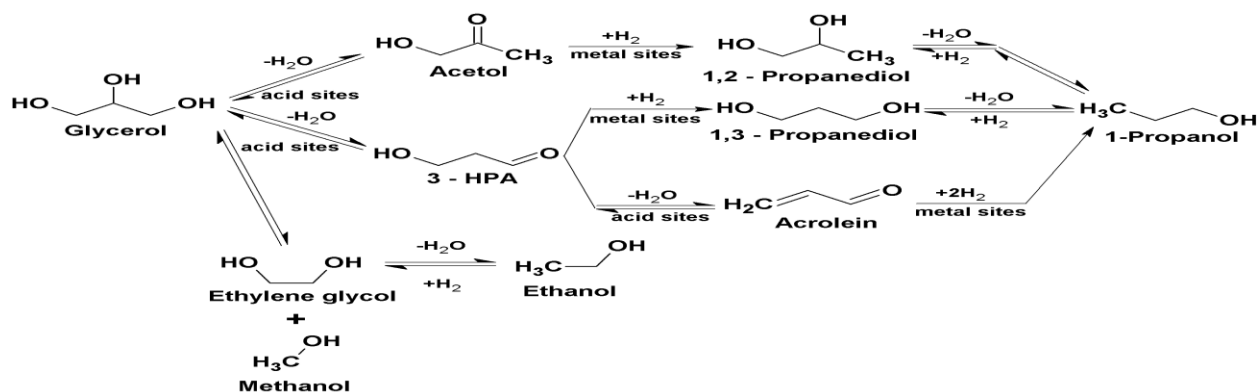
In glycerol hydrogenolysis, the first step involves an initial protonation of the hydroxyl group that leads to the formation of a carbocation and water [161,162]. The initial acid catalyzed dehydration is the selectivity controlling step. If the primary hydroxyl group is eliminated 1,2-PD will be obtained; if the secondary alcohol is eliminated then 1,3-PD will form. The dehydration of a primary alcohol produces acetol that is thermodynamically more stable than the dehydration of a secondary alcohol to form 3-HPA. Although dehydration of a secondary alcohol will occur via a relatively more stable intermediate secondary carbocation [105,163], the reaction is kinetically controlled [164,165]. This is likely due to the steric hindrance of the two primary alcohol functional groups in the glycerol.

Acetol is formed via the elimination of the primary hydroxyl group; while the elimination of secondary hydroxyls will produce 3-HPA. Although 3-HPA is more reactive compared to acetol [59,166], it was not observed as an intermediate in the liquid phase under our reaction conditions. The hydrogen activated on the metal facilitates the hydrogenation of acetol or 3-HPA to release 1,2-PD or 1,3-PD respectively. However, the dehydration of 3-HPA on the acid sites to form acrolein is very facile [204-208], therefore it is not easy to obtain 1,3-PD unless the hydrogenation reaction can be facilitated by a very active hydrogenation environment .



Further hydrogenolysis of propanediols will form 1-PO. Again the protonation of the hydroxyl groups of propanediols can produce reactive carbocation intermediates. A dehydration reaction of propanediols requires protonation of the alcohol group on the primary or secondary carbon to form primary or secondary carbocation ions respectively [172]. 1,2-PD having the secondary hydroxyl group can be easily dehydrated to produce 1-PO. Dehydration of 1,3-PD also leads to 1-PO although it is expected to be less facile as the dehydration produces the less stable primary carbocation. The pseudo first order rate constants shown in Chapter 4 (Fig 4-5) shows the rate constant for the conversion of 1,2-PD is the highest, followed by glycerol. The conversion of 1,3-PD is slower than the glycerol conversion while the conversion of 1-PO is the slowest. The conversion of 1,2-PD and 1,3-PD shows the rate constants for the conversion of 1,2-PD is 15 times faster than for 1,3-PD. These rate constants provide important information on the proposed reaction pathway for glycerol hydrogenolysis and also the product selectivity.

Based on the literature review [50, 59, 64, 108, 116] and our experimental results, we propose the following detailed mechanism to explain the formation of the 1-PO in the glycerol hydrogenolysis over the 10Ni30HSiW/Al<sub>2</sub>O<sub>3</sub> catalyst (Scheme 5-1). The intermediate products that are formed from glycerol are acetol, 3-hydroxypropylaldehyde (3-HPA), 1,2-PD, 1,3-PD and acrolein. 3-HPA and acetol are formed via the dehydration on acid sites of the hydroxyl group at the secondary and primary carbon atoms. While the overdehydration of 3-HPA forms acrolein following by the hydrogenation to form 1-PO; the hydrogenation of acetol or 3-HPA leads to 1,2-PD or 1,3-PD formation with further hydrogenolysis of 1,2-PD or 1,3-PD to give 1-PO. Since 3-HPA is more reactive compared to acetol [59, 166], it was not observed as an intermediate in the liquid phase.



**Scheme 5-1.** Proposed mechanism for hydrogenolysis of glycerol via bifunctional metal-acid catalysis.

From the mechanism proposed, we suggest that the main route for the formation of 1-PO from glycerol is via either the hydrogenation of acrolein or further hydrogenolysis of 1,2-PD (and 1,3PD) where 1,2-PD (and 1,3-PD) and acrolein are the intermediates in the formation of 1-PO from glycerol. In the absence of hydrogen, acetol and acrolein were the major products. Therefore hydrogen is required for the next step of hydrogenation of these intermediates to form 1-PO.

## 5.5 Leaching and recyclability of catalyst

The solid bifunctional catalyst used in the reaction can be separated from the reaction mixture as it is heterogeneous. However whether the catalyst suffers from leaching and if it could be reused for the same purpose are one of the aspects that must be explored.

The leaching of catalyst can be measured by using a hot filtration method. The catalyst was filtered out from the reaction mixture at the stage of 50% conversion. If reaction further proceed, that means leaching of catalyst happened. On other hand, if there is no further progress in the reaction that indicates either there is no leaching or the leaching of component is not sufficient to keep the reaction proceeding. To study the leaching of HSiW supported catalyst, the catalyst was filtrated from the liquid after 7h of experiment. Then the liquid was placed back into the autoclave. The experiment was carried out for 6h to test for catalyst leaching. The results are shown in Table 5-15.

**Table 5-15** Continuing reaction after filtering the 10Ni/30HSiW/Al<sub>2</sub>O<sub>3</sub> catalyst

Leaching	C <sub>GL</sub> mol/l	Selectivity, mol%					
		1,3-PD	1,2-PD	Acetol	EG	1-PO	OP*
<b>Before testing</b>	<b>3.111</b>	<b>0.0</b>	<b>2.9</b>	<b>1.21</b>	<b>0.0</b>	<b>80.9</b>	<b>14.9</b>
<b>After testing of 6h</b>	<b>3.088</b>	<b>0.0</b>	<b>1.6</b>	<b>1.16</b>	<b>0.0</b>	<b>78.4</b>	<b>18.9</b>

OP\*: methanol, ethanol and light unidentified products

As can be seen from the Table 5-15, there is a slight decrease in the concentration of glycerol and selectivity to 1-PO and an increase in OP which suggest that the leaching is not significant or the components that leached out from catalyst are essentially catalytically inactive for the reaction.

To confirm if the leaching of catalyst affects the catalyst activity, the recyclibility of the catalyst was studied. To study the recyclability of the HSiW supported catalyst 3 type of catalysts that were reduced at different temperature (350°C, 400°C and 450°C) were used and recycled. For each type of catalyst, two experiments were carried out using 2g of catalyst and then the catalysts were recovered and reused one time.

The results were presented in the Table 5-16. It is shown that the activity and acidity of the catalyst reduced at 350°C and 400°C decreases after recycling. For both catalysts the conversion of glycerol shows a decrease of around 10% and there is a change in the distribution of products. The selectivity to 1-PO decreases while the selectivity to 1,2-PD, EG and by-products increases. It is believed that the loss in activity and acidity may be a result of leaching of HSiW. As a result the basicity of the catalyst may increase leading to an increase in selectivity to EG. It is unexpected that the catalyst reduced at 450°C showed an increase in activity with respect to the conversion of glycerol and selectivity to 1-PO, an increase in selectivity to EG was still observed. It is thought that after the catalyst involved in the hydrogenolysis of glycerol in water media, water may be added to recover the heteropoly acid so the catalytic activity was increased.

**Table 5-16** 10Ni/30HSiW/Al<sub>2</sub>O<sub>3</sub> catalyst recycling study

Red. Temp	Catal	Conv mol%	Selectivity, mol%					
			13PD	12PD	Acetol	EG	1-PO	OP
350	Fresh	72.3	0.0	1.1	0.6	0.0	91.7	6.6
	Reused	69.6	0.0	1.8	0.5	2.7	87.7	9.9
400	Fresh	67.4	0.0	1.7	0.6	0.0	91.2	6.5
	Reused	57.4	0.0	8.3	0.7	5.8	71.9	13.3
450	Fresh	43.8	0.0	2.9	1.2	0.0	80.9	14.9
	Reused	63.1	0.0	3.6	0.7	2.7	79	14.1

## 5.6 Conclusions

The catalyst of 10/Ni/30HSiW/Al<sub>2</sub>O<sub>3</sub> was prepared using the impregnation method and a parametric study was performed to understand the effect of different factors such as catalyst loading, reaction temperature, and hydrogen pressure.

It is found that the hydrogenolysis of glycerol is chemically controlled at a stirring speed of 500RPM which is sufficient to further hydrogenolysis of 1,2-PD to 1-PO but not increase the side reactions to produce by products.

The conversion of glycerol is inversely related to the hydrogen pressure due to most likely to the reduction of W<sup>6+</sup> to W<sup>5+</sup> or <sup>4+</sup> and a reduction in acidity. However the high H<sub>2</sub> pressure is necessary to suppress the undesired dehydration or a side reactions and decrease the undesired products. Optimal operating H<sub>2</sub> pressures are required to obtain a high yield of 1-PO.

Dilute feed solutions results in an increase of selectivity to 1-PO but lower the conversions of glycerol. Increasing the glycerol concentration (decreasing the initial water content) decreased the selectivity to 1-PO but the selectivity to 1,2-PD and acrolein increased. Optimal glycerol feed concentration is required to obtained high yield of 1-PO.

Conversion increased with catalyst loading, but selectivity to 1-PO reached a maximum of 92.7% at 4.5% loading. It is thought that high catalyst loadings may increase the decomposition of the product or promote side reactions. Optimal catalyst loading is required to obtain a high yield of 1-PO.

Increasing temperature may promote further hydrogenolysis of 1,2-PD to 1-PO. However excessive heat may cause the degradation of 1-PO to other products.

The total acidity linearly increases with an increase in HSiW loading. Acidity favors 1-PO while basicity favors 1,2-PD and EG. The loading of HSiW should be 20% or higher to promote the further hydrogenolysis of 1,2-PD to 1-PO.

The catalyst having 5% loading of Ni is the best catalyst compared to others; it can give the highest selectivity to 1-PO, and reduce the by-products as a result of better dispersion of NiO on the surface of the catalyst. It is believed that part of 1-PO came from the hydrogenation of acrolein that was

produced from the consecutive dehydration of glycerol. The total number of acidic sites and the acid strength was found to decrease with increasing Ni content. A decrease in acidity may possibly be due to the covering of acid sites by Ni or it can be suggested that this behavior may result from direct anchoring on the proton sites and from blockage of acid channels by Ni particles.

The sequence of adding the catalyst component during the preparation of the catalyst can affect the catalyst activity and the catalyst properties. Among these catalysts, the catalyst prepared by co-impregnation is the best for the hydrogenolysis of glycerol to 1-PO with high selectivity to 1-PO and low by-products are produced. Furthermore the catalyst prepared by the co-impregnation method possesses the highest acidity and the easy reducibility of Ni.

The mechanism proposed suggests that the main route for the formation of 1-PO from glycerol is via either the hydrogenation of acrolein or further hydrogenolysis of 1,2-PD (and 1,3-PD) where 1,2-PD (and 1,3-PD) and acrolein are the intermediates in the formation of 1-PO from glycerol. In the absence of hydrogen; acetol and acrolein were the main products which suggested that hydrogen is necessary for the next step of hydrogenation of intermediates to produce desired products.

Although 10Ni/30HSiW/Al<sub>2</sub>O<sub>3</sub> catalyst shows a good activity for the production of 1-PO from glycerol; the leaching of the catalyst is a concern and should be addressed in future studies.

## Chapter Six

### **Keggin type Heteropolyacid supported catalyst for hydrogenolysis of glycerol to 1-Propanol**

Heteropolyacids (HPAs) present several advantages as catalysts that make them economically and environmentally attractive. [66,167]. Among the HPAs, the best known of these structures is the Keggin-type heteropolyacids, HPAs which are very strong Brønsted acids; stronger than common inorganic acids (HCl, H<sub>2</sub>SO<sub>4</sub>...) and are even sometimes classified as super acids [168,169]. However their acid properties can be tuned by modifying their compositions.

From the previous section, the hydrogenolysis of glycerol over silicotungstic acid (HSiW), one of most well-known Keggin type HPAs structures, results in high selectivity to 1-PO at moderate glycerol conversion. It is found that the acidity of HSiW is crucial to providing high selectivity to 1-PO since it is required for further hydrogenolysis of 1,2-PD to 1-PO. In this chapter the effect of different Keggin-type heteropolyacids, the effect of Cs, the effect of treatment temperature and the effect of support were studied for the hydrogenolysis of glycerol to other chemicals in particular the conversion to 1-PO will be investigated as these factors can tune the acidity of the catalyst. The catalyst characterizations were carried out to study the relationship between the catalyst physicochemical properties and the catalytic activities. The characterization techniques including NH<sub>3</sub> temperature programmed desorption (TPD), temperature programmed reduction (TPR), thermogravimetric analysis (TGA), X-Ray diffraction (XRD), Fourier transform infrared (FTIR) and Brunauer–Emmett–Teller (BET) surface area analysis. The characterization results were analyzed according to the experimental results.

#### **6.1 Efficient hydrogenolysis catalysts based on Keggin polyoxometalates**

Heteropoly acids (HPAs) with the Keggin structure that are well-known as environmentally friendly and economically viable solid acids [170] have been used for the upgrading of glycerol to other chemicals. Different forms of HPAs are used as catalysts, among them silicotungstic acid (HSiW), phosphotungstic acid (HPW) and phosphomolybdic acid (HPMo) as a consequence of their high catalytic activity in the selective dehydration of glycerol [72, 73, 76, 85, 142, 171]. The

acidity of the HPAs strongly depends on the nature of the addenda atoms. For example, the HPAs containing W are more acidic than those containing Mo. Since the Mo-O terminal bond is more polarizable than the W-O terminal bond. The O atoms linked to Mo atoms are negatively charged and protons are less mobile in this case. Hernández-Cortez J.G. et al. [172] studied the dehydration of secondary alcohols using HPAs supported on different solids and it was found that the interaction between supports and HPAs affects the physicochemical properties of the prepared catalysts. The Keggin structure was retained when they were supported. The product distribution depends on different type of HPAs (HPMo, HSiW and HPW) due to the difference in acid and base properties. In 2005 Thomas stated that the acidity of HPW can be changed by high temperature variation and HPW loses its protons at a lower temperature than HSiW [173]. Although work has been done to study different type of HPAs (HPMo, HSiW and HPW) for the dehydration of glycerol [73, 76], hardly any work has been done on the direct conversion of glycerol to 1-PO using different HPAs supported catalyst.

Thus in this work, Keggin-type heteropolyacids, including phosphotungstic acid (HPW), phosphomolybdic acid (HPMo) and silicotungstic acid (HSiW), and nickel were loaded onto alumina for the hydrogenolysis of glycerol. The aim was to investigate the effect of HPAs composition on the catalytic activity, the role of acidity of the catalyst and to follow the effect of temperature treatment of the catalyst on the Keggin structure and surface acidity properties of the catalyst during the course of the hydrogenolysis reaction. For this study, the catalysts were prepared via the sequential impregnation method. The properties of the prepared catalysts were characterized using TPD, XRD, FTIR techniques. Activity tests were performed in a 300ml Hastelloy Parr batch autoclave using 30g glycerol, 70g DI water, 580PSI Hydrogen at 240°C and 2g catalysts. Prior to each experiment, the catalyst was reduced in a quartz tubular reactor for 5 hours. The main products observed in the liquid phase were: Acetol, 1,2-Propanediol (1,2-PD), 1,3-Propanediol (1,3-PD), 1-Propanol (1-PO) and ethylene glycol (EG). Some other products such as methanol, ethanol, acrolein were also obtained and named as other products (O.P.).

### **Experimental condition**

The effect of different HPAs was examined at constant reaction conditions. The experiment was performed in a 300ml Hastelloy Parr batch autoclave at 240°C under 580PSI of H<sub>2</sub> pressure using 2g of 10Ni/30HSiW/Al<sub>2</sub>O<sub>3</sub> catalyst, 30wt% starting materials (30g of glycerol), for 7 hours. Two

catalysts reduced at different temperature were studied. One was reduced at 350°C and another was reduced at 450°C for 5 hours.

## Results and discussion

The effect of heteroatom substitution on the catalytic activity of the HPA catalysts for the hydrogenolysis of glycerol to other chemicals was examined at different reduction temperature. The results after reaction for 7 h are shown in Table 6-1. The main products observed in the liquid phase were: acetol, 1,2-PD, 1,3-PD, Acr, 1-PO and EG. Some other products (OP) such as methanol (MeOH), ethanol (EtOH) were also obtained.

**Table 6-1** Effect of different HPAs supported 10Ni/Al<sub>2</sub>O<sub>3</sub> catalyst on the conversion of glycerol and the distribution to products in the hydrogenolysis of glycerol

Catalyst	Red. temp °C	Conv mol%	Selectivity, mol%						
			1,3-PD	1,2-PD	Acetol	EG	1-PO	Acr	OP*
10Ni/30HSiW/Al <sub>2</sub> O <sub>3</sub>	350	72.3	0.0	1.1	0.6	0.0	91.7	3.3	3.3
	450	43.8	0.0	2.9	1.2	0.0	80.9	5.4	9.5
10Ni/30HPW/Al <sub>2</sub> O <sub>3</sub>	350	51.1	0.0	2.9	0.7	2.2	87.7	3.2	3.3
	450	48.9	0.0	6.1	1.0	3.7	80.3	3.3	5.7
10Ni/30HPMo/Al <sub>2</sub> O <sub>3</sub>	350	1.0	0.0	10.7	35.2	0.0	54.1	0.0	0.0
	450	1.0	0.0	10.1	36.5	0.0	53.4	0.0	0.0

**Reaction condition:** 10Ni/30HPAs/Al<sub>2</sub>O<sub>3</sub> catalyst, 240°C, 700RPM, 2g catalyst, 30g of glycerol (30wt%), 70g of DI water and 580PSI of H<sub>2</sub>. \*OP: By-products included methanol and ethanol

The data shows that the activity of the HPA supported catalyst is affected by reduction temperature. As can be seen from Table 6 -1 at a low reduction temperature of 350°C the catalyst activity of HPAs is in the order of HSiW >HPW >HPMo. Over a HSiW supported catalyst the selectivity to 1-PO reached 90% at 72% conversion of glycerol while the selectivity of 1,2-PD was low at 1.1%. Compared to HSiW, other supported HPAs catalysts showed lower activity towards glycerol



conversion and selectivity to 1-PO. While the HSiW supported catalyst achieved the best catalytic performance in terms of glycerol conversion and selectivity to 1-PO, the HPMo supported catalyst is inactive. In all cases, 1-PO is produced as the main product and acrolein, methanol, ethanol are the by-products of the reaction.

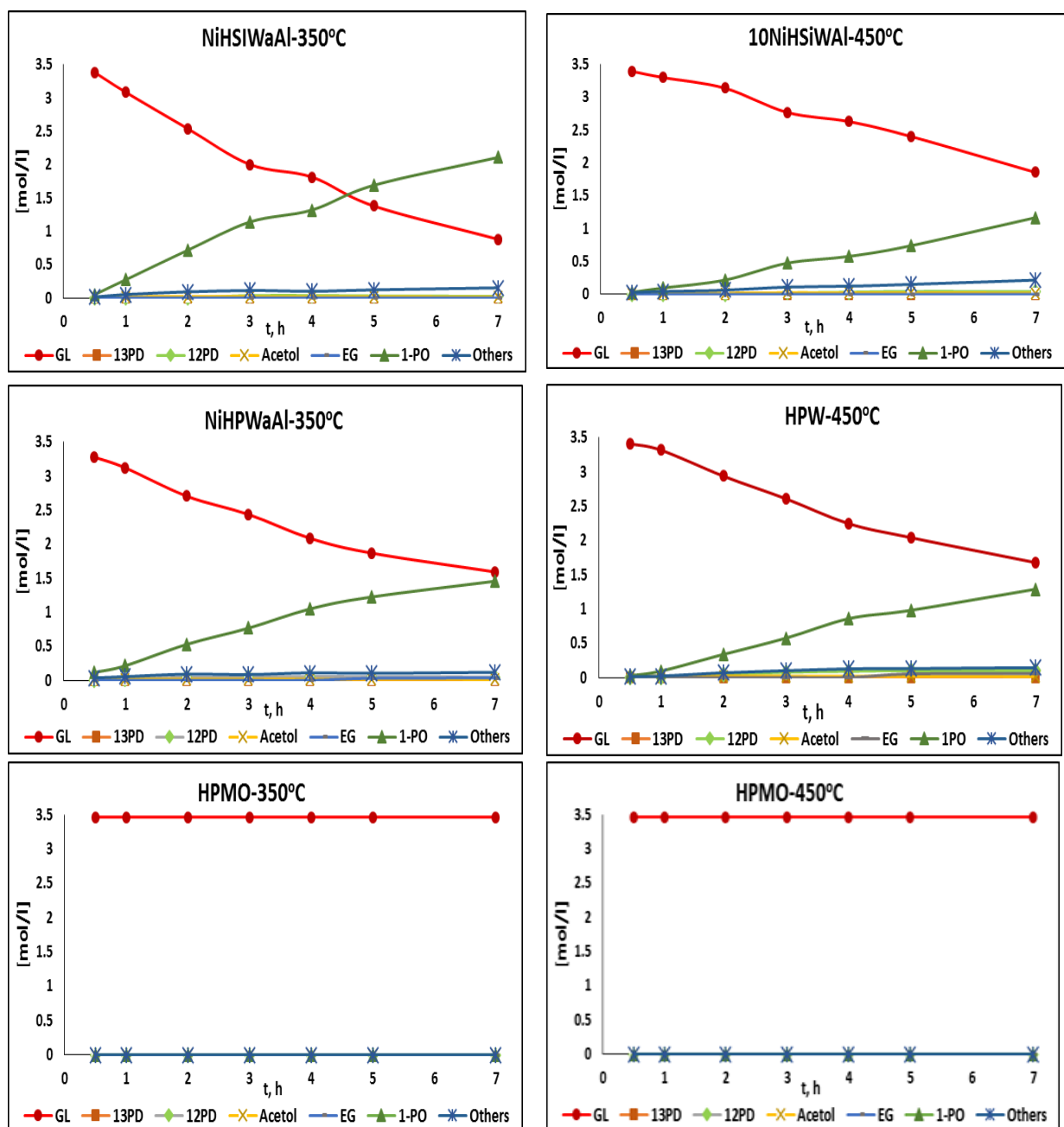


**Figure 6-1** Concentration profiles of different HPAs supported 10Ni/Al<sub>2</sub>O<sub>3</sub> catalyst at different reduction temperature at 350 and 450°C. **Reaction condition:** 30g of glycerol (30wt%), 70g of DI water, 580PSI of H<sub>2</sub>, 240°C, 700RPM, 2g catalyst reduced at 350°C and 450°C, 7 hours

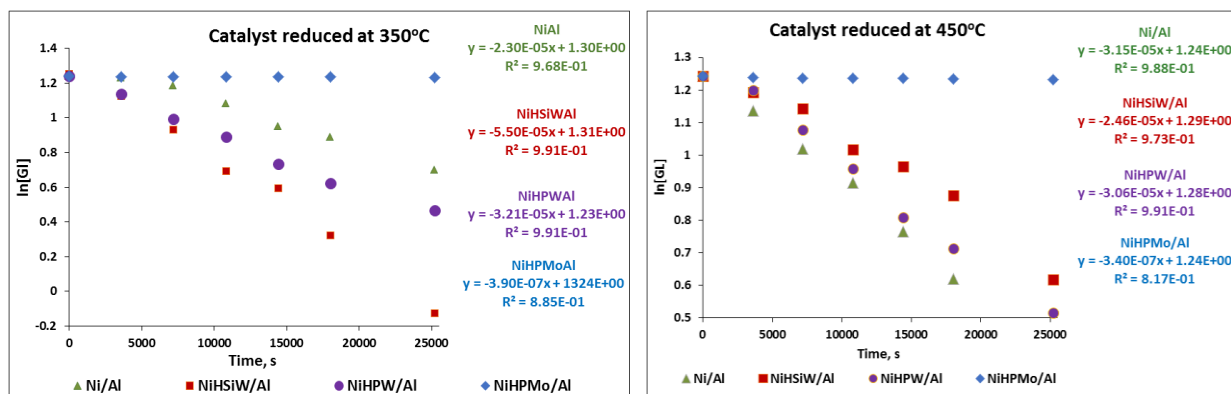


**Figure 6-2** Pseudo-First-Order kinetic plots of effect of HPAs on hydrogenolysis of glycerol in the presence of 10Ni/30HPA/Al<sub>2</sub>O<sub>3</sub> catalyst; **Reaction condition:** 240°C, 700RPM, 2g catalyst, 30g of glycerol (30wt%), 70g of DI water and 580PSI H<sub>2</sub>

When the reduction temperature increases to 450°C, glycerol conversion decreased to low values of 43% over HSiW supported catalyst. Accordingly, selectivity to 1-PO slightly decreased. While the conversion of glycerol remained similar at around 50% over the HPW supported catalyst; the selectivity to 1-PO also slightly decreased. In all cases, higher reduction temperature reduces the activity of the catalyst but not the selectivity, with the exception of the HPMo supported catalyst that is inactive already at 350°C treatment.

## Characterization of catalysts

### The catalysts were characterized by different techniques

The relationship between catalytic activity and catalyst properties in particular the acid concentration of the catalysts was studied using different techniques.

The NH<sub>3</sub>-TPD was performed from 50 to 750°C to study the acidic properties on the catalyst surface in order to elucidate the catalytic activity of catalysts, and thus, to find a comprehensive correlation between catalytic activity and acid property of the HPA catalysts. The TPD data was deconvoluted into 3 peaks (namely weak, medium and strong acid sites) using a Gaussian fitting method. Two different NH<sub>3</sub>-TPD profiles of the catalysts reduced at 350°C and 450°C with different Keggin-type heteropolyacids loaded are shown in Fig. 6-3 and Fig. 6-4. The total acidity of the catalysts is recorded in Table 6-2 and was then correlated with the catalytic activity of HPA catalysts.

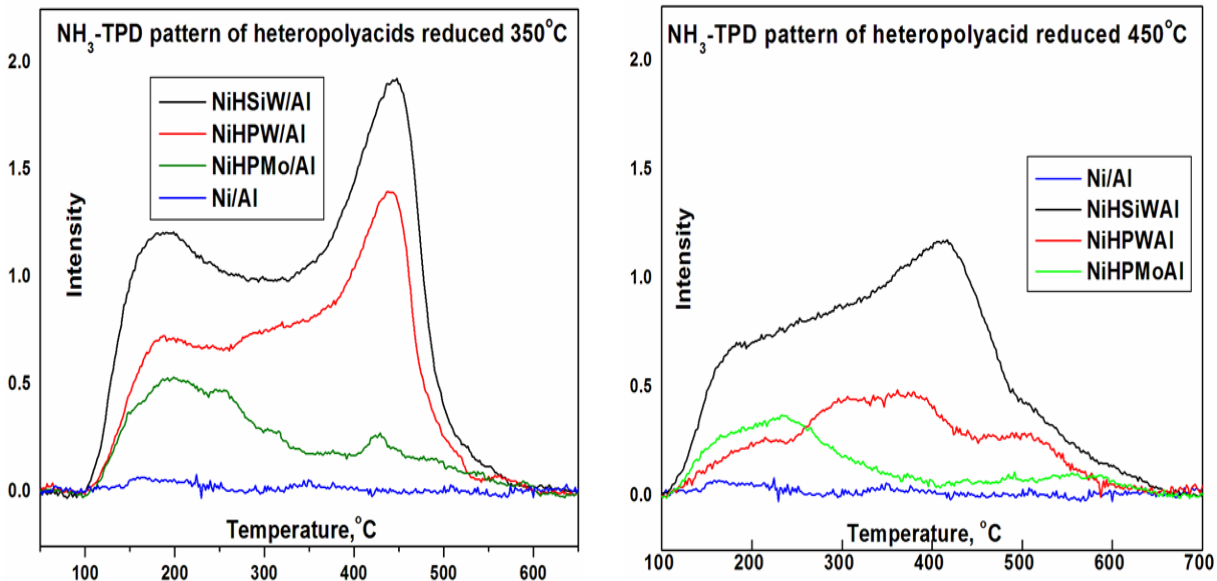


**Figure 6-3** NH<sub>3</sub>-TPD patterns for different HPAs reduced at 350 and 450°C

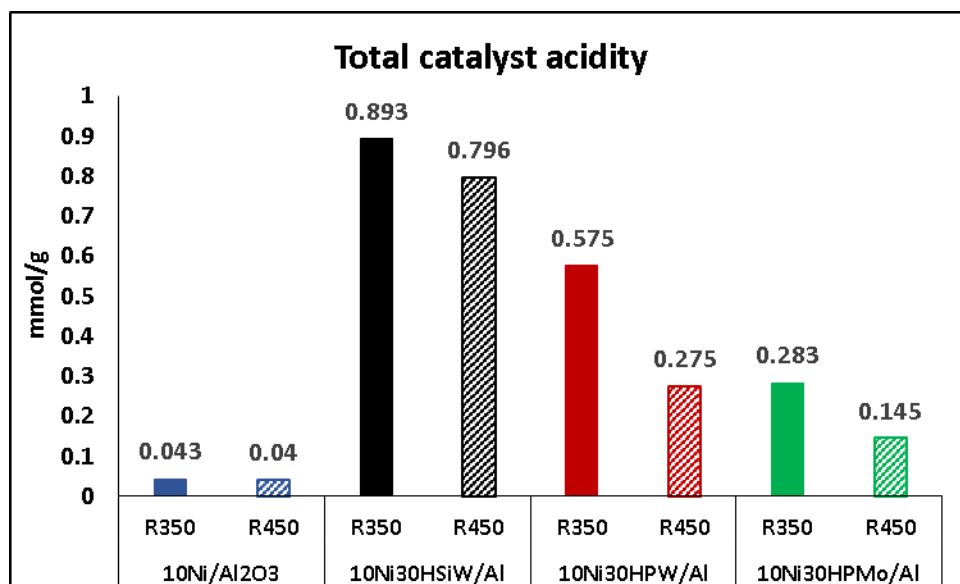


**Figure 6-4** Total acidity amount for different HPAs reduced at 350 and 450°C

**Table 6-2** Effect of different HPAs supported 10Ni/Al<sub>2</sub>O<sub>3</sub> catalyst and reduction temperature on acidity and catalyst performance

Catalyst	Red. temp, °C	k, s <sup>-1</sup> E-05	Weak acid site /(Temp.)	Medium acid site /(Temp.)	Strong acid site/(Temp.)	Total acid amount, mmol/g	Conv. mol %
Ni/Al <sub>2</sub> O <sub>3</sub>	350	2.3	0.027/(185°C)	0.016/(372°C)	-	0.043	40.4
	450	3.1	0.028/(175°C)	0.013/(350°C)	-	0.041	51.6
Ni/HSiW/Al <sub>2</sub> O <sub>3</sub>	350	5.5	0.180/(182°C)	0.504/(335°C)	0.196/(441°C)	0.880	72.3
	450	2.4	0.232/(189°C)	0.396/(335°C)	0.168/(436°C)	0.796	43.8
Ni/HPW/Al <sub>2</sub> O <sub>3</sub>	350	3.21	0.090/(185°C)	0.365/(338°C)	0.120/(438°C)	0.575	51.2
	450	3.06	0.020/(180°C)	0.226/(340°C)	0.029/(511°C)	0.275	48.9
Ni//HPMo/Al <sub>2</sub> O <sub>3</sub>	350	0.039	0.040/(167°C)	0.135/(234°C)	0.108/(426°C)	0.283	1.0
	450	0.034	0.068/(207°C)	0.043/(292°C)	0.034/(536°C)	0.145	1.0

Qualitatively, a positive correlation is observed between glycerol conversion and acid concentration over HSiW supported catalyst. However, the correlations are not observed for the other 2 catalysts, i.e. HPW and HPMo.

As can be seen from Fig. 6-3, Fig 6-4 and Table 6-2, for both reduction temperatures of 350 and 450°C, the HSiW supported catalyst shows the highest total acid amount while the HPMo supported catalyst possesses the lowest total acid amount among all catalysts. The total acidity is in the order of 10Ni/30HSiW/Al<sub>2</sub>O<sub>3</sub> > 10Ni/30HPW/Al<sub>2</sub>O<sub>3</sub> > 10Ni/30HPMo/Al<sub>2</sub>O<sub>3</sub> > 10Ni/Al<sub>2</sub>O<sub>3</sub> and the total acidity decreases as the reduction temperature increases (Fig. 6-4). Without HPAs, it was found that the acidity of 10Ni/Al<sub>2</sub>O<sub>3</sub> was low; only 2 broad small peaks of weak and medium acidity were observed at around 200°C and 350°C. After heteropolyacids loading, all curves are composed of overlapped 3-peaks between 100 and 600°C, indicating the presence of 3 acid centers with different strengths. These results illustrated that the Keggin-type heteropolyacids loading increases the acidity of the catalysts, offering acid sites for catalysis. Different kinds of Ni-HPAs/Al catalysts provide a difference in the acidity. It can be seen from Table 6-2 that the order

of acidity amount is: HSiW > HPW > HPMo. It is noticeable that the performance in catalytic activity is consistent with the trend of the amount of acidity of these HPA catalysts. When the catalysts were reduced at a low temperature of 350°C, the TPD pattern of HSiW and HPW is almost similar, illustrating that this low reduction temperature does not affect the acidity of these two HPAs catalysts. However, there was a reduction in the proton content for all of the heteropolyacids when the catalyst was reduced at 450°C. HPW and HPMo lost their acidity much more readily than HSiW. While the TPD pattern over HSiW supported catalyst was similar at both reduction temperature, new patterns of the acidity for HPW and HPMo were observed at a high reduction temperature - there was a shift toward higher temperature of strong acid sites with increasing reduction temperature.

These results suggest that the acidity of Keggin-type heteropolyacids was affected by the high temperature, that the structures of the heteropolyacids were probably changed or damaged. The decomposition of the crystal structure upon heating at high temperature leads to a loss in acidity and the removal of protonated water under heat treatment which may account for the acidity loss, mainly decreasing Brønsted acidity.

It is interesting to note that the activities of the HSiW and HPW catalysts reduced at 450°C have similar activity as they also have similar acidity in medium acid site as can be seen from Table 6-2. It is suggested that medium acid sites affect to some extent the activity of the catalyst.

The catalysts were characterized using XRD to explore the crystal phases and to check possible HPAs support interactions giving rise to distortion of the HPAs structure of the catalysts. The XRD pattern of the alumina support, Ni supported alumina and the supported HPAs catalyst is shown in Fig. 6-5.

Generally, bulk HSiW exhibits characteristic crystalline peaks at 8°~10°, 20°~24°, 26°~28°, 32°~35° [158]. As can be seen for the HSiW and HPW catalysts some minor characteristics crystalline peaks of HSiW (20°~24°, 26°~28°) can be observed but no significant changes in the diffraction patterns occurred compared to the Ni/Al catalyst, indicating that there is no change in the structure. However the XRD pattern of the HPMo supported catalyst is different from the other two catalysts. There are diffraction peaks that do not coincide with the diffraction of HPMo but

resemble orthorhombic  $\text{MoO}_3$ . This can be explained by considering the decomposition of HPMo into  $\text{MoO}_3$  species under preparation treatment.

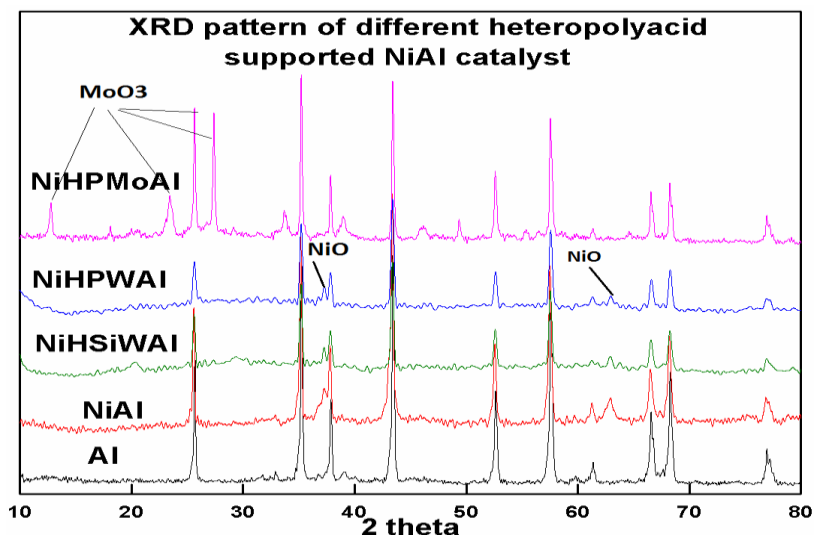


**Figure 6-5** XRD patterns for different HPAs calcined at 350°C

Infrared spectra are also an informative fingerprint of the Keggin heteropoly cage structure. Therefore the prepared catalysts were analyzed by FTIR in order to confirm the structural integrity of the Keggin unit of these catalysts. All the catalysts were calcinated at 350°C prior to analysis. The FTIR spectra of the catalysts are presented in Fig. 6-6.

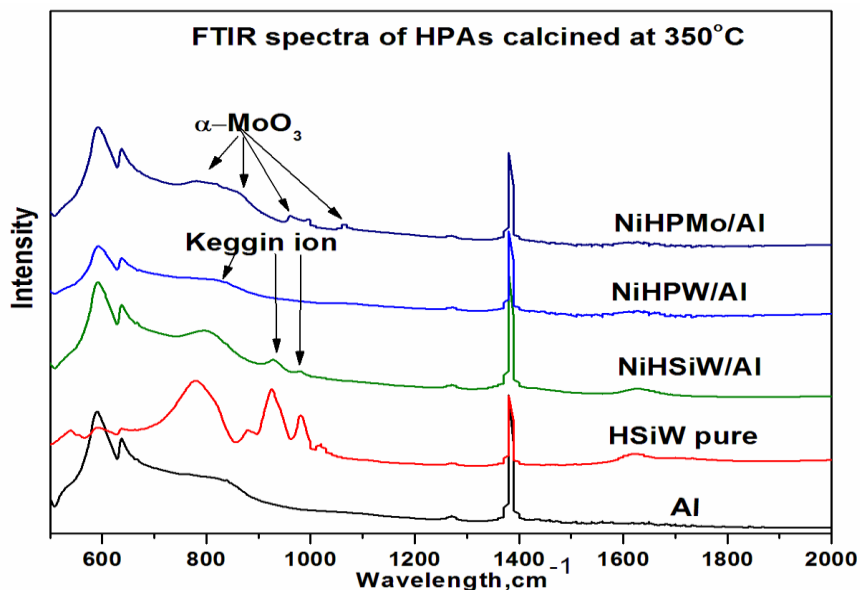


**Figure 6-6** FTIR patterns for different HPAs calcined at 350°C

It is shown that the evidence for the retention of the Keggin ion structure on the surface of HSiW and HPW supported catalysts was provided; however the HPMo supported catalyst was already decomposed under the preparation condition at 350°C of calcination. The fingerprint bands of the HSiW Keggin anion appeared at 978, 915, and 798  $\text{cm}^{-1}$ , which could be assigned to the typical antisymmetric stretching vibrations of W=O, Si-O, and W-Oe-W [145]. This indicated that the Keggin phase remains intact for the HSiW supported catalyst. For the supported HPW catalyst, 3 bands of HPW appear around 1079, 983 and 810  $\text{cm}^{-1}$  that can be assigned to the typical antisymmetrical stretching vibrations of P-O, W=O, and W-O-W [174]. These spectra exhibit similar bands for the structure of the  $\text{PW}_{12}\text{O}_{40}^{3-}$  anion also suggesting that HPW in the catalyst still retains the Keggin structure. However, the FTIR spectra of HPMo supported catalyst was different from HSiW and HPW. The spectra of Keggin ion was not observed for HPMo sample but only the spectra of orthorhombic  $\alpha\text{-MoO}_3$  appeared. This confirmed that the decomposition of HPMo to  $\text{MoO}_3$  occurred at 350°C. It is believed that the decomposition of HPMo into  $\text{MoO}_3$  at higher temperatures is responsible for the decrease in catalytic performance. The Keggin structure of HSiW is rather stable and is the best candidate for 1-PO production

## Summary

The activation process is associated with structural changes and these structural changes match with those that occur during thermal treatment – in fact, thermal stability is known to be extremely important for catalyst stability [175,176]. The effect of reduction temperature on the activity of different HPA supported catalyst was not the same for all catalysts. Under our reaction conditions, the HSiW supported catalyst seems to be more stable than other catalysts up until a treatment temperature of 450°C and is the best candidate for 1-PO production. The decomposition of HPMo already occurred at 350°C of treatment. The decomposition of HPMo into  $\text{MoO}_3$  is likely to be responsible for the inactivity of the catalyst for glycerol conversion.

## 6.2 The effect of thermal treatment on activity and structure of 10Ni/30HSiW/ $\text{Al}_2\text{O}_3$ catalyst

It has been shown that the performance of a heterogeneous catalyst not only depends on the intrinsic catalyst components but also on its texture and stability. One of the most important factors affecting the texture and activity of a catalyst is the proper choice of the activation step. HPAs

have proved their remarkable and unique simultaneous acid and redox properties but their rapid degradation at high temperature by decomposition is still a major drawback [177]. The stability of these compounds is thus a critical parameter that has been extensively studied. The effect of temperature on the catalyst structure was studied. However, the effect of temperature on the HPAs supported catalyst activity for the conversion of glycerol is rarely studied. In 2014 Liu et. al. [171] studied the effect of calcined temperature on the structural evolution of  $\text{Al}_2\text{O}_3$  supported HSiW and the catalytic performance during glycerol conversion to acrolein. The decomposition of supported HSiW crystal structure and the degradation of Keggin unit occurred after calcination of HSiW/ $\text{Al}_2\text{O}_3$  at 350 and 450°C, but to a small extent. However the Keggin structure was decomposed totally at 550 and 650°C. One important property of HPAs; is their thermal stability, is discussed in this section. The effect of the calcination temperature and reduction temperature of the HSiW on the physico-chemical properties of supported Ni catalysts will be investigated. The change of the acidity with the increasing temperature and the performance of the catalysts in the hydrogenolysis of glycerol will be investigated.

### **6.2.1 The effect of calcined temperature**

Although HPAs showed high activity for glycerol dehydration, the tendency to decompose under thermal treatments always leads to a loss of active sites and deactivation [72-75]. It is well known that calcination is basically thermal decomposition with air at the decomposition temperature. During this process, the active centers are usually generated, where calcination of supported HPA catalysts below the decomposition temperature would favor the creation of proper interaction between the heteropolyanions and the support surface, improving the stability of HPAs as solid acid catalysts. However, if the temperature is further increased, the Keggin structure can be gradually decomposed. For HSiW supported catalyst, calcination is generally carried out at about 350°C under atmospheric pressure to remove the precursor decomposition products efficiently. The upper level of temperature can be put as the limit where all the acidic properties are lost. Kozhevnikov [170] proposed a mechanism related to losses during heating. The process consists of three steps of which the first is vaporization of water at 100°C. At 200°C and 450-470°C, water molecules bonded to the acidic protons and the remaining protons are removed respectively. At temperatures higher than 600°C, the component is totally converted to  $\text{P}_2\text{O}_5$  and  $\text{WO}_3$  which shows no acidic property. Martin et al. studied the decomposition behaviors of HSiW and HPMo HPAs



using DTA technique [76]. The loss of water, the interaction with the support and the formation of new species were observed. Ezzat Rafiee et al. [178] synthesized the green core nanorod catalyst for the C-N coupling reactions at room temperature. The effect of calcination temperature at 100, 150, 200, 250, and 300°C was investigated and it is found that the catalyst calcined at 150°C was observed to have very low leaching of the HPW in the heterogeneous catalytic system. This catalyst was easily recyclable with slight loss of catalytic activity. Devassy prepared the catalysts with different HSiW loadings and calcination temperatures (600–850°C) for veratrole benzylation [179]. It is found that 15% HSiW on zirconia calcined at 750°C that was highly dispersed on the support had the highest Brønsted acidity and total acidity and the added HSiW stabilizes the tetragonal phase of zirconia. The catalytic activity was found to depend mainly on the HSiW coverage. A bifunctional catalyst with alumina as the support was produced by Liu and co-workers in 2015. They showed that increasing the calcination temperature from 350 to 650°C can lead to structural evolution of the supported HSiW and a subsequent activity change. The Keggin structure of HSiW began to dissociate around 450°C, causing the formation of various  $WO_x$  species [171, 180].  $TiO_2$  nanoparticles stabilized HPW in SBA-15 was prepared and calcined at different temperatures (650–1000°C) it was found that the catalytic activity is mainly related with the textural parameters and the acidity of the catalyst depends on the HPW coverage on the surface of the catalyst and the calcination temperature. The calcination temperature 850°C was found to be the best which is mainly due to the availability of the highest Brønsted acidity together with the perfect monolayer coverage of HPW on the surface of the catalytic support [181a]. However, the detailed structure evolution and the consequent activity changes with thermal treatment at elevated temperature are still not clearly unveiled. Therefore thermal stability is one of the factors that is considered in the design of heterogeneous HPAs based catalysts.

In this section, the effect of the calcination temperature of the 10Ni/30HSiW supported alumina on the physico-chemical properties of catalysts and performance of the catalysts will be investigated to optimize the catalytic properties and performance.

### **Experimental condition**

The catalysts were prepared via the impregnation method. The obtained catalyst was heated in flowing air to a particular temperature (350, 450, 550, and 650°C at 5°C/min), calcined for 5 h, and then cooled to room temperature. Prior to each experiment, the catalyst was reduced in a quartz

tubular reactor at 350°C. The effects of the calcined temperature on catalytic performance was performed in a 300ml Hastelloy Parr batch autoclave using 30g glycerol, 70g DI water, 580PSI Hydrogen at 240°C and 2g catalyts. The main products observed in the liquid phase were: acetol, 1,2-PD, 1,3-PD, acrolein (Acr), 1-PO and ethylene glycol (EG). Some other products (OP) such as methanol (MeOH), ethanol (EtOH) were also obtained. The properties of the prepared catalysts were characterized using TPD, TPR, XRD and FTIR techniques.

## Result and discussion

The performance of the catalyst calcined at different temperature is shown in Table 6-3 and Fig. 6-7. The main products observed in the liquid phase were: acetol, 1,2-PD, 1,3-PD, Acr, 1-PO and EG. Some other products (OP) such as methanol (MeOH), ethanol (EtOH) were also obtained.

**Table 6-3** Effect of calcination temperature on the conversion of glycerol and the distribution to products in the hydrogenolysis of Glycerol

T, °C	Conv. mol%	Selectivity, mol%						
		1,3-PD	1,2-PD	Acetol	EG	1-PO	Acr	OP
350	86.5	0.0	0.0	0.4	0.0	91.7	2.9	5.0
450	90.1	0.0	0.0	0.3	0.0	92.9	2.6	4.2
550	46.2	0.0	2.9	1.7	0.0	71.5	2.9	21.0
650	21.3	0.0	0.0	4.4	0.0	64.9	7.6	23.1

**Reaction condition:** 10Ni/30HSiW/Al<sub>2</sub>O<sub>3</sub> catalyst, 240°C, 700RPM, 2g catalyst, 30g of glycerol (30wt%), 70g of DI water and 580PSI of H<sub>2</sub>. OP: By-products included methanol and ethanol.

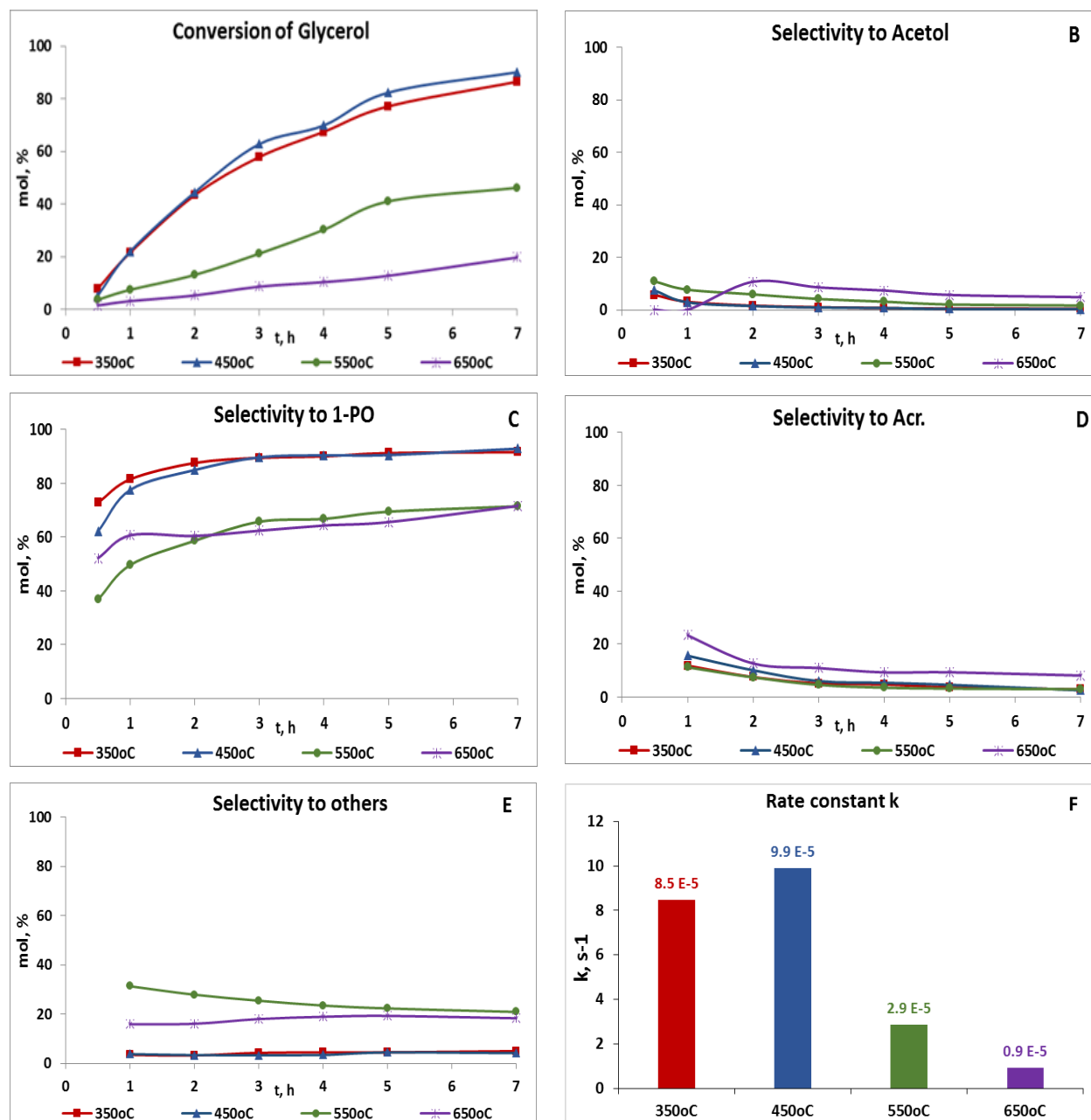


**Figure 6-7** Effect of calcination temperature on the conversion of glycerol and the distribution to products as a function of time; A) Glycerol Conversion; B,C,D,E,F) Selectivity of acetol, 1,2-PD, 1-PO, Acr., other products, respectively. **Reaction condition:** 10Ni/30HSiW/Al<sub>2</sub>O<sub>3</sub> catalyst, 240°C, 700RPM, 2g catalyst, 30g of glycerol (30wt%), 70g of DI water and 580PSI of H<sub>2</sub>.

It is evident that the calcined temperature above 450°C affects both the conversion of glycerol and product distribution significantly. Increasing the temperature of calcination, the conversion of glycerol and selectivity went through a maximum of 90.1% and 92.9% respectively at a

temperature of 450°C. The catalyst calcined at a temperature 450°C was found to produce the best results with respect to 1-PO selectivity (92.9%) at high conversion (90.1%). The catalyst activity is not affected by the calcination temperature below 450°C; there is only a slight difference in the conversion of glycerol and product distribution and it is shown that the catalyst that was calcined at 450°C had the optimal catalytic properties with respect to the conversion of glycerol and the selectivity to 1-PO (90.1% and 92.9% respectively). On increasing of calcination temperature to 550°C, the conversion of glycerol and the selectivity to 1-PO decreased remarkably to 46.2% and 71.5% respectively; however the selectivity to acetol, acrolein and byproducts (mainly ethanol) increase. The by-products significantly increased from 4.2% (450°C) to 21% (550°C). The conversion of glycerol and selectivity to 1-PO decrease continuously to 23.1% and 64.9% respectively with a further increase in the calcination temperature to 650°C. It is noticed that a further increase of calcination temperature to 650°C does not show an increase in by-products but results in an increase in the selectivity of acetol and acrolein (acetol increased from 1.7% (550°C) to 4.8% (650°C) and acrolein increased from 2.9 to 7.6%). The catalytic performance of the catalyst calcined at a higher temperature of 550°C and 650°C was depressed to a certain degree compared to the catalyst calcined at 350 and 450°C.

### **Characterization**

The acidic properties of the catalysts were probed using NH<sub>3</sub>-TPD. For a detailed analysis, the TPD curves were deconvolved into 3 peaks (namely weak, medium and strong acid sites) using a Gaussian fitting method, NH<sub>3</sub>-TPD profiles of the catalysts are shown in Fig. 6-8, and analysis of the data is presented in Table 6-4.

It is seen that the calcination temperature plays an important role in controlling acid properties of the catalysts. From the overall TPD curve areas, it was found that the total amount of acid sites decreased monotonously with increasing calcination temperature. However the decrease in total acidity does not accompany the activity of the catalyst in term of glycerol conversion.

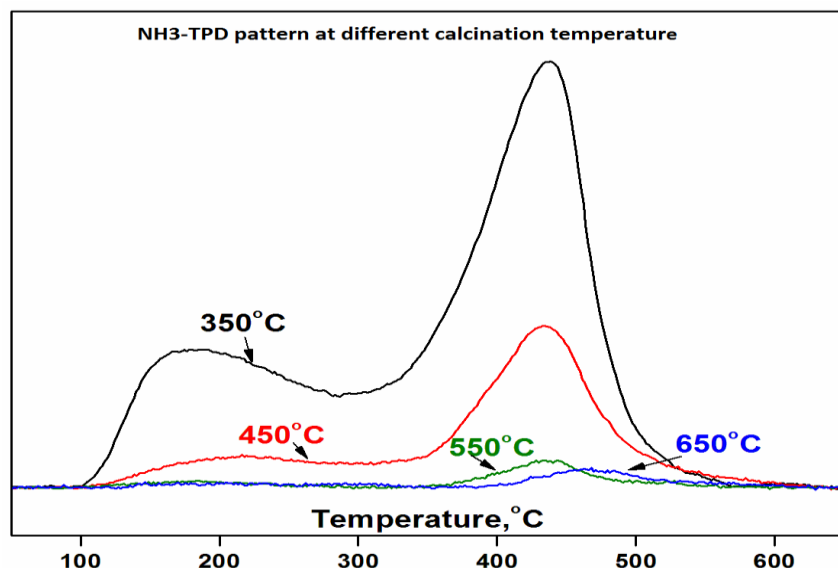


**Figure 6-8** NH<sub>3</sub>-TPD patterns for catalyst calcined at different temperature

**Table 6-4** Effect of calcination temperature on acidity of 10Ni/30HSiW/Al<sub>2</sub>O<sub>3</sub> catalyst

Calc. Temp °C	Weak acid site mmol/g /(Temp.)	Medium acid site mmol/g /(Temp.)	Strong acid site mmol/g /(Temp.)	Total acid amount, mmol/g
350	0.365/(196°C)	0.559/(389°C)	0.383/(432°C)	1.306
450	0.080/(207°C)	0.126/(396°C)	0.232/(433°C)	0.438
550	0.014/(185°C)	-	0.051/(439°C)	0.065
650	0.011/(227°C)	-	0.038/(470°C)	0.049

Increasing the temperature of calcination the conversion of glycerol and selectivity went through a maximum of 90.1 and 92.9% respectively at 450°C. The catalyst calcined at a temperature of 450°C was found to produce the best results for 1-PO selectivity (92.9%) at high conversion (90.1%). The reason for the high selectivity maybe due to the decrease in the acidity of the catalyst making it less selective towards coke and the catalyst had a proper balance between dehydration functions (acid sites) and hydrogenation (metal surface atoms). The classification of acid site strength is indicated by the NH<sub>3</sub>-TPD; weak sites corresponding to 180–230°C, medium sites 390–400°C and strong sites 430–470°C. The deconvoluted results showed two distinct trends as shown

in Table 6-4. First, the total number of acid sites decreased significantly as the calcination temperature was increased. In particular, a large decline in acid site number was observed after calcination at 550°C. The second trend was that apparently stronger acid sites were present as the calcination temperature increased, the desorption maxima for NH<sub>3</sub> were 432, 433, 439 and 470°C after calcination at 350, 450, 550 and 650°C, respectively. When the catalyst was calcined at temperatures below 450°C, 3 distinguished acid sites were observed and the intensity decreases with the increasing calcination temperature. Further increases in calcination temperature results in a significant decrease in intensity of the acid sites in particular the medium acid sites that became almost undetectable. The NH<sub>3</sub>-TPD experiments provide a good correlation between the adsorbed amount of ammonia and the temperature of calcination: the higher the calcination temperature, the lower is the amount of desorbing ammonia. Hence it could be concluded, that the proton as it is suggested for the acidity of the catalyst are sufficient for chemically adsorption of ammonia and that increasing the temperature reduces the amount of proton of the catalyst which are responsible for bonding ammonia. The relevance of the proton is emphasized by the effect of the calcination temperature. The samples calcined at 650°C adsorb a lower amount of ammonia than those calcined at 350°C which can be attributed to the loss of hydroxyl groups during calcination. The reason for this loss is conceivable: dehydration at the surface.

Variations of the TPR profiles of the catalysts as a function of calcination temperature can be helpful to interpret how components interact. The TPR profiles for the catalysts are shown in Fig. 6-9. As can be seen the TPR profiles of catalysts calcinated at 350 and 450°C are similar and as a combination of two species of Ni and HSiW. However the TPR of the catalysts calcinated at higher temperatures of 550 and 650°C were different from these two. It is suggested that the modification in the structure of the catalyst occurred.

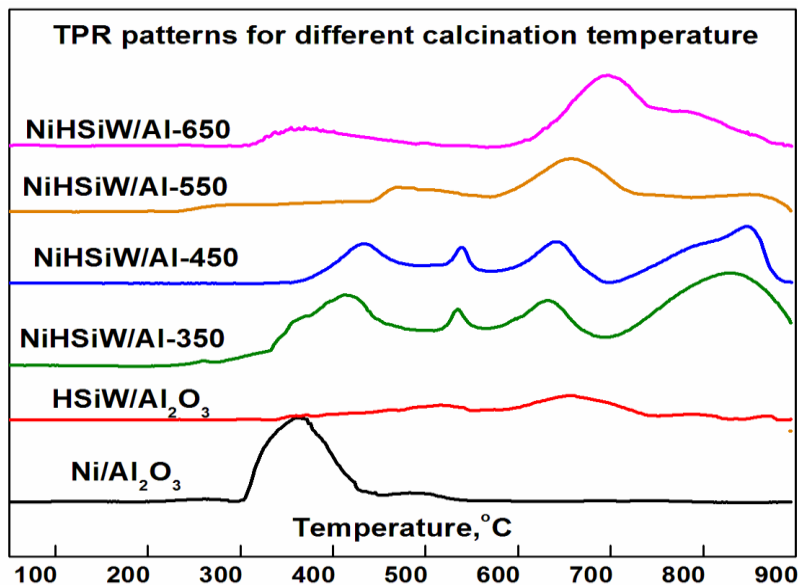


**Figure 6-9** TPR patterns for catalyst calcined at different temperature

The catalysts were characterized with XRD to explore the crystal phases and to check possible calcination temperature giving rise to distortion of the Keggin structure of the catalysts. The XRD pattern of alumina support, bulk HSiW and the catalysts was showed in the Fig. 6-10.

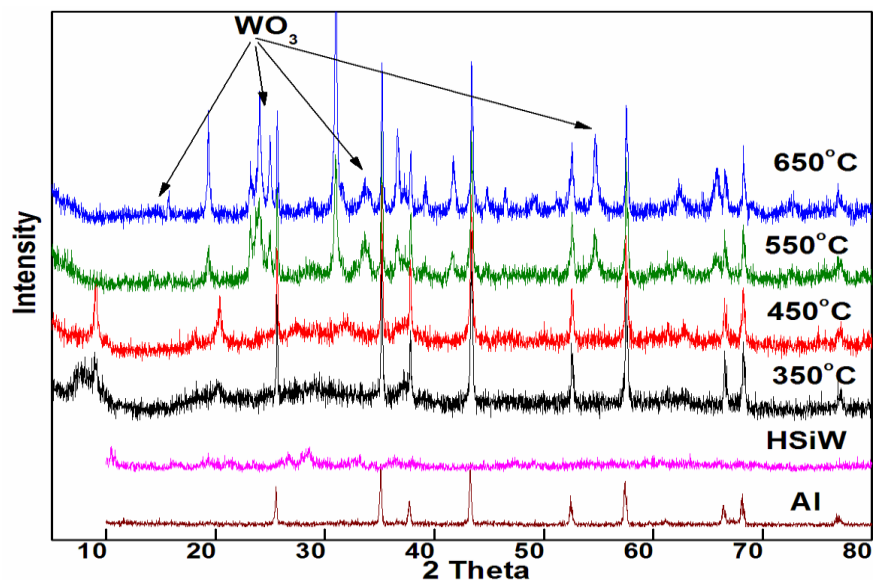


**Figure 6-10** XRD signal for catalyst calcined at different temperature

In Fig. 6-10, the same diffraction peaks of  $\text{Al}_2\text{O}_3$  support are observed in all catalysts, well corresponding to diffraction peaks of standard cubic  $\text{Al}_2\text{O}_3$  [JCPDS No. 01-078- 2427]. XRD

patterns for the bulk HSiW showed distinct reflections (at  $20^{\circ}\sim 24^{\circ}$ ,  $26^{\circ}\sim 28^{\circ}$ ,  $32^{\circ}\sim 35^{\circ}$ ). The peak of HSiW could also be observed on the catalysts calcinated at 350 and 450°C, indicating the presence of crystalline HSiW that proves that the Keggin structure is retained on the catalyst. However, the diffraction peak of HSiW diminished and clear diffraction peaks assigned to orthorhombic  $\text{WO}_3$  (654048-ICSD) nanocrystals were observed when the calcination temperature was increased to 550 and 650 °C and the intensity of the diffraction peaks of orthorhombic the  $\text{WO}_3$  phase increased with increasing calcination temperature. The result demonstrates that tungstosilicic acid in the catalyst is, at least partially, dissociated into tungsten trioxide species after treatment at 550 and 650°C. It is consistent with the results Liu L. [171] observed on a HSiW/ $\text{Al}_2\text{O}_3$  catalyst.

FTIR spectra were employed to characterize the supported HSiW catalysts to investigate the Keggin structure of the catalysts under thermal treatment. This technique can be used to confirm the presence of the Keggin structure of HSiW on the support surface. Keggin anion at 978, 915, 885 and 798  $\text{cm}^{-1}$  could be assigned to the typical antisymmetric stretching vibrations of W-O, Si-O, W-O-W and W-O-W respectively [145]. The FTIR spectra of the catalysts are shown in Fig. 6-11.

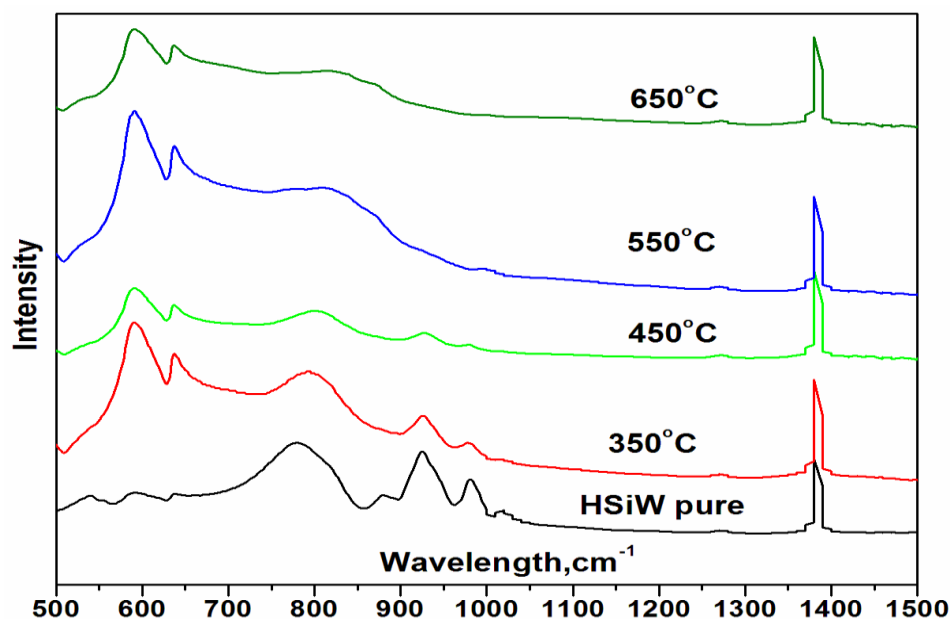


**Figure 6-11** FTIR signal for catalyst calcined at different temperature



As can be seen, bulk HSiW has distinct absorption peaks at 978, 915, 885 and 798  $\text{cm}^{-1}$ , which could be assigned to the typical antisymmetric stretching vibrations of W-O, Si-O, W-Oc-W and W-Oe-W, respectively and the positions are in good agreement with those reported earlier, [145,181b, 182]. It can be seen from the Fig. 6-11 that there was almost no change in the positions of the characteristic bands for samples up to 450°C, confirming that the Keggin anion was preserved in the catalyst up to this temperature. These peaks that present the Keggin structure of HSiW also present on the catalyst calcined at 350 and 450°C but with relatively low intensity and decreasing with increasing calcination temperature. This implies the presence of the Keggin ion in the two catalysts, is well consistent with the TPD, XRD and TPR results. However, the first changes in spectrum were registered at 550°C, which indicate the appearance of some new species in the catalyst structure. It is evident that at high temperature, the Keggin anion had decomposed to  $\text{SiO}_4^{4-}$  (bands at about 1000 $\text{cm}^{-1}$ ) and  $\text{WO}_4^{2-}$  ions (bands at about 860, 700 and 525 $\text{cm}^{-1}$ ). After calcinations, the broad absorption peaks in the range 750–900 $\text{cm}^{-1}$  are characteristic of the different O-W-O stretching vibrations in the  $\text{WO}_3$  crystal lattice [183-185]. On the other hand, the observed broad peak at a wave number of 835 $\text{cm}^{-1}$  is assigned to the symmetric stretching vibrations band of Si-O-Si, implying the formation of  $\text{SiO}_2$  [186]. Based on this analysis, dissociation of the Keggin structure of HSiW is evidenced to occur at a calcination temperature of 550°C and above

## Summary

The total amount of acid sites decreased monotonously with an increase in calcination temperature. However the decrease in total acidity does not accompany the activity of the catalyst in term of glycerol conversion. Increasing the temperature of calcination, the conversion of glycerol and selectivity went through a maximum of 90.1 and 92.9% respectively at 450°C. The catalyst calcined at a temperature of 450°C was found to produce the best results for 1-PO selectivity (92.9%) at high conversion (90.1%). The reason for the high selectivity maybe due to the decrease in the acidity of the catalyst making it less selective towards coke and the catalyst had a proper balance between dehydration functions (acid sites) and hydrogenation (metal surface atoms). To achieve good performance, catalysts must retain Keggin species on the surface, but they must also have a proper balance between acid sites and metal sites. The supported silicotungstic acid (HSiW) calcinated at 350 and 450°C retained their crystal structure of Keggin

units; the decomposition and the degradation in the crystal structure of the catalyst may occur but to a small extent. However increasing the calcination temperature to 550 and 650°C causes clear decomposition of the Keggin structure.

### **6.2.2 The effect of reduced temperature**

Reduction is also a crucial step in the catalyst preparation process. The reduction temperature can influence the catalyst reducibility, thereby influencing the catalytic performance [187,188]. This section deals with the effects of reduction temperature on the catalytic performance of 10Ni/30HSiW/Al<sub>2</sub>O<sub>3</sub> catalysts for the hydrogenolysis of glycerol. The aim is to get some insight into the relations between the catalyst preparation conditions (here catalyst reduction temperature) and the catalytic properties of the studied catalysts (here catalyst activity and acidity). A set of 4 experiments were carried out under H<sub>2</sub> media and the effect of reduction temperature (300°C, 350°C, 450°C and unreduced catalyst) on the catalytic performance was studied.

#### **Experimental condition**

The catalysts were prepared via the impregnation method. The obtained catalyst was calcinated in flowing air at 350 for 5 h, and then cooled to room temperature. Prior to each experiment, the catalyst was reduced in a quartz tubular reactor at different temperatures (300°C, 350°C, 450°C and unreduced catalyst). The effects of the reduction temperature on catalytic performance was performed in a 300ml Hastelloy Parr batch autoclave using 30g glycerol, 70g DI water, 580PSI Hydrogen at 240°C and 2g catalysts. The main products observed in the liquid phase were: acetol, 1,2-PD, 1,3-PD, acrolein (Acr), 1-PO and ethylene glycol (EG). Some other products (OP) such as methanol (MeOH), ethanol (EtOH) were also obtained. The acidity of the prepared catalysts were characterized using a TPD technique.

#### **Result and discussion**

The performance of the catalyst reduced at different temperature is shown in Table 6-5 and Fig. 6-12.

**Table 6-5** Effect of reduction temperature on the conversion of glycerol and the distribution to products in the hydrogenolysis of Glycerol

Reduced Temp.	Conv. mol%	Selectivity, mol%						
		1,3-PD	1,2-PD	Acetol	EG	1-PO	Acr.	OP
No	71.3	0.0	0.0	1.1	0.0	66.5	26.2	6.2*
300°C	76.3	0.0	0.8	0.5	0.0	92.7	2.4	3.6**
350°C	81.1	0.0	0.0	0.6	0.0	90.6	3.7	5.1**
400°C	64.3	0.0	0.9	0.8	0.0	89.7	5.0	3.7**
450°C	43.8	0.0	2.9	1.2	0.0	80.9	5.4	9.5

**Reaction condition:** 10Ni/30HSiW/Al<sub>2</sub>O<sub>3</sub> catalyst, 240°C, 700RPM, 2g catalyst, 30g of glycerol (30wt%), 70g of DI water and 580PSI of H<sub>2</sub>. OP: By-products included methanol and ethanol and \*: light and heavy, \*\*: light

From the results summarized in Table 6-5, it is evident that the reduction is a crucial step in catalyst treatment to obtain high selectivity to 1-PO and reduce the production of the by-products. Without reducing, the selectivity to 1-PO was low at 67.5% but the selectivity to acrolein was high at 26.2% at 71.3% glycerol conversion. Once the catalyst was reduced at 300°C the selectivity to 1-PO significantly increased to 92.7% followed by a decrease of acrolein from 26.2% to only 2.4% at 76.3 conversion of glycerol. It is shown that a reduction temperature below 350°C affects slightly the catalyst activity in term of conversion of glycerol and product distribution and the catalyst that was reduced at 350°C had optimal catalytic properties for the formation of 1-PO (the yield of 1-PO was 73.5%). With a further increase in the reduction temperature to 450°C the catalyst activity in term of glycerol conversion remarkably decreases; the conversion of glycerol was only 43.8%. The selectivity to 1-PO was also affected by the reduction temperature but it only as much as the conversion of glycerol. Obviously, increasing the reduction temperature causes an inhibition effect on the catalytic activity and selectivity to 1-PO, but it seems to be beneficial to promote the 1,2-PDO selectivity. To be specific, as the reduction temperature was raised from 350 °C to 450 °C, the conversion of glycerol decreased from 81.1% to 43.8%, and the selectivity to 1-PO decreases from 90.6 to 80.9% while the 1,2-PD and acrolein selectivity increased from 0% to 2.9% and

3.7% to 5.4% respectively. The decrease in activity of catalyst at high reduction temperature may be caused by partial thermal decomposition that leads to a loss in protons. Hence the acidity of the catalyst decreases and the catalyst becomes less effective for the dehydration step. As a result the conversion of glycerol decreases and the further hydrogenolysis of 1,2-PD was slowed down.

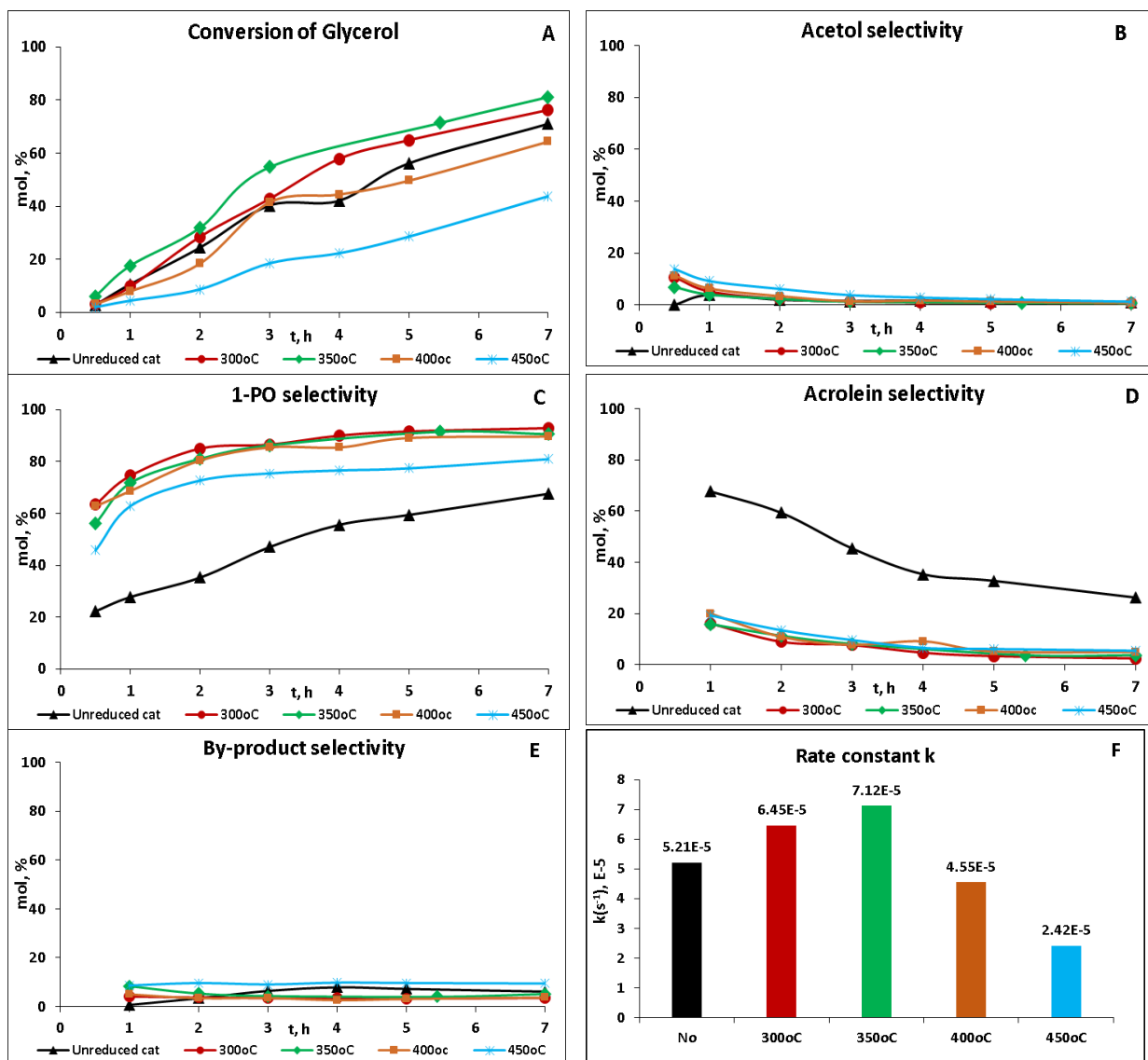


**Figure 6-12** Effect of reduction temperature on the conversion of glycerol and the distribution to products as a function of time; A) Glycerol Conversion; B,C,D) Selectivity of acetol, 1-PO, Acr., other products, respectively. F) A comparison in rate constant k. **Reaction condition:** 10Ni/30HSiW/Al<sub>2</sub>O<sub>3</sub> catalyst, 240°C, 700RPM, 2g catalyst, 30g of glycerol (30wt%), 70g of DI water, 70g of DI water and 580 PSI of H<sub>2</sub>.

It is worth noting that the unreduced catalyst exhibited even higher activity than that of the catalysts reduced at 400°C and 450°C. Although the activity of unreduced catalyst is similar to the activity of catalysts reduced below 350°C in terms of glycerol conversion but there was a remarkable difference in product distribution. The conversion of glycerol can reach 71%; however, the selectivity to 1-PO was only 67.6% whilst the selectivity to acrolein was high. The glycerol conversion and product selectivity as a function of time are shown in Figure 6-12. It can be seen from Figure 6-12 that the selectivity to 1-PO (C) is increased but the selectivity to acrolein (D) decreased. Using reduced catalyst, the selectivity to 1-PO and acrolein likely reached a stable state and hardly changed after 2 hours of reaction. On the contrary, the selectivity to 1-PO increases monotonously, while the selectivity to acrolein decreases gradually with increasing time when an unreduced catalyst is used. One reasonable explanation for this trend is that under H<sub>2</sub> media the unreduced catalyst can be reduced in situ during the glycerol hydrogenolysis reaction so it can promote the hydrogenation of acrolein as an intermediate to 1-PO leading to the selectivity to a 1-PO increase but the selectivity to acrolein decreased with increasing time. This may be indicating that the reduced catalyst can influence the catalytic performance by promoting active hydrogen species on the metal sites and generate in the active sites of the catalyst.

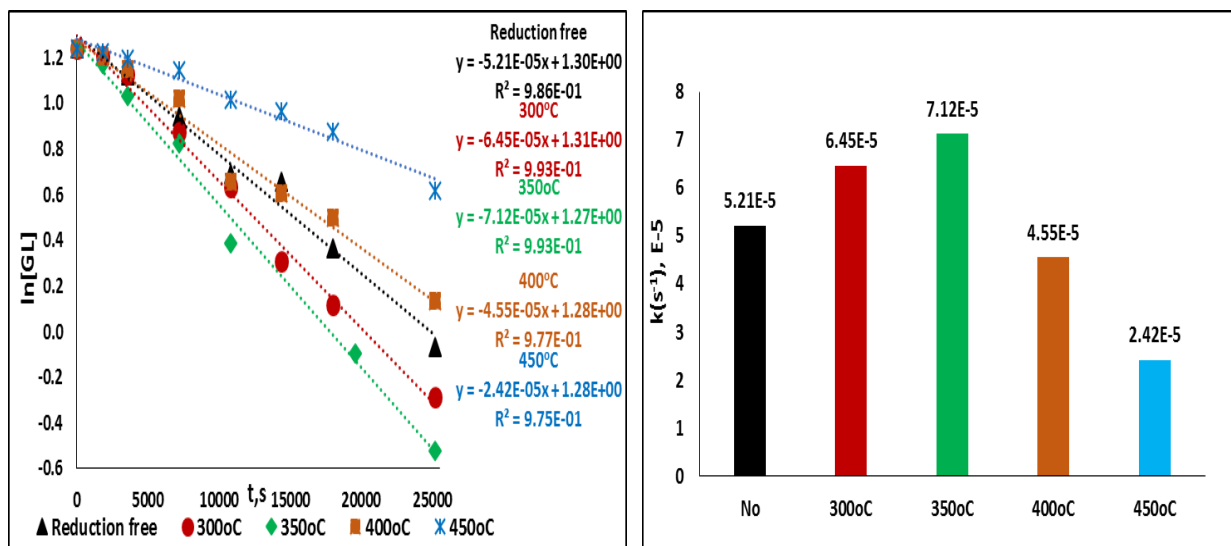


**Figure 6-13** Pseudo-first-order kinetic plots for 10Ni/30HSiW/Al<sub>2</sub>O<sub>3</sub> Catalyst reduced at different temperature. **Reaction condition:** 240°C, 580PSI of H<sub>2</sub>, 700RPM, 2g catalyst, 30g of glycerol (30wt%), 70g of DI water.

## Characterization

To examine surface acidity,  $\text{NH}_3$ -TPD was performed and the results are shown in Table 6-6 and Fig. 6-14. For a detailed analysis, the TPD curves were deconvoluted, using a Gaussian curve fit of three bands as shown in Table 6-6. Thus the low temperature peak at around  $190^\circ\text{C}$  is attributed to weak acid sites,  $330^\circ\text{C}$  is attributed to medium acid sites and the peak at around  $440^\circ\text{C}$  is attributable to strong acid sites. From the overall TPD curve areas, it can be seen that on increasing the reduction temperature the acidity of the catalyst went through a maximum of  $0.911 \text{ mmol/g}$  at a  $400^\circ\text{C}$  reduction temperature. First, the total number of acid sites increased monotonously as the reduction temperature increased from  $300$  to  $400^\circ\text{C}$ . A further increase in the reduction temperature leads to a decrease in the total number of acid sites. The increase in the amount of acidity was also accompanied by the change in the strength of the acidity. It can be seen that there is a similar change in strong acid sites with increasing reduction temperature. First, the strength of the acidity also increased as the reduction temperature was increased from  $300$  to  $400^\circ\text{C}$  (shift of strong acid sites from  $419^\circ\text{C}$  to  $443^\circ\text{C}$ ). A further increase in the reduction temperature leads to a decrease in the strength of the acidity (shift of strong acid sites to  $436^\circ\text{C}$ ).

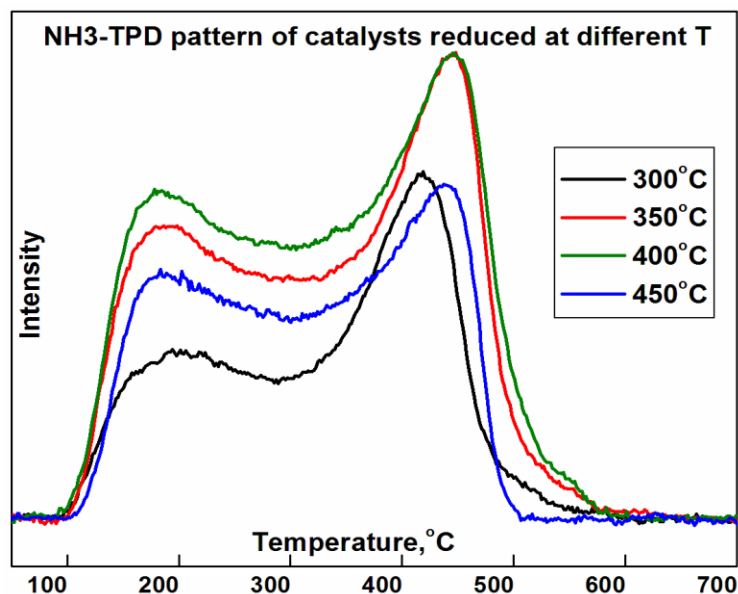


**Figure 6-14**  $\text{NH}_3$ -TPD patterns for catalyst reduced at different temperature

**Table 6-6** Effect of reduced temperature on acidity of 10Ni/30HSiW/Al<sub>2</sub>O<sub>3</sub> catalyst

<b>Reduced Temp.</b>	<b>Weak acid site, mmol/g /(Temp.)</b>	<b>Medium acid site mmol/g /(Temp.)</b>	<b>Strong acid site mmol/g /(Temp.)</b>	<b>Total acid amount, mmol/g</b>
<b>300°C</b>	<b>0.146/ (187°C)</b>	<b>0.270/ (346°C)</b>	<b>0.151/ (419°C)</b>	<b>0.568</b>
<b>350°C</b>	<b>0.180/ (182°C)</b>	<b>0.504/ (335°C)</b>	<b>0.196/ (441°C)</b>	<b>0.880</b>
<b>400°C</b>	<b>0.208/ (179°C)</b>	<b>0.460/ (319°C)</b>	<b>0.242/ (443°C)</b>	<b>0.911</b>
<b>450°C</b>	<b>0.230/ (189°C)</b>	<b>0.396/ (335°C)</b>	<b>0.170/ (436°C)</b>	<b>0.796</b>

However an increase in total acidity does not absolutely accompany the activity of the catalyst in terms of glycerol conversion. The catalyst that was reduced at 350°C had the optimal catalytic properties with respect to the conversion of glycerol and the selectivity to 1-PO. The reaction rate is the highest when the catalyst was reduced at 350°C (Fig. 6-13).

### Summary

In summary, it is crucial to reduce the catalyst to obtain high selectivity of 1-PO. The selectivity to 1-PO decreased with increasing catalyst reduction temperature above 400°C indicating that the catalyst activity may be weakened at high reduction temperature. However over the range of 300 to 450°C of reduction temperature, the change in acidity of the catalyst was not accompanied by a change in the activity of the catalyst. Although the catalyst reduced at 300°C has the lowest acidity it can possess an activity similar to the catalyst reduced at 350°C that has much higher acidity. The catalyst reduced at 450°C has the highest acidity but its activity was much lower than the catalysts reduced at 300 and 350°C. The reason for the low activity maybe due to the increase in acidity of catalyst making it more selective towards coke formation [189]. The catalyst that has low acidity but high activity, is a result of a proper balance between dehydration functions (acid sites) and hydrogenation (metal surface atoms). To achieve good performance, catalysts must have a proper balance between acid sites and metal sites

### 6.3 Effect of different supports on activity of 10Ni/30HSiW supported catalyst

It is well-known that the disadvantage of HPAs relates to low thermal stability, low surface area (<10 m<sup>2</sup>/g) and leaching problems of the species into reaction mixture which limit the application of HPA catalysts in current industry to some extent. Amongst the main factors determining activity and the stability of such catalysts is the nature of the supports. Therefore to overcome these disadvantages and make the catalyst more feasible, proper supports should be employed to disperse the active phase. The choice of a support is generally guided by the increased specific surface area, which leads to a high number of accessible active sites. However the development of HPA catalysts possessing higher thermal stability is an important challenge. [190,191]. Besides, the acidity and catalytic activity of the supported HPAs also depend mainly on the type of carrier and on the loading. The increased thermal stability is ascribed to the aforementioned interaction between the support and the heteropoly anion. If the interaction with the support is strong, the acidic strength of the HPA may reduce due to the distortion of its structure leading to the activity of the final catalyst being much lower than that of the HPAs itself, but this interaction also stabilizes the Keggin structure and hinders its thermal decomposition; whereas low interactions of HPAs with the supports could lead to dramatic leaching. This effect has been described by Alta et al for alumina supported heteropoly acids [76].

It is of high interest to obtain a deeper insight of the influence of the support character on the catalytic behavior of Ni/HSiW catalysts. In order to be able to clearly present many aspects concerning the 10Ni/30HSiW catalysts, it was decided to investigate the influence of different supports on the catalytic behavior of 10Ni/30HSiW catalysts. The aim of this work was to study the acidity and catalytic activity of different supports.

Atia et al. [192] claimed that alumina-supported HPA showed higher catalytic activity and acrolein selectivity than silica-supported acid, although the reported selectivity did not exceed that of what Tsukuda [170].

It has been reported that MCM41 that has higher surface area, a regular pore size arrangement and is a thermally stable material (T>1000), which can be a promising candidate as a supporting material in doping of heteropolyacids for catalytic applications in acidic regions. Good dispersion of the active component over the whole surface enhances the yield of the processes by increasing



the accessibility to active sites [193-196]. Titania, is a widely used catalyst support [197], and is known to enhance the activity in many cases due to the strong interaction between the active phase and the support [198]. It is reported that TiO<sub>2</sub>-supported HPAs are more active and resistant and preserves the Keggin unit at a higher temperature than the corresponding bulk HPAs. [199, 200]. The crystalline structure and thermal stability of HSiW are not compromised after deposition on TiO<sub>2</sub> and the Keggin structure is preserved at temperatures up to 450°C [201]

In this section, several supports for 10Ni/30HSiW catalyst were prepared, characterized, and tested in aqueous solution for glycerol hydrogenolysis. The aim of the present investigation was to compare the catalytic activity of catalysts containing HSiW, one of the strongest heteropolyacids, supported on alumina with the activity of the catalysts containing the same heteropolyacids supported on commonly used oxides: Titania and MCM-41.

### **Experimental condition**

The effects of the different support on catalytic performance was performed in a 300ml Hastelloy Parr batch autoclave using 30g glycerol, 70g DI water, 580PSI Hydrogen at 240°C and 2g catalysts. The catalysts were prepared via the impregnation method. Prior to each experiment, the catalyst was reduced in a quartz tubular reactor for 5 hours. The main products observed in the liquid phase were: acetol, 1,2-PD, 1,3-PD, acrolein (Acr), 1-PO and ethylene glycol (EG). Some other products (OP) such as methanol (MeOH), ethanol (EtOH) were also obtained. The properties of the prepared catalysts were characterized using TPD, XRD techniques.

### **Result and discussion**

Effect of the support on the catalytic activity of 10Ni30HSiW catalysts in the hydrogenolysis of glycerol to other chemicals was examined at 2 different reduction temperatures of 350°C and 450°C. The results after reaction for 7 h are shown in Table 6-7.

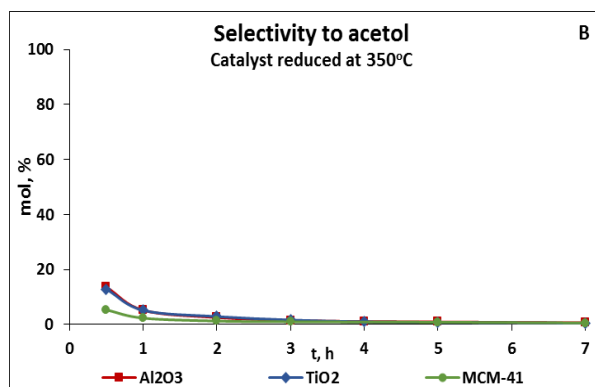
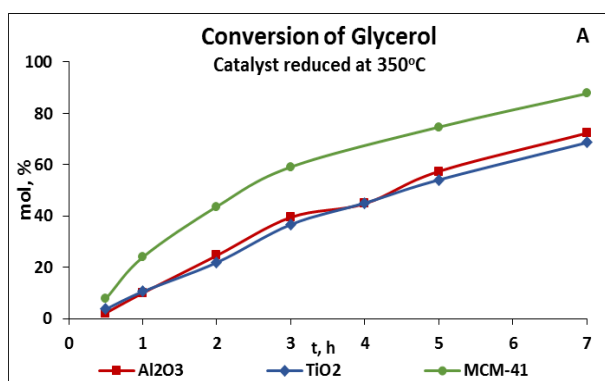
As can be observed, the activity of MCM-41 and TiO<sub>2</sub> supported catalysts seems to be not affected by high treatment temperature of 450°C; however, the catalyst supported alumina does. The activity of the different supported catalyst was in the order of Al<sub>2</sub>O<sub>3</sub><TiO<sub>2</sub><MCM-41. In all cases, 1-PO is produced as the main product. Among the catalysts, the catalyst supported MCM-41 appears to be the most active for the production of 1-PO from glycerol and its activity is apparently

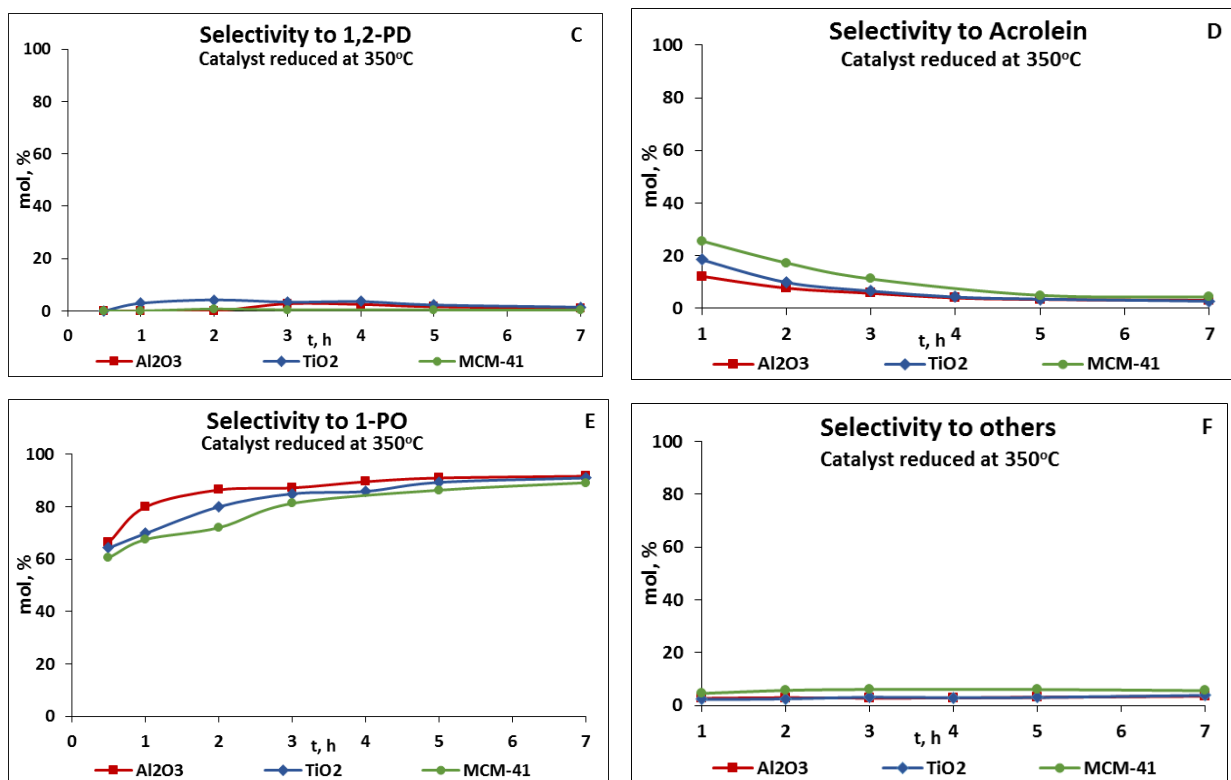
not affected by the reduction temperature. The conversion of glycerol and the product distribution are similar for both catalysts reduced at 350 and 450°C that the selectivity to 1-PO can reach around 90% at 87% glycerol conversion.

**Table 6-7** Effect of support on the conversion of glycerol and the distribution to products in the hydrogenolysis of Glycerol

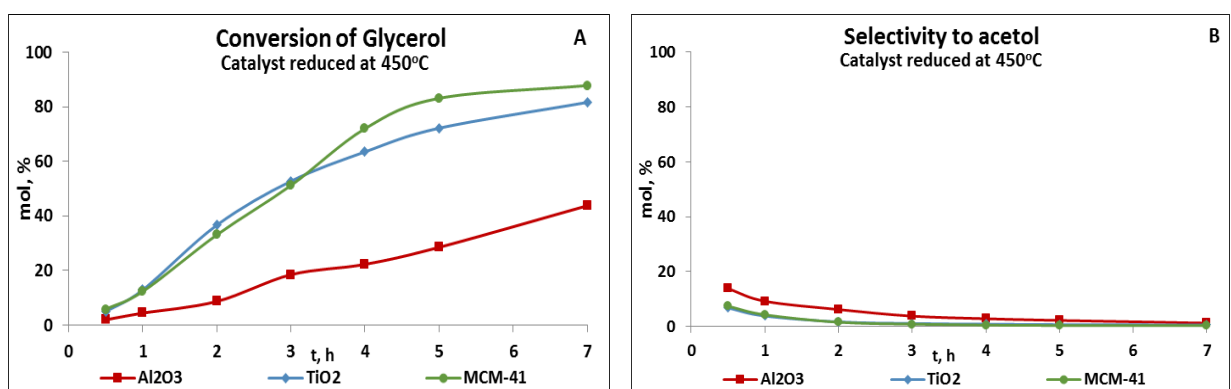
Support	Red. temp	Conv. mol%	Selectivity, mol%						
			1,3-PD	1,2-PD	Acetol	EG	1-PO	Acr	OP
Al <sub>2</sub> O <sub>3</sub>	350	72.3	0.0	1.1	0.6	0.0	91.7	3.1	3.5*
	450	43.8	0.0	2.9	1.2	0.0	80.9	5.4	9.6*
TiO <sub>2</sub>	350	68.5	0.0	1.4	0.5	0.0	91.5	2.7	3.9*
	450	81.7	0.0	0.5	0.6	0.0	88.9	6.6	3.5*
MCM-41	350	87.7	0.0	0.3	0.6	0.0	89.2	4.3	5.6**
	450	87.8	0.0	0.9	0.3	0.0	90.9	2.7	5.2*

**Reaction condition:** 10Ni/30HSiW/Al<sub>2</sub>O<sub>3</sub> catalyst, 240°C, 700RPM, 2g catalyst, 30g of glycerol (30wt%), 70g of DI water and 580PSI of H<sub>2</sub>. \*OP: By-products included methanol and ethanol; \*\*OP: By-products included methanol and ethanol;





**Figure 6-15** Effect of supports reduced at 350°C on the conversion of glycerol and the distribution to products as a function of time; A) Glycerol Conversion; B,C,D,E,F) Selectivity of acetol, 1,2-PD, Acr., 1-PO, other products, respectively. **Reaction condition:** 10Ni/30HSiW supported catalyst, 240°C, 700RPM, 2g catalyst, 30g of glycerol (30wt%), 70g of DI water and 580PSI of H<sub>2</sub>



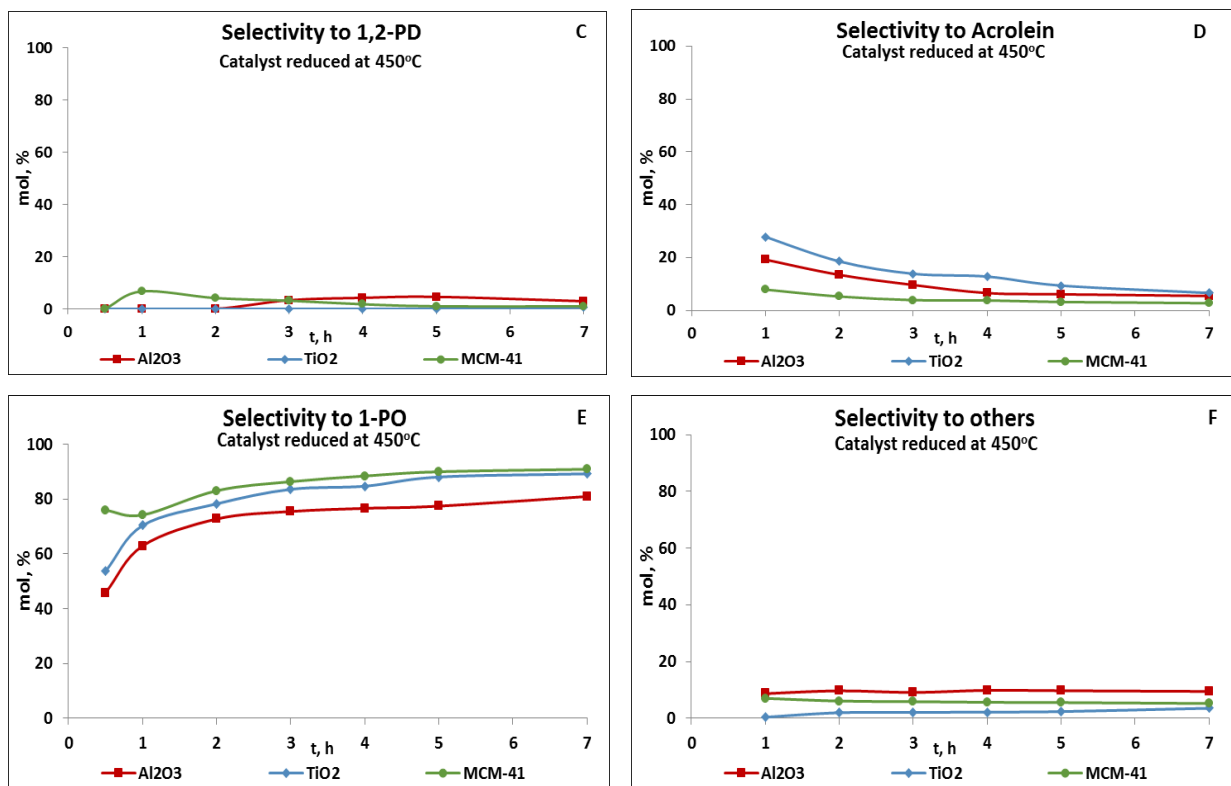


**Figure 6-16** Effect of supports reduced at 450°C on the conversion of glycerol and the distribution to products as a function of time; A) Glycerol Conversion; B,C,D,E,F) Selectivity of acetol, 1,2-PD, Acr., 1-PO, other products, respectively. **Reaction condition:** 10Ni/30HSiW supported catalyst, 240°C, 700RPM, 2g catalyst, 30g of glycerol (30wt%), 70g of DI water and 580PSI of H<sub>2</sub>

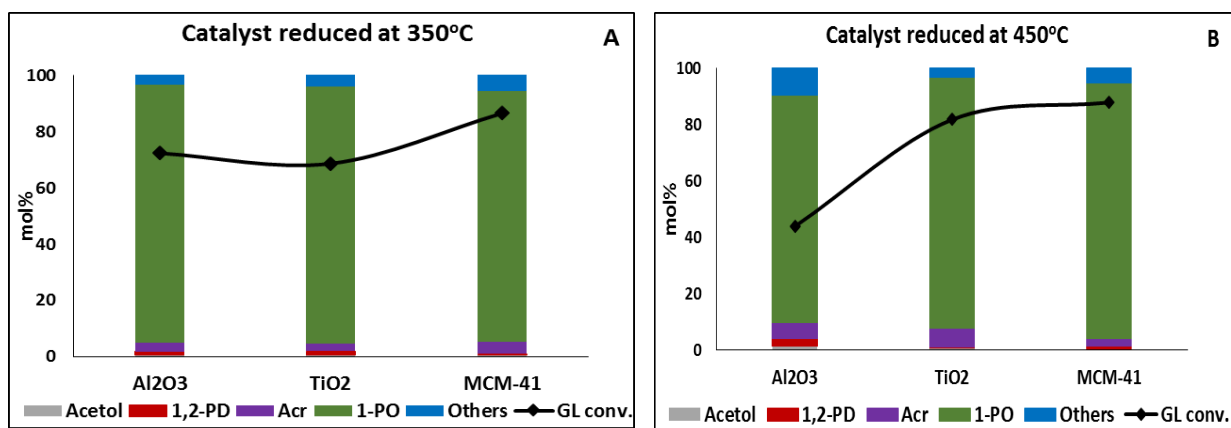


**Figure 6-17** Effect of supports on Glycerol Hydrogenolysis and products selectivity: A) Catalyst reduced at 350°C; B) Catalyst reduced at 450°C. **Reaction condition:** 240°C, 700RPM, 2g catalyst, 30g of glycerol (30wt%), 70g of DI water and 580PSI of H<sub>2</sub>.

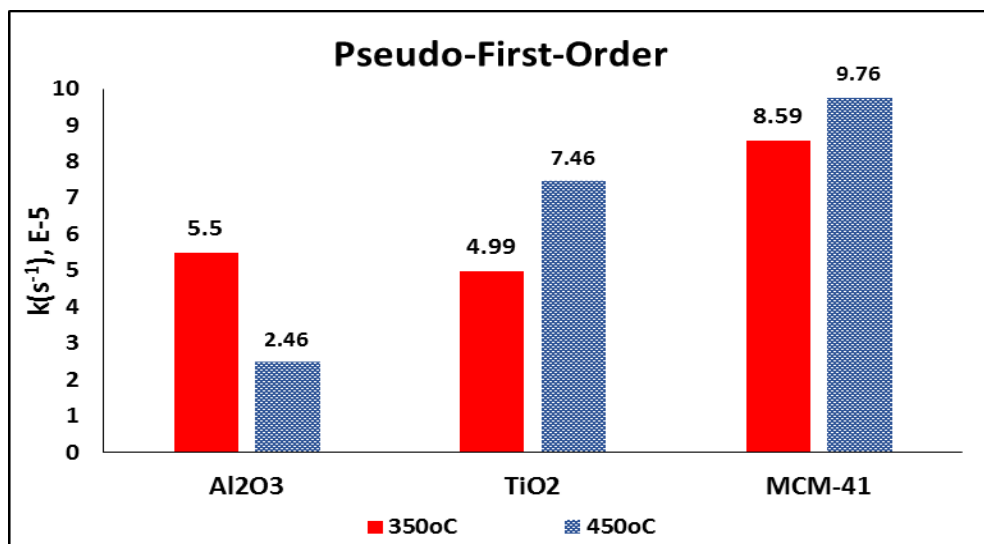


**Figure 6-18** Pseudo-First-Order kinetic analysis of effect of support on hydrogenolysis of glycerol in the presence of 10Ni/30HSiW/Al<sub>2</sub>O<sub>3</sub> catalyst; **Reaction condition:** 240°C, 700RPM, 2g catalyst, 30wt% aqueous glycerol and 580PSI H<sub>2</sub>

The high reduction temperature affects slightly the activity of the catalyst supported TiO<sub>2</sub> in terms of glycerol conversion to some extent but it does not affect the product distribution. The selectivity to 1-PO can reach around 89.2% at the 81.7% glycerol conversion. Although at a low treatment temperature of 350°C, the activity of alumina supported catalyst can compete with the activity of Titania supported catalyst with respect to both glycerol conversion and the product distribution; however, the reduction temperature at 450°C affects strongly the activity of alumina supported catalyst. Increasing of treatment temperature to 450°C decreases the activity of alumina supported catalyst significantly. The conversion of glycerol significantly decreases from 72.3% to only 43.8% and the selectivity drops from 91.7% to only 80.9%.

### Charaterization

The NH<sub>3</sub>-TPD was performed from 50 to 750°C to study the acidic properties on the catalyst surface conducted in order to elucidate the catalytic activity of catalysts, and thus, to find out how a support can affect the catalytic activity and acid property of the 10Ni/30HSiW supported catalysts. The NH<sub>3</sub>-TPD profiles of different support catalysts reduced at 450°C were deconvoluted into 3 peaks (namely weak, medium and strong acid sites) using a Gaussian fitting method and are shown in Fig. 6-19. The total acidity of the catalysts was recorded and is shown in Table 6-8 and

was then correlated with the catalytic activity of 10Ni/30HSiW supported catalysts (Fig. 6-18 and Fig. 6-19). Roughly, different kinds of support represented a difference in the total acidity amount, the strength of acid sites and a positive correlation is observed between activity of the catalyst and acid amount over different supported catalysts.

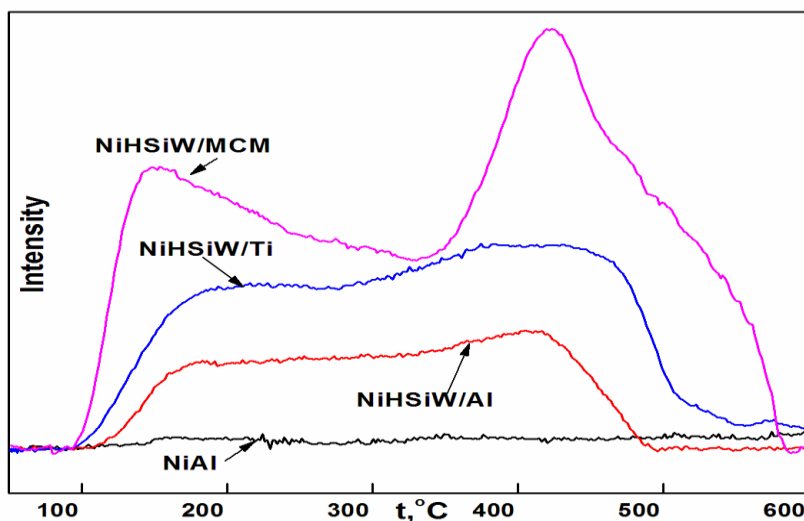


**Figure 6-19** NH<sub>3</sub>-TPD patterns for different support.

**Table 6-8** Surface area and acidities of 10Ni/30HSiW supported catalysts

Support	SAA m <sup>2</sup> /g	Weak acid site mmol/g /(Temp.)	Medium acid site, mmol/g /(Temp.)	Strong acid site, mmol/g /(Temp.)	Total acid amount, mmol/g	Acidity/SAA mmol/m <sup>2</sup>
Al <sub>2</sub> O <sub>3</sub>	21.2	0.232/ (189°C)	0.396/ (335°C)	0.168/ (436°C)	0.796	0.038
TiO <sub>2</sub>	18.1	0.219/ (191°C)	0.462/ (342°C)	0.153/(449°C)	0.834	0.046
MCM-41	560.5	0.354/ (176°C)	0.702/ (355°C)	0.483/ (446°C)	1.539	0.0027

As can be seen, the MCM-41 supported catalyst shows the highest acidity while the alumina supported catalyst gives a low acidity among all catalysts (Fig. 6-20). The total acidity is in the order of MCM-41>TiO<sub>2</sub>>Al<sub>2</sub>O<sub>3</sub>, a similar trend was also observed for the strength of medium acid sites. These results suggest that the acidity of HSiW is affected by the support. It is noticeable that the trend of catalytic activity is well consistent with the trend of the amount of acidity of these catalysts; the most active catalyst is the one that possesses the highest acidity and the strength of

medium acid sites (Table 6-7 and Fig. 6-20). The higher the acidity the higher the conversion of glycerol and selectivity to 1-PO (Fig. 6-21)

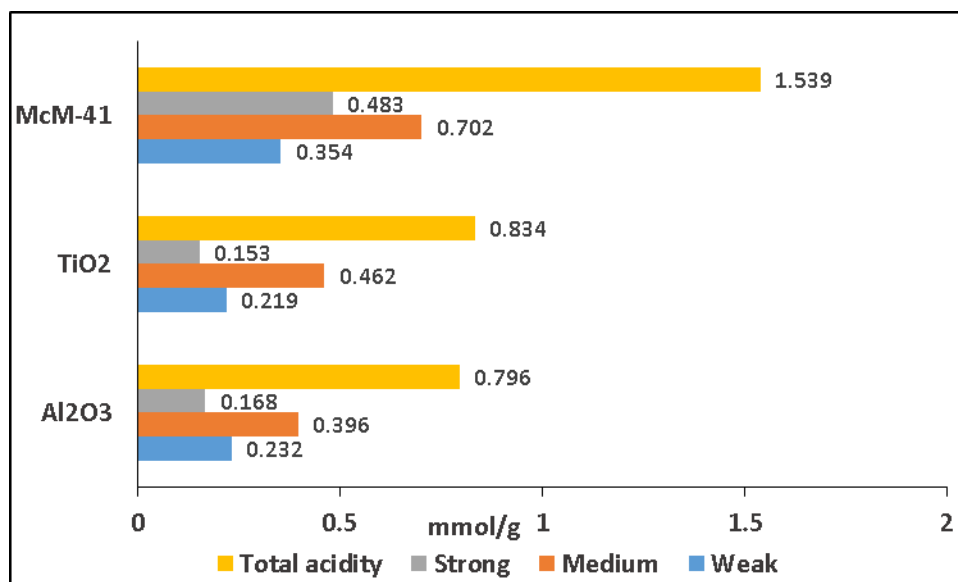


**Figure 6-20** Effect of supports on total acidity and acid strength of catalyst reduced at 450°C

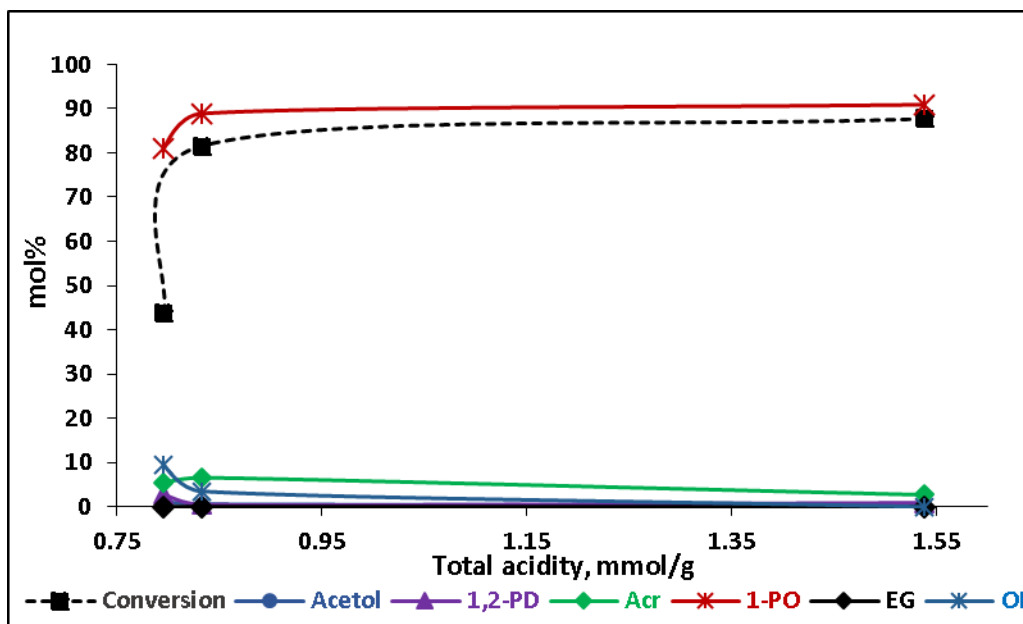


**Figure 6-21** Effect of acidity of catalyst on glycerol conversion and selectivity of products

The catalysts were characterized with XRD to explore the crystal phases and to check possible if the interactions between the support and HSiW can affect and distort the structure of the HSiW

supported catalysts. Fig. 6-22 shows the X-ray diffraction patterns of alumina support, bulk HSiW and 10Ni/30HSiW supported catalysts

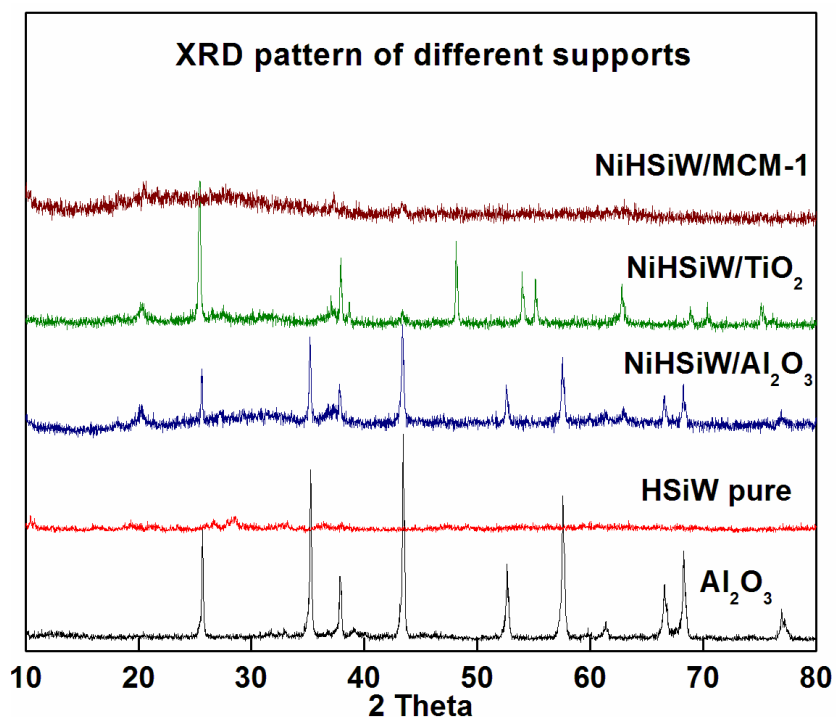


**Figure 6-22** XRD patterns for different support

As shown in Fig. 6-20, all supported catalysts show that the diffraction peaks corresponded to the support itself that is referred to the JCPDS database. Anatase TiO<sub>2</sub> (centered at  $2\theta = 25.4, 38.0,$  and  $48.2, 54, 55, 63, 69, 71$ ) are in good agreement with the standard spectrum (JCPDS no.: 84-1286) [202]. Alpha alumina (centered at  $2\theta = 25.6, 35.2, 37.8, 43.4, 52.6, 57.5$  and  $61.3$ ) are in good agreement with the standard spectrum (JCPDS no.: 42-1468)[203]. Wide angle X-ray diffraction patterns of MCM-41 are in good agreement with that of Jha A. et al. reported in his work, a broad band in the range of  $2\theta = 15-40^\circ$ , which is a characteristic of siliceous material [195]. Besides the diffraction peaks that attributed to HSiW are observed for all catalysts confirms that the Keggin structure is preserved upon the impregnation of the HSiW onto different supports under the catalytic system.

BET surface area was calculated from desorption isotherms and the result are listed in Table 6-8. As can be seen from Table 6-8, amongst the supports, the MCM-support catalysts have the largest surface area. This may contribute to more acid sites that this catalyst possesses and as a result the



increase in glycerol conversion is believed to be higher when the amount of acid sites produced is higher by introducing more surface area.

## Summary

The support clearly affects the catalyst activity. Among the supports, the catalyst supported MCM-41 possesses the highest acidity and catalyst activity. This support can retain the activity of catalyst at high reduction of 450°C. This was also observed for the catalyst supported TiO<sub>2</sub> but the catalyst activity is a bit lower compared to that of MCM-41. At low temperature treatment, an alumina support can compete with TiO<sub>2</sub>; however the catalyst loses its activity quickly at high temperature. MCM-41 and TiO<sub>2</sub> can be a good support for the hydrogenlysis of glycerol to 1-PO using a 10Ni/30HSiW supported catalyst.

## 6.4 Conclusion

In this chapter, catalysts have been tested and characterized using different catalyst characterization techniques to study the relationship between the catalyst structure and the catalytic activity.

It is found that the structure of catalyst can be affected in the activation process such as calcination or reduction. The loss in activity of catalyst may occur if the treatment temperature is higher than 450°C. Under our catalytic system, the HSiW supported catalyst calcined at 450°C and reduced at 350°C is the best candidate for 1-PO production and the catalyst needs to be reduced to obtain high selectivity of 1-PO. The decomposition of HPMo already occurred at 350°C treatment and HPMo supported catalyst is inactive in this reaction.

To achieve good performance, catalysts must retain the Keggin species on the surface which is probably beneficial to induce Brønsted acid site that can cleave the secondary – OH group in glycerol; they must also have a proper balance between acid sites and metal sites. The crystal structure of the Keggin unit of the HSiW supported catalyst is decomposed at least partially when the calcination temperature increased to 550°C. The support clearly affects the catalyst activity. Among the supports, the catalyst supported MCM-41 possesses the highest acidity and catalyst activity. MCM-41 and TiO<sub>2</sub> can be a good supports for the hydrogenlysis of glycerol to 1-PO using 10Ni/30HSiW supported catalyst.

## Chapter Seven

### Conclusion and Recommendation

#### 7.1 Conclusions on glycerol hydrogenolysis to 1-PO using 10Ni/30HSiW supported catalyst

To my knowledge, this is the first time the one-pot hydrogenolysis of glycerol to 1-PO using non-noble-metal of Ni-based supported HSiW/Al<sub>2</sub>O<sub>3</sub> catalyst have been successfully carried out in water with high selectivity to 1-PO (92%) at high conversion of glycerol (90%). Further development could potentially lead to a new green process for the production of sustainable 1-PO.

The bifunctional catalyst of 10Ni/30HSiW/Al<sub>2</sub>O<sub>3</sub> was successfully prepared in water through a one step of impregnation (co-impregnation of Ni and HSiW) with high catalyst activity. This served as a cheaper and efficient alternatives method compared to that was prepared by a conventional sequential impregnation method.

Among the metals (Cu, Ni, Pd, and Pt) supported on 30HSiW/Al<sub>2</sub>O<sub>3</sub>, Pt is the best promoter for the production of 1,3-PD from glycerol, however using Ni, a much cheaper metal has fairly comparable reactivity to Pt. Although it is reported that Cu possesses good hydrogenation activity that is comparable with Ni, Cu does not show activity for the production of 1,3-PD under these reaction conditions.

Cs<sup>+</sup> has little effect on glycerol conversion; however it shows a significant effect on the product distribution – due to reduction of acidity. The 10Ni/30HSiW/Al<sub>2</sub>O<sub>3</sub> catalyst was found to be an effective catalyst for the production of 1-PO, whereas, Cs<sup>+</sup> exchanged catalyst becomes effective for the production of 1,2-PD and EG. A greater quantity of acid sites of a medium strength corresponded to a higher selectivity of 1-PO. XRD data shows that hydrogen protons in the secondary structure may be replaced by Cs<sup>+</sup> that corresponds to the decrease in the acidity of the catalyst. Among the catalysts tested, 1Cs<sup>+</sup> catalyst showed the best catalytic performance for 1,3-PD and 1-PO; however, fully substituted NiCs<sub>4</sub>SiW<sub>12</sub>O<sub>40</sub> is catalytically inert to 1-PO as it possesses very low acid sites. Ni plays an important role for the production of lower alcohols due to its hydrogenation activity. Without Ni, the substitution of H<sup>+</sup> by Cs<sup>+</sup> decreases the activity of 30HSiW/Al<sub>2</sub>O<sub>3</sub> significantly.

It is found that the hydrogenolysis of glycerol is chemically controlled at a stirring speed of 500 RPM in a batch reactor. The conversion of glycerol is inversely proportional to the hydrogen pressure. This possibly could be attributed to the fact that the reduction of W under high pressure of H<sub>2</sub> results in the loss of activity of the catalyst for the dehydration step that leads to a decrease in the conversion of glycerol. However a high H<sub>2</sub> pressure is necessary to suppress the undesired dehydration and to decrease the undesired products. Optimal operating H<sub>2</sub> pressures are required to obtain high yields of 1-PO.

Dilute feed solutions favor the selectivity to 1-PO but decreases the conversions of glycerol. Increasing the glycerol concentration (decreasing the initial water content) decreased the selectivity to 1-PO while meanwhile the selectivity to 1,2-PD and acrolein increased. The increase in the concentration of glycerol may result in less active sites becoming available for the conversion of 1,2-PD and/or acrolein to 1-PO, so more 1,2-PD and/or acrolein can be retained and less 1-PO is produced. Optimal glycerol feed concentration is required to obtain a high yield of 1-PO.

Conversion increased with catalyst loading, but selectivity had a maximum of 92.7% at 4.5% loading. It is thought that high catalyst loadings tend to provide excess active sites resulting in increased exposure of 1-PO to the surface of catalyst that can promote the further degradation of 1-PO or promote the side reactions from glycerol to produce undesired products causing a decrease in 1-PO selectivity. Optimal catalyst loading is required to obtain a high yield of 1-PO.

Increasing temperature may promote further hydrogenolysis of 1,2-PD to 1-PO. However excessive heat may cause the degradation of 1-PO to other products or promote other side reactions. Therefore it is suggested that the operation at high hydrogen pressures may prevent degradation of products.

According to acidity, 1-PO was favored by catalyst acidity while 1,2-PD and EG are likely favored by basicity and the loading of HSiW should be at least 20% to promote the further hydrogenolysis of 1,2-PD to 1-PO. It is believed that part of 1-PO came from the hydrogenation of acrolein that was produced from the consecutive dehydration of glycerol. The total number of acidic sites and the acid strength was found to decrease with increasing Ni content. A decrease in acidity may

possibly be due to the covering of acid sites by Ni or it can be suggested that this behavior may result from direct anchoring on proton sites and from blockage of acid channels by Ni particles.

It is found that the structure of catalyst can be affected in the activation process such as calcination or reduction. The loss in activity of the catalyst may occur if the treatment temperature is higher than 450°C. Under our catalytic system condition, the HSiW supported catalyst calcined at 450°C and reduced at 350°C is the best candidate for 1-PO production and the catalyst needs to be reduced to obtain high selectivity of 1-PO. The decomposition of HPMo already occurred at 350°C of treatment and HPMo supported catalyst is inactive in this reaction.

To achieve good performance, catalysts must retain the Keggin species on the surface which is probably beneficial to induce Brønsted acid sites that can cleave the secondary – OH group in glycerol; they must also have a proper balance between acid sites and metal sites. The crystal structure of the Keggin unit of the HSiW supported catalyst decomposed at least partially when the calcination temperature increased to 550°C. A greater quantity of acid sites of a certain strength corresponded to a higher selectivity of 1-PO.

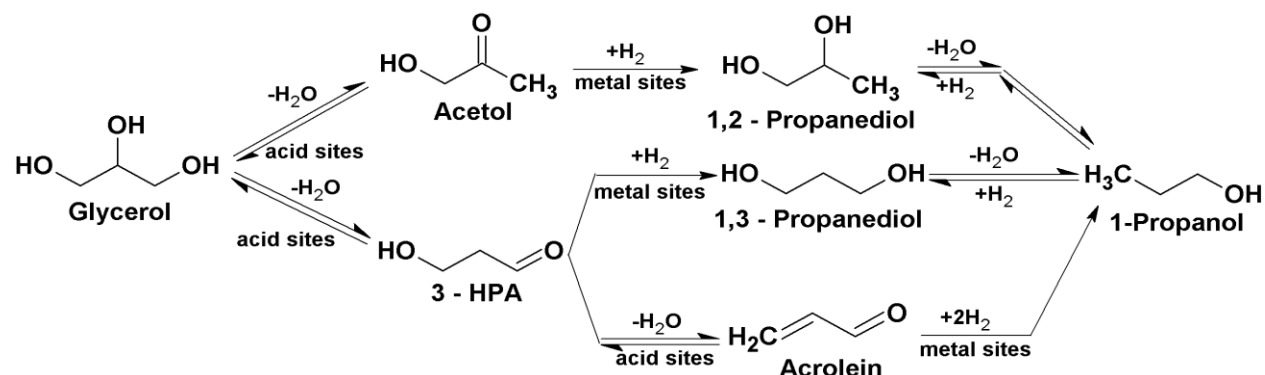
The support clearly affects the catalyst activity. Among the supports, the catalyst supported MCM-41 possesses the highest acidity and catalyst activity. Preliminary results indicated that MCM-41 and TiO<sub>2</sub> are good supports for the hydrogenolysis of glycerol to 1-PO using a 10Ni/30HSiW supported catalyst.

Although 10Ni/30HSiW supported catalyst shows a good activity for the production of 1-PO from glycerol; the leaching of catalyst is a concern.

## **7.2 Proposed reaction pathway**

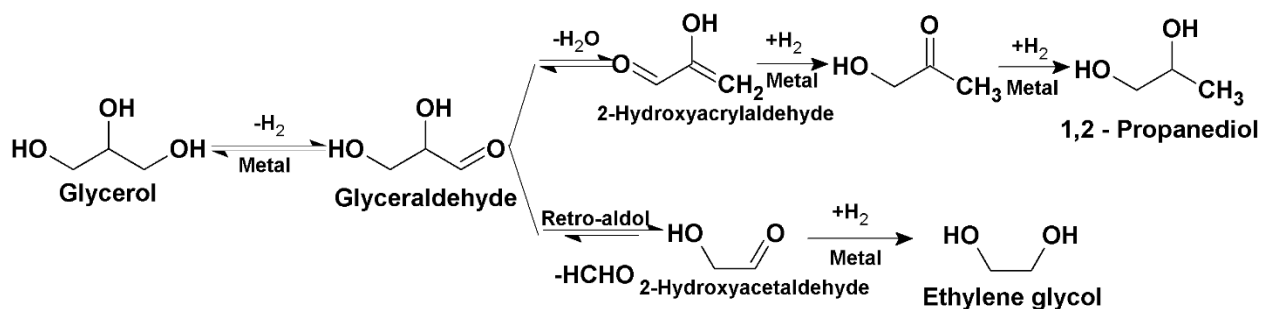
Based on our experimental results, we propose the following reaction pathway to explain the glycerol hydrogenolysis over a 10Ni/30HSiW supported catalyst (Scheme 7-1). The first intermediate products for glycerol conversion are acetol and 3-hydroxypropionaldehyde (3-HPA) which are formed via the dehydration of the hydroxyl group at the secondary and primary carbon atom respectively. 1,2-PD is formed from the hydrogenation of acetol while hydrogenation of 3-HPA produces 1,3-PD. In the absence of an efficient hydrogenation function on an acidic catalyst, 3-HPA will undergo dehydration to form acrolein. Further hydrogenolysis of 1,2-PD or 1,3-PD

gives 1-PO. Since 3-HPA is more reactive compared to acetol [59, 166], it was not observed as an intermediate in the reaction. From the mechanism proposed, 1-PO could be obtained from the hydrogenolysis of 1,2-PD and 1,3-PD, or the hydrogenation of acrolein.



**Scheme 7-1** Reactions in the hydrogenolysis of glycerol to 1-PO using bifunctional catalyst of 10Ni/30HSiW/Al<sub>2</sub>O<sub>3</sub>

With acidic catalysts, the formation of 1,2-PD, 1,3-PD and 1-PO is proposed as in the scheme 7-1. When H<sup>+</sup> was substituted by Cs<sup>+</sup> or at low HSiW loading proposed pathways for the conversion of glycerol to glycols (1,2-PD and EG) are shown in Scheme 7-2.



**Scheme 7-2** Proposed pathways in the hydrogenolysis of glycerol to 1,2-PD and EG using a bifunctional catalyst with low acidity

When H<sup>+</sup> was replaced by an alkaline metal ion, Cs<sup>+</sup>, the acidity of the catalyst decreases while the basicity of the catalyst may increase. Hence it is possible that the formation of 1,2-PD and EG takes place through a reversible dehydrogenation of glycerol to glyceraldehyde (GA) on metal sites, followed by dehydration or retro-aldolization of GA on basic sites to 2-

hydroxyacrylaldehyde or 2-hydroxyacetaldehyde, and finally, the two aldehyde precursors are hydrogenated on metal sites to 1,2-PD and EG, respectively.

### 7.3 Recommendations

The much lower price of Ni compared to Pt is very attractive for a new green process development for the conversion of glycerol to sustainable higher value products. To obtain a desired product selectively, the control of reaction conditions and catalyst properties such as acid strength, the amount of appropriate acid sites and metal hydrogenation activity will be needed. Optimization of the catalyst preparation techniques and a balance of Ni and HiSiW loading on various supports could lead to high yields of value-added chemicals from glycerol. Due to the inexpensive Ni-based catalyst and the high selectivity, an economical production of green and sustainable 1-PO from glycerol hydrogenolysis may be feasible for future commercial development.

10Ni/30HSiW supported catalysts seem to be a good catalyst system for the production of 1-PO from glycerol. MCM-41 or TiO<sub>2</sub> can be a choice of support to make the catalyst work effectively.

It is suggested that that catalyst should be prepared by co-impregnation, since under this catalytic system this catalyst can perform better compared to other catalyst preparation sequences. This method also saves time and requires less work to prepare the catalyst. However, the direct interaction between the components during the preparation should be considered.

The studied catalytic system is effective for the production of 1-PO from glycerol and it is known that the dehydration of 1-PO will produce propene. Therefore it is promising to develop new route for one-step propylene production from glycerol based on this catalytic system.

It is found that the 10Ni/30HSiW/Al<sub>2</sub>O<sub>3</sub> catalyst is effective for the hydrogenolysis of 1,2-PD to 1-PO (at high conversion of glycerol of 98.1% and high selectivity to 1-PO of 91%) so the 2 layer catalyst packing can also be developed for the production of 1-PO from glycerol.

However, it has been discussed that the catalyst leaching and deactivation in a glycerol hydrogenolysis process is possible; therefore, the development of a catalyst supported heteropolyacid needs to be studied to facilitate the improvement of catalytic performance and to make it widely used.

It was found that when the hydrogenolysis of glycerol was performed in a Stainless steel reactor, the reaction rate was much lower compared to when it was carried out in a Hastelloy reactor; however, the selectivity to 1,3-PD was much higher. It is thought that the release of metal constituent from stainless steel reactor into the solution may occur and affect the product selectivity. This was also reported by Chaminand J. et. al. that partial dissolution of metals from the inox walls of the reactor increased the selectivity to 1,3-PD in the hydrogenolysis of glycerol on heterogeneous catalysts [56]. Therefore, a study of promoter effects, e.g. adding another metal component such as Fe, for the activity of catalyst to form 1,3-PD may be of interest. To improve the selectivity of 1,3-PD it is suggested that the catalyst should have high hydrogenation activity for the intermediate 3-HPA. The equilibrium between acrolein and 3-HPA in the hydration-dehydration step is important, so it is essential to tune the bi-functional catalyst and the conditions of the reaction to form 1,3-PD from 3-HPA. A statistical analysis on the effect of catalyst compositions, the conditions of the reaction on 1,3-PD selectivity from glycerol can be applied to this study. The effect of catalyst composition can be studied through response surface methodology (RSM) combined with a central composite rotatable design (CCRD). A DRIFT technique can be applied for in-situ studying of the intermediate species for 1,3-PD on the catalyst. Chemisorption studies and density functional density theory (DFT) modelling can be applied to investigate the structures and interactions between the reactants and the catalyst surface to elucidate a potential mechanistic pathway for the catalytic reactions.

## References

1. Hatti-Kaul, R., Törnvall U., Gustafsson L., Börjesson P., Industrial biotechnology for the production of bio-based chemicals—a cradle-to-grave perspective. *Trends Biotechnol.*, 2007, 25, 3, 119-124
2. Sheldon R.A., Why green chemistry and sustainability of resources are essential to our future. *J. Environ. Monit.*, 2008, 10, 4, 406-407
3. Okkerse C. and Bekkum H.V., From fossil to green. *Green Chem.*, 1999, 1, 2, 107-114
4. James H.C., Fabien I. D., Introduction to chemical from biomass, John Wiley and Sons, United Kingdom, 2008
5. Anastas. P. T., Warner. J. C., *Green Chemistry: Theory and Practice*, Oxford University Press: New York, 1998
6. Bagheri S. et al., Catalytic conversion of biodiesel derived raw glycerol to value added products, *Renewable and Sustainable Energy Reviews*, 2015, 41, 113–127
7. Ye X. P., Ren S., *Value-Added Chemicals from Glycerol*, ACS Symposium Series; American Chemical Society: Washington, DC, 2014, Chapter 3, pp 43–80
8. Pagliaro M., Ciriminna R., Kimura H., Rossi M., Pina C.D., Recent advances in the conversion of bioglycerol into value-added products, *Eur. J. Lipid Sci. Technol.*, 2009, 111, 788–799
9. Bozell J. J., Petersen G. R., Technology development for the production of biobased products from biorefinery carbohydrates—the US Department of Energy’s “Top 10” revisited, *Green Chem.*, 2010, 12, 539-554
10. Förare J., *Swedish Research and Innovation Strategy for a Bio-based Economy*, 2012, ISBN:978-91-540-6068-2,
11. Christoph R., Schmidt B., Steinberner U., Dilla W., Karinen R., "Glycerol", *Ullmann's Encyclopedia of Industrial Chemistry*. Online Edn, 2006, Germany, Wiley-VCH, Weinheim.
12. Patel M.K., Crank M., Dornburg V., Recchia E., Medium and long-term opportunities and risks of the biotechnological production of bulk chemicals from renewable resources- The potential of white biotechnology. *The BREW Project*, 2006



13. Dasari M.A., Kiatsimkul P.P., Sutterlin W.R., and Suppes G.J., Low-pressure hydrogenolysis of glycerol to propylene glycol, *Applied Catalysis A: General*, 2005, 281, 1-2, 225-2311
14. Nilles D., Combating the glycerin glut. *Biodiesel Magazine*, 2006
15. Yang F. X., Hanna M. A., Sun R. C., Value-added uses for crude glycerol-a byproduct of biodiesel production, *Biotechnol. Biofuels*, 2012, 5, 13
16. Johnson D. T., Taconi K. A., "The glycerin glut: Options for the value-added conversion of crude glycerol resulting from biodiesel production," *Environmental Progress*, 2007, 26, 338-348
17. Pagliaro M., Ciriminna R., Kimura H., Rossi M., Pina C. D., "From glycerol to value-added products." *Angewandte Chemie - International Edition*, 2007, 46, 24, 4434-4440
18. Werpy T., Peterson G., Aden A., Bozell J., Holladay J., White J., Manheim, A. Top value added chemicals from biomass, Volume 1: Results of screening for potential candidates from sugars and synthesis gas. United States Department of Energy Efficiency and Renewable Energy, 2004
19. Jong, E.D., et al., Bio-based chemicals - value added products from biorefineries. IEA Bioenergy, 2012
20. Jang, Y.-S., et al., Bio-based production of C2–C6 platform chemicals. *Biotechnology and Bioengineering*, 2012, 109, 10, 2437-2459
21. Pagliaro M., Rossi M., *The Future of Glycerol*. Cambridge, The Royal Society of Chemistry, 2010
22. Kenar J. A., "Glycerol as a platform chemical: Sweet opportunities on the horizon?" *Lipid Technology*, 2007, 19, 249-253.
23. Dube M. A., Tremblay A. Y., Liu Y., "Biodiesel production using a membrane reactor." *Bioresource Technology*, 2007, 98, 3, 639-647
24. Zhou C.H., Beltramini J.N., Fan Y.X. and Lu G.Q., Chemoselective catalytic conversion of glycerol as a biorenewable source to valuable commodity chemicals, *Chemical Society Reviews*, 2008, 37, 527–549
25. M. Pagliaro and M. Rossi, *The Future of Glycerol: New Usages for a Versatile Raw Material*. Cambridge: RSC Publishing, 2008

26. Corma, S. Iborra, and A. Velty, "Chemical Routes for the Transformation of Biomass into Chemicals," *Chemical Reviews*, 2007, 107, 2411-2502
27. Behr A., J. Eilting, K. Irawadi, J. Leschinski, and F. Lindner, "Improved utilisation of renewable resources: New important derivatives of glycerol," *Green Chemistry*, 2007, 10, 13-30
28. a. [https://www.zauba.com/shipment\\_search](https://www.zauba.com/shipment_search); b. Jiang W. et al., Key enzymes catalyzing glycerol to 1,3-propanediol, *Biotechnol Biofuels*, 2016, 9, 57-75
29. Wang Y et al., Catalytic hydrogenolysis of glycerol to propanediols: a review, *RSC Adv.*, 2015, 5, 74611–74628
30. Saxena R.K., Anand P., Saran S., Jasmine I., Microbial production of 1,3-propanediol: Recent developments and emerging opportunities, *Biotechnology Advances*, 2009, 27, 895-913
31. Product Safety Summary Sheet - DuPont Tate & Lyle BioProducts™ 1,3-Propanediol
32. Value-added Utilization of Crude Glycerol from biodiesel Production: A Survey of Current Research Activities, An ASABE Meeting Presentation, Paper Number: 066223
33. Hellman T.M., Small F.H., Characterization of the odor properties of 101 petrochemicals using sensory methods. *J. Air Pollut. Control Assoc.*, 1974, 24, 979-982
34. Jain R, Yan Y, Dehydratase mediated 1-propanol production in metabolically engineered *Escherichia coli*. *Microb Cell Fact* 2011, 10,1–10
35. Shen C.R., Liao J.C., 2008. Metabolic engineering of *Escherichiacoli* for 1-butanol and 1-propanol production via the keto-acid pathways. *Metab.Eng.* 2008, 10, 312–320
36. "1-Propanol. <http://www.inchem.org/documents/ehc/ehc/ehc102.htm>
37. Material Safety Data Sheet 1-Propanol. Caledon Laboratory chemicals [<http://www.caledonlabs.com/upload/msds/8500-1e.pdf>]
38. Product Safety Assessment: DOW™ 1-propanol, page 2; James L. Unmack, 1-propanol Health-Base Assessment and Recommendation for HEAC
39. <http://www.syntecbiofuel.com/propanol.php>
40. Atsumi S, Liao JC, Directed evolution of *Methanococcus jannaschii* citramalate synthase for biosynthesis of 1-propanol and 1-butanol by *Escherichia coli*, *Appl Environ Microbiol* 2008, 74, 7802–7808

41. Atsumi S., Cann A.F., Connor M.R., Shen C.R., Smith K.M., Brynildsen M.P., Chou K.J.Y., Hanai T., Liao J.C., Metabolic engineering of *Escherichia coli* for 1-butanol production. *Metab Eng* 2008, 10, 305–311
42. Bioalcohols". [Biofuel.org.uk](http://Biofuel.org.uk). Retrieved 2014-04-16
43. <http://www.inchem.org/documents/ehc/ehc/ehc102.htm>
44. Schlaf M., Ghosh P., Fagan P.J., Hauptman E., Bullock R.M., Catalytic Deoxygenation of 1,2-Propanediol to Give n-Propanol, *Advanced Synthesis & Catalysis*, 2009, 351, 789 – 800
45. Amada Y., Koso S., Nakagawa Y., Tomishige K., Hydrogenolysis of 1,2-Propanediol for the Production of Biopropanols from Glycerol, *ChemSusChem*, 2010, 3, 728–736
46. Foskey A.T.J., Heinekey D.M., Goldberg K.I., Partial Deoxygenation of 1,2-Propanediol Catalyzed by Iridium Pincer Complexes, *ACS Catalysis* 2012, 2, 1285–1289
47. Kusunoki Y., Miyazawa T., Kunimori K., Tomishige K., Highly active metal–acid bifunctional catalyst system for hydrogenolysis of glycerol under mild reaction conditions, *Catalysis Communications*, 2005, 6, 645–649;
48. Furikado I., Miyazawa T., Koso S., Shima A., Kunimori K., Tomishige K., Catalytic performance of Rh/SiO<sub>2</sub> in glycerol reaction under hydrogen, *Green Chemistry*, 2007, 9, 582–588 ;
49. Shinmi Y., Koso S., Kubota T., Nakagawa Y., Tomishige K., Modification of Rh/SiO<sub>2</sub> catalyst for the hydrogenolysis of glycerol in water, *Appl. Catal., B*, 2010, 94, 318–326;
50. Gandarias I., Arias P.L., Requies J., Guñemez M.B. , Fierro J.L.G., Hydrogenolysis of glycerol to propanediols over a Pt/ASA catalyst: The role of acid and metal sites on product selectivity and the reaction mechanism, *Appl. Catal., B*, 2010, 97, 248–256
51. Nakagawa Y., Ning X., Amada Y. , Tomishige K., Solid acid co-catalyst for the hydrogenolysis of glycerol to 1,3-propanediol over Ir-ReO<sub>x</sub>/SiO<sub>2</sub>, *Applied Catalysis A: General*, 2012, 433–434, 128–134
52. Feng J., Xu B., REVIEW: Reaction mechanisms for the heterogeneous hydrogenolysis of biomass-derived glycerol to propanediols, *Progress in Reaction Kinetics and Mechanism*, 2014, 39, 1, 1–15

53. Amada Y., Shinmi Y., Koso S., Kubota T., Nakagawa Y., Tomishige K., Reaction mechanism of the glycerol hydrogenolysis to 1,3-propanediol over Ir–ReOx/SiO<sub>2</sub> catalyst, *Applied Catalysis B: Environmental*, 2011, 105, 117-127
54. Qin L.Z., Aqueous-phase deoxygenation of glycerol to 1,3-propanediol over Pt/WO<sub>3</sub>/ZrO<sub>2</sub> catalysts in a fixed-bed reactor, *Green Chemistry*, 2010, 12, 1466–1472
55. Longjie L., Yanhua Z., Aiqin W., Tao Z., Mesoporous WO<sub>3</sub> Supported Pt Catalyst for Hydrogenolysis of Glycerol to 1,3-Propanediol, *Chinese Journal of Catalysis*, 2012, 33, 1257–1261
56. Chaminand J., Djakovitch L., Gallezot P., Marion P., Pinel C., Rosier C., Glycerol hydrogenolysis on heterogeneous catalysts, *Green Chemistry*, 2004, 6, 359 – 361
57. Wang S., Liu H., Selective hydrogenolysis of glycerol to propylene glycol on Cu–ZnO Catalysts, *Catalysis Letters*, 2007, 117, 1–2, 62-67
58. Huang L., Zhu Y.L., Zheng H.Y., Li Y.W., Zeng Z.Y., Continuous production of 1,2-propanediol by the selective hydrogenolysis of solvent-free glycerol under mild conditions, *Journal of Chemical Technology and Biotechnology*, 2008, 83, 1670-1675
59. Miyazawa T. et al., Glycerol conversion in the aqueous solution under hydrogen over Ru/C + an ion-exchange resin and its reaction mechanism, *J. Catal.*, 2006, 240, 213–221
60. Ryneveld E.V. et al, A catalytic route to lower alcohols from glycerol using Ni-supported Catalysts, *Green Chem.*, 2011, 13, 1819-1827
61. Wang M. et al, Catalytic transformation of glycerol to 1-propanol by combining zirconium phosphate and supported Ru catalysts, *RSC Adv.*, 2016, 6, 29769–29778
62. Yu L. et al., Propylene from Renewable Resources: Catalytic Conversion of Glycerol into Propylene, *ChemSusChem*, 2014, 7, 743 – 747
63. Sun D. et al, Efficient production of propylene in the catalytic conversion of glycerol, *Applied Catalysis B: Environmental*, 2015, 174–175, 13–20
64. Nakagawa Y. et al., Heterogeneous catalysis of the glycerol hydrogenolysis, *Catal. Sci. Technol.*, 2011, 1, 179–190
65. Gascon J et al., Amino-based metal-organic frameworks as stable, highly active basic catalysts, *Journal of Catalysis*, 2009, 261, 75-87

66. Wang S. S., Yang G. Y. , Recent Advances in Polyoxometalate-Catalyzed Reactions, *Chem. Rev.*, 2015, 115, 11, 4893–4962
67. Brückman K., Che M., Haber J., On the physicochemical and catalytic properties of H<sub>5</sub>PV<sub>2</sub>Mo<sub>10</sub>O<sub>40</sub> supported on silica, *J. M. Tatibouët, Catal. Lett.*, 1994, 25, 225-240
68. Trolliet A., G. Coudurier, J. C. Vedrine, Influence of the nature and porosity of different supports on the acidic and catalytic properties of H<sub>3</sub>PW<sub>12</sub>O<sub>40</sub>, *Topics in Catal.*, 2001, 15, 73-81
69. E. Lopez-Salinas, J. G. Hernandez-Cortez, I. Schifer, E. Torres-Garcia, J. Navarrete, A. Gutierrez-Carrillo, T. Lopez, P. P. Lottici, D. Bersani, Thermal stability of 12-tungstophosphoric acid supported on zirconia, *Appl. Catal. A: General*, 2000, 193 , 215
70. Zhou Y., Guo Z., Hou W., Wang Q. and Wang J., Polyoxometalate-based phase transfer catalysis for liquid–solid organic reactions: a review, *Catal. Sci. Technol.*, 2015, 5, 4324-4335
71. Misono M., Unique acid catalysis of heteropoly compounds(heteropolyoxometalates) in the solid state, *Chem. Commun.*, 2001, 1141–1152
72. Atia H., Armbruster U., Martin A., Influence of alkaline metal on performance of supported silicotungstic acid catalysts in glycerol dehydration towards acrolein , *Appl. Catal. A: Gen.*, 2011, 393, 331–339
73. Martin A., U. Armbruster, H. Atia, Recent developments in dehydration of glycerol toward acrolein over heteropolyacids, *Eur. J. Lipid Sci. Technol.*, 2012, 114, 10–23
74. Liu L., Ye X.P., Bozell J.J., A Comparative Review of Petroleum-Based and Bio-Based Acrolein Production, *ChemSusChem*, 2012, 5 2012, 1162–1180
75. Katryniok A., S. Paul, F. Dumeignil, Recent Developments in the Field of Catalytic Dehydration of Glycerol to Acrolein, *ACS Catal.*, 2013, 3, 1819–1834
76. Hanan Atia, Udo Armbruster, Andreas Martin, Dehydration of glycerol in gas phase using heteropolyacid catalysts as active compounds, *Journal of Catalysis*, 2008, 258, 71–82
77. Zhu S., Zhu Y., Hao S., Chen L., Zhang B. and Li Y., Aqueous-Phase Hydrogenolysis of Glycerol to 1,3-propanediol Over Pt-H<sub>4</sub>SiW<sub>12</sub>O<sub>40</sub>/SiO<sub>2</sub>, *Catalysis Letters*, 2012, 142, 267–274

78. Zhu S., Zhu Y., Hao S., Zheng H., Mo T., Li Y., One-step hydrogenolysis of glycerol to biopropanols over Pt–H<sub>4</sub>SiW<sub>12</sub>O<sub>40</sub>/ZrO<sub>2</sub> catalysts, *Green Chemistry*, 2012, 14, 2607–2616
79. Zhu S., Qiu Y., Zhu Y., Hao S., Zheng H., Li Y., Hydrogenolysis of glycerol to 1,3-propanediol over bifunctional catalysts containing Pt and heteropolyacids, *Catalysis Today*, 2013, 212, 120–126
80. Cavani F, Guidetti S, Marinelli L, Piccinini M, Ghedini E, Signoretto M, The control of selectivity in gas-phase glycerol dehydration to acrolein catalysed by sulfated zirconia, *Applied Catalysis B: Environmental*, 2010, 100, 197–204
81. Alhanash A., Kozhevnikova E.F., Kozhevnikov I.V., Hydrogenolysis of Glycerol to Propanediol Over Ru: Polyoxometalate Bifunctional Catalyst, *Catalysis Letters*, 2008, 120, 307–311
82. Gong L., Selective hydrogenolysis of glycerol to 1,3-propanediol over a Pt/WO<sub>3</sub>/TiO<sub>2</sub>/SiO<sub>2</sub> catalyst in aqueous media, *Applied Catalysis A: General*, 2010, 390, 119–126
83. Zhang Y., Zhao X.C., Wang Y., Zhou L., Zhang J., Wang J., Wang A., Zhang T., Mesoporous Ti–W oxide: synthesis, characterization, and performance in selective hydrogenolysis of glycerol, *Journal of Materials Chemistry A*, 2013, 1, 3724–3732
84. Oh J., Dash D., Lee H. Selective conversion of glycerol to 1,3-propanediol using Pt-sulfated zirconia, *Green Chemistry*, 2011, 13, 2004–2007
85. Alhanash A., Kozhevnikova E.F., Kozhevnikov I.V., Gas-phase dehydration of glycerol to acrolein catalysed by caesium heteropoly salt, *Applied Catalysis A: General*, 2010, 378, 11–18
86. Zhu S., Gao X., Zhu Y., Xiang X., C. Hu, Li Y., Alkaline metals modified Pt–H<sub>4</sub>SiW<sub>12</sub>O<sub>40</sub>/ZrO<sub>2</sub> catalysts for the selective hydrogenolysis of glycerol to 1,3-propanediol, *Applied Catalysis B: Environmental*, 2013, 140–141, 60–67
87. Kongpatpanich K., T. Nanok, B. Boekfa, M. Probst, J. Limtrakul, Structures and reaction mechanisms of glycerol dehydration over H-ZSM-5 zeolite: a density functional theory study, *Physical Chemistry Chemical Physics*, 2011, 13, 6462–6470
88. Kurosaka T., Production of 1,3-propanediol by hydrogenolysis of glycerol catalyzed by Pt/WO<sub>3</sub>/ZrO<sub>2</sub>, *Catalysis Communications*, 2008, 9, 1360–1363

89. Pope M.T., "Heteropoly and Isopoly Oxometallates." Springer-Verlag, Berlin, 1983
90. Barton D.G., Soled S.L., Meitzner G.D., Fuentes G.A., Iglesia E., Structural and Catalytic Characterization of Solid Acids Based on Zirconia Modified by Tungsten Oxide, *Journal of Catalysis* 1999, 181, 57–72
91. Petkovic L. M., Bielenberg J. R. , Larsen G., A Comparative Study of n-Pentane and n-Butane Isomerization over Zirconia-Supported Tungsten Oxide: Pulse and Flow Studies and DRIFTS Catalyst Characterization *J. Catal.*, 1998, 178, 533-539
92. Misono M., Recent progress in the practical applications of heteropolyacid and perovskite catalysts: Catalytic technology for the sustainable society, *Catalysis Today*, 2009, 144, 285–291
93. Kozhevnikov I.V., Heterogeneous acid catalysis by heteropoly acids: Approaches to catalyst deactivation, *Journal of Molecular Catalysis A: Chemical*, 2009, 305, 104–111
94. Ferreira P., Fonseca I.M., Ramos A.M., Vital J., Castanheiro J.E., Valorisation of glycerol by condensation with acetone over silica-included heteropolyacids, *Applied Catalysis B: Environmental*, 2010, 98, 94–99
95. Timofeeva M.N., Acid catalysis by heteropoly acids, *Applied Catalysis A: General*, 2003, 256, 19-35
96. Jin H., Yi X., Sun X., Qiu B., Fang W., Weng W., Wan H., Influence of H<sub>4</sub>SiW<sub>12</sub>O<sub>40</sub> loading on hydrocracking activity of non-sulfide Ni–H<sub>4</sub>SiW<sub>12</sub>O<sub>40</sub>/SiO<sub>2</sub> catalysts, *Fuel*, 2010, 89, 1953-1960
97. Xu S., Wang L., Chu W., Yang W., Influence of Pd precursors on the catalytic performance of Pd– H<sub>4</sub>SiW<sub>12</sub>O<sub>40</sub>/SiO<sub>2</sub> in the direct oxidation of ethylene to acetic acid, *Journal of Molecular Catalysis A: Chemical*, 2009, 310, 138–143
98. Mizugaki T., Yamakawa T., Arundhathi R., Mitsudome T., Selective Hydrogenolysis of Glycerol to 1,3-Propanediol Catalyzed by Pt Nanoparticles AlO<sub>x</sub>/WO<sub>3</sub>, *Catalysis Letters*, 2012, 41, 1720-1722
99. Dam J.T., Djanashvili K., Kapteijn F., Hanefeld U., Pt/Al<sub>2</sub>O<sub>3</sub> Catalyzed 1,3-Propanediol Formation from Glycerol using Tungsten Additives, *ChemCatChem*, 2013, 5, 497 – 505
100. Arundhathi R., Mizugaki T., Mitsudome T., Jitsukawa K., Kaneda K., Highly Selective Hydrogenolysis of Glycerol to 1,3-Propanediol over a Boehmite-Supported Platinum/Tungsten Catalyst, *ChemSusChem*, 2013, 6, 1345 – 1347

101. Delgado S. N., Influence of the nature of the support on the catalytic properties of Pt-based catalysts for hydrogenolysis of glycerol, *Journal of Molecular Catalysis A: Chemical*, 2013, 367, 89–98
102. Zhu S., Gao X., Zhua Y., Cuia J., Zheng H., Li Y., SiO<sub>2</sub> promoted Pt-WO<sub>x</sub>/ZrO<sub>2</sub> catalysts for the selective hydrogenolysis of glycerol to 1,3-propanediol, *Applied Catalysis B: Environmental* 2014, 158–15, 391–399
103. Deng C., Duan X., Zhou J., Chen D., Zhou X., Yuan W., Size effects of Pt-Re bimetallic catalysts for glycerol hydrogenolysis, *Catalysis Today*, 2014, 234, 208–214
104. Vanama P. K., Kumar A., Ginjupalli S. R., Komandur V.R.C, Vapor-phase hydrogenolysis of glycerol over nanostructured Ru/MCM-41 catalysts, *Catalysis Today*, 2015, 250, 226–238
105. Huang L., Zhu Y., Zheng H., Ding G., Li Y., Direct conversion of Glycerol into 1,3-Propanediol over Cu-H<sub>4</sub>SiW<sub>12</sub>O<sub>40</sub>/SiO<sub>2</sub>, *Catalysis Letters*, 2009, 131, 312–320
106. Feng Y. Yin H., Wang A., Shen L., Yu L., Jiang T., Gas phase hydrogenolysis of glycerol catalyzed by Cu/ZnO/MO<sub>x</sub> (MO<sub>x</sub> = Al<sub>2</sub>O<sub>3</sub>, TiO<sub>2</sub>, and ZrO<sub>2</sub>) catalysts, *Chemical Engineering Journal*, 2011, 168, 403–412
107. Nakagawa Y., Shinmi Y., Koso S., Tomishige K., Direct hydrogenolysis of glycerol into 1,3-propanediol over rhenium-modified iridium catalyst, *Journal of Catalysis*, 2010, 272, 191–194
108. Thibault M.E., DiMondo D. V., Jennings M., Abdelnur P. V., Eberlin M. N., Schlaf M., Cyclopentadienyl and pentamethylcyclopentadienyl ruthenium complexes as catalysts for the total deoxygenation of 1,2-hexanediol and glycerol, *Green Chemistry*, 2011, 13, 357-366
109. Perosa A., Tundo P., Selective Hydrogenolysis of Glycerol with Raney Nickel, *Industrial & Engineering Chemistry Research*, 2005, 44, 8535-8537
110. Yu W., Xu J., Ma H., Chen C., Zhao J., Miao H., Song Q., A remarkable enhancement of catalytic activity for KBH<sub>4</sub> treating the carbothermal reduced Ni/AC catalyst in glycerol hydrogenolysis, *Catalysis Communications*, 2010, 11, 493-497
111. Zheng Z., Wang J., Lu Z., Luo M., Zhang M., Xu L., Ji J., Hydrogenolysis of 2-Tosyloxy-1,3-propanediol into 1,3-Propanediol over Raney Ni Catalyst, *Journal of the Brazilian chemical society*, 2013, 24, 3, 385-391



112. Komplin G.C, Smegal J.A., Hydrogenation catalyst and hydrogenation method, US Pat., 7 335 800 B2, 2008
113. Peng G., Wang X., Chen X., Jiang Y., Mu X., Zirconia-supported niobia catalyzed formation of propanol from 1,2-propanediol via dehydration and consecutive hydrogen transfer, *J. Ind. Eng. Chem.*, 2014, 20, 2641–2645.
114. Lebugle A., Axelsson U., Nyholm R., Martensson N. *Phys. Scripta* 1981, 23, 825
115. Wachs, I.E., Fitzpatrick, L.E., “Characterization of Catalytic Materials”, Manning Publications Co., 1992, Greenwich
116. Wang F. et al., Catalytic dehydration of glycerol over vanadium phosphate oxides in the presence of molecular oxygen, *J. Catal.*, 2009, 268, 260–267
117. Hao S. L. et al, Hydrogenolysis of glycerol to 1,2-propanediol catalyzed by Cu-H<sub>4</sub>SiW<sub>12</sub>O<sub>40</sub>/Al<sub>2</sub>O<sub>3</sub> in liquid phase, *J Chem Technol Biotechnol*, 2010, 85, 1499–1503
118. Tsunoda T., Nomura K., Process for producing 1,3-propanediol, US Pat., 6 911 566 B2, 2005
119. Arntz D., Haas T., Schafer-sindlinger A., Process for the preparation of 1,3-propanediol by the hydrogenation of hydroxypropionaldehyde, U.S. Patent No. 5 364 984, 1994
120. Hatch L.F., Evans T.W., Process for hydrating olefinic aldehydes, U.S. Patent No. 2 434 110, 1948
121. Haas T., Wiegand N., Arntz D., Process for the production of 1,3-propanediol, U.S. Patent No. 5 334 778, 1994
122. Lin X. et al, Hydrogenolysis of Glycerol by the Combined Use of Zeolite and Ni/Al<sub>2</sub>O<sub>3</sub> as Catalysts: A Route for Achieving High Selectivity to 1-Propanol; *Energy Fuels* 2014, 28, 3345–3351
123. T. Okuhara, T. Nishimura, H. Watanabe, K. Na, M. Misono, Novel Catalysis of Cesium Salt of Heteropoly Acid and its Characterization by Solid-state NMR, *Stud. Surf. Sci. Catal.*, 1994, 90, 419–428
124. T. Okuhara and T. Nakato, Catalysis by porous heteropoly compounds, *Catal. Surv. JPN*, 1998, 2, 1, 31–44
125. He, W. Huang, J. Liu, Q. Zhu, Condensation of formaldehyde and methyl formate to methyl glycolate and methyl methoxy acetate using heteropolyacids and their salts, *Catal. Today*, 1999, 51, 127–134

126. Haber J., Pamin K., Matachowski L., Napruszewska B., Poltowicz J., "Potassium and Silver Salts of Tungstophosphoric Acid as Catalysts in Dehydration of Ethanol and Hydration of Ethylene", *Journal of Catalysis*, 2002, 207, 296–306
127. Soled, S., Miseo, S., McVicker, G., Gates, W.E., Gutierrez, A., Paes, J., "Preparation of bulk and supported heteropolyacid salts", *Catalysis Today*, 1997, 36, 441-450, 42
128. Kozhevnikov, I.V., "Fine organic synthesis with the aid of heteropolycompounds", *Russian Chemical Reviews*, 1993, 62, 5, 473-491.
129. Okuhara T., Watanabe H., Nishimura T., Inumaru K., Misono M., Microstructure of Cesium Hydrogen Salts of 12-Tungstophosphoric Acid Relevant to Novel Acid Catalysis, *Chem. Mater.*, 2000, 12, 2230–2238
130. Friesen D.A., Gibson D.B., Langford C.H., Heterogeneous  $\text{Cs}_3\text{PW}_{12}\text{O}_{40}$  photocatalysts, *Chem. Commun.*, 1998, 543–544
131. Rana S, Mallick S, Rath D, Parida KM, Characterization of novel Cs and K substituted phosphotungstic acid modified MCM-41 catalyst and its catalytic activity towards acetylation of aromatic alcohols, *J Chem Sci*, 2012, 124, 1117–1125
132. Dias JA, Caliman E, Dias SCL, Effects of cesium ion exchange on acidity of 12 tungstophosphoric acid. *Microporous Mesoporous Mater*, 2004, 76, 221–232
133. Izumi Y., Ogawa M., Urabe K., Alkali metal salts and ammonium salts of Keggin-type heteropoly acids as solid acid catalysts for liquid-phase Friedel–Crafts reactions. *Appl Catal A Gen*, 1995, 132, 127–140
134. Okuhara T., Nishimura T., Misono M., Novel Microporous Solid "Superacids":  $\text{Cs}_x\text{H}_{3-x}\text{PW}_{12}\text{O}_{40}$  ( $2 < x < 3$ ), 11 th International Congress on Catalysis - 40<sup>th</sup> Anniversary, *Studies in Surface Science and Catalysis*, 1996, 101, 581-590
135. Essayem N. et al, Acidic and catalytic properties of  $\text{Cs}_x\text{H}_{3-x}\text{PW}_{12}\text{O}_{40}$  heteropolyacid compounds, *Catalysis Letters*, 1995, 34 , 223-235
136. Bardin B.B., Davis R.J., Heteropolyacid and sulfated zirconia catalysts, *Topics in Catalysis*, 1998, 6, 77–86
137. Ezzat Rafiee et al, Cesium Salts of Phosphotungstic Acid: Comparison of Surface Acidity, Leaching Stability and Catalytic Activity for the Synthesis of  $\alpha$ -Ketoenol Ethers, *S. Afr. J. Chem.*, 2013, 66, 145–149

138. Shaimaa M. Ibrahim, Catalytic Activity and Selectivity of Unsupported Dodecatungstophosphoric Acid, and Its Cesium and Potassium Salts Supported on Silica, *Modern Research in Catalysis*, 2013, 2, 110-118
139. K. Narasimharao et al., Structure–activity relations in Cs-doped heteropolyacid catalysts for biodiesel production, *Journal of Catalysis*, 2007, 248, 226–234
140. Pesaresia L., Brown D.R., Lee A.F., Montero J.M., Williams H., Wilson K., Cs-doped  $H_4SiW_{12}O_{40}$  catalysts for biodiesel applications, *Applied Catalysis A: General*, 2009, 360, 50–58
141. Sujiao F et al, Catalytic Hydroxylation of Benzene to Phenol with Hydrogen Peroxide over Cesium Salts of Keggin-type Heteropoly Acids, *Acta Chim. Sinica*, 2012, 70, 2316-2322
142. Haider M.H., Dummer N. F., Zhang D., Miedziak P., Davies T. E., Taylor S. H., Willock D. J., Knight D. W., Chadwick D., Hutchings G. J., Rubidium- and caesium-doped silicotungstic acid catalysts supported on alumina for the catalytic dehydration of glycerol to acrolein, *Journal of Catalysis*, 2012, 286, 206–213
143. Li X. K., Zhao J., Ji W. J., Zhang Z. B., Chen Y., Au C. T., Hanc S., Hibst H., Effect of vanadium substitution in the cesium salts of Keggin-type heteropolyacids on propane partial oxidation, *J. Catal.*, 2006, 237, 58-66
144. Kamiya Y, Okuhara T, Misono M, Miyaji A, Tsuji K, Nakajo T. Catalytic Chemistry of Supported Heteropolyacids and Their Applications as Solid Acids to Industrial Processes, *Catal Surv from Asia*, 2008, 12, 101-113
145. Bhatt N., Patel A., Esterification of 1° and 2° alcohol using an ecofriendly solid acid catalyst comprising 12-tungstosilicic acid and hydrous zirconia, *J. Mol. Catal.*, 2005, 238, 223-228.
146. Guo X. et al , Effect of cesium content on the structure and catalytic performances of heteropoly compounds in one-step synthesis of methylmethacrylate from methacrolein, *Korean J. Chem. Eng.*, 2008, 25, 697-702
147. Langpape M., Millet J. M. M., Ozkan U. S., Boudeulle M., Study of Cesium or Cesium-Transition Metal-Substituted Keggin-Type Phosphomolybdic Acid as Isobutane Oxidation Catalysts: I. Structural Characterization, *J. Catal.*, 1999, 181, 8

148. Maris E. P., Davis R. J., Hydrogenolysis of glycerol over carbon-supported Ru and Pt catalysts. *J. Catal.*, 2007, 249 , 328–337
149. Montassier C., Ménézo J.C., Hoang L.C., Renaud C., Barbier J., Aqueous polyol conversions on ruthenium and on sulfur-modified ruthenium, *J. Mol. Catal.*, 1991, 70, 99-110
150. Wang K., Hawley M. C., Furney T. D., Mechanism Study of Sugar and Sugar Alcohol Hydrogenolysis Using 1,3-Diol Model Compounds, *Ind. Eng. Chem. Res.*, 1995, 34, 3766–3770
151. Auneau F., Michel C., Delbecq F., Pinel C., Sautet P., Unravelling the mechanism of glycerol hydrogenolysis over rhodium catalyst through combined experimental-theoretical investigations, *Chem. A Eur. J.*, 2011, 17, 50, 14288–14299
152. Ramachandran P. A., Chaudhari R. V., *Three Phase Catalytic Reactors*; Gordon and Breach Science Publishers: New York, 1983.
153. *Fundamentals of Reaction Engineering*, Rafael Kandiyoti, 2009
154. Wang M., Catalytic transformation of glycerol to 1-propanol by combining zirconium phosphate and supported Ru catalysts, *RSC Adv.*, 2016, 6, 29769-29778
155. Dasari M. A., *Catalytic Conversion of Glycerol and Sugar Alcohols to Value-Added Products*. Ph.D. Thesis, University of Missouri-Columbia, Columbia, MO, USA, 2006.
156. Karwowska B., Solid State Electrochemical Characterization of Tungsten Oxides and Related Heteropoly-12-Tungstic Acid Single Crystals, *Electroanalysis*, 1995, 7, 11, 1005-1009
157. Misono M. Heterogeneous Catalysis by Heteropoly Compounds of Molybdenum and Tungsten, *catal. Rev., Sci Eng*, 1987, 29, 269-321
158. Lan L.W., Li J., Chen Q.Y., Photocatalytic Properties for Photocatalytic Water Splitting of  $H_4SiW_{12}O_{40}/TiO_2$ , *Nonferrous Metals*, 2009, 3, 35-38
159. Chia M et al, Selective Hydrogenolysis of Polyols and Cyclic Ethers over Bifunctional Surface Sites on Rhodium–Rhenium Catalysts. *Journal of the American Chemical Society*, 2011, 133, 32, 12675-12689
160. Aramendía M. A. et al., Liquid-phase heterogeneous catalytic transfer hydrogenation of citral on basic catalysts. *Journal of Molecular Catalysis A: Chemical*, 2001, 171, 1-2, 153-158

161. Schlaf M., Selective deoxygenation of sugar polyols to  $\alpha,\omega$ -diols and other oxygen content reduced materials-a new challenge to homogeneous ionic hydrogenation and hydrogenolysis catalysis. *Dalton Transactions*, 2006, 39, 4645-4653
162. Braga T. P. et al., Gas-Phase Conversion of Glycerol to Acetol: Influence of Support Acidity on the Catalytic Stability and Copper Surface Properties on the Activity; *J. Braz. Chem. Soc.*, 2016, 00, 00, 1-11
163. Coll D. et al., Stability of intermediates in the glycerol hydrogenolysis on transition metal catalysts from first principles, *Phys. Chem. Chem. Phys.*, 2011, 13, 1448-1456
164. Dam J. T., Renewable Chemicals: Dehydroxylation of Glycerol and Polyols, *ChemSusChem*, 2011, 4, 1017 – 1034
165. Auneau F. et al., Unravelling the Mechanism of Glycerol Hydrogenolysis over Rhodium Catalyst through Combined Experimental–Theoretical Investigations, *Chem. Eur. J.*, 2011, 17, 14288 – 14299.
166. Wawrzetz A. et al., Towards understanding the bifunctional hydrodeoxygenation and aqueous phase reforming of glycerol, *J. Catal.*, 2010, 269, 411–420;
167. Gascon J et al., Amino-based metal-organic frameworks as stable, highly active basic catalysts, *Journal of Catalysis*, 261 (2009) 75-87.
168. Misono M. et al, catalysis by heteropoly compounds, successful design of catalysis, Amsterdam, Elsevier Science publisher, 1988, 267-278;
169. Misono M., Mizuno N., Katamura K., Kasai A., Konishi Y., Sakata K., Okuhara T., Yoneda Y., Catalysis by heteropoly compounds. III: The structure and properties of 12 heteropolyacids of molybdenum and tungsten and their salts pertinent to heterogeneous catalysis, *Bull. Chem. Soc Jpn.* 1982, 55, 400-406
170. Kozhevnikov I. V., Catalysis by Heteropoly Acids and Multicomponent Polyoxometalates in Liquid-Phase Reactions, *Chem. Rev.*, 1998, 98, 171-198
171. Liu L. et al. Supported  $H_4SiW_{12}O_{40}/Al_2O_3$  solid acid catalysts for dehydration of glycerol to acrolein: Evolution of catalyst structure and performance with calcination temperature / *Applied Catalysis A: General*, 2015, 489, 32–41
172. a. Hernández-Cortez J.G. et al, Study of acid–base properties of supported heteropoly acids in the reactions of secondary alcohols dehydration, *Catalysis Today*, 2014, 220–

- 222, 32– 38; b. D. Zhang et al., Dehydration of 1,2-propanediol to propionaldehyde over zeolite catalysts, *Applied Catalysis A: General*, 2011, 400, 148–155
173. Thomas A., Dablemont C., Basset J. M. , Lefebvre, F. Comparison of H<sub>3</sub>PW<sub>12</sub>O<sub>40</sub> and H<sub>4</sub>SiW<sub>12</sub>O<sub>40</sub> heteropolyacids supported on silica by <sup>1</sup>H MAS NMR, *C. R. Chim.*, 2005, 8, 1969–1974
174. Deltcheff C. R., Fournier M., Franck R. , Thouvenot R., Vibrational Investigations of Polyoxometalates. 2. Evidence for Anion-Anion Interactions in Molybdenum(VI) and Tungsten(VI) Compounds Related to the Keggin Structure, *Inorg. Chem.*, 1983, 22, 207-216
175. Ressler T., Timpe O., Girgsdies F., Wienold J., Neisius T., In situ investigations of the bulk structural evolution of vanadium-containing heteropolyoxomolybdate catalysts during thermal activation, *J. Catal.*, 2005, 231, 2, 279–291
176. Janik M.J., Bardin B.B., Davis R.J., Neurock M.A., A Quantum Chemical Study of the Decomposition of Keggin-Structured Heteropolyacids, *J. Phys. Chem. B*, 2006, 110, 9, 4170–4178
177. Watzenberger O., Emig G. , Lynch D. T , Oxydehydrogenation of isobutyric acid with heteropolyacid catalysts: Experimental observations of deactivation, *J. catal.* 1990, 124, 247-258
178. Rafiee, M. Joshaghani and P. Ghaderi-Shekhii Abadi, Synthesis and characterization of carbon@HPW core/shell nanorod using potato as a novel precursor: Efficient catalyst for C–N coupling reaction, *Arabian J. Chem.*, 2015
179. Biju M. Devassy et al., Zirconia-supported heteropoly acids: Characterization and catalytic behavior in liquid-phase veratrole benzoylation, *Journal of Catalysis*, 2005, 236, 313–323
180. Liu L., Wang B., Du Y., Zhong Z., Borgna A., Bifunctional Mo<sub>3</sub>VO<sub>x</sub>/H<sub>4</sub>SiW<sub>12</sub>O<sub>40</sub>/Al<sub>2</sub>O<sub>3</sub> catalysts for one-step conversion of glycerol to acrylic acid: Catalyst structural evolution and reaction pathways, *Appl. Catal., B*, 2015, 174–175, 1-12
181. a. Sawant-Dhuri D., Balasubramanian V. V., Ariga K., Park D. H., Choy J. H., Cha W. S., Al-deyab S. S., Halligudi S. B., Vinu A., Titania Nanoparticles Stabilized HPA in SBA-15 for the Intermolecular Hydroamination of Activated Olefins, *ChemCatChem*,

- 2014, 6, 3347; b. T. Okuhara, N. Mizuno, M. Misono, *Catalytic Chemistry of Heteropoly Compounds*, *Adv. Catal.*, 1996, 41, 113
182. Parida K.M., Mallick S., Silicotungstic acid supported zirconia: An effective catalyst for esterification reaction, *Journal of Molecular Catalysis A: Chemical*, 2007, 275, 77–83
  183. Phuruangrat A, Ham DJ, Hong SJ, Thongtem S, Lee JS. Synthesis of hexagonal WO<sub>3</sub> nanowires by microwaveassisted hydrothermal method and their electrocatalytic activities for hydrogen evolution reaction, *J. Mater. Chem.*, 2010, 20, 1683-1690
  184. Zhao Y, Fan H, Li W, Bi L, Wang D, Wu L. Incorporation of polyoxotungstate complexes in silica spheres and in situ formation of tungsten trioxide nanoparticles. *Langmuir.*, 2010, 26, 18, 14894–14900
  185. Bai S et al, Synthesis mechanism and gas-sensing application of nanosheet-assembled tungsten oxide microspheres, *J. Mater. Chem. A*, 2014, 2, 7927–7934
  186. Katumba G, Mwakikunga BW. FTIR and Raman spectroscopy of carbon nanoparticles in SiO<sub>2</sub>, ZnO and NiO matrices. *Nanoscale Res Lett.*, 2008, 3, 11, 421–426
  187. Priya S.S et al, Metal–acid bifunctional catalysts for selective hydrogenolysis of glycerol under atmospheric pressure: A highly selective route to produce propanols, *Applied Catalysis A: General*, 2015, 498, 88–98
  188. Mauriello F., Ariga H., Musolino M.G., Pietropaolo R., Takakusagi S., Asakura K., Exploring the catalytic properties of supported palladium catalysts in the transfer hydrogenolysis of glycerol. *Appl. Catal. B*, 2015, 166–167, 121–131
  189. A. Laurance B, Bright NPRA Annual meeting, Am-91 53, 1995; B. Wang J. S., Li B. L., Xu X. Z., Ke, X. M., High metal tolerance matrix for FCC catalyst, *Fluid cracking catalyst*, 111-119; C. Travers C., Isomerization of light paraffins, *Petroleum refining*. Vol.3. Conversion Processes.
  190. Shi C., Wang R., Zhu G., Qiu S., Long J., Synthesis, characterization, and catalytic properties of SiPW-X mesoporous silica with heteropolyacid encapsulated into their framework, *European Journal of Inorganic Chemistry*, 2005, 4801-4807
  191. Dufaud V., Lefebvre F., Niccolai G.P., Aouine M., New insights into the encapsulation and stabilization of heteropolyacids inside the pore walls of mesostructured silica materials, *Journal of Materials Chemistry*, 2009, 19, 1142-1150

192. Atia H., Armbruster U., Martin A., Dehydration of glycerol in gas phase using heteropolyacid catalysts as active compounds. DGMK Tagungsbericht, 2008. 2008-3 (Preprints of the DGMK-Conference "Future Feedstocks for Fuels and Chemicals"), 2008, 177-184.
193. Beck J. S., Vartuli J. C., Roth W. J., Leonowicz M. E., Kresge C. T., Schmitt K. D., Chu C. T-W., Olson D. H., Sheppard E. W., McCullen S. B., Higgins J. B., Schlenker J. L., "A new family of mesoporous molecular sieves prepared with liquid crystal templates", *Journal of American Chemical Society*, 1992, 27, 10834-10843
194. Liu Q., Wu W., Wang J., Ren X., Wang Y., "Characterization of 12-tungstophosphoric acid impregnated on mesoporous silica SBA-15 and its catalytic performance in isopropylation of naphthalene with isopropanol", *Microporous and Mesoporous Materials*, 2004, 76, 51-60
195. Jha A., Garade A. C., Mirajkar S. P., Rode C. V., MCM-41 supported phosphotungstic acid for the hydroxyalkylation of phenol to phenolphthalein *Ind. Eng. Chem. Res.*, 2012, 51, 3916
196. Kozhevnikov I.V., Sinnema A., Jansen R.J.J., Pamin K., Bekkum H., New acid catalyst comprising heteropoly acid on a mesoporous molecular sieve MCM-41, *Catal. Lett.*, 1994, 30, 241-252
197. Satterfield C.N., *Heterogeneous Catalysis in Industrial Practice*, 2nd ed., McGraw-Hill, New York, 1991, p. 123
198. Arco M. del, Caballero A., Malet P., Rives V., Effect of consecutive and alternative oxidation and reduction treatments on the interactions between titania (anatase and rutile) and copper, *J. Catal.*, 1998, 113, 120-128
199. Lingaiah N. et al, Influence of Vanadium Location in Titania Supported Vanadomolybdophosphoric Acid Catalysts and Its Effect on the Oxidation and Ammoxidation Functionalities, *J. Phys. Chem. C* 2008, 112, 8294–8300
200. Rosa María Ladera et al., TiO<sub>2</sub>-supported heteropoly acid catalysts for dehydration of methanol to dimethyl ether: relevance of dispersion and support interaction, *Catal. Sci. Technol.*, 2015, 5, 484–491



201. Ladera R. M., Fierro J. L. G., Ojeda M. and Rojas S., TiO<sub>2</sub>-supported heteropoly acids for low-temperature synthesis of dimethyl ether from methanol, *J. Catal.*, 2014, 312, 195–203
202. Thamaphat K., Phase Characterization of TiO<sub>2</sub> Powder by XRD and TEM, *Kasetsart J. (Nat. Sci.)*, 2008, 42, 357 - 361
203. Buck E. C., Arey B. W., Fiskum S. K., Geeting J. G. H., Jenson E. D., McNamara B. K., Poloski A. P., Identification of Washed Solids from Hanford Tanks 241-AN-102 and 241-AZ-101 with X-Ray Diffraction, Scanning Electron Microscopy, and Light-Scattering Particle Analysis, WTP Project Report, 2003
204. Park H., Yun Y. S., Kim T. Y., Lee K. R., Baek J., J. Kinetics of the dehydration of glycerol over acid catalysts with an investigation of deactivation mechanism by coke, *Applied Catalysis B: Environmental*, 2015, 176, 1–10
205. Kim Y.T., You S.J., Jung K.D., Park E.D., Effect of Al Content on the Gas-Phase Dehydration of Glycerol over Silica-Alumina-Supported Silicotungstic Acid Catalysts, *Bull. Korean Chem. Soc.*, 2012, 33, 2369–2377
206. Bühler W., Dinjus E., Ederer H.J., Kruse A., Mas C., J. Y, *Supercrit. Fluids*, 2002, 22, 37–53
207. Tsukuda E., Sato S., Takahashi R., Sodesawa T., Production of acrolein from glycerol over silica-supported heteropoly acids, *Catal. Commun.*, 2007, 8, 1349–1353
208. Yun D., Yun S., Kim T. Y., Park H., Lee J. M., Han J. W., Yi J., Mechanistic study of glycerol dehydration on Brønsted acidic amorphous aluminosilicate, *Journal of Catalysis*, 2016, 341, 33–43
209. Jia Wang, Xiaochen Zhao, Nian Lei, Lin Li, Leilei Zhang, Shutao Xu, Shu Miao, Xiaoli Pan, Aiqin Wang, Tao Zhang, Hydrogenolysis of Glycerol to 1,3-propanediol under Low Hydrogen Pressure over WO<sub>x</sub>-Supported Single/Pseudo-Single Atom Pt Catalyst, *ChemSusChem*, 2016, 9, 784 – 790

## Appendix A Literature Data

**Table A-1 Summary of Reported Catalysts and Reaction Conditions for Converting Glycerol into 1,3-PD in batch reactor**

	Catalyst	Catalyst loading, wt%	Glycerol content,	Temp. oC	Press. Mpa	React. Time, h	Conv %	Selectivity			Reference
								1,3PD	1,2PD	1-PO	
1	Cu/SiO <sub>2</sub>	0.6	40(n-	240	8	5	20	2	92	-	Vasiliadou
2	5Pt-Re/CNTs	14μmol	1	170	4	8	55	26	52	26.0	Chenghao
3	Ir-ReOx/SiO <sub>2</sub>	3.75	66.7	120	8	24	38.6	59	9.4	24.4	Tamura M., (2014)
	Ir-ReOx/SiO <sub>2</sub>	None H <sub>2</sub> SO <sub>4</sub>					9.4	66.2	11.9	15.8	
		H+/Ir = 1					23	57.7	7.9	27.0	
4	1Ru/SBA-15(H2-500)	3.75	40	160	8	8	4	7.2	44	19.8	Li Y. et al., (2014)
	5Ru/SBA-15(Air-300/H2-300)						12.4	4.1	29	21.8	
5	Ru/Al <sub>2</sub> O <sub>3</sub>	3.75 Ru/Al <sub>2</sub> O <sub>3</sub> ,	40	160	8	8	18	1.7	30.5	17.7	Li Y. et al., (2014)
	Ru/HZSM5(360)	3.75					19	4	27.2	28.0	
	Ru/Al <sub>2</sub> O <sub>3</sub> + HZSM5(25)	3.75 Ru/Al <sub>2</sub> O <sub>3</sub> ,		120			6.4	6.2	36	20.4	
6	5Pd-5Re/Al <sub>2</sub> O <sub>3</sub>	3.75	40	200	8	18	23.6	13.6	54.5	26.6	Li Y. et al., (2014)
	5Pd/Al <sub>2</sub> O <sub>3</sub>						3.3	9.9	63.3	19.3	
7	Pt/Ti <sub>100</sub> W <sub>0</sub>	25	10	180	5.5	12	7.8	7.2	83	9.6	Zhang Y., (2013)
	Pt/Ti <sub>90</sub> W <sub>10</sub>						18.4	40.3	13.7	32.5	
	Pt/Ti <sub>80</sub> W <sub>20</sub>						24.2	33.5	11.6	36.6	
	Pt/Ti <sub>50</sub> W <sub>50</sub>						6.7	40.9	7.2	44.3	
8	Pt/Al <sub>2</sub> O <sub>3</sub> +STA	0.5mol%		200	4	18	49	28	3	31.0	Dam J.T.,
9	Pt/WO <sub>x</sub> /AlOOH	108.6	3	180	5	12	100	66	2	11.0	Arundhathi
	Pt/TiO <sub>2</sub>						24	0	61.8	6.2(1+2)	

10	Pt/Al <sub>2</sub> O <sub>3</sub>	22	4.5	210	6	6	10	12.1	33.8	2.6	Delgado S. N., (2013)
11	PtAlO <sub>x</sub> /WO <sub>3</sub>	108.6	3	180	3	10	90	44	2.2	37.8	Mizugaki T., (2012)
	PtMnO <sub>x</sub> /WO <sub>3</sub>						87	33	1.14	48.3	
	PtZrO <sub>x</sub> /WO <sub>3</sub>						87	33	3.45	48.3	
12	Ir-ReO <sub>x</sub> /silica-alumina	3.75	20	120	8	24	31.5	59.8	13.3	17.7	Nakagawa
13	Rh-MoO <sub>x</sub> /SiO <sub>2</sub>	1.4	20	120	8 (initial)	4	7.1	9.6	41	34.0	Koso S. et al., (2012)
	Rh-ReO <sub>x</sub> /SiO <sub>2</sub>						9.7	21	32	31.0	
14	Pt/m-WO	10	25	180	5.5	12	18	39.3	4.1	33.8	Longjie L., (2012)
	Pt/c-WO <sub>3</sub>						4.5	29.9	14.1	23.6	
15	Pt-Sulfated ZrO <sub>2</sub>	12	57 (water)	170	7.3 (initial)	24	62.9	12.3	32.1	0.0	Jinho Oh (2011)
	Pt-Sulfated ZrO <sub>2</sub>		57 (in DMI)				66.5	55.6	2.9	0.0	
	Fe-Sulfated ZrO <sub>2</sub>						51.4	13.8	0	0.0	
	Mn-Sulfated ZrO <sub>2</sub>						56.4	14.5	0	0.0	
	Pt/STA/ZrO <sub>2</sub>						50.2	17.2	5.4	0.0	
	Pt/PTA/ZrO <sub>2</sub>						48.4	15.4	3.8	0.0	
16	Pt/WO <sub>3</sub> /TiO <sub>2</sub> /SiO <sub>2</sub>	2ml/40ml	10	180	5.5	12	15.3	50.5	9.2	25.1	Gong L.,
17	Ir-ReO <sub>x</sub> /SiO <sub>2</sub>	3.75 + H <sub>2</sub> SO <sub>4</sub>	80	120	8	24	62.8	49	10	33.0	Nakagawa
18	Pt-Re/C Sintered (5.7 wt% Pt,	Substrate/	1	170	4		20	34	33	22.0	Daniel O.M.
19	Ru-Re/SiO <sub>2</sub> -r450	4	40	160	8		23.8	13.6	51.1	23.0	Ma L. (2010)
	Ru-Re/SiO <sub>2</sub> -r200						51	8.3	49.1	26.1	
20	Pt/WO <sub>3</sub> /ZrO <sub>2</sub>	10		170	5.5	Ethanol-	45.7	21.2	8	32.1	Leifeng G. et al., (2009)
						Ethanol	38.2	23	13.6	46.6	
						Water	24.7	25.7	15	21.3	
21	2Pt/19.6WO <sub>3</sub> /ZrO <sub>2</sub>	36		170		18	86	28	14.5	32.0	
	2Pt/19.6WO <sub>3</sub> /Al <sub>2</sub> O <sub>3</sub>						44	30	25	26.4	

	<b>Pt/WO<sub>3</sub>/TiO<sub>2</sub></b>		57 (in		8		16.9	38.4	42	30.2	Kurosaka
22	<b>5% Rh/Cs<sub>2.5</sub>H<sub>0.5</sub>[PW<sub>12</sub>O<sub>40</sub>]</b>	20	20	180	0.5	10	6.3	7.1	65.4	27.5	Alhanash A., (2008)
	<b>5% Ru/Cs<sub>2.5</sub>H<sub>0.5</sub>[PW<sub>12</sub>O<sub>40</sub>]</b>						23	0	73.6	4.3	
23	<b>Rh/SiO<sub>2</sub> + Amberlystb</b>	3.75	20	120	8	10	14.3	9.8	26	42.2	Furikado I.
24	<b>Ru/C+Amberlyst</b>	4+8%amberlyst	20	120	8	10	12.9	4.9	55.4	14.1	Miyazawa T., (2006)
	<b>Rh/C+Amberlyst</b>						3	9	32.7	40.4	
25	<b>Rh/C</b>	20	4	initial	8	10	0.3	3.4	58.6	0.0	Kusunoki Y. (2005)
	<b>Rh/C + H<sub>2</sub>WO<sub>4</sub></b>			180			1.3	20.9	56.7	10.4	
26	<b>Rh/C (5%)</b>	0.3 + H <sub>2</sub> WO <sub>4</sub>	19%	180	8	168	32	12	6	80.0	Chaminand J. et al. (2004)
	<b>Rh/Al<sub>2</sub>O<sub>3</sub> (5%)</b>		19% in				27	12	45	-	
	<b>Rh/C (5%)</b>		water				21	6	70	-	
	<b>Rh/HY (3.5%)</b>						3	0	0	100.0	

**Table A-2 Summary of Reported Catalysts and Reaction Conditions for Converting Glycerol into 1,3-PD in fix-bed reactor**

	Catalyst	Catalyst loading,	Glycerol w %	Temp. °C	H <sub>2</sub> flow rate,	Press. Mpa	Conv. %	Selectivity, %			Reference
								1,3-PD	1,2-	1-PO	
1	<b>3Ru/MCM-41</b>	0.5		230	140		62	20	38	13.0	Vanama
2	<b>5PtW/ZrSi</b>	3	10	180	100	5	54.3	52	6.8	34.0	Zhu S.,
3	<b>Pt-STA/ZrO<sub>2</sub></b>	2	10	180	100	5	24.1	48.1	16.5	21.8	Zhu S.,
4	<b>Pt-STA/ZrO<sub>2</sub></b>	2	10	180	100	5	26.7	38.9	9.2	39.9	Zhu S., (2013)
	<b>Pt-LiSiW/ZrO<sub>2</sub></b>						43.5	53.6	14.2	24.1	
	<b>Pt-KSiW/ZrO<sub>2</sub></b>						24	36.8	22	27.4	
	<b>Pt-RbSiW/ZrO<sub>2</sub></b>						16.6	31.6	25.4	28.9	
	<b>Pt-CsSiW/ZrO<sub>2</sub></b>						41.2	40.2	20.5	30.2	
5	<b>Pt-STA/ZrO<sub>2</sub></b>	4	10	200	100	5	99.7	0.9	5.1	80.0	Zhu S., (2012)
	<b>Pt-STA/ZrO<sub>2</sub>+1%</b>						90.1	3.8	8.8	72.5	
	<b>Pt-HPW/ZrO<sub>2</sub></b>						92.4	8.6	9.2	65.2	
	<b>Pt-WO<sub>3</sub>/ZrO<sub>2</sub></b>						90.7	9.3	8.7	64.0	
	<b>Pd-STA/ZrO<sub>2</sub></b>						25.3	10.9	49.2	27.4	
	<b>Pt-STA/ZrO<sub>2</sub></b>			180			85.2	22.1	5.7		
6	<b>Pt-15STA/SiO<sub>2</sub></b>	4	10	200	100	6	81.2	38.7	20	28.0	Zhu S.,
7	<b>CuZnTi(2-2-1)</b>		20	280	25	0.1	100	9	2		Feng Y. et
8	<b>3.0Pt/WZ10</b>	2ml	60	130	10	4	70.2	45.6	2.6	44.2	Qin L. Z.,
9	<b>10Cu-15STA/SiO<sub>2</sub></b>	8	100	210		0.54	83.4	32.1	22.2	-	Huang L.,

**Table A-3 Summary of Reported Catalysts and Reaction Conditions for Converting Glycerol into 1-propanol**

	Catalyst	React., conten	Cat. loading, wt%	Condition			Conv	Selectivity			Reference			
				T,	MPa	Time,		1-PO	1,3P	1,2P				
1	Raney Cu	GL	2.5	18	initia	6	12.4	50.5		5.5	Yue			
	Raney Cu/Al <sub>2</sub> O <sub>3</sub>			0	11		16.3	81 (1,2PP)	0	7.3	C.J.(2014)			
2	3Ru/MCM-41	GL		23			fix bed	62	13	20	38	P.K.		
3	5Pt-Re/CNTs				17	4	8		55	26	15	52	Chenghao	
4	2.5PtW/ZrSi	GL	3g	18	5		fix bed	41.5	35.3	46.3	9.8	Shanhui		
5	Ru(0.9)-Ir-		4	12	8	24		77.9	43.7	38.9	6	Masazumi		
6	5% Ru/HY	GL		20	4	4		10.3	3.4	0	77.4	Jin S. (2014)		
	5% Ru/HY-0.5H			0			17.9	2.9	78.5					
7	5Pd-5Re/SBA-15	GL	4	20	8	18		40.7	24.6	8.2	59.9	Yuming Li (2014)		
	5Pd/SBA-15							1.5	14.6	4.4	72.2			
	5Re/SBA-15	GL						3.1	38.7	6.7	49.6			
	5Pd-5Re/CNTs						49.6	30	8.2	52.5				
8	Cu/boehmite	GL	5	20	4	6		77.5	6.1		92.5	Z. Wu (2013)		
	Cu/γ-Al <sub>2</sub> O <sub>3</sub>							54.2	15.7		81.2			
	Cu/SiO <sub>2</sub>	GL						0		51.7	9.8			88.7
	Ru/C								55.7	5.8			59.4	
9	Pt/WO <sub>x</sub> /AlOOH	GL	BET SSA 123					100	18	37	2	Arundhathi R., (2013)		
	Pt/WO <sub>x</sub> /AlOOH		BET SSA 56					100	32	37	1			
10	Pt-STA/ZrO <sub>2</sub>	GL		18	5		fix bed	26.7	39.9	38.9	9.2	Zhu S. (2013)		
	Pt-CsSiW/ZrO <sub>2</sub>			0				41.2	30.2	40.2	20.5			
11	Pt/Al <sub>2</sub> O <sub>3</sub> +STA	GL	0.5mol%	20	4	18		49	30	28	7	Dam J.T. (2013)		
	Pt/SiO <sub>2</sub> +STA							10	73	10	5			

12	Pt-H <sub>4</sub> SiW <sub>12</sub> O <sub>40</sub> /SiO <sub>2</sub>	GL	4g	20	5		In fix bed	88.5	36.9	27.2	24.8	Zhu
13	PtAlO <sub>x</sub> /WO <sub>3</sub>	GL	108.6	18	3	10		90	34	40	2	Mizugaki
	Pt/WO <sub>3</sub>			0				75	47	21	1	T. (2012)
14	Pt/m-WO		25	18	5.5	12		18	33.8	39.3	4.1	Longjie L.
15	NiSiO <sub>2</sub>	GL	8.5 g + carborundum	32	6		In fix bed	99.9	42.8	0.6	4.6	Ryneveld
	NiAlO <sub>3</sub>			0				96.1	35.5	2.2	1.8	E. V.(2011)
16	Homogenous Ru	GL		20	3.45	24	water-		18 yield			Michelle E.
17	Pt/WO <sub>3</sub> /TiO <sub>2</sub> /SiO <sub>2</sub>	GL		18	5.5			15.3	25.1	50.5	9.2	Gong L.
	Pt/WO <sub>3</sub> /TiO <sub>2</sub>						7.5	28.2	43.7	11.7	(2010)	
18	Pt-Re/C			17	4	24		33	41	25	20	O.M.
19	Ru-Re/SiO <sub>2</sub> -r200	GL	4	16	8			51	26.1	8.3	49.1	Ma
20	Rh-ReOx/SiO <sub>2</sub>	GL	4	12	8	5		79	35.3	13.8	38	Shinmi Y.
	Rh-MoOx/SiO <sub>2</sub>			12	8	5		44.1	49	5.6	30.4	(2010)
21	Pt/WO <sub>3</sub> /ZrO <sub>2</sub>	GL		17	5.5		Ethanol	38.2	46.6	23	13.6	Leifeng G.
22	Pt/WO <sub>3</sub> /ZrO <sub>2</sub>	GL		17	initia	12	Ethanol	38.2	46.6	23	13.6	Leifeng
				0	1 5.5			Ethanol-	45.7	32.1	21.2	8
23	Ru/Al <sub>2</sub> O <sub>3</sub>	GL	5	24	8	5		69	45 (1+2PrP)	0.7	37.9	Vasiliadou
24	[Ru(OH <sub>2</sub> ) <sub>3</sub> (4'-			25	5.5	24		100	35			Taher
25	Pt/WO <sub>3</sub> /ZrO <sub>2</sub>	GL	36.2	17	8	18	DMI	85.8	32.1	28.2	14.6	Kurosaka
	Rh/WO <sub>3</sub> /ZrO <sub>2</sub>			0				86.4	26.3	5.4	32.6	T.(2008)
26	Ru/C +Amberlyst	GL		12	8			12.9	14.1	4.9	55.4	Miyazawa
				14				40.7	18.2	1	43.1	T.(2006)
				20				6.5	19.9	1.5	74.1	
27	Rh_ReOx/SiO <sub>2</sub>	GL	4	12	initia	24		100	76		3	Amada Y.
	(Re/Rh=0.5)	1,2PD	4	12	8	48	water	98.2	68			(2010)
		GL	37.5	12	8	10	Water	29.3	41.3	5.4	22.6	

28	<b>Rh/SiO<sub>2</sub> (G-6) + Amberlyst</b>	1,2PD						17.5	56.5			Furikado I. (2007)	
		1,3PD						22.6	68.2				
	<b>Ru/C+ Amberlyst</b>	GL						38.8	28.9	0.8	28.8		
		1,2PD						6.3	28.2				
		1,3PD					77.7	32.8					
29	<b>Ir-ReOx/SiO<sub>2</sub>, H<sub>2</sub>SO<sub>4</sub>, (H+/Re = 1), Re:Ir=2</b>	GL	4	12 0	8	12		58.6	40.7	44.8	5.4	Amada Y. (2011)	
		1,2PD						2	46.9	87			
		1,3PD						2	10	93			
30	<b>Ir-ReOx/SiO<sub>2</sub> (Re/Ir = 1), sulfuric, acid (H+/Ir = 1)</b>	GL	4	12 0	8	24		62.8	33	49	10	Nakagawa Y.(2010)	
		1,2PD							71.7	85			
		1,3PD							22.6	>99			
31	<b>Pt-H<sub>4</sub>SiW<sub>12</sub>O<sub>40</sub>/ZrO<sub>2</sub></b>	GI10%	4g	20 0	5		In fix bed	99.7	80	0.9	5.1	Zhu S.(2012)	
		1,2PD							100	84.9			
		1,3PD							92.6	95.4			
	<b>Ni-STA/ZrO<sub>2</sub></b>	GI						24.7	16.1	5.7	52.6		
								<b>Cu-STA/ZrO<sub>2</sub></b>	15.2	11.3	7.2		70.9
32	<b>4.0Pt/WZ10</b>	GL	2ml	13 0	4	24	In fix bed	84.5	66.5	26.4	0.7	Qin L.Z. (2010)	
								41.6	44.2	44	3.6		
	1,2PD							78.3	90.7				
	1,3PD							22	99.9				
33	<b>Pt/SiO<sub>2</sub>-Al<sub>2</sub>O<sub>3</sub></b>	20%G	166	22	4.5	24		19	53.8(1+2Pr)	4.5	31.9	Gandarias I. (2010)	
		L		24				87.6	59.7	0.7	11.2		
		1,2-						12.9	92.9(1+2PP)				
		1,3-						10.5	98(1+2PP)				
34	<b>Rh-ReOx/SiO<sub>2</sub></b>	20%G	4		8	5		79	32.9	14	41.5		
	<b>Rh-ReOx/SiO<sub>2</sub></b>	100%						15	16.3	28	51.2		



	<b>Rh-ReOx/SiO<sub>2</sub></b> <b>(Re/Rh = 0.5)</b>	20GL		12		2		38.4	26.7	16.1	46.9	Shimao A. (2009)	
		1,2PD		0				14	81.7				
		1,3PD						11.8	97.9				
35	<b>Ru/Al<sub>2</sub>O<sub>3</sub></b>	GL,		16	8	8		18	17.7	1.7	30.5	Yuming Lia, (2014)	
	<b>Ru/Al<sub>2</sub>O<sub>3</sub> +</b>	4%		0				30.5	19.1	1.6	20.9		
	<b>Ru/Al<sub>2</sub>O<sub>3</sub></b>	1,2PD				3		2.3	11.9				
		1,3PD				3		5.8	16.8				
36	<b>Pt-HPW/ZrO<sub>2</sub></b>	Gl	2	18	5	12		25.5	37.9	32.9	10.9	Zhang Y.(2013)	
	<b>Pt-STA/ZrO<sub>2</sub></b>	Gl						24.1	21.8	48.1	16.5		
	<b>Pt-STA/ZrO<sub>2</sub></b>	1,2-						47.1	85.2				
	<b>Pt-STA/ZrO<sub>2</sub></b>	1,3-						9.1	96.5				
37	<b>Ir- ReOx/SiO<sub>2</sub>+H<sub>2</sub>SO<sub>4</sub></b>	GL20	4	12	8	24		61.1	36.6	43.2	9.2	Nakagawa Y.(2012)	
		1,2-				4		38.9	89.7				
		1,3-						4	99.1				
	<b>Ir-</b>						69.3	43.6	39	7			
38	<b>Ru/C + Amberlyst</b>	GL	4+8%amberly st	12	8	10		38.8	28.9	28.8	0.8	Miyazawa T.(2006)	
		1,2PD		0					6.3	28.2			
		1,3PD							77.7	31			
39	<b>Rh/C + Amberlyst</b>	20		14				64	53.2	7.2	19.5	Kusunoki Y. (2005)	
	<b>Ru/C + Amberlyst</b>	GL	4	12	8	10		12.9	14.1	4.9	55.4		
		1,2PD		0					3.5	55.8			
		1,3PD							12.8	27.7			
40	<b>Homogeneous Ru</b>	1,2PD		11	5.2	72	HBf <sub>4</sub> ·Et <sub>2</sub>	85	10			Schlaf M.	

## Appendix B GC Calibration Curve

Compound	1-PO	1-Butanol	Ac.	1,2-PD	EG	1,3PD	1,4-Buta-diol	Glycerol
Retention Time (min)	2.129	2.788	4.57	9.165	10.09	15.61	22.35	32.23
Response Factor	0.795	-	1.555	1.257	1.676	1.232	1.0	1.651

1-PO							
Entry	m <sub>1-PO</sub> , mg	A <sub>1-PO</sub>	mis, mg	A <sub>is</sub>	A <sub>1-PO</sub> /A <sub>is</sub>	m <sub>ac</sub> /mis	y/x
1	33.7	3104.5	25	1949.78	1.59	1.35	0.847
2	60.1	5702.6	25	1968.70	2.90	2.40	0.829
3	101.7	10113.0	25	1946.54	5.20	4.07	0.783
4	152.4	15302.6	25	2000.65	7.65	6.11	0.799
5	202.2	19708.3	26	1956.05	9.82	7.78	0.792
Acetol							
Entry	m <sub>Ac</sub> , mg	A <sub>Ac</sub>	mis, mg	A <sub>is</sub>	A <sub>Ac</sub> /A <sub>is</sub>	m <sub>ac</sub> /mis	y/x
1	44.3	2173.5	25	1949.78	1.09	1.77	1.634
2	87.9	4455.7	25	1968.70	2.29	3.52	1.537
3	133.5	6765.1	25	1946.54	3.38	5.34	1.579
4	175.9	8740.5	25	2000.65	4.44	7.04	1.585
5	227.1	11921.3	25	1956.05	5.94	9.08	1.530
1,2-PD							
Entry	m <sub>1,2-PD</sub> , mg	A <sub>1,2-PD</sub>	mis, mg	A <sub>is</sub>	A <sub>1,2-PD</sub> /A <sub>is</sub>	m <sub>ac</sub> /mis	y/x
1	56.1	3135.3	25	1949.78	1.61	2.24	1.395
2	107.2	6281.6	25	1968.70	3.19	4.30	1.346
3	155.7	9506.8	25	1946.54	4.88	6.22	1.273
4	204.6	12975.7	25	2000.65	6.49	8.18	1.262

5	303.7	19200.3	25	1956.05	9.82	12.15	1.238
6	602.1	38403.5	25	2005.18	19.15	24.08	1.258
<b>EG</b>							
Entry	m <sub>EG</sub> , mg	A <sub>EG</sub>	mis, mg	A <sub>is</sub>	A <sub>EG</sub> /A <sub>is</sub>	m <sub>EG</sub> /mis	y/x
1	33.0	1453.1	25	1949.78	0.75	1.32	1.771
2	51.8	2396.7	25	1968.70	1.22	2.07	1.702
3	86.1	3992.9	25	1946.54	2.05	3.44	1.679
4	125.9	5973.4	25	1956.05	3.03	5.04	1.664
<b>1,3-PD</b>							
Entry	m <sub>1,3-PD</sub> , mg	A <sub>1,3-PD</sub>	mis, mg	A <sub>is</sub>	A <sub>1,3-PD</sub> /A <sub>is</sub>	m <sub>1,3-PD</sub> /mis	y/x
1	28.6	1789.0	25	1949.78	0.92	1.14	1.247
2	53.2	3399.9	25	1968.70	1.73	2.13	1.232
3	79.6	5137.0	25	2000.65	2.57	3.18	1.240
4	103.7	6457.0	25	1946.54	3.32	4.15	1.250
5	155.5	10233.5	25	1956.05	5.09	6.22	1.222
<b>Glycerol</b>							
Entry	m <sub>GL</sub> , mg	A <sub>GL</sub>	mis, mg	A <sub>is</sub>	A <sub>GL</sub> /A <sub>is</sub>	m <sub>GL</sub> /mis	y/x
1	49.5	2195.7	25	2000.65	1.10	1.98	1.804
2	103.3	4611.2	25	1946.54	2.37	4.13	1.744
3	151.3	7012.5	25	1968.70	3.56	6.05	1.699
4	202.3	9293.1	25	1949.78	4.77	8.09	1.698
5	303.9	14513.7	25	1956.05	7.42	12.16	1.638
6	602.4	29275.7	25	1996.32	14.66	24.10	1.643

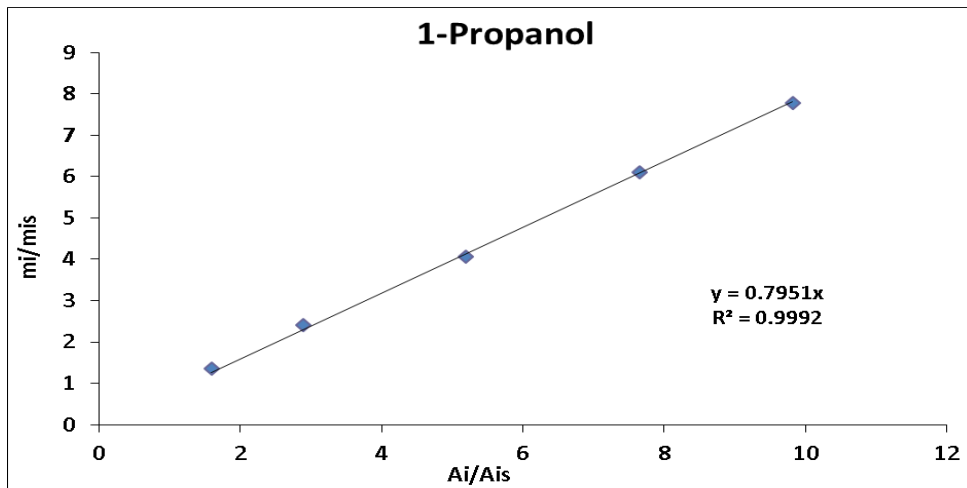


**Figure B-1** Calibration Curve for Propanol

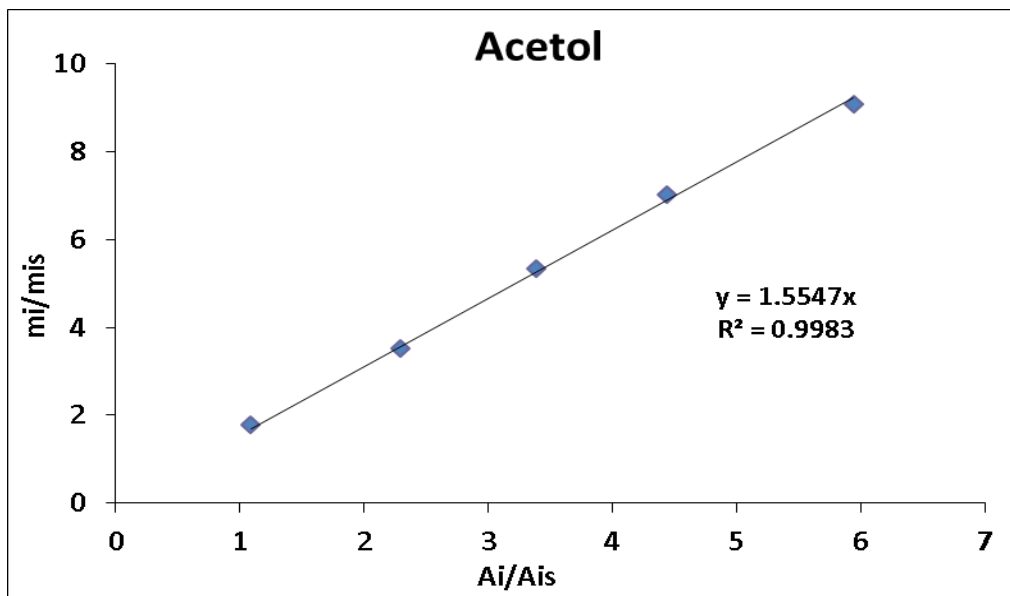


**Figure B-2** Calibration Curve for Acetol.

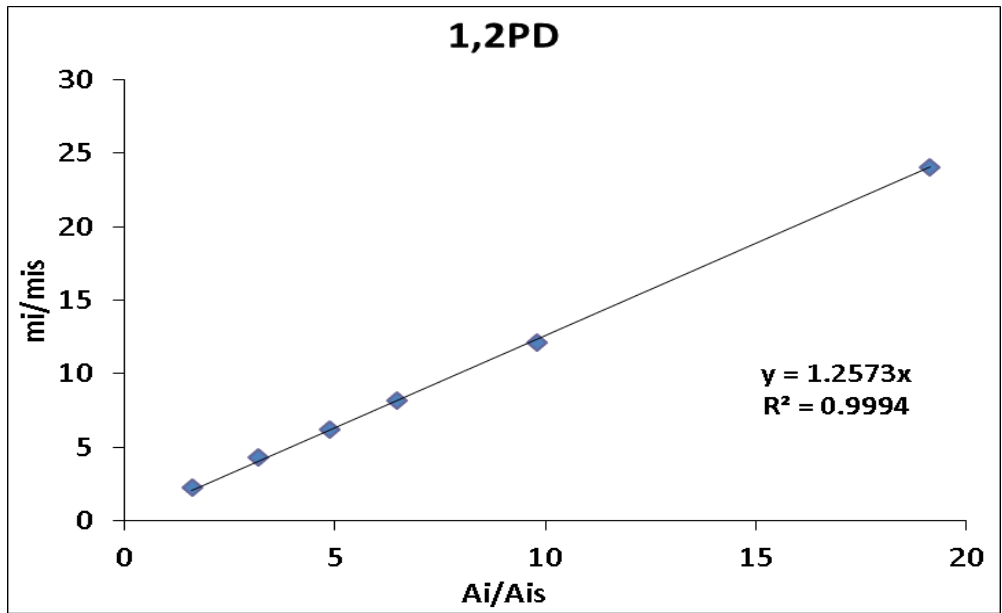


**Figure B-3 Calibration Curve for 1,2-PD**

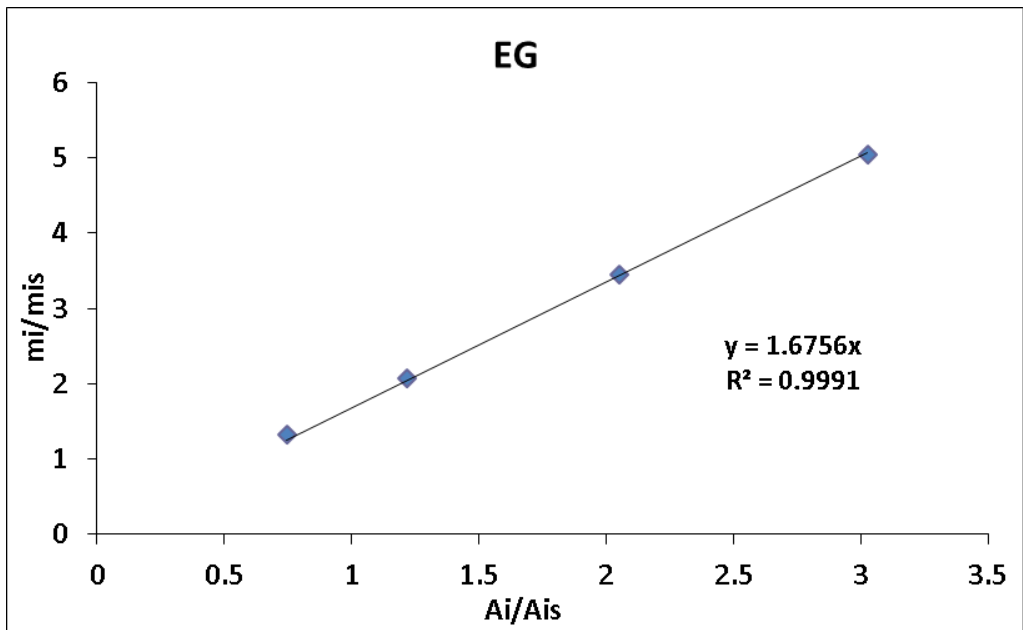


**Figure B-4 Calibration Curve for EG.**

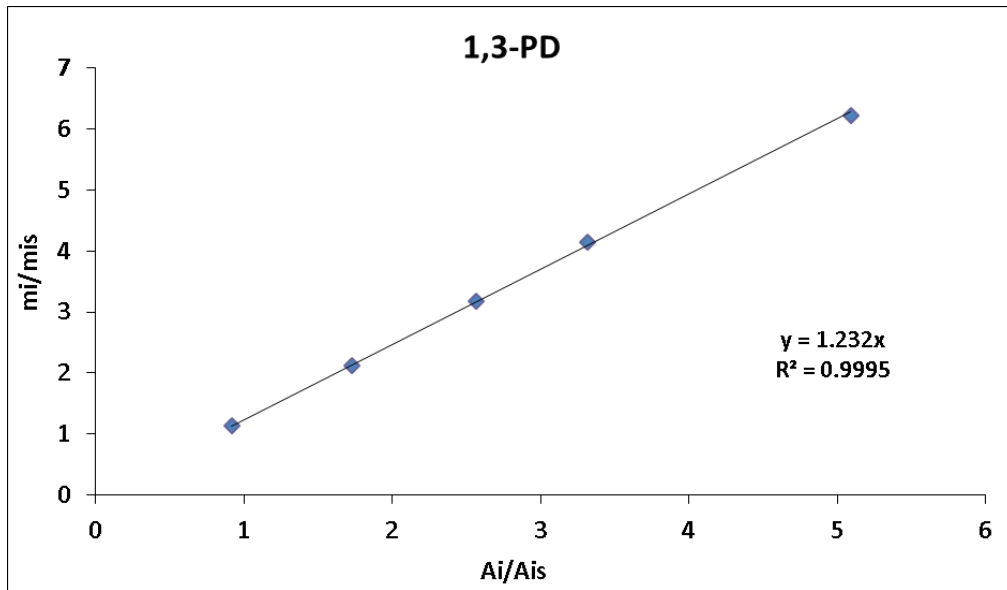


**Figure B-5** Calibration Curve for 13PD.

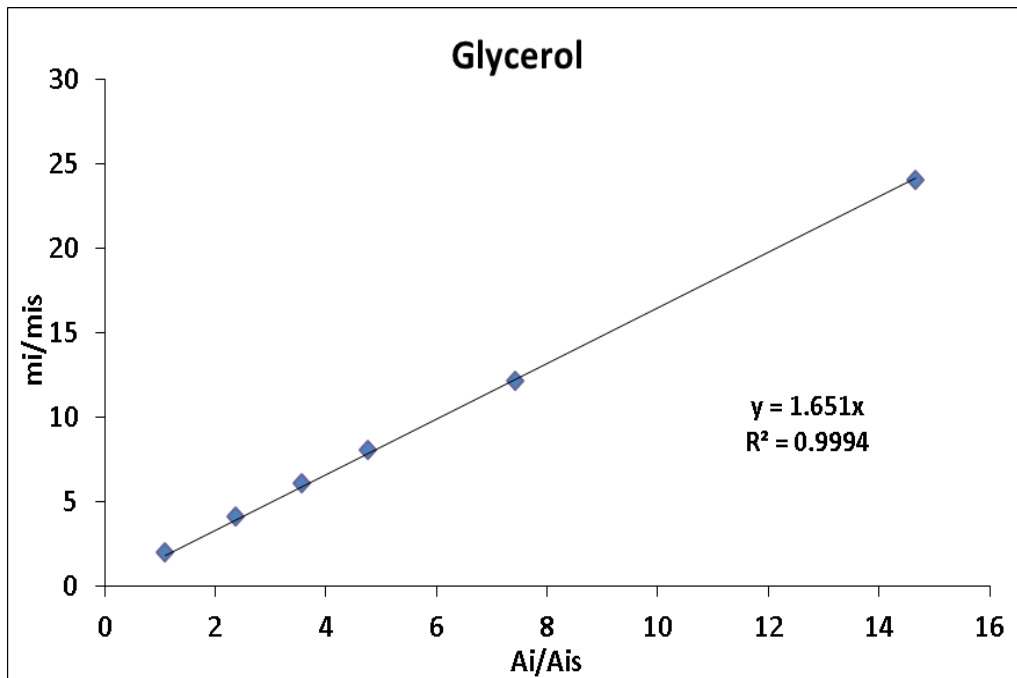


**Figure B-6** Calibration Curve for Glycerol.

## Identification of products by GC

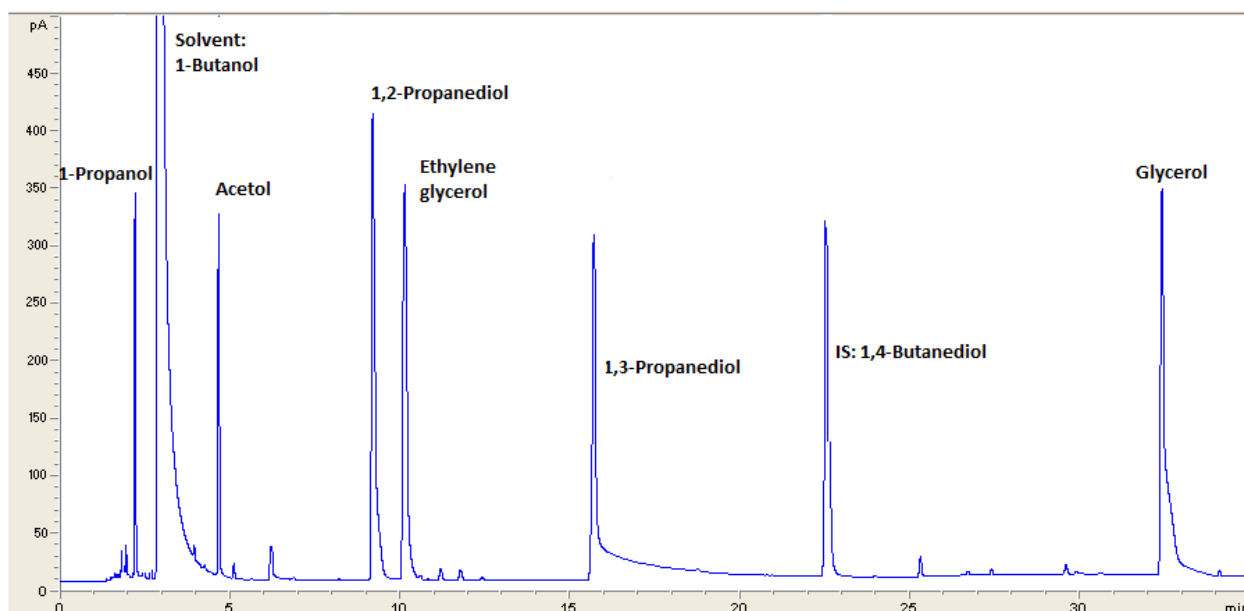


**Figure B-7** A typical Chromatogram of a GC Calibration Standard

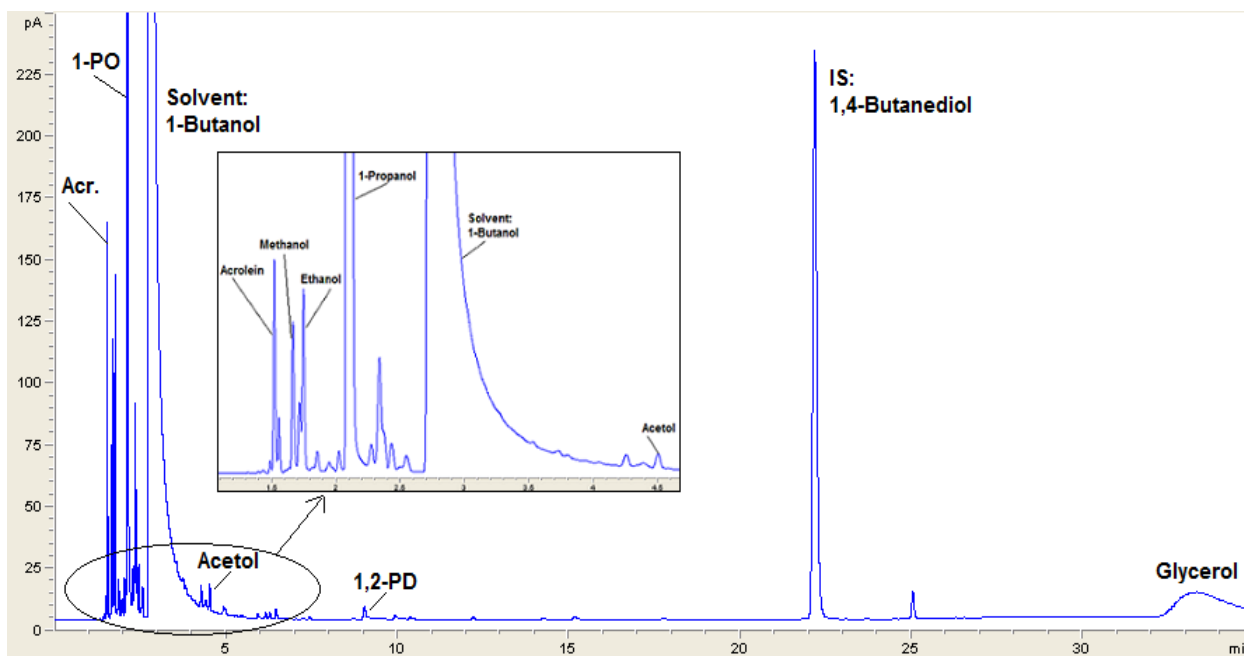


**Figure B-8** Chromatogram of a GC products using 10Ni/30HSiW/Al<sub>2</sub>O<sub>3</sub> calcinated at 450°C

## Appendix C Acid concentration calculation (mmol/g<sub>cat</sub>)

The TPD data was deconvoluted into 3 peaks (namely weak, medium and strong acid sites) using a Gaussian fitting method. Lower temperature desorption corresponds to weak acid sites and higher temperature to medium, strong acid sites. The number of moles of NH<sub>3</sub> desorbed during desorption step can be calculated using Equation C-1 and Equation C-2.

$$\text{Calibration\_Value} = \frac{(\text{loop\_volume}) * (\text{percent\_analytical\_gas})}{(\text{mean\_calibration\_area}) * 100} \quad \text{C-1}$$

$$\text{Uptake}(\text{mmol/g}_{\text{cat}}) = \frac{(\text{analytical\_area}) * (\text{calibration\_value})}{(\text{sample\_weight}) * 24.5} \quad \text{C-2}$$

### Calculation NH<sub>3</sub> desorbed using catalyst of 1Ni30HSiW/Al<sub>2</sub>O<sub>3</sub>

Sample weight: 0.123g

Loop volume: 0.524ml

Percent analytical gas 5.16%

Analytical area: Weak acid site (167°C): 18464; Medium acid site (259°C): 24998; Strong acid site (460°C): 26702

Weak acid site: 0.228 mmol/g<sub>cat</sub>. Medium acid site 0.308 mmol/g<sub>cat</sub>. Strong acid site: 0.330 mmol/g<sub>cat</sub>

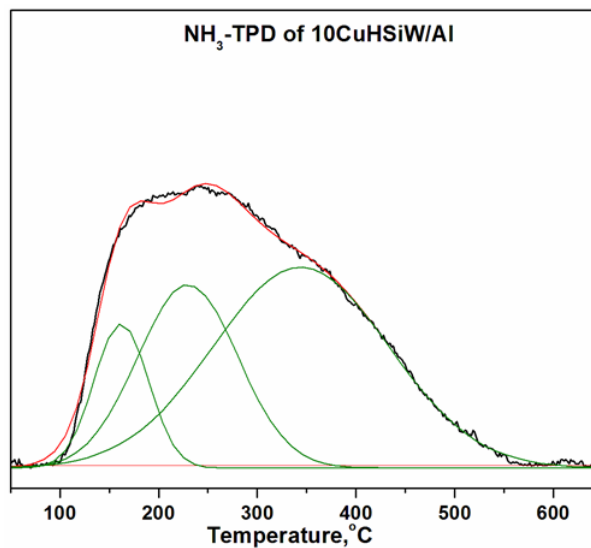
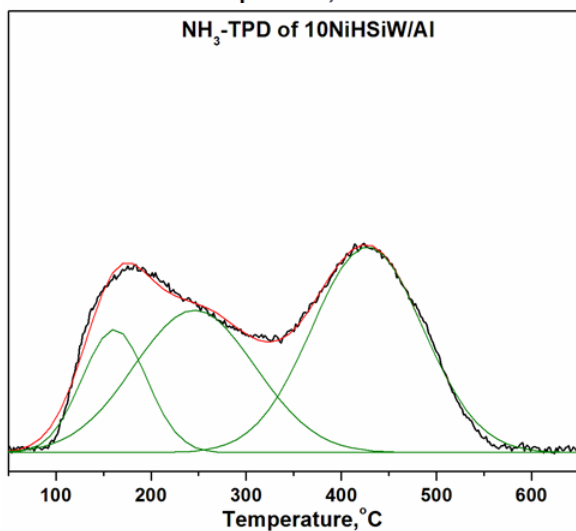
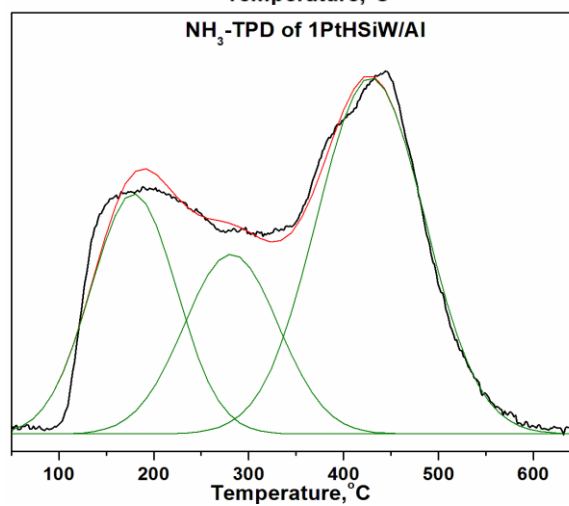
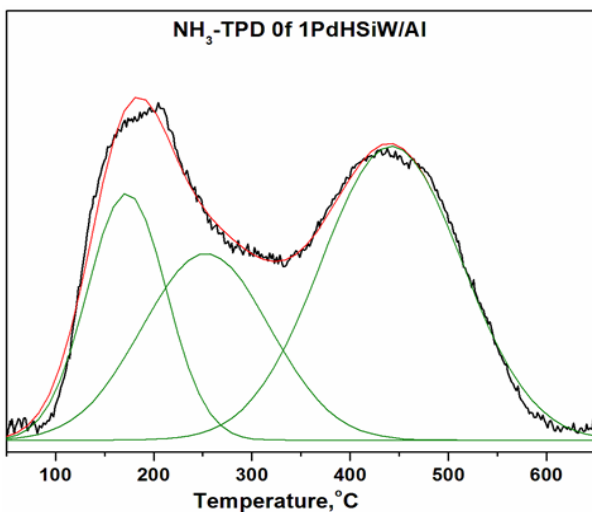
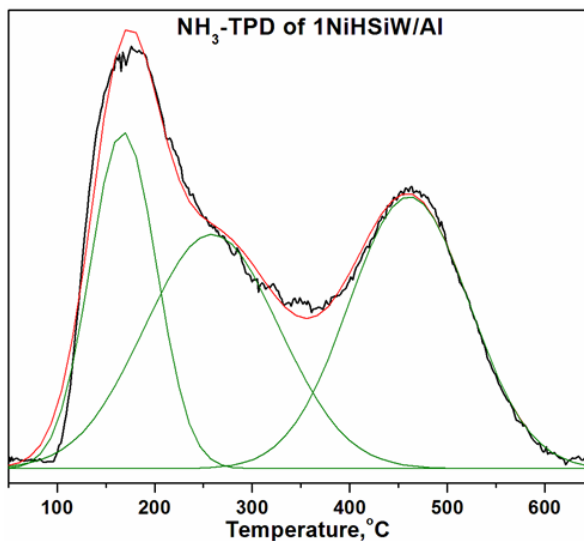
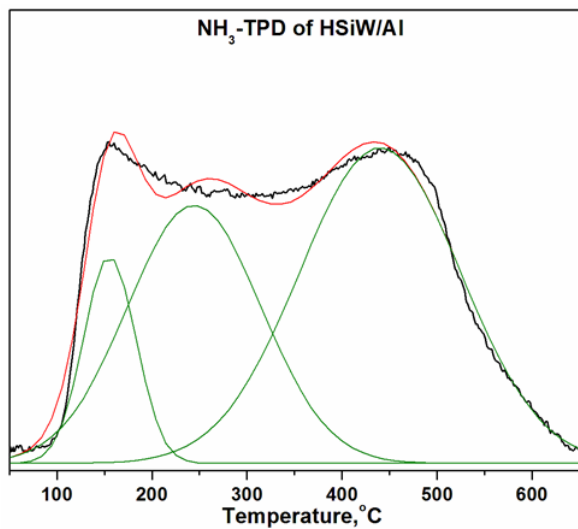
Total acidity: 0.228 + 0.308 + 0.330 = 0.866 mmol/g<sub>cat</sub>

Calculation for Table 4-1

Pulse	HSiW/Al	1Ni	1Pd	1Pt	10Ni	10Cu
1	679.34	726.83	709.41	678.09	658.09	687.26
2	722.35	712.06	733.96	739.37	650.99	692.84
3	721.08	697.22	670.72	710.22	716.37	687.25
4	734.46	680.82	681.88	714	694.44	649.37
5	802.38	720.28	700.18	708.81	691.67	645.05
Mean area	731.92	707.44	699.23	710.10	682.31	672.35
Loop volume (mL)	0.524	0.524	0.524	0.524	0.524	0.524
Sample weight (g)	0.123	0.123	0.120	0.122	0.120	0.120
Calibration value	3.6E-05	3.7E-05	3.7E-05	3.7E-05	3.8E-05	3.9E-05
Total acid amount mmol/g	0.989	0.866	0.873	0.869	0.572	0.657



The TPD curves are deconvoluted into 3 peaks using a Gaussian curve-fitting



<b>Catalyst</b>	<b>Weak acid site mmol/g /(Temp.)</b>	<b>Medium acid site mmol/g /(Temp.)</b>	<b>Strong acid site mmol/g /(Temp.)</b>	<b>Total acid amount, mmol/g</b>
<b>30HSiW/Al<sub>2</sub>O<sub>3</sub></b>	<b>0.149/ (155°C)</b>	<b>0.379/ (243°C)</b>	<b>0.461/ (439°C)</b>	<b>0.989</b>
<b>1Ni//30HSiW/Al<sub>2</sub>O<sub>3</sub></b>	<b>0.228/ (167°C)</b>	<b>0.308/ (259°C)</b>	<b>0.330/ (460°C)</b>	<b>0.866</b>
<b>1Pd/30HSiW/Al<sub>2</sub>O<sub>3</sub></b>	<b>0.205/ (172°C)</b>	<b>0.242/ (254°C)</b>	<b>0.425/ (442°C)</b>	<b>0.873</b>
<b>1Pt/30HSiW/Al<sub>2</sub>O<sub>3</sub></b>	<b>0.235/ (178°C)</b>	<b>0.194/ (281°C)</b>	<b>0.441/ (428°C)</b>	<b>0.869</b>
<b>10Ni/30HSiW/Al<sub>2</sub>O<sub>3</sub></b>	<b>0.124/ (162°C)</b>	<b>0.233/ (246°C)</b>	<b>0.215/ (427°C)</b>	<b>0.572</b>
<b>10Cu/30HSiW/Al<sub>2</sub>O<sub>3</sub></b>	<b>0.108/ (162°C)</b>	<b>0.201/ (230°C)</b>	<b>0.347/ (345°C)</b>	<b>0.657</b>

## Appendix D Glycerol conversion, product selectivity and rate constant calculations

$$\text{glycerol\_conversion} = \frac{\sum \text{mole\_of\_all\_carbon\_based\_product}}{\sum \text{mole\_of\_all\_carbon\_based\_product} + \text{mole\_of\_glycerol\_remain}} \quad \text{D-1}$$

$$1\_PO\_selectivity = \frac{\text{mole\_of\_1\_PO}}{\sum \text{mole\_of\_all\_carbon\_based\_product}} \quad \text{D-2}$$

$$13\_PD\_selectivity = \frac{\text{mole\_of\_13\_PD}}{\sum \text{mole\_of\_all\_carbon\_based\_product}} \quad \text{D-3}$$

$$\text{Glycerol\_mass\_balance} = \frac{\sum \text{mole\_of\_all\_carbon\_based\_product} + \text{mole\_of\_glycerol\_remain}}{\text{mole\_of\_initial\_glycerol}} * 100\% \quad \text{D-4}$$

**Calculation for Table 5-6 “Effect of temperature on the conversion of glycerol and the distribution to products in the hydrogenolysis of glycerol”**

### Experimental Conditions:

Temperature: 240°C; Initial Hydrogen Pressure: 580PSI; Stirring Speed: 700RPM

Catalyst: 10Ni/30HSiW/Al<sub>2</sub>O<sub>3</sub>; prepared by incipient wetness impregnation

Reactant Feed: 30g glycerol, 70g water, 2g catalyst

**Table D-1.** GC data

Compound	Retention time	Area
1-PO	2.129	7050.218
Acetol	4.57	27.455
1,2-PD	9.165	106.253
EG	10.095	0
1,3-PD	15.608	0
Glycerol	23.25	2752.582
I.S.	22.35	1782.696
Others		289.115

**Table D-2.** Response Factor for Each Compound

	<b>1-PO</b>	<b>Acetol</b>	<b>1,2-PD</b>	<b>EG</b>	<b>1,3-PD</b>	<b>Glycerol</b>	<b>Others</b>
<b>MW</b>	60.1	74.08	76.09	62.07	76.09	92.09	73.52
<b>RF</b>	0.795	1.555	1.257	1.676	1.232	1.651	1.361

Mass of GC sample: 131mg

Solvent: 1ml of 1-butanol and 5mg of 1,4-butanediol (I.S.) mixture (5mg of I.S.)

$$m(\text{propanol}) = m_{I.S.} \times k_P \times \frac{A_P}{A_{I.S.}} = 5 \times 0.795 \times \frac{7050.212}{1782.7} = 15.72\text{mg}$$

$$n(\text{propanol}) = \frac{m(\text{propanol})}{MW(\text{propanol})} = \frac{15.72\text{mg}}{60.1\text{mmol/mg}} = 0.2616\text{mmol}$$

$$m(\text{acetol}) = m_{I.S.} \times k_A \times \frac{A_A}{A_{I.S.}} = 5 \times 1.555 \times \frac{27.456}{1782.7} = 0.1197\text{mg}$$

$$n(\text{acetol}) = \frac{m(\text{acetol})}{MW(\text{acetol})} = \frac{0.19\text{mg}}{74.1\text{mmol/mg}} = 0.0016\text{mmol}$$

$$m(12PD) = m_{I.S.} \times k_{12PD} \times \frac{A_{12PD}}{A_{I.S.}} = 5 \times 1.257 \times \frac{106.25}{1782.7} = 0.375\text{mg}$$

$$n(12PD) = \frac{m(12PD)}{MW(12PD)} = \frac{0.447\text{mg}}{76.1\text{mmol/mg}} = 0.0049\text{mmol}$$

$$m(GL) = m_{I.S.} \times k_{GL} \times \frac{A_{GL}}{A_{I.S.}} = 5 \times 1.651 \times \frac{2752.6}{1782.7} = 12.75\text{mg}$$

$$n(GL) = \frac{m(GL)}{MW(GL)} = \frac{12.75\text{mg}}{92.1\text{mmol/mg}} = 0.138\text{mmol}$$

$$m(\text{unknown}) = m_{I.S.} \times k_{\text{unknowns}} \times \frac{A_{\text{unknown}}}{A_{I.S.}} = 5 \times 1.346 \times \frac{289.12}{1782.7} = 1.104\text{mg}$$

$$n(\text{unknown}) = \frac{m(\text{unknown})}{MW(\text{unknown})} = \frac{1.104\text{mg}}{73.52\text{mmol/mg}} = 0.015\text{mmol}$$

$$n(\text{products}) = \sum n_{\text{product}} = n(nPO) + n(\text{Acetol}) + n(12PD) + n(EG) + n(13PD) + n(\text{unknown}) \\ = 0.2616 + 0.0016 + 0.0049 + 0.000 + 0.00 + 0.015 = 0.2831 \text{mmol}$$

$$\text{Conversion}_{GL} = \left( \frac{n_{\text{products}}}{n_{\text{products}} + n_{GL}} \right) \times 100\% = \left( \frac{0.2831}{0.2831 + 0.138} \right) * 100\% = 67.4\%$$

$$\text{Selectivity}_{n-PO} = \left( \frac{n_{nPO}}{n_{\text{products}}} \right) \times 100\% = \left( \frac{0.2616}{0.2831} \right) * 100\% = 92.4\%$$

$$\text{Yield}_{nPO} = \left( \frac{n_{nPO}}{n_{\text{products}} + n_{GL}} \right) \times 100\% = \left( \frac{0.2616}{0.2831 + 0.138} \right) * 100\% = 62.3\%$$

$$\text{Selectivity}_{12PD} = \left( \frac{n_{12PD}}{n_{\text{products}}} \right) \times 100\% = \left( \frac{0.0049}{0.2831} \right) * 100\% = 1.7\%$$

$$\text{Yield}_{12PD} = \left( \frac{n_{12PD}}{n_{\text{products}} + n_{GL}} \right) \times 100\% = \left( \frac{0.0049}{0.2831 + 0.138} \right) * 100\% = 1.2\%$$

$$\text{Glycerol}_{\text{mass\_balance}} = \frac{(n_{\text{products}} + n_{GL}) * MW_{GL}}{m_{\text{Sample}}} * 100\% = \frac{(0.2831 + 0.138) * 92.1}{0.131 * 30} * 100\% = 98.7\%$$

### Calculation of the reaction rate for the hydrogenolysis of glycerol to 1-PO (Table 5-7 for 240°C)

A sample calculation of the kinetic determination of glycerol hydrogenolysis using an integral method was performed under the following condition: Temperature of 240°C; initial Hydrogen Pressure of 580PSI; Stirring Speed - 700RPM; 30g glycerol, 70g water, 2g catalyst). The samples taken from the reaction mixture after 0.5, 1, 2, 3, 4, 5 and 7 hours were analyzed by GC.

Experimental data for this reaction are listed in Table D-3; they are provided as [GL], ln[GL] versus time. A plot of ln[GL] vs. time in Figure D2 has the form of a straight line, hydrogen was supplied continuously for the whole reaction thus it is suggested that the reaction is first-order in Gl and a pseudo-first-order kinetics has been used to calculate the rate constant of reaction. The plot of ln[GL] vs. time is represented by the equation D-5.

**Table D-3.** Concentration of glycerol as a function of time using the 10Ni30HSiW/Al<sub>2</sub>O<sub>3</sub> catalyst

Time, h	0	0.5	1	2	3	4	5	7
[GL], mol/l	3.47	3.27	2.97	2.17	1.71	1.46	1.30	1.04
ln[GL]	1.24	1.19	1.09	0.78	0.54	0.38	0.26	0.04

$$-\frac{d[GL]}{dt} = k_{obs} * [GL] \Rightarrow \ln[GL] = -k_{obs} * t + \ln[GL_{t=0}] \quad \text{D-5}$$

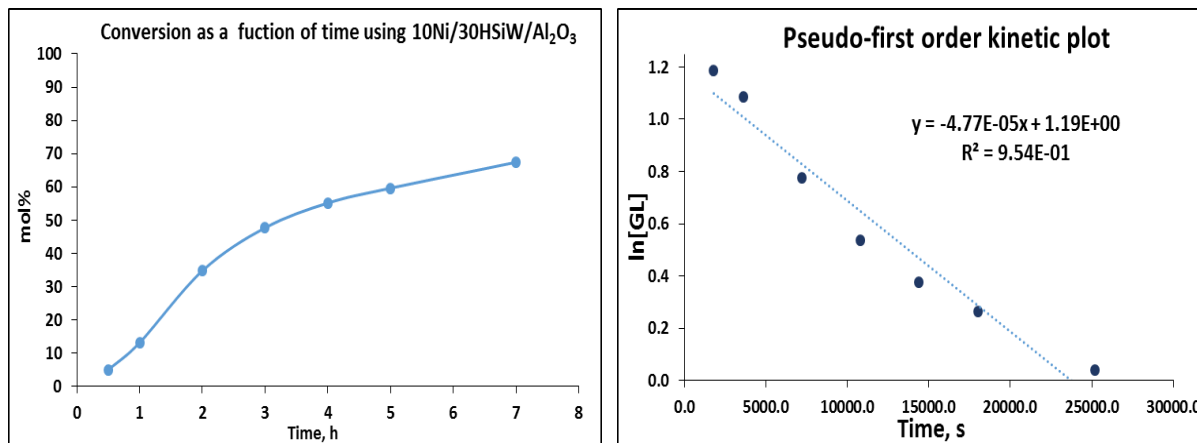


**Figure D-1 Conversion as a time function      Figure D-2 Pseudo-first order kinetic plot**

The plot of  $\ln[GL]$  vs. time is represented by the following equation:

$$y = -4.77E-05x + 1.19E+00$$

From the kinetic plot it is suggested that the rate constant is  $k_{obs}=4.77E-05 \text{ s}^{-1}$ .

# Appendix E Data of hydrogenolysis of Glycerol (some typical experiments)

## E1. Effect of metals on the hydrogenolysis of glycerol using Stainless Steel batch reactor

### Experiment #1

30HSiW/Al <sub>2</sub> O <sub>3</sub> catalyst, T = 240°C, P <sub>H<sub>2</sub></sub> = 880PSI, SR = 700 rpm, 30g of glycerol, 70g of DI water, 4g catalyst, t = 8 hours							
Time (h)	Conv (mol%)	Selectivity (mol%)					
		1,3PD	12PD	Act	EG	1-PO	Others
1	1.6	0.0	0.0	5.5	0.0	9.5	85.0
2	4.8	0.0	0.0	4.9	0.0	13.1	82.0
3	6.7	0.0	0.0	6.5	0.0	14.3	79.2
4	10.3	0.0	0.0	5.7	0.0	18.6	75.7
6	13.2	0.0	0.0	6.1	0.0	23.7	70.2
8	14.5	0.0	0.0	6.0	0.0	30.5	63.5

### Experiment #2

1Ni/30HSiW/Al <sub>2</sub> O <sub>3</sub> catalyst, T = 240°C, P <sub>H<sub>2</sub></sub> = 880PSI, SR = 700 rpm, 30g of glycerol, 70g of DI water, 4g catalyst, t = 8 hours							
Time (h)	Conv (mol%)	Selectivity (mol%)					
		1,3PD	12PD	Act	EG	1-PO	Others
1	6.7	0.0	8.1	15.5	0.0	37.2	39.2
2	9.6	0.0	7.6	12.8	0.0	46.0	33.6
3	17.6	0.0	7.2	6.9	0.0	50.0	36.0
4	20.6	0.0	9.0	6.5	0.0	53.2	31.3
6	29.9	3.9	5.5	4.5	0.0	51.2	35.0
8	39.2	3.0	4.1	3.3	0.0	54.7	34.9

### Experiment #2

1Pd/30HSiW/Al <sub>2</sub> O <sub>3</sub> catalyst, T = 240°C, P <sub>H<sub>2</sub></sub> = 880PSI, SR = 700 rpm, 30g of glycerol, 70g of DI water, 4g catalyst, t = 8 hours							
Time (h)	Conv (mol%)	Selectivity (mol%)					
		1,3PD	12PD	Act	EG	1-PO	Others
1	6.4	0.0	9.7	15.3	0.0	29.5	45.5
2	12.9	0.0	7.7	10.4	0.0	36.2	45.6

3	17.5	0.0	6.0	6.1	0.0	43.5	44.4
4	22.3	0.0	5.0	4.6	0.0	48.0	42.3
6	29.0	4.2	3.8	3.7	0.0	44.9	43.4
8	34.1	5.4	4.7	4.1	0.0	51.4	34.5

#### Experiment #4

1Pt/30HSiW/Al <sub>2</sub> O <sub>3</sub> catalyst, T = 240°C, P <sub>H<sub>2</sub></sub> = 880PSI, SR = 700 rpm, 30g of glycerol, 70g of DI water, 4g catalyst, t = 8 hours							
Time (h)	Conv (mol%)	Selectivity (mol%)					
		1,3PD	12PD	Act	EG	1-PO	Others
1	7.8	0.0	17.9	15.5	0.0	56.8	9.7
2	13.5	9.3	15.5	8.5	0.0	57.8	8.9
3	19.1	10.3	12.0	4.6	0.0	56.1	17.0
4	25.5	11.5	10.1	4.2	0.0	57.4	16.8
6	36.0	11.0	7.1	3.0	0.0	58.2	20.7
8	45.3	10.5	5.7	2.5	1.8	59.2	20.3

#### Experiment #5

10Ni/30HSiW/Al <sub>2</sub> O <sub>3</sub> catalyst, T = 240°C, P <sub>H<sub>2</sub></sub> = 880PSI, SR = 700 rpm, 30g of glycerol, 70g of DI water, 4g catalyst, t = 8 hours							
Time (h)	Conv (mol%)	Selectivity (mol%)					
		1,3PD	12PD	Act	EG	1-PO	Others
1.0	10.7	0.0	13.5	12.0	0.0	55.2	19.4
2.3	16.0	10.0	13.5	5.8	4.9	52.4	13.3
4.0	18.5	4.9	9.4	5.3	0.0	47.7	32.8
6.0	29.3	4.5	8.9	4.8	2.7	51.3	27.8
8.0	33.2	7.9	10.5	3.8	4.4	60.3	12.7

#### Experiment #6

10Cu/30HSiW/Al <sub>2</sub> O <sub>3</sub> catalyst, T = 240°C, P <sub>H<sub>2</sub></sub> = 880PSI, SR = 700 rpm, 30g of glycerol, 70g of DI water, 4g catalyst, t = 8 hours							
Time (h)	Conv (mol%)	Selectivity (mol%)					
		1,3PD	12PD	Act	EG	1-PO	Others
1.0	1.1	0.0	0.0	4.4	0.0	10.6	85.0
2.0	5.7	0.0	0.0	6.0	0.0	12.2	81.9
3.0	8.0	0.0	2.5	5.8	0.0	15.4	76.2
4.0	11.4	0.0	3.6	4.6	0.0	17.6	74.2
6.0	14.7	0.0	3.8	8.0	0.0	26.4	61.8
8.0	18.4	0.0	4.2	5.3	0.0	31.8	58.7



## E2. Effect of calcination temperature on the hydrogenolysis of glycerol using a Hasteylloy reactor

### Experiment #1

10Ni/30HSiW/Al <sub>2</sub> O <sub>3</sub> catalyst, T = 240°C, P <sub>H2</sub> = 580PSI, SR = 700 rpm, 30g of glycerol, 70g of DI water, 2g catalyst, t = 7 hours, calcination temperature = 350°C							
Time (h)	Conv (mol%)	Selectivity (mol%)					
		1,3PD	12PD	Act	EG	1-PO	Others
1.0	21.5	0.0	0.0	3.1	0.0	81.6	15.3
2.0	43.3	0.0	0.0	1.6	0.0	87.6	10.8
3.0	57.8	0.0	0.0	1.0	0.0	89.5	9.5
4.0	67.4	0.0	0.0	0.7	0.0	90.1	9.3
5.0	77.1	0.0	0.0	0.5	0.0	91.3	8.2
7.0	86.5	0.0	0.0	0.4	0.0	91.7	7.9

### Experiment #2

10Ni/30HSiW/Al <sub>2</sub> O <sub>3</sub> catalyst, T = 240°C, P <sub>H2</sub> = 580PSI, SR = 700 rpm, 30g of glycerol, 70g of DI water, 2g catalyst, t = 7 hours, calcination temperature = 450°C							
Time (h)	Conv (mol%)	Selectivity (mol%)					
		1,3PD	12PD	Act	EG	1-PO	Others
1.0	21.9	0.0	0.0	2.9	0.0	77.7	19.4
2.0	44.4	0.0	0.0	1.4	0.0	85.0	13.5
3.0	62.7	0.0	0.0	0.9	0.0	89.7	9.4
4.0	69.8	0.0	0.0	0.7	0.0	90.5	8.8
5.0	82.3	0.0	0.0	0.4	0.0	90.6	9.1
7.0	90.1	0.0	0.0	0.3	0.0	92.9	6.8

### Experiment #3

10Ni/30HSiW/Al <sub>2</sub> O <sub>3</sub> catalyst, T = 240°C, P <sub>H2</sub> = 580PSI, SR = 700 rpm, 30g of glycerol, 70g of DI water, 2g catalyst, t = 7 hours, calcination temperature = 550°C							
Time (h)	Conv (mol%)	Selectivity (mol%)					
		1,3PD	12PD	Act	EG	1-PO	Others
1.0	7.4	0.0	0.0	7.7	0.0	49.7	42.6
2.0	13.1	0.0	0.0	5.9	0.0	58.7	35.4
3.0	21.1	0.0	0.0	4.1	0.0	65.8	30.1
4.0	30.2	0.0	3.0	3.1	0.0	66.8	27.1
5.0	41.0	0.0	2.9	2.1	0.0	69.5	25.6
7.0	46.2	0.0	2.9	1.7	0.0	71.5	23.9

#### Experiment #4

10Ni/30HSiW/Al <sub>2</sub> O <sub>3</sub> catalyst, T = 240°C, P <sub>H2</sub> = 580PSI, SR = 700 rpm, 30g of glycerol, 70g of DI water, 2g catalyst, t = 7 hours, calcination temperature = 650°C							
Time (h)	Conv (mol%)	Selectivity (mol%)					
		1,3PD	12PD	Act	EG	1-PO	Others
1.0	3.1	0.0	0.0	0.0	0.0	60.7	39.3
2.0	5.3	0.0	0.0	10.7	0.0	60.5	28.8
3.0	8.6	0.0	0.0	8.6	0.0	62.4	29.0
4.0	10.3	0.0	0.0	7.4	0.0	64.4	28.3
5.0	12.7	0.0	0.0	5.7	0.0	65.6	28.7
7.0	21.3	0.0	0.0	4.4	0.0	64.9	30.7

# Appendix F Permission to Re-print Copyrighted Material



RightsLink®

Home

Account Info

Help



**Book:** Soy-Based Chemicals and Materials  
**Chapter:** Value-Added Chemicals from Glycerol  
**Author:** X. Philip Ye, Shoujie Ren  
**Publisher:** American Chemical Society  
**Date:** Jan 1, 2014

Copyright © 2014, American Chemical Society

Logged in as:  
Chau Mai  
Waterloo University  
Account #:  
3001059113

LOGOUT

## PERMISSION/LICENSE IS GRANTED FOR YOUR ORDER AT NO CHARGE

This type of permission/license, instead of the standard Terms & Conditions, is sent to you because no fee is being charged for your order. Please note the following:

- Permission is granted for your request in both print and electronic formats, and translations.
- If figures and/or tables were requested, they may be adapted or used in part.
- Please print this page for your records and send a copy of it to your publisher/graduate school.
- Appropriate credit for the requested material should be given as follows: "Reprinted (adapted) with permission from (COMPLETE REFERENCE CITATION). Copyright (YEAR) American Chemical Society." Insert appropriate information in place of the capitalized words.
- One-time permission is granted only for the use specified in your request. No additional uses are granted (such as derivative works or other editions). For any other uses, please submit a new request.

If credit is given to another source for the material you requested, permission must be obtained from that source.

## ROYAL SOCIETY OF CHEMISTRY LICENSE TERMS AND CONDITIONS

Oct 25, 2016

This Agreement between Waterloo University – Chau Mai ("You") and Royal Society of Chemistry ("Royal Society of Chemistry") consists of your license details and the terms and conditions provided by Royal Society of Chemistry and Copyright Clearance Center.

License Number	3939431235235
License date	Aug 31, 2016
Licensed Content Publisher	Royal Society of Chemistry
Licensed Content Publication	Catalysis Science & Technology
Licensed Content Title	Heterogeneous catalysis of the glycerol hydrogenolysis
Licensed Content Author	Yoshinao Nakagawa, Kelichi Tomishige
Licensed Content Date	Feb 10, 2011
Licensed Content Volume Number	1
Licensed Content Issue Number	2
Type of Use	Thesis/Dissertation
Requestor type	academic/educational
Portion	figures/tables/images
Number of figures/tables/images	1
Format	print and electronic
Distribution quantity	1
Will you be translating?	no
Order reference number	
Title of the thesis/dissertation	Catalytic upgrading of glycerol into
Expected completion date	Oct 2016
Estimated size	210
Requestor Location	Waterloo University 200 University Ave. W  Waterloo, ON N2L3G1 Canada Attn: Chau Thi Guynh Mai
Billing Type	Invoice
Billing Address	Waterloo University 200 University Ave. W

<https://s100.copyright.com/MyAccount/viewPrintableLicenseDetails?ref=965243f-3864-...> 10/25/2016

RightsLink - Your Account

Page 2 of 4

	Waterloo, ON N2L3G1 Canada Attn: Chau Thi Guynh Mai
Total	0.00 USD

### Terms and Conditions

This License Agreement is between (Requestor Name) ("You") and The Royal Society of Chemistry ("RSC") provided by the Copyright Clearance Center ("CCC"). The license consists of your order details, the terms and conditions provided by the Royal Society of Chemistry, and the payment terms and conditions.

### RSC / TERMS AND CONDITIONS

#### INTRODUCTION

The publisher for this copyrighted material is The Royal Society of Chemistry. By clicking "accept" in connection with completing this licensing transaction, you agree that the following terms and conditions apply to this transaction (along with the Billing and Payment terms and conditions established by CCC, at the time that you opened your RightsLink

# ELSEVIER LICENSE TERMS AND CONDITIONS

Oct 25, 2016

This Agreement between Waterloo University – Chau Mai ("You") and Elsevier ("Elsevier") consists of your license details and the terms and conditions provided by Elsevier and Copyright Clearance Center.

License Number	3939431079137
License date	Aug 31, 2016
Licensed Content Publisher	Elsevier
Licensed Content Publication	Applied Catalysis B: Environmental
Licensed Content Title	Hydrogenolysis of glycerol to propanediols over a Pt/ASA catalyst: The role of acid and metal sites on product selectivity and the reaction mechanism
Licensed Content Author	I. Gandarias, P.L. Arias, J. Requies, M.B. Gómez, J.L.G. Fierro
Licensed Content Date	9 June 2010
Licensed Content Volume Number	97
Licensed Content Issue Number	1-2
Licensed Content Pages	9
Start Page	248
End Page	256
Type of Use	reuse in a thesis/dissertation
Intended publisher of new work	other
Portion	figures/tables/illustrations
Number of figures/tables/illustrations	1
Format	both print and electronic
Are you the author of this Elsevier article?	No
Will you be translating?	No
Order reference number	
Original figure numbers	Figure 5
Title of your thesis/dissertation	Catalytic upgrading of glycerol into
Expected completion date	Oct 2016
Estimated size (number of pages)	210
Elsevier VAT number	GB 484 6272 12
Requestor Location	Waterloo University 200 University Ave. W

Waterloo, ON N2L3G1

<https://s100.copyright.com/MvAccount/viewPrintableLicenseDetails?ref=0af0772e-cb3f-...> 10/25/2016

RightsLink - Your Account

Page 2 of 5

Canada  
Attn: Chau Thi Quynh Mai  
Total **0.00 USD**  
Terms and Conditions

#### INTRODUCTION

1. The publisher for this copyrighted material is Elsevier. By clicking "accept" in connection with completing this licensing transaction, you agree that the following terms and conditions apply to this transaction (along with the Billing and Payment terms and conditions established by Copyright Clearance Center, Inc. ("CCC"), at the time that you opened your Rightslink account and that are available at any time at <http://myaccount.copyright.com>).

#### GENERAL TERMS

2. Elsevier hereby grants you permission to reproduce the aforementioned material subject to the terms and conditions indicated.

# ELSEVIER LICENSE TERMS AND CONDITIONS

Oct 25, 2016

This Agreement between Waterloo University – Chau Mai ("You") and Elsevier ("Elsevier") consists of your license details and the terms and conditions provided by Elsevier and Copyright Clearance Center.

License Number	3939430906270
License date	Aug 31, 2016
Licensed Content Publisher	Elsevier
Licensed Content Publication	Journal of Catalysis
Licensed Content Title	Glycerol conversion in the aqueous solution under hydrogen over Ru/C + an ion-exchange resin and its reaction mechanism
Licensed Content Author	Tomohisa Miyazawa, Yohei Kusunoki, Kimio Kunimori, Keiichi Tomishige
Licensed Content Date	10 June 2006
Licensed Content Volume Number	240
Licensed Content Issue Number	2
Licensed Content Pages	9
Start Page	213
End Page	221
Type of Use	reuse in a thesis/dissertation
Portion	figures/tables/illustrations
Number of figures/tables/illustrations	1
Format	both print and electronic
Are you the author of this Elsevier article?	No
Will you be translating?	No
Order reference number	
Original figure numbers	Figure 5
Title of your thesis/dissertation	Catalytic upgrading of glycerol into
Expected completion date	Oct 2016
Estimated size (number of pages)	210
Elsevier VAT number	GB 494 6272 12
Requestor Location	Waterloo University 200 University Ave. W

Waterloo, ON N2L3G1  
Canada  
Attn: Chau Thi Quynh Mai

<https://s100.copyright.com/MvAccount/viewPrintableLicenseDetails?ref=c12e395a-01e4...> 10/25/2016

RightsLink - Your Account

Page 2 of 5

Total 0.00 USD  
Terms and Conditions

## INTRODUCTION

1. The publisher for this copyrighted material is Elsevier. By clicking "accept" in connection with completing this licensing transaction, you agree that the following terms and conditions apply to this transaction (along with the Billing and Payment terms and conditions established by Copyright Clearance Center, Inc. ("CCC"), at the time that you opened your Rightslink account and that are available at any time at <http://myaccount.copyright.com>).

## GENERAL TERMS

2. Elsevier hereby grants you permission to reproduce the aforementioned material subject to the terms and conditions indicated.

3. Acknowledgement: If any part of the material to be used (for example, figures) has appeared in our publication with credit or acknowledgement to another source, permission must also be sought from that source. If such permission is not obtained then that material may not be included in your publication/copies. Suitable acknowledgement to the source

# ROYAL SOCIETY OF CHEMISTRY LICENSE TERMS AND CONDITIONS

Oct 25, 2016

This Agreement between Waterloo University – Chau Mai ("You") and Royal Society of Chemistry ("Royal Society of Chemistry") consists of your license details and the terms and conditions provided by Royal Society of Chemistry and Copyright Clearance Center.

License Number	3939430094025
License date	Aug 31, 2016
Licensed Content Publisher	Royal Society of Chemistry
Licensed Content Publication	Catalysis Science & Technology
Licensed Content Title	Polyoxometalate-based phase transfer catalysis for liquid–solid organic reactions: a review
Licensed Content Author	Yu Zhou,Zengqiang Guo,Wei Hou,Qian Wang,Jun Wang
Licensed Content Date	Jul 21, 2015
Licensed Content Volume Number	5
Licensed Content Issue Number	9
Type of Use	Thesis/Dissertation
Requestor type	academic/educational
Portion	figures/tables/images
Number of figures/tables/images	1
Format	print and electronic
Distribution quantity	1
Will you be translating?	no
Order reference number	
Title of the thesis/dissertation	Catalytic upgrading of glycerol into
Expected completion date	Oct 2016
Estimated size	210
Requestor Location	Waterloo University 200 University Ave. W  Waterloo, ON N2L3G1 Canada Attn: Chau Thi Quynh Mai
Billing Type	Invoice
Billing Address	Waterloo University 200 University Ave. W

<https://s100.copyright.com/MyAccount/viewPrintableLicenseDetails?ref=9d89300f-c8a6-...> 10/25/2016

RightsLink - Your Account

Page 2 of 4

Total	0.00 USD
-------	----------

#### Terms and Conditions

This License Agreement is between (Requestor Name) ("You") and The Royal Society of Chemistry ("RSC") provided by the Copyright Clearance Center ("CCC"). The license consists of your order details, the terms and conditions provided by the Royal Society of Chemistry, and the payment terms and conditions.

#### RSC / TERMS AND CONDITIONS

##### INTRODUCTION

The publisher for this copyrighted material is The Royal Society of Chemistry. By clicking "accept" in connection with completing this licensing transaction, you agree that the following terms and conditions apply to this transaction (along

# ROYAL SOCIETY OF CHEMISTRY LICENSE TERMS AND CONDITIONS

Oct 25, 2016

This Agreement between Waterloo University – Chau Mai ("You") and Royal Society of Chemistry ("Royal Society of Chemistry") consists of your license details and the terms and conditions provided by Royal Society of Chemistry and Copyright Clearance Center.

License Number	3939421471272
License date	Aug 31, 2016
Licensed Content Publisher	Royal Society of Chemistry
Licensed Content Publication	Chemical Communications (Cambridge)
Licensed Content Title	Unique acid catalysis of heteropoly compounds (heteropolyoxometalates) in the solid state
Licensed Content Author	Makoto Misono
Licensed Content Date	Jun 18, 2001
Licensed Content Issue Number	13
Type of Use	Thesis/Dissertation
Requestor type	academic/educational
Portion	figures/tables/images
Number of figures/tables/images	1
Format	print and electronic
Distribution quantity	1
Will you be translating?	no
Order reference number	
Title of the thesis/dissertation	Catalytic upgrading of glycerol into
Expected completion date	Oct 2016
Estimated size	210
Requestor Location	Waterloo University 200 University Ave. W  Waterloo, ON N2L3G1 Canada Attn: Chau Thi Quynh Mai
Billing Type	Invoice
Billing Address	Waterloo University 200 University Ave. W  Waterloo, ON N2L3G1

<https://s100.copyright.com/MyAccount/viewPrintableLicenseDetails?ref=6abc7449-24b5...> 10/25/2016

RightsLink - Your Account

Page 2 of 4

Canada  
Attn: Chau Thi Quynh Mai  
Total 0.00 USD

#### Terms and Conditions

This License Agreement is between (Requestor Name) ("You") and The Royal Society of Chemistry ("RSC") provided by the Copyright Clearance Center ("CCC"). The license consists of your order details, the terms and conditions provided by the Royal Society of Chemistry, and the payment terms and conditions.

#### RSC / TERMS AND CONDITIONS

##### INTRODUCTION

The publisher for this copyrighted material is The Royal Society of Chemistry. By clicking "accept" in connection with completing this licensing transaction, you agree that the following terms and conditions apply to this transaction (along with the Billing and Payment terms and conditions established by CCC, at the time that you opened your RightsLink



# ROYAL SOCIETY OF CHEMISTRY LICENSE TERMS AND CONDITIONS

Oct 25, 2016

This Agreement between Waterloo University – Chau Mai ("You") and Royal Society of Chemistry ("Royal Society of Chemistry") consists of your license details and the terms and conditions provided by Royal Society of Chemistry and Copyright Clearance Center.

License Number	3939421242209
License date	Aug 31, 2016
Licensed Content Publisher	Royal Society of Chemistry
Licensed Content Publication	Chemical Society Reviews
Licensed Content Title	Chemoselective catalytic conversion of glycerol as a biorenewable source to valuable commodity chemicals
Licensed Content Author	Chun-Hui (Clayton) Zhou, Jorge N. Beltrami, Yong-Xian Fan, G. Q. (Max) Lu
Licensed Content Date	Nov 22, 2007
Licensed Content Volume Number	37
Licensed Content Issue Number	3
Type of Use	Thesis/Dissertation
Requestor type	academic/educational
Portion	figures/tables/images
Number of figures/tables/images	1
Format	print and electronic
Distribution quantity	1
Will you be translating?	no
Order reference number	
Title of the thesis/dissertation	Catalytic upgrading of glycerol into
Expected completion date	Oct 2016
Estimated size	210
Requestor Location	Waterloo University 200 University Ave. W  Waterloo, ON N2L3G1 Canada Attn: Chau Thi Guynh Mai
Billing Type	Invoice
Billing Address	Waterloo University 200 University Ave. W

<https://s100.copyright.com/MyAccount/viewPrintableLicenseDetails?ref=698def41-2b0e-...> 10/25/2016

RightsLink - Your Account

Page 2 of 4

	Waterloo, ON N2L3G1 Canada Attn: Chau Thi Guynh Mai
Total	0.00 CAD

#### Terms and Conditions

This License Agreement is between (Requestor Name) ("You") and The Royal Society of Chemistry ("RSC") provided by the Copyright Clearance Center ("CCC"). The license consists of your order details, the terms and conditions provided by the Royal Society of Chemistry, and the payment terms and conditions.

#### RSC / TERMS AND CONDITIONS

##### INTRODUCTION

The publisher for this copyrighted material is The Royal Society of Chemistry. By clicking "accept" in connection with